PhD candidate
Elena Verticchio

An integrated approach for the climate-induced risk assessment within historic libraries combining microclimate data and modelling

PhD thesis

Sapienza Università di Roma, Department of Earth Sciences
Cycle XXXIV (2018-2021), *curriculum Environment and Cultural Heritage*

Academic Disciplines: FIS/06, ING-IND/11

Advisors

Prof. Anna Maria Siani
Department of Physics
Sapienza Università di Roma

Prof. Chiara Bertolin
Department of Mechanical and Industrial Engineering
Norwegian University of Science and Technology

Prof. Cristina Cornaro
Department of Enterprise Engineering
Università degli Studi di Roma "Tor Vergata"

A precious — mouldering pleasure — 'tis
to meet an Antique Book
In just the dress his century wore.
A privilege — I think
[…]
His presence is Enchantment —
You beg him not to go

Emily Dickinson

Abstract

The durability of historic libraries is affected by deterioration processes driven by the environmental conditions in which the collections are kept. The present research aimed to infer meaningful information from the combination of microclimate observations (i) and modelling (ii) so to outline an integrated approach to assess the climate-induced risks (iii) in historic libraries.

Four historic libraries in Italy, associated with different climates, were used as case studies: the Meteorology Library of CREA (Consiglio per la Ricerca in Agricoltura e l'Analisi dell'Economia Agraria) at Collegio Romano and the repository of the Alessandrina Library in Rome, the Ca' Granda Library in Milan and the Delfiniana Library in Udine. The study of the microclimate (i) enhanced the understanding of the interaction between the heritage material properties and the environmental forcing. For the first time, a comparative study was carried out to provide useful insight into the impact on the climate-induced conservation risks for paper collections of conditioned and unconditioned microclimates in historic buildings. Modelling (ii) allowed to simulate the microclimate inside historic buildings housing the libraries using both sinusoidal heat and moisture transfer functions and whole-building dynamic simulation. For the latter method, the thermal model of the Collegio Romano Library was built in IDA ICE (Indoor Climate and Energy) environment and calibrated using on-site measurements. Then, the capability of IDA ICE extended with HMWall (Heat Air and Moisture) model was tested in the simulation of 1D hygrothermal exchanges across a wall made in paper. To this aim, the physical and hygrothermal properties of ancient and modern papers were investigated through a sensitivity analysis to identify the most influential parameters in the simulation of moisture gradients. Finally, dose-response/damage functions for library materials and NDT (Non-Destructive Testing) measurements were used to evaluate the climate-induced risks for paper collections (iii). The climate-induced risk assessment involved mechanical, chemical and biological mechanisms. The allowable microclimate bands to avoid mechanical stress to organic hygroscopic materials and the risk of wear and tears due to handling were studied to draw recommendations to limit mechanical deterioration in case of consultation and loans. The isochrones of equal expected lifetime of paper allowed to evaluate the chemical risk for different paper-based collections as a function of their intrinsic vulnerability (i.e., acidity and degree of

polymerisation) and considering the typical response time of paper books to the environmental temperature and humidity changes. In addition, the Time Weighted Expected Lifetime (TWEL) index was defined to explore the effect on paper conservation of changes in the microclimate conditions resulting from climate control strategies, retrofitting measures and/or the possible future climate change. The biological threats were estimated by using Sedlbauer curves for mould germination and growth and the Brimblecombe model for potential production of cloth moth eggs. Finally, the colorimetric change on some faded book covers in the repository of the Alessandrina library was monitored over a year to estimate the photodeterioration rate due to solar exposure.

The results highlighted that, at all climate zones considered, the historic libraries were characterised by high thermal inertia and moisture buffering capacity due to the combined effect of massive building envelopes, low air exchanges and large total volumes of hygroscopic materials. The modelling of the hygrothermal conditions inside paper collections showed that the relative humidity levels and fluctuations collected in the libraries would affect only the first layers of the books, showing a low impact on their conservation. Temperature was found to be a key microclimate stressor to be studied for preventive conservation of paper collections, as it controls the rate of cellulose hydrolysis and favours insect proliferation. In terms of paper chemical deterioration, the annual microclimate conditions inside the libraries would lead to the loss of their acidic collections in less than 300 years. The use of winter heating markedly reduced the expected lifetime with respect to that estimated in the unconditioned microclimates in the same season. For this reason, the natural microclimates within historic buildings in winter could be suggested as a sustainable preservation strategy for paper collections. This result was confirmed in simulation environment reconstructing the natural microclimate in Collegio Romano Library through its validated whole-building model. The observed summer overheating is particularly alarming in view of the predicted climate change, as the expected lifetime for acidic paper was found to potentially decrease up to −46% in the Far Future (2071-2100) if compared to the Recent Past (1981-2010) scenario. Finally, although spore germination could be excluded, the risk of insect proliferation was high in all the libraries. The annual discolouration rate of the faded book covers in Alessandrina was too low to be measured; however, the estimated luminous exposure was found to be incompatible for the conservation of photosensitive materials.

The integrated approach followed in this thesis enabled a wide-ranging study on the conservation of historic libraries, enhancing the understanding of the role of climate on the deterioration risks and supporting the design of rational and sustainable mitigation strategies. The same approach could be effectively adapted to most library and archival collections made of paper.

Preface

Preventive conservation involves all the measures addressed towards mitigating the risks affecting heritage objects before irreversible damages occur. In this framework, the study of microclimate plays a key role, as the environment is among the principal causes of deterioration to the artworks. A successful management of the climate-induced deterioration risks must be grounded in the scientific research on the interactions between the environment and the materials. In the times of a growing concern about the effect of climate change, we are commited to find timely and sustainable mitigation strategies.

I embraced the study of the microclimate for cultural heritage during my bachelor programme and developed a deep interest in the topic. In the following years, I applied the underlying principles to a variety of cultural objects (e.g., paintings, mineralogical collections, wood ceilings) and spaces (e.g., museums, churches, historic buildings, hypogea). My interest in library conservation was the natural evolution of my early passion for books as material objects. This thesis is the result of an academic and professional journey started in 2018, when I had the chance to carry out a joint internship at the British Library and the London Metropolitan Archives in London (United Kingdom). Once back in Italy, I enriched the experience collaborating at the Istituto Centrale per la Patologia degli Archivi e del Libro with the Laboratories of Environment and Preventive Conservation.

This PhD project focused on the preventive conservation of historic libraries, combining microclimate observations and modelling to assess the climate-induced risks for paper collections. My project was sewn stitching together expertise with passion. During these years, I have learnt valuable professional and collateral skills, becoming more independent as a young researcher. I designed and set up the two-year-long monitoring campaigns of the indoor climate in two prestigious case studies in Rome: the Historic Meteorology Library of CREA (Consiglio per la Ricerca in Agricoltura e l'Analisi dell'Economia Agraria) at the historical complex of Collegio Romano and the vast storage facility of the Alessandrina Library at Sapienza University Campus. The availability of long time series of microclimate observations collected in the historic libraries Ca' Granda in Milan and Delfiniana in Udine gave me the opportunity to perform a comprehensive comparative analysis.

Since March 2019, I have been involved in the European project *Collection-Care: Innovative and affordable service for the Preventive Conservation monitoring of individual Cultural Artefacts during display, storage, handling and transport* (European Union's Horizon 2020, under grant agreement No 814624) as a member of the Research Unit Sapienza (URO1 - responsible: Prof. A.M. Siani) . From August to November 2021, I was a visiting student at the Jerzy Haber Institute of Catalysis and Surface Chemistry of the Polish Academy of Science in Krakow (Poland), joining the Cultural Heritage Research group led by Prof. Łukasz Bratasz. My research activities were funded by Sapienza University of Rome through the grants "Avvio alla Ricerca" and "Joint Mobility" for PhD students.

I hope that the results of this work can support the decision-making for the preventive conservation of historic libraries by informing on their main climate-induced deterioration risks. To whom might be interested, my synthetic curriculum vitae is included at the end of the dissertation.

Contents

Dissemination of research

Publications in peer-reviewed journals

[1] **Verticchio, E.**, Frasca, F., Bertolin, C., and Siani, A.M. Climate-induced risk for the preservation of paper collections: Comparative study among three historic libraries in Italy. *Building and Environment* **206**, 108394 (2021).

[2] Frasca, F., **Verticchio, E.**, Cornaro C., and Siani, A.M. Performance assessment of hygrothermal modelling for diagnostics and conservation in an Italian historical church. *Building and Environment* **193**, 107672 (2021).

[3] Frasca, F. ,**Verticchio, E.**, Caratelli, A., Bertolin, C., Camuffo, D., and Siani, A.M. A Comprehensive study of the microclimate-induced conservation risks in hypogeal sites. The mithraeum of the Baths of Caracalla (Rome). *Sensors* **20** (11), 3310 (2020).

[4] **Verticchio, E.**, Frasca, F., García-Diego, F.-J., and Siani, A.M. Investigation on the Use of Passive Microclimate Frames in View of the Climate Change Scenario. *Climate* 7 (8), 98 (2019).

Conference papers

[5] **Verticchio, E.**, Frasca, F., Cornaro, C., and Siani, A.M. Investigation on the use of hygrothermal modelling for paper collections. *IOP Conference Series: material science and engineering* **949** (1), 015604 (2020).

[6] Frasca, F., **Verticchio, E.**, Cornaro, C., and Siani, A.M. Optimising Conservation of Artworks, Energy Performance and Thermal Comfort Combining Hygrothermal Dynamic Simulation and On-Site Measurements in Historic Buildings. IBPSA 2019 Conference (2-4 September 2019) (2019).

Other related publications

i. D'Erme, C., **Verticchio, E.**, Frasca, F., Caseri, W., Cornaro, C., Siani, A.M. and Santarelli, M. L. Preliminary study of the mechanical and hygrothermal performance of concrete reinforced with nanofibrillated cellulose. *AIP Conference Proceedings*. **2416**, 020012 (2021).

ii. Siani, A.M., Frasca, F., **Verticchio, E.**, Bile, A., and Fazio, E. Definition of protocols for deployment of sensor node devices III. *H2020 Collection Care* Deliverable number: D4.10 (2021).

iii. García-Castillo, A.M, Mercado, R., Laborda, J., Fuster López, L., Frasca, F., Siani, A.M., and **Verticchio, E.** Training materials for the correct installation, configuration and usage of CollectionCare system. *H2020 Collection Care* Deliverable number: D7.4 (2021).

iv. Siani, A.M., Frasca, F., **Verticchio E.**, Bile, A., Peiró Vitoria, A., Favero G., and Fazio, E. Definition of protocols for deployment of sensor node devices II. *H2020 Collection Care* Deliverable number: D4.9 (2020).

v. Siani, A.M., Frasca, F., **Verticchio E.**, Bile, A., and Fazio, E. Definition of protocols for deployment of sensor node devices I. *H2020 Collection Care* Deliverable number: D4.2 (2020).

vi. **Verticchio, E.** IBPSA Student Modelling Competition. Deliverable Report. (2019).

Conference participation

a. **Verticchio, E.**, Frasca, F., Iafrate, L., Bertolin, C., and Siani, A.M. *An investigation on the climate-induced conservation risks in historic libraries*. Oral presentation at SyMBoL final Conference, 2-3 September 2021.

b. **Verticchio, E.**, Frasca, F., Iafrate, L., Bertolin, C., and Siani, A.M. *Past and future scenarios of conservation conditions of paper collections in three historic libraries in Italy*. Oral presentation at 107^{th} SIF National Congress, 13-17 September 2021.

c. **Verticchio, E.**, Frasca, F., Iafrate, L., and Siani, A.M. *La Biblioteca Meteorologica Storica del CREA al Collegio Romano: analisi critica del microclima al fine della conservazione del suo patrimonio librario*. Poster at AISAM National Congress, 9-12 February 2021.

d. Frasca, F., **Verticchio, E.**,Bile, A., Fazio, E., Favero, G., Grinde, A., and Siani, A.M. *Definition of allowable targets from indoor climate observations in exhibition rooms: the case study of the Rosenborg Castle (Denmark)*. Poster at AISAM National Congress, 9-12 February 2021.

e. Mazzei, G., Frasca, F., **Verticchio, E.**, and Siani, A.M. *Sperimentazione di uno strumento per la misura dell'umidità relativa in ambienti ad elevata umidità*. Poster at AISAM National Congress, 9-12 February 2021.

f. **Verticchio, E.**, Frasca, F., Cornaro, C., and Siani, A.M. *Investigation on the use of hygrothermal modelling for paper collections*. Oral presentation at Heri-Tech Conference, 14-16 October 2020.

g. **Verticchio, E.**, Frasca, F., Iafrate, L., and Siani, A.M. *Preliminary study on the environmental conditions within a scientific historic library in Rome*. Poster at INAF workshop "Preventive conservation in museum, libraries and archives", 16-18 October 2019.

h. **Verticchio, E.**, Frasca, F., Bartolucci, B., Favero, G., and Siani, A.M. *Verso un nuovo rapporto tra microclima e beni culturali nell'ambito della conservazione preventiva: il caso dell'edificio storico di Villa Blanc (Roma)*. Poster at AISAM National Congress, 24-26 September 2019.

i. Frasca, F., **Verticchio, E.**, Grottesi, G., Cornaro, C., Siani, A.M., Botticelli, M., and Maras, A. *Verso un nuovo rapporto tra microclima e beni culturali nell'ambito della conservazione preventiva: il caso di un soffitto ligneo nel Museo Archeologico di Priverno*. Oral presentation at AISAM National Congress, 24-26 September 2019.

j. Siani, A. M., Frasca, F., **Verticchio, E.**, Fazio, E., Perles, A., and Garcia-Diego, F.J. *CollectionCare: Innovative and affordable service for the Preventive Conservation monitoring of individual Cultural Artefacts during display, storage, handling and transport*. Poster at AISAM National Congress, Naples, 24-26 September 2019.

Manuscripts under review

I. **Verticchio, E.**, Frasca, F., Fugaro, D., Cavalieri, P., Teodonio, L., and Siani, A.M. *Conservation risks for paper collections due to the microclimate in the repository of the Alessandrina Library in Rome (Italy)*.

Manuscripts in preparation

I. Frasca, F., **Verticchio, E.**, Merello, P., Zarzo, M., García-Diego, F.-J., Grinde, A. and Siani, A.M. *A multivariate approach for the deployment of the microclimate sensors in museums: a case study*.

List of Figures

CHAPTER 7

List of Tables

Nomenclature

Abbreviations

ANSI	American National Standards Institute
ASHRAE	American Society of Heating, Refrigerating and Air-Conditioning Engineers
BSI	British Standards Institution
CEN	European Committee for Standardization
CMCC	Centro Euro-Mediterraneo sui Cambiamenti Climatici
CMIP	Coupled Model Intercomparison Project
CREA	Consiglio per la Ricerca in Agricoltura e l'Analisi dell'Economia Agraria
D65	CIE standard illuminant for the average midday light in Western Europe
EEs	Elementary Effects
EN	European Norm
EU	European Union
HMWall	Heat and Moisture wall model
HVAC	Heating, Ventilation, and Air Conditioning
IDA ICE	IDA Indoor Climate and Energy
IFLA	International Federation of Library Associations and Institutions
ISO	International Organization for Standardization
LIM	Lowest Isopleth for Mould
MiC	Italian Ministry of Culture
NISO	National Information Standards Organization
PAS	Publicly Available Specification
PD	Portable Document
RHT	Probes measuring T and RH
SA	Sensitivity Analysis
TR	Technical Report
UNI	Italian National Unification Institute
UNESCO	United Nations Educational Scientific and Cultural Organization

Variables and parameters - Greek symbols

A_{ω}	Gain of the building (-)
Γ_d	Adiabatic gradient of vertical temperature for dry air (°C·m^{-1})
Δa*	Colorimetric difference in red and green (-)
Δb*	Colorimetric difference in yellow and blue (-)
ΔE*	Total colorimetric difference (-)
ΔL*	Colorimetric difference in lightness and darkness (-)
ΔMR	Absolute difference between outdoor and indoor mixing ratio (g·kg^{-1})
ΔRH_{24h}	Daily relative humidity fluctuation (%)
ΔT	Vertical temperature gradient (°C)
ΔT_{24h}	Daily temperature fluctuation (°C)
Δz	Vertical distance between probes (m)

Variables and parameters - Greek symbols (continued)

λ	Dry thermal conductivity ($W \cdot m^{-1} \cdot K^{-1}$)
μ	Dry diffusion resistance factor (-)
ρ	Bulk density ($kg \cdot m^{-3}$)
ω	Angular frequency (-)
ϕ	Relative humidity fraction (-)
Φ_ω	Phase shift of the building (-)
Ψ	Weighted function (%)

Variables and parameters - Roman symbols

A_w	Water absorption coefficient ($kg \cdot m^{-2} \cdot s^{-0.5}$)
ACH	Air Changes per Hour (h^{-1})
AER	Air Exchange Rate
C_p	Specific heat capacity ($J \cdot kg^{-1} \cdot K^{-1}$)
CO_2	Carbon dioxide (ppm)
DP	Paper degree of polymerisation (-)
DP0	Initial paper degree of polymerisation (-)
GCM	Global Climate Model
GHI	Global Horizontal Irradiance (-)
k	Rate of paper degradation ($years^{-1}$)
MA	Centred 30-day moving average of RH observations (%)
MET	Metabolic Equivalent of Task (-)
MR	Mixing Ratio ($g \cdot kg^{-1}$)
PDH	Predicted Discomfort Hours (h)
pH	Acidity of paper (-)
RH	Relative Humidity (%)
RH_{30d}	Centred 30-day moving mean of relative humidity (%)
RH_{90d}	Centred 90-day moving mean of relative humidity (%)
RH_{ratio}	RH ratio (%)
s	Thermal conductivity supplement (-)
SHGC	Solar Heat Gain Coefficient (-)
T	Temperature (°C)
T_{24h}	Centred 24-hour moving mean of temperature (°C)
$T_{d,14}$,$T_{d,22}$	Temperature at 14:00 and 22:00 of d^{th} calendar day (°C)
$T_{d,mean}$,$T_{d,max}$	Mean and maximum temperature of d^{th} calendar day (°C)
T-vis	Visible solar transmittance (-)
U-value	Thermal transmittance ($W \cdot m^{-2} \cdot K^{-1}$)
w	Equilibrium water content ($kg \cdot m^{-3}$)
w_{80}	Equilibrium water content at $\phi = 0.8$ ($kg \cdot m^{-3}$)
w_f	Equilibrium water content at saturation ($kg \cdot m^{-3}$)

Indexes

CI	Continuity Index (-)
CoI	Completeness Index (-)
CV-RMSE	Coefficient of the Variation of the Root Mean Square Error (%)
$n_{eggs-laid}$	Number of eggs laid by webbing cloth moths (-)
EL	Expected Lifetime of historic paper (years)
EMC	Equilibrium Moisture Content (%)
LM	Lifetime Multiplier (-)
MAE	Mean Absolute Error
NDR	Normalized Diurnal Range (-)
PI	Preservation Index (-)
r	correlation coefficient (-)
RH_{ratio}	Relative Humidity ratio (%)
RMSE	Root Mean Square Error
SD	Standard Deviation
TWEL	Time Weighted Expected Lifetime (years)
TWPI	Time Weighted Preservation Index (-)

Part I

Background

Chapter 1

Rationale

1.1 Context

The priority to preserve our cultural heritage is promoted worldwide by the *United Nations Educational, Scientific, and Cultural Organization* (UNESCO) [133]. In Italy, it is affirmed in the Legislative Decree D.Lgs. 42/2004 [5] under the auspices of the Constitution, commiting us to study effective preventive conservation strategies to mitigate the potential causes of damage and loss. In this context, caring about cultural heritage must be considered as a duty as well as a valuable long-term investment for all nations [52].

Over the last decades, scientific research has made substantial progress in the knowledge of the materials constituting cultural objects and multidisciplinary studies have allowed a global approach to diagnose conservation issues [70]. Most of the deterioration processes (mechanical, chemical and biological) is driven by the interaction between the objects and the environment [48]. For this reason, the study of microclimate plays a key role to define appropriate strategies to minimise the impact of climate-induced deterioration. The development of risk assessment strategies based on evidence-based studies is advocated to optimise decision-making for preventive conservation [31]. In the times of climate change, new threats have to be faced, as the ongoing global warming may further reduce the durability of the vulnerable objects [35].

Modelling is increasingly adopted as a versatile tool for the diagnosis and prognosis of conservation needs related to the indoor climate [77]. The growing demand for sustainability in the cultural heritage field induced the need to avoid (or at least reduce) the use of invasive and expensive Heating, Ventilation and Air-Conditioning (HVAC) systems [48]. The European standard EN 16883:2017 [14], which provides guidelines for improving the energy performance of historic buildings, encourages the adoption of passive methods to design effective retrofit solutions.

Several projects have lately received funding from the European Union's Horizon 2020 Research and Innovation programme to investigate on heritage science for the preventive conservation and sustainable management of cul-

tural assets [109]. In this framework, CollectionCare *Innovative and affordable service for the Preventive Conservation monitoring of individual Cultural Artefacts during display, storage, handling and transport* (2019-2022) [20] aims to develop an innovative preventive conservation decision support system by integrating environmental monitoring with multi-scale modelling of different heritage materials. A previous European project, Climate for Culture *Damage risk assessment, economic impact and mitigation strategies for sustainable preservation of cultural heritage in the times of climate change* (2009-2014) [6], laid the foundations to assess the possible future impact of the expected climate change on the conservation of historic buildings and their interiors by combining outdoor climate predictions and building simulation models.

Historic libraries

Not many studies have investigated so far the microclimate in historic buildings conserving libraries. Libraries are unique witnesses of the human knowledge over the centuries [150]. Italy has a rich patrimony of libraries [90], among which about one third of those founded before the XX century dates back to XVI-XVIII centuries [88]. Library collections are made of a wide range of organic and inorganic materials, which all undergo an unavoidable ageing process [47]. The different needs of the materials constituting the collections must be prioritised to ensure their long-term preservation through appropriate preventive conservation strategies [44].

The study of historic libraries can be addressed either to the ancient book collections or to the historic building where such collections are conserved. Among the available studies on the microclimate inside historic libraries, only few of them were based on long-term microclimate observations and there is lack of uniformity in the use of modelling and risk assessment methods [158].

Comparative studies are useful to investigate to what extent the differences in the external climate, building features and microclimate control strategies can affect the climate-induced risk for library collections. Moreover, they can provide useful insight into the impact of conditioned (i.e., controlled by HVAC systems [65, 129]) and unconditioned (i.e., natural free-floating [23, 72]) indoor climates within historic libraries.

Integrating the study of microclimate through observations and modelling for the diagnosis and prognosis of the climate-induced conservation risks for library collections [86, 123] enables to improve the potentialities of both the approaches, thus contributing to the definition of rational and sustainable preventive conservation strategies [36].

1.2 Aim of the study

My research focussed on defining an integrated approach to inform and support decision-making for the preventive conservation of historic libraries. To achieve this aim, microclimate observations and modelling have been jointly studied to assess climate-induced deterioration risks.

Three specific objectives were pursued: 1) to gain insight into the microclimate of conditioned and unconditioned historic libraries located in different climate zones in Italy; 2) to assess the capability of whole-building models to simulate the microclimate of historic libraries including the heat and moisture exchanges of hygroscopic library collections; 3) to identify synthetic indexes to characterise the microclimate and assess the climate-induced risks for paper collections which may be informative for conservators and heritage scientists.

Taking advantage of the availability of annual time series of microclimate observations, four historic libraries in Italy (Milan, Udine and Rome) were used as case studies within a comprehensive comparative study.

1.3 Outline

The structure of the thesis is articulated into the following chapters:

Chapter 2 provides an overview on the state-of-the-art about preventive conservation, microclimate analysis and modelling, and climate-induced risk assessment in historic libraries;

Chapter 3 introduces the general workflow of the thesis and presents the four historic libraries in Italy under study (i.e., the CREA Historical Meteorological Library at Collegio Romano in Rome, the repository of the Biblioteca Universitaria Alessandrina in Rome, the Ca' Granda Library in Milan, and the Delfiniana Library in Udine);

Chapter 4 describes the methodology followed, from the on-site microclimate monitoring campaigns to the analysis of collected data, from the approach adopted for modelling library buildings and collections to the dose-response and damage functions applied for the climate-induced risk assessment;

Chapter 5 summarises the results of the microclimate analysis, with particular attention to the thermal buffering capacity of the buildings, the thermal vertical gradients in high-ceilinged libraries, and the RH buffering influenced by the hygroscopic behaviour of the collections;

Chapter 6 presents the main outcomes derived from modelling, focussing on the use of sinusoidal heat and moisture transfer models and dynamic simulation for modelling the hygrothermal conditions inside historic libraries and paper collections;

Chapter 7 outlines the most relevant results obtained from the integration of microclimate observations and simulations for the assessment of the climate-induced risks, also discussing possible alternative mitigation strategies;

Chapter 8 draws the general conclusions and perspectives of the research.

This manuscript also includes seven appendices that provide the supplementary equations and present the relevant articles and conference papers reporting some results of the PhD research (Appendix A–F):

Appendix A provides an approach to comparatively assess the climate-induced deterioration risks for paper collections in historic libraries;

Appendix B proposes a multi-step methodology to investigate the capability of a hygrothermal model as a tool for diagnostic and conservation;

Appendix C investigates the use of a hygrothermal model to simulate the hygroscopic response of paper in steady-state and transient conditions;

Appendix D discusses the moisture buffering of paper inside microclimate frames in view of the climate change scenario;

Appendix E defines an approach to design indoor climate control strategies balancing conservation, energy demand and thermal comfort;

Appendix F presents the results of the assessment of the climate-induced deterioration risks in a library repository.

Chapter 2

State-of-the-art

2.1 Preventive conservation in historic libraries

Preventive conservation includes all the *measures and actions aimed at avoiding or minimizing future damage, deterioration and loss and, consequently any invasive intervention* [16]. Nowadays, preventive conservation is considered as the most cost-effective approach to preservation [112], as it is able to safe around 40–70% of the total maintenance expense by avoiding traditional remedial actions [116].

The microclimate[1] in which the objects are kept greatly affect their preservation, because it influences both cumulative and irreversible ageing and deterioration mechanisms. In the framework of preventive conservation, the study of microclimate allows to better understand the interaction between the materials and the environment, and to study the environmental conditions that may cause damage (Figure 2.1). Over the last decades, the Physics of the Atmosphere and the Material Sciences have made considerable progress on this topic, deriving empirical expressions relating variations in the material properties to the environmental conditions. These dose-response functions are pivotal to investigate past damage and to assess current and future climate-induced deterioration risks for vulnerable collections.

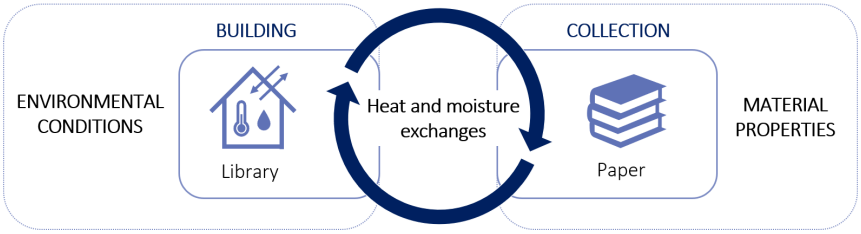

Figure 2.1. Scheme of the climate-induced risk assessment approach based on the study of the interactions between the environment and the heritage materials.

[1] The microclimate is defined as *the synthesis of the ambient physical conditions due to either atmospheric variables or exchanges with other bodies over a period of time representative of all the conditions determined by the natural and artificial forcing factors* [48].

The risk assessment approach entails the *identification, analysis and evaluation of threats that might alter significance, and the probability of their occurrence* [16]. In this way, it allows to prioritise the risks affecting the collections, making it possible to plan more effective strategies of preventive conservation [44] as well as to empower communication of conservation needs in order to gain funding [134]. Disposing of accurate microclimate data is pivotal to obtain a reliable risk assessment [19].

Preventive conservation of historic libraries may be addressed towards both the ancient collections and the buildings themselves (if with cultural value). The term "library" can refer either to a collection of books and other sources of recorded information or to the building where such a collection is conserved. The adjective "historic" underlines the significance of the collections and/or building from the cultural point of view, as opposite to "historical" that can be referred to anything from the past [107].

Within historic libraries, preventive conservation strategies are grounded in a critical balance between preservation and access [131]. Digitization is being increasingly proposed as a way to preserve books thanks to reduced handling [153]. Although broadening dissemination through digital media is unquestionably worthy [17], the current decrease in consultation and loans [114] might reduce investments and supervision of the collections' material conditions. Since digital surrogates cannot fully replace the information carried by the originals, the preservation of physical libraries must remain our priority.

2.2 Standards and guidelines on the microclimate for the conservation of heritage libraries

Over the last decades, the growing need for recommendations to preserve cultural heritage led to the proliferation of official documents on microclimate specifications [2–4, 7, 11–13, 16, 18, 19]. Standards are documents being published by national or international standardisation bodies, whereas guidelines are usually formulated by unions. Table 2.1 summarises some of the international standards and guidelines that can be applied to the case of historic libraries. The Technical Committee TC 346 [73] of the European Committee for Standardization (CEN) has published so far several standards specifying methods, procedures and instruments for accurate measurement of the microclimate and its interactions with materials constituting cultural objects [10].

The earlier standards specified recommendations about the temperature (T) and relative humidity (RH) ranges for various types of materials including paper, parchment and leather [2–4]. Nevertheless, the suggested T and RH ranges for the same classes of materials reported in these standards are sometimes contradictory, thus arising doubts about which indication has to be followed.

TABLE 2.1. Italian and international policy framework on the preservation of cultural heritage including library and archive materials. Remarks' field provides the microclimate specifications indicated in each document.

Document	Institution	Type of document	Remarks
UNI 10586	Italian National Unification Institute (UNI)	Standard	T=14÷20°C, RH=50÷60% (illustrative documents). T=18÷23°C, RH=50÷65% (consultation and reading). Acclimatisation is advised if T and RH in consultation places differ more than ±4°C and ±5% respectively from storage facilities conditions.
UNI 10829	Italian National Unification Institute (UNI)	Standard	T=13÷18°C, RH=50÷60% (archival document and books); T=19÷24°C, RH=45÷55% and ΔT_{24h}=±1.5ºC, ΔRH_{24h}=±6% (book bindings in leather and parchment).
D. lgs. 112/98, art.150, comma 6	Italian Ministry of Cultural Heritage (MIBAC)	Legislative Decree	T=19÷24°C, RH=50÷60% (books and manuscripts). T<21°C, RH = 40÷55% to avoid microbiological attacks on organic materials.
EN 15757	European Committee for Standardization (CEN)	Standard	T = no limits; RH = within safe bands calculated from the historical climate.
ISO 11799	International Organization for Standardization (ISO)	Standard	Recommended T and RH ranges not explicitly specified.
IFLA - Principles for the Care and Handling of Library materials	International Federation of Library Associations and Institutions (IFLA)	Guidelines	T<10°C to favour paper chemical stability and physical appearance; RH=50÷65% to minimise mechanical damage (while reducing the risk of biological attacks).
BS 4971	British Standards Institution (BSI)	Standard	T=13÷23°C, with annual average T<18°C; RH=35÷60% (mixed archives).
EN 16893	European Committee for Standardization (CEN)	Standard	Tables on the relative risk of damage and deterioration due to T and RH [26] as a function of the sensitivity to hydrolysis (rag paper = low; wood pulp paper = medium) are reported as an informative appendix.
ISO/TR 19815	International Organization for Standardization (ISO)	Standard	Tables on the relative risk of damage and deterioration due to T and RH [26] as a function of the sensitivity to hydrolysis (rag paper = low; wood pulp paper = medium) are reported as an informative appendix.
ASHRAE Handbook—Chapter 24	American Society of Heating, Refrigerating and Air-Conditioning Engineers (ASHRAE)	Guidelines	Class B is the reference for historic buildings (no risk to most books): T ≤ 30ºC, RH = 30÷70%, seasonal adjustment from annual average T+10ºC, T-20°C) and RH±10%, short-term fluctuations T±5ºC, RH±10%.

The introduction of the concepts of "proofed fluctuations" [111] and "historical climate" [7] led to more flexible T and RH ranges with respect to the target values previously recommended as satisfactory to mitigate mechanical risks for organic hygroscopic materials. As a result of the above concepts and of the advances in the research on damage functions for heritage science [146], the standards have evolved along different paths: ISO (International Organization for Standardization) and BSI (British Standards Institution) updated their documents with new specifications [11, 13, 16], while UNI (Ente Italiano di

Normazione) has not changed yet the original version of the norms [2, 3]. The ASHRAE (American Society of Heating, Refrigerating and Air-Conditioning Engineers) handbook, since the version published in 2003, introduced museum climate classes without prescriptive T and RH specifications [111]. These guidelines have been extensively adopted for both environmental design and risk management in museums, galleries, archives and libraries.

In the last years, EN 16893 [16], ISO/TR 19815 [18] and the updated ASHRAE guidelines [19] focused on sustainability and greater flexibility in the climate control strategy by adopting risk management principles. Although EN 16893 [16] gives useful recommendations for buildings intended for the storage and use of heritage collections (including reading rooms), no European standards exist by CEN/TC 346, which specifically deals with the conservation in libraries and archives.

2.3 Microclimate monitoring studies within libraries

A survey was conducted using the Scopus database to obtain an overview on the microclimate monitoring studies within libraries (Figure 2.2). Over the last 30 years, the interest of the scientific community on the study of the microclimate for the conservation of libraries and archives has been increasingly growing, with more than five-hundred publications reported since 1991 (Figure 2.2a) among articles, books, conference papers and reviews. However, it is worth to notice that only less than 10% of the total publications dealt with the specific reality of libraries and archives (Figure 2.2b), highlighting that the topic still needs to be further investigated.

In Italy, microclimate studies were conducted in prestigious historic libraries as the Malatestiana (Cesena) [72], Palatina (Parma) [123] and Classense (Ravenna) [23]. Among the microclimate monitoring studies within historic libraries, a significant variability can be observed in the length of the monitoring period as well as in the policy framework adopted for microclimate analysis and, more in general, in the methods followed for damage risk assessment [158]. The T and RH ranges recommended by the standards and guidelines summarised in Table 2.1 have been frequently used as threshold values to evaluate the quality of the environmental conditions for the conservation of library materials [23, 72, 123]. Sedlbauer spore germination isopleths and fungal growth curves have been employed in [138, 141] to evaluate the biological risk for collections. In terms of chemical deterioration, synthetic indexes - such as the equivalent Lifetime Multiplier (eLM) and the Time Weighted Preservation Index (TWPI) - have been used in [141] and [152] to account for an average risk over the monitored period.

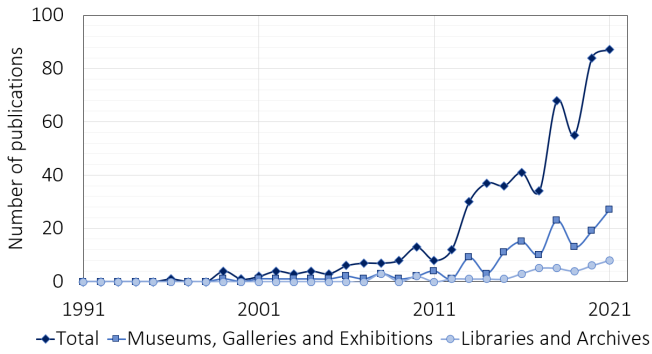

(A) Number of scientific publications per year

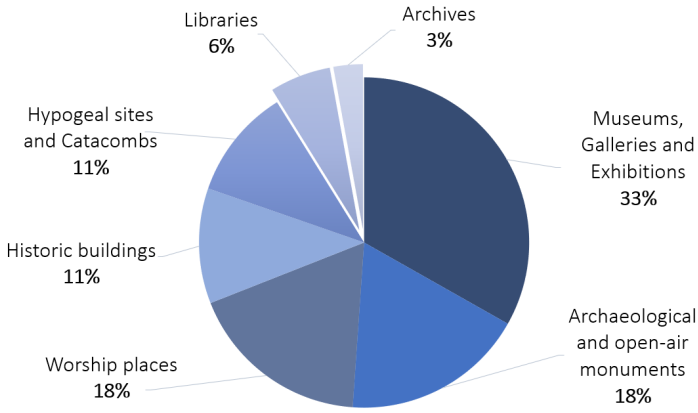

(B) Types of cultural site involved in the studies

FIGURE 2.2. Survey on scientific publications about microclimate for cultural heritage conservation. Data retrieved from Scopus (last update October 2021) by using the words: ("indoor climate" OR "microclimate") AND cultural heritage AND conservation".

A synthetic overview on the indoor microclimate monitoring studies in historic libraries conducted over the last 20 years is provided in Appendix A.

2.4 MICROCLIMATE MODELLING IN HISTORIC LIBRARIES

Historical buildings represent a considerable amount of the total architectural monuments in Italy [91]. Preserving the cultural value of these buildings and their interiors requires a thorough understanding of the indoor climate and of the object-environment and building-environment interactions, which are influenced by the local climate, the features of the building envelope and the management of the site [80, 104].

In the last decades, the use of mathematical models has attracted a broad interest in the scientific community as a method to diagnose conservation conditions and to study the suitability of retrofit measures in historical buildings [46, 159]. A simplified approach in indoor climate modelling is the use of transfer functions that derive the indoor hygrothermal conditions from the outdoor climate [37, 50]. A more powerful tool is the whole-building dynamic simulation (Figure 2.3), which can provide both energy and hygrothermal assessment [63]. The capability of these tools to predict the indoor microclimate offers the chance to investigate mitigation strategies of the climate-induced damages [28, 75] and to design retrofit solutions that concurrently fulfill different needs, e.g., the reduction of energy consumption and occupants' discomfort along with the mitigation of climate-induced deterioration risks [78, 140].

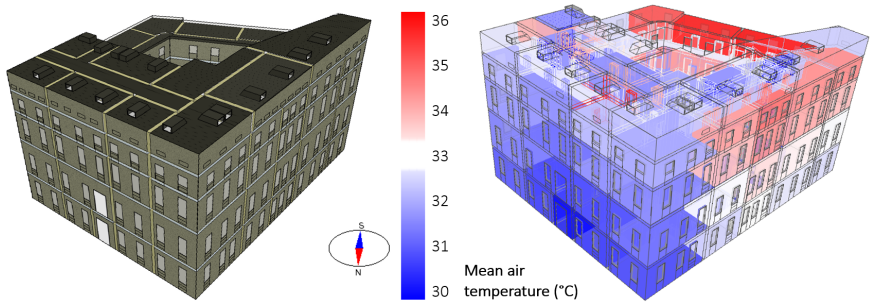

FIGURE 2.3. Example of the use of whole-building dynamic simulation to study the distribution of temperature inside a historical building [155]

Some Building Energy Simulation (BES) tools integrate heat and moisture transfer equations using Heat, Air and Moisture (HAM) models. The hygrothermal modelling of historical buildings can be problematic, as ancient construction techniques and materials are frequently not fully known (e.g., they may be rebuilt many times, the properties of aged materials may have changed [137]), resulting in a high risk of modelling errors [58]. In the hygrothermal modelling of historical buildings, Akkurt et al. [22] identified four sources of uncertainties: a) the geometrical model, b) the thermo-physical properties of the envelope, c) the schedules of internal gains and occupancy and d) the outdoor climate data. For this reason, a necessary prerequisite to reliably use these tools for risk assessment is to verify their accuracy in the simulation of the time behaviour of the key hygrothermal variables (e.g., temperature and relative humidity) responsible for climate-induced deterioration [80]. Increasing precision in the determination of internal gains (e.g., electronic supplies and occupants) may result to be mostly negligible on the simulation output [137].

In modelling the environmental conditions within library and archival repositories, it is fundamental to include the analysis of the hygrothermal in-

teractions between the building and its hygroscopic content (i.e. the paper collections). Indeed, hygroscopic materials, which continuously exchange moisture with their surrounding environment, can act as buffers on RH fluctuations [67]. The moisture buffering behaviour of paper collections is usually simplified by using the effective moisture capacity approach, where the moisture buffering capacity of the indoor air is integrated with that of the books [68]. However, the hygrothermal response of cellulose-based objects can be more effectively modelled by means of tools commonly used for the simulation of the simultaneous heat and moisture transfer through porous envelope materials such as those of the HAM-family [93, 99, 129, 144]. In the simulation of moisture buffering effects, the HAM models are indicated as the most appropriate to account for moisture exchange in hygroscopic materials [22].

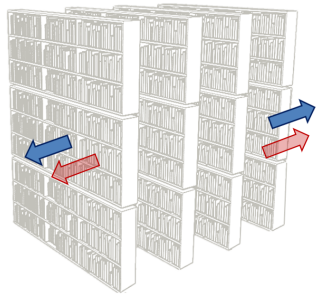

FIGURE 2.4. Heat and moisture exchanges through library collections can be modelled as hygrothermal walls having assigned the material properties of paper.

Steeman et al. [144] used a HAM model to simulate the hygrothermal conditions within a library repository and found the obtained results to be more accurate and reliable with respect to those obtained with simplified approaches. More recently, Kupczak et al. [99] have proposed a way to model the water vapour diffusion in 3-D objects using 1-D moisture transport equations so that the buffering effects of paper collections can be integrated. In Kompatscher et al. [93], the archival collections are modelled as internal walls (Figure 2.4) having assigned the material properties of paper based on literature studies. It has to be noticed that none of these studies provided an in-depth investigation on the uncertainties to be associated with the simulation outputs. Furthermore, most of them focussed on the impact of the RH stabilization in terms of energy savings [99] and in the design of the air-conditioning systems [144] rather than on the implications on the conservation of paper collections.

2.5 Climate-induced risk assessment to library collections

Library materials

All library materials undergo an unavoidable ageing process, with a rate of decay which is dependent on the properties of the constituent materials (e.g., acidity of paper and physical strength) and is greatly affected by the indoor climate [108]. Traditional materials include media such as paper, leather, parchment, cloth and wax.

Paper is usually the most widely occurring material in libraries as it has been extensively used since its diffusion from the XI-XII century in the Mediterranean region [40]. Paper usually appears in the form of thin sheets made from fibrous plant materials containing cellulose. Cellulose is a natural polymer forming long chains (i.e., fibres), which are subject hydrolysis catalysed by acid compounds, light and adequate thermo-hygrometric conditions.

Paper can be classified into three main types: rag paper, acidic paper and contemporary paper. Paper made from linen and cotton rags has long fibres and generally contains few additives, making it a high-quality and resistant paper type. Since the 19th century, the growing demand for printing media led to the introduction of the machine-made paper, having shorter wood fibres and possibly containing lignin and acidic chemical, making it a poor-quality and acidic paper type. Contemporary paper, made from highly processed wood pulp, is usually comparable to rag paper in durability thanks to its alkaline reserves. It follows that each paper type is characterised by different average acidity (pH) and degree of polymerisation (DP) [149], as shown in Table 2.2.

Table 2.2. Average acidity (pH) and degree of polymerisation (DP) of common paper types according to [66].

Paper type	pH	DP
Rag	6.4	1481.2
Acidic	5.2	826.3
Contemporary	7.6	1526.2

Hygroscopic collections are known to stabilise air relative humidity fluctuations [99]. The RH buffering can be observed both at smaller scale (e.g., in sealed boxes containing paper [156]) and inside libraries through microclimate analysis [158] and hygrothermal simulation [144]. Since hygroscopic materials respond with a certain delay to the environmental humidity changes, when performing the assessment of the climate-induced risks, the response time of the objects [106] has to be taken into account in order to correctly evaluate the conditions to which they are equilibrated.

The main causes of paper deterioration are the intrinsic instability due to

the production process, inadequate environmental conditions and improper handling. Table 2.3 summarises mechanical and chemical risks for library materials as reported in the ASHRAE guidelines [19]. Although the sensitivity of most paper-based books can be considered low, materials frequently used in book bindings such as vellum, wood, parchment and leather are moderately sensitive to RH fluctuations. It is worth to notice that these materials, if weakened due to ageing or UV exposure, become highly vulnerable to mechanical risks. In terms of chemical stability, wood, parchment and leather are safe, while acidic paper and natural materials acidified have low stability.

Table 2.3. Mechanical and chemical risks for objects that can be found in library collections (extract from ASHRAE guidelines [19], Tables 3 and 5). Sensitivity to mechanical deterioration refers to unproofed objects assuming they can fully respond to RH fluctuations based on their response time.

Mechanical deterioration	
Low sensitivity	Most case-bound books Most single sheets of paper
Medium sensitivity	Book bindings of vellum and/or wood Gilded parchment, leather Most photographs, films and magnetic records
High sensitivity	Thick images on parchment Objects listed as medium sensitivity that have weakened because of UV exposure or ageing already causing flaking
Very high sensitivity	Large paper sheets adhered to stretchers
Chemical deterioration	
High stability	Wood, glue, linen, cotton, leather, rag paper, parchment
Medium stability	Stable photographic materials
Low stability	Acidic paper (e.g., newsprint, low-quality books) Natural materials acidified
Very low stability	Typical magnetic media Least-stable photographic materials

Digital platforms, such as HERIe [1, 94] and Collection Demography app [66], are freely available for conservation professionals and decision makers to easily and effectively carry out the quantitative assessment of the climate-induced risks for paper collections based on the prevailing environmental conditions where the objects are displayed or stored.

Mechanical deterioration

Library collections are mostly composed of hygroscopic organic materials, which continuously exchange moisture with the surrounding air [68]. Since materials such as paper can shrink/swell as they lose/gain moisture, differential dimensional changes can lead to deformation [41] and tensile stresses [48].

Temperature and relative humidity fluctuations might accelerate historical paper degradation [105], as they can increase the risk of tears in restrained and/or layered objects made in materials having different dimensional response [42]. However, a consensus on the influence of hygrothermal fluctuations on historic paper degradation has not been reached yet among researchers [108].

Handling is the main responsible for the accumulation of wear and tears of paper. The time required for a library collection to become unfit for use by readers due to the combined effect of handling and cellulose hydrolysis can be estimated through a dose-response function [147] that depends on the percentages of paper types constituting the collection (i.e., its demography).

Chemical deterioration

Cellulose hydrolysis represents the main concern for damage risk of paper collections, being the rate of chemical degradation mainly driven by temperature. This deterioration mechanism has been studied by using the dose-response functions, such as the Lifetime Multiplier (LM) for varnishes and cellulose [110] and the Preservation Index (PI) for organic materials (e.g. paper, textiles, leather) [118]. Strlič et al. [148] derived the isochrones for historic paper (i.e., curve of equal expected lifetime), based on a damage function which relates the loss of degree of polymerisation with the acidity of paper and the indoor temperature and relative humidity at the reference conditions of dark storage (i.e., without considering natural and artificial light). The damage function for historic paper [148] was effectively used in [60] for the estimation of the collection expected lifetimes in various conservation scenarios.

Pollutants do not generally represent a significant threat to the overall rate of chemical degradation, as their concentrations are small (e.g., acetic acid<250 $g \cdot m^{-3}$; formic acid<35 $g \cdot m^{-3}$; nitrogen dioxide<15 $g \cdot m^{-3}$; ozone<25 $g \cdot m^{-3}$; sulphur dioxide< 3 $g \cdot m^{-3}$ [23, 101]) and their effect on historic paper preservation is limited [108]. Dust particles can affect paper conservation in terms of cellulose degree of polymerisation, thus increasing the vulnerability of paper to the other environmental parameters [29].

Biological deterioration

In museum contexts, the biological agents more interfering with conservation are usually moulds, as spores are ubiquitous and their spread is hard to control. Fungal spores may become a biological risk when RH>65% for a sufficient period of time. This risk is frequently assessed using the Sedlbauer isopleths for spore germination and mould growth for biologically recyclable materials [96], which defines combinations of minimum temperature and relative humidity that favour their proliferation.

Insects have rapidly spread over the last decades in conservation institutions probably due to global warming and the banning of some pesticides [56]. The most dangerous insects in libraries are beetles, weevils and termites; however, the most common are silverfish and booklice [124]. Insects are favoured by the presence of dust and mould, and are mostly temperature-dependent.

Photodeterioration

Visible light, and particularly UV radiation if not filtered out [142], can accelerate embrittlement to poor-quality paper and colour fading to most of dyes, inks and colourants [108]. Colorimetry is frequently used in the field of conservation to objectively assess colour changes that may reduce the aesthetic value of books and documents and, in the worst cases, their readability.

2.6 Sustainability in microclimate control strategies

Preventive conservation strategies for cultural heritage collections should support preservation in an economically and environmentally sustainable way. To this aim, in the latest release of the ASHRAE Chapter dedicated to Museum, Galleries, Archives and Libraries [19], it was recommended the design of performance targets being proportionate to the effective hygrothermal loads associated with the specific climate zone. Among the obstacles in the transition towards sustainability in libraries, the major one is likely the lack of a common framework for estimating emission and sustainability policy [92]. A method for sustainable lighting, preventive conservation, energy design and lighting in a historical church converted into a library was recently proposed in [27].

Energy consumption in libraries can be high due to the need for lighting, heating and air conditioning. As an example of a large modern building, the British Library in London (United Kingdom) reported a total of 30 MWh in the period 2020/2021 [100]. In accordance to the international call for reducing energy use [8, 15], various green building rating system have been developed, such as the LEED (Leadership in Energy and Environmental Design) and BREEAMS (Building Research Establishment Environmental Assessment Method) [59]. Although newly built libraries are frequently designed to comply with the requirements of sustainability, this target is rarely achieved by existing ones, especially if housed in historical buildings.

In view of the expected climate change, we must consider that the present energy loads will likely increase. In the study of Hong [84], hygrothermal simulations were used to propose climate change mitigation strategies for mechanically controlled repositories in The National Archives, Kew (London, UK). The research highlighted that, although less energy will be necessary for

winter heating, an increase in total energy load is predicted in 2050 and 2080 due to higher cooling requirements (Figure 2.5).

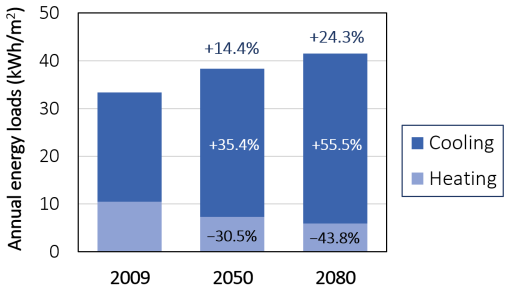

FIGURE 2.5. Heating and cooling energy loads under the present (2009) and future climate scenarios at The National Archives, Kew in London (UK). The reported percent change was calculated in comparison to 2009 baseline [84].

Passive solutions should be preferred whenever possible for the indoor climate control. Examples of passive solutions for historic libraries are, on a small scale, the use of enclosures and boxes for items needing special care (to a certain extent similar to the microclimate frames used for paintings [81, 156]) and, on a large scale, passive retrofit interventions to the building envelopes [127]. If only active solutions are feasible, it has to be borne in mind that even slight refinements in the climate management (e.g., allowing for intermittent use of the HVAC systems [27, 93]) can lead to a significant reduction of energy consumption [44].

FIGURE 2.6. The first cool and passive storage for the National Archives in Krakow designed to be a passive building that will use 15 times less energy compared to other facilities of this type in Poland. Source: Cultural Heritage Research Group

The compelling need to reduce energy costs and to face the impact of the expected climate change led to the design of passive storage facilities (Figure 2.6).

In these low-energy repositories, temperature control is effectively obtained through a combination of thermal insulation and air-tightness of the building and heat capacity of the underlying ground [121, 135]. Compared to traditional library and archival storage facilities, semi-passive solutions can reduce the energy consumption per year up to 1.1 kWh/m^3 in comparison to a modern facility relying on HVAC systems (67 kWh/m^3) [143].

Part II

Methodology

Chapter 3

Workflow and case studies

3.1 Workflow

The approach followed in this thesis integrated the study of microclimate observations and modelling for the assessment of the associated climate-induced risks inside historic libraries (Figure 3.1).

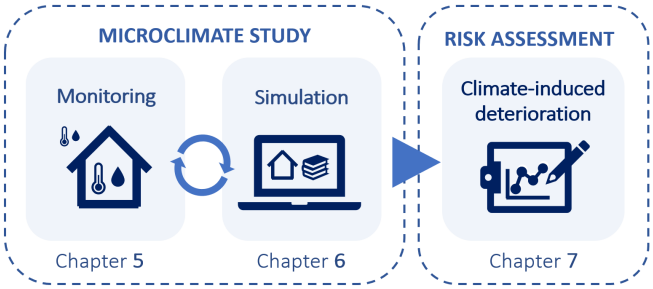

Figure 3.1. Workflow of the integrated approached followed in the thesis for the climate-induced risk assessment within historic libraries.

The microclimate study aimed at investigating the interactions between the building environment and the hygroscopic collections (Chapter 5). The modelling of both paper collections and whole buildings was used to simulate the conditions inside the libraries (Chapter 6). Finally, a comprehensive risk assessment including mechanical, chemical, biological and light-induced deterioration mechanisms was carried out to evaluate the impact of conditioned and unconditioned microclimates on paper collections as well as to explore the effectiveness of possible retrofit strategies (Chapter 7).

The integrated approach was applied to four historic libraries in Italy (Figure 3.2). The libraries are associated with different temperate climate zones corresponding to the Köppen-Geiger classes [30]: Csa (dry and hot summer) in Rome [69], Cfa (fully humid with hot summer) in Milan and Cfb (fully humid with warm summer) in Udine. In Collegio Romano and Alessandrina, Heating, Ventilation and Air Conditioning (HVAC) systems were used, whereas Ca' Granda and Delfiniana had natural free-floating climates.

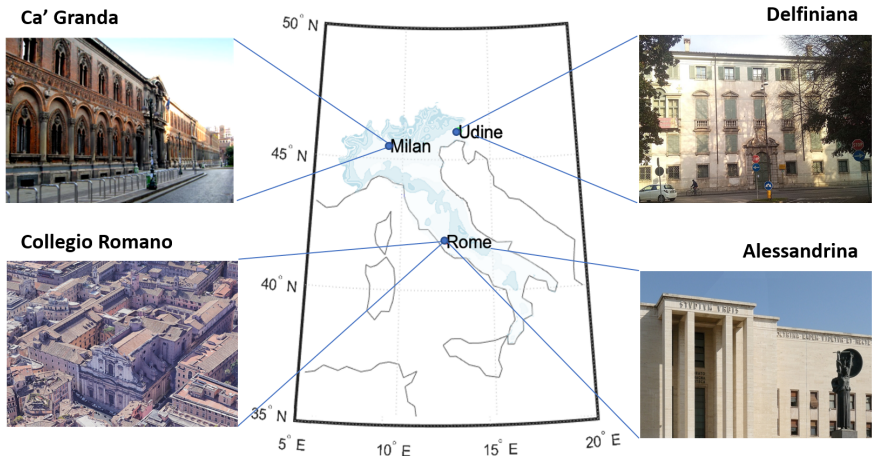

Figure 3.2. The geographical position of the historic libraries under study (Italy): the CREA Meteorological Library and the Alessandrina Library repository in Rome, the Ca' Granda Archive in Milan, and the Delfiniana Library in Udine.

3.2 CREA Meteorological Library (Rome)

The CREA Historical Meteorological Library in the monumental complex of Collegio Romano (Rome, Lat. 41.9°N and Long. 12.5°E, 21 m a.m.s.l.), hereafter called simply Collegio Romano, is considered as the most important collection in Italy devoted to Atmospheric Sciences, Meteorology and Geophysics of the Modern Age. Although its original nucleus, gathered by Jesuits, dates back to the foundation of the building (1584), the current location on the fourth floor of the building was elected in 1879, after the establishment of the first Central Meteorological Office in Italy (currently an important sector of CREA, the leading Italian research organization dedicated to the agri-food supply chains). The collection includes several national and international periodicals published by scientific societies, CREA's interesting publications and original books and manuscripts, mostly from the XIX century [32, 33].

Building Collegio Romano is a monumental masonry construction, with an approximately overall plant of 14300 m^2 deployed on more than four levels. The construction started at the end of the XVI century, under Gregorio XIII papacy. The building currently houses the headquarters of the Italian Ministry of Culture (MiC) and the Liceo Statale Ennio Quirino Visconti and it adjoins the baroque church of St. Ignatius of Loyola at Campus Martius. The library has a 4.5 m high ceiling and a small volume, with a wooden roof and four SW-W-facing windows on two orders.

Figure 3.3. CREA Meteorological Library at Collegio Romano in Rome.

The library is naturally ventilated and heated by cast iron radiators from November 1st to April 15th (operating from 6 a.m. to 6 p.m. local time) and cooled through fan-coils (switched on when needed).

Collection The library collection is mostly made of mid-19th–mid-20th century paper of Western origin (lignin containing, rosin sized, printed and non-coated). The percentage of paper types constituting the collections, as estimated on private communication with the library conservator, is: 96% acidic, 1% contemporary and 3% rag paper.

3.3 Alessandrina Library repository (Rome)

The Alessandrina library (Rome, Lat. 41.9°N and Long. 12.5°E, 21 m a.m.s.l.) is considered one of the most important university libraries in Italy, also being among the 46 prestigious public libraries belonging to the Italian Ministry of Culture [114]. The Library was founded in 1667 by pope Alexander VII Chigi as the library of the *Studium Urbis* (i.e., the University of Rome). Originally housed in the Roman Baroque church of Sant'Ivo alla Sapienza designed by the architect Francesco Borromini (1642-1660), its historical nucleus comprised duplicates from the Chigiana Library, the Vatican Library and the valuable library of the Dukes of Urbino. From 1935, the Alessandrina Library was relocated in the newly built Sapienza University Campus, acquiring the pre-existent libraries of the Faculties of Humanities, Law, Political Science and

important donations. Nowadays, the Library was elected as the legal repository for all the documents of cultural interest destined to public use and published by editors from the province of Rome. High-resolution pictures and metadata of some of the most valuable documents belonging to the Alessandrina collection are publicly available on the web through digitisation [17].

Figure 3.4. Alessandrina Library repository in Rome.

Building The Alessandrina library is housed on the upper floors (from third to fifth) of the Rectorate building, in the hearth of Sapienza University Campus in Rome. The repository (Figure 3.4) has a total volume of more than 4000 m^3, with floors having ceilings 2.2 m high and surfaces more than 500 m^2 wide. Windows are located on both the E and W walls of the repository and have simple glass panes with UV-filters, which however are severely deteriorated. The large E-oriented windows are exposed to direct natural light during the morning hours and have a total area of approximately 85 m^2. These windows are mostly closed during the year. The W-oriented windows, shaded under the prostyle of the Rectorate building, have a total area of approximately 30 m^2. These windows are frequently open during the warmer months. The repository is naturally ventilated and is equipped with fan-coils for both heating and cooling. However, the air-conditioning system is old and scarcely effective in controlling temperature over the year.

Collection The library collection includes two major assets associated with different periods of production: the Ancient collection, deployed on three floors

in the S-oriented part of the repository, and the Modern collection, which occupies most of the repository space. Paper is the most represented material among both the Ancient and the Modern collection assets. According to private communications with the Director of the Library, the Ancient collection is mainly made in paper produced from XVI to XIX century and around 3% in parchment, while the Modern collection is mostly made of XX-XXI century paper, with small amounts of cardboard, plastics and canvas.

3.4 Ca' Granda Library (Milan)

The library is hosted in the Ca' Granda Ospedale Maggiore Policlinico (Milan, Lat. 45.5°N and Long. 9.2°E, 120 m a.m.s.l.). The library and archival collections of the IRCC Foundation (Istituto di Ricovero e Cura a Carattere Scientifico) represents a national unicum in terms of richness and specialisation on medical sciences, with a patrimony estimated in about 100.000 printed volumes among monographies, periodicals and magazines from XV to XX century [54].

Figure 3.5. Ca' Granda Library in Milan. Copyright: M. Balsamini. Source: I tesori della Ca' Granda

Building Ca' Granda has a large volume (approximately 2100 m^3), with rectangular shape and high ceiling (up to 12 m). The beautiful room of the "Capitolo d'estate" was built in 1637, during the enlargement interventions of the ancient hospital complex. The room is covered by a wooden roof and has SW-W-facing windows on two orders with simple glass panes and wooden shadings, which are closed most of time during the year. During the microclimate monitoring campaigns, Ca' Granda had no HVAC (Heating, Ventilation and Air-Conditioning) system.

Collection The history of the collection dates back to the foundation of the Hospital (1456), but the main core is from the XIX century and it is continuously updated thanks to private donations. Although the collection conserved in "Capitolo d'estate" is mostly composed of archival documents, Ca' Granda was here studied among libraries due to its specific architectural features and use. The collection is deployed in a three-level wooden shelf on the perimeter of a room at the ground floor (Figure 3.5). The percentage of paper types constituting the collections, as estimated on private communication with the library conservator, is: 90% acidic, 8% contemporary and 2% rag paper.

3.5 Delfiniana Library (Udine)

Figure 3.6. Delfiniana Library in Udine. Source: Wikimedia Commons

The Library of the Archbishop's Palace (Udine, Lat. 46.1°N and Long. 13.2°E, 113 m a.m.s.l.) was named "Delfiniana" after his founder, Dionisio Delfino, which was the patriarch of the diocese of Aquileia from 1699 to 1734 [125]. The foundation of the library dates back to 1708, when the patriarch commissioned the construction of its building, to be donated to eternal public utility. The library is nowadays part of the touristic itinerary of the Diocesan Museum of Udine.

Building Delfiniana has similar features as Ca' Granda, but smaller dimensions (approximately 1150 m^3). New air-tight windows with UV-IR-filtered glass were mounted in May 2017 in place of the previous single panes [34]. During the microclimate monitoring campaigns, Delfiniana had no HVAC (Heating, Ventilation and Air-Conditioning) system.

Collection The collection comprises printed volumes, manuscripts (dated from XVI to XIX century) and some illuminated liturgical codices (dated from IX to XIV century). It is organised in a two-level wooden shelf deployed on the perimeter of a hall at the second floor of the patriarchal palace (Figure 3.6). According to private communications with the conservators of the library, the main core of the collection is however mostly made of mid-19th–mid-20th century paper of Western origin (lignin containing, rosin sized, printed and non-coated).

Chapter 4

Materials and methods

4.1 Microclimate study

4.1.1 On-site monitoring campaigns

The position of the thermo-hygrometers (hereafter called as RHT) installed in each library to measure temperature (T) and relative humidity (RH) is sketched in Figure 4.1. In Collegio Romano, two RHT probes were positioned on the shelves leaning against the wall opposite to the windows. In Alessandrina, six RHT probes were deployed at 1.7 m above the floor of each of the three levels constituting the repository. In Ca' Granda and Delfiniana, where ceilings are high, two RHT probes were deployed at different heights (1.5 m and 6.5 m above the floor) to monitor vertical temperature gradients [130].

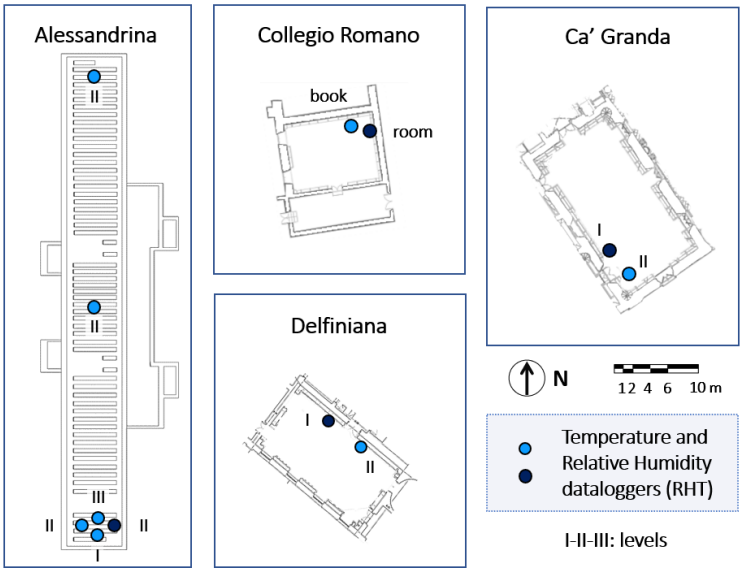

Figure 4.1. Deployment of the microclimate probes in the monitoring campaigns. Darker blue points indicate the position of the sensors whose data were used in the following analysis.

In Collegio Romano, one RHT probe was placed on a shelf and the other one inside a mock-up book on the same shelf with the aim to derive the book response time, i.e., the lag between the RH values measured inside the book with respect to those collected in the room. The mock-up book (250 mm × 180 mm × 28 mm) was made using modern rag paper sheets, with cardboard covers and leather spine (Figure 4.2). An extra probe (HOBO® U12-012 Data Logger) measuring light intensity and carbon dioxide (CO_2) concentrations was also used from June 2019 to June 2020 to estimate the air change rate (ACH) and to infer the space management in terms of the opening of windows and shadings.

Figure 4.2. Thermo-hygrometer placed inside a mock-up book made in cellulose paper and put on a shelf in the Collegio Romano library.

The indoor climate monitoring campaigns to study the hygrothermal behaviour of the four libraries covered different periods (Table 4.1), as they were independently planned. The metrological features of the indoor T sensors (Pt100 resistance thermometers) and RH sensors (thin film capacitive sensors), reported in Table 4.1, were in accordance with the current European Standards on the instruments to be used in cultural heritage conservation [7, 9]. The choice of the instruments was limited due to technical and financial reasons. Hence, it was not possible to measure more environmental variables nor to dispose of a higher number of sensors in order to increase the monitoring representativeness.

4.1.2 Analysis of collected data

The long time series of temperature and relative humidity measurements collected in the four case studies underwent a quality control in terms of the Completeness Index (CoI) and the Continuity Index (CI) [76]. In this way, the time intervals having the highest scores of CoI=1 and CI=1 were selected (Table 4.1) to carry out the microclimate study presented in Chapter 5.

The buffering capacity of the building envelopes to smooth out the maximum outdoor temperatures occurring in daylight hours was evaluated using

TABLE 4.1. Microclimate monitoring campaigns in the four case studies.

Library	City	Monitoring period	Instrument (uncertainty)	Sampling frequency	Outdoor climate	Analysed period
Alessandrina	Rome	Jul 2019 – Jul 2021	Rotronic®, model HygroLog (0.3°C for T, 0.8% for RH)	15 min	Climate Network Weather station (Lat. 41.9° N and Long. 12.5° E)	1st Jan 2020 – 31st Dec 2020
Collegio Romano	Rome	Jun 2019 – ongoing	Rotronic®, model HC2A-S3 (0.3°C for T, 1.5% for RH)	10 min*	CREA Weather station (Lat. 41.9° N and Long. 12.5° E)	1st Jun 2020 – 31st May 2021
Ca' Granda	Milan	Sep 2011 – Jan 2013	Comet®, model R3121 (0.4°C for T, 2.5% for RH)	15 min	ARPA Weather station (Lat. 45.5°N and Long. 9.2°E)	1st Jan 2012 – 31st Dec 2012
Delfiniana	Udine	Oct 2016 – Mar 2018	Testo®, model 175H1 (0.4°C for T, 2% for RH)	15 min	ARPA Weather station (Lat. 46.1°N and Long. 13.2°E)	1st Jan 2017 – 31st Dec 2017

*recorded every 30 min as averaged values

the Normalized Diurnal Range (NDR). NDR is an index defined in [51] as the ratio between the observed diurnal indoor temperature range (calculated as the difference between the temperatures at 14:00 ($T_{d,14}$) and 22:00 ($T_{d,22}$) of dth calendar day) in the monitored period (MP) with respect to the average reference period (RP). $T_{d,14}$ and $T_{d,22}$ were chosen as they are close to the outdoor diurnal maximum and mean temperatures, respectively. The outdoor temperatures in the 1991–2020 reference period were extracted from the E-OBS v23.1e [64] gridded observational dataset (spatial resolution of 0.1° x 0.25°) via the Climate Data Store (CDS) infrastructure. As E-OBS v23.1e does not include hourly data, the daily maximum temperature ($T_{d,max}$) and the daily mean temperature ($T_{d,mean}$) in the reference period were extracted and used in the place of $T_{d,14}$ and $T_{d,22}$ [51]. The formulation of NDR was adjusted to enhance its capability to sense the active climate control [158] and calculated in each site as follows:

$$NDR = \frac{(T_{d,14} - T_{d,22})_{MP}}{\frac{(T_{d,max} - T_{d,mean})_{RP}}{n_{RP}}} \tag{4.1}$$

where n_{RP} is the total number of days in the reference period (i.e. 30 years). When NDR is around zero, the building has a high thermal buffering capacity and low ventilation, while if NDR is close to unity, the indoor and outdoor temperatures are practically identical. The latter condition can be experienced when there is a persistence of sufficient ventilation due, for example, to windows' opening. Negative NDR occur mainly in summer, when the indoor evening temperatures register the effect of the highest outdoor temperature

values with a certain delay. Since the NDR value results from the combined effect of building envelope, solar exposure, room ventilation and use [51], this index is not able to distinguish among their individual contributions.

The thermal vertical gradients ($\Delta T/\Delta z$) in the high-ceilinged libraries were compared with the adiabatic gradient of vertical temperature for dry air (Γ_d=0.1°C/10m). In Alessandrina, the thermal vertical gradient was calculated as the difference between the T values collected at 1.7 m above the floor on the upper (III) and the lower (I) levels of the repository, where level III is distant approximately 4.5 m from level I along the vertical direction. In Ca' Granda and Delfiniana, $\Delta T/\Delta z$ was computed as the difference between T values collected at levels II and I (Figure 4.1), distant approximately 5 m along the vertical direction.

The air change rate per hour (ACH) in Collegio Romano was estimated from the monitored concentration values of the CO_2 by fitting a decay curve to the gas concentration peaks (e.g., after prolonged presence of people in the room) [61]. The ACH was obtained by applying the following equation [58]:

$$ACH = -ln\left(\frac{c_{\text{int,t}} - c_{\text{ext}}}{c_{\text{int,0}} - c_{\text{ext}}}\right) \cdot \frac{1}{t} \tag{4.2}$$

where $c_{\text{int,t}}$ is the internal gas concentration at the end of the slope (in ppm), $c_{\text{int,0}}$ the internal gas concentration at the beginning of the slope (in ppm), c_{ext} is the external gas concentration (in ppm) and t is time. As only the indoor CO_2 concentration was monitored, the outdoor gas concentration was approximated as the indoor CO_2 concentration corresponding to the steady state reached some time after people had left, following the same approach used in [58].

MR values were derived from T and RH observations using the formula given in Supplementary equations. The differences between simultaneous outdoor and indoor MR values (ΔMR) were used as a proxy of the extent of the air exchanges between the indoors and the outdoors [86]. Nevertheless, it has to be taken into account that in historic libraries also moisture exchanges with the hygroscopic materials may contribute to the calculated MR values [99, 144].

4.1.3 *Hygroscopic behaviour of the collections*

The response time of hygroscopic material to the environmental RH variability was experimentally determined by fitting an approximate formula relating consecutive RH values measured on the object at regular time interval [106]:

$$RH_{\text{response,i}} = \frac{RH_{\text{response,i}-1} + \frac{RH_i}{n/3}}{1 + \frac{1}{n/3}} \tag{4.3}$$

where $RH_{\text{response,i}}$ is the material response in terms of RH to the surrounding environmental RH_i at each time i and n equals the number of measured data points in the response time [87].

Since RH is not an independent variable, it must be studied together with air temperature or mixing ratio, which both influence its behaviour. The possible effect of the moisture exchanges between the hygroscopic collections and the surrounding air on the stabilisation of the indoor RH values was explored based on the following approach, as defined in Appendix A:

a) analysis of the concurrent time evolution of indoor measurements of T, RH and MR over the year;

b) analysis of the frequency distribution of the indoor RH observations;

c) calculation of the Relative Humidity ratio (RH_{ratio});

d) assessment of the average absolute differences between simultaneous outdoor and indoor MR values ($\overline{\Delta \text{MR}}$).

The RH_{ratio} was defined as the ratio (in percentage) between the indoor (in) and the outdoor (out) seasonal spreads, i.e., the sum over a year of the absolute differences between the i-th centered 90-day moving average of relative humidity ($RH_{\text{i,90d}}$) and the i-th relative humidity observation (RH_i):

$$RH_{\text{ratio}} = \frac{\left(\sum_{i=1}^{n} \mid RH_{\text{i,90d}} - RH_i \mid\right)_{in}}{\left(\sum_{i=1}^{n} \mid RH_{\text{i,90d}} - RH_i \mid\right)_{out}} \tag{4.4}$$

When the RH ratio is low, the library has limited air exchanges with the outdoors together with high moisture buffering capacity by the hygroscopic materials (if present); when the RH ratio is close to 100%, the indoor and outdoor RH seasonal spread are practically identical.

Moreover, to further discuss the role of hygroscopic collections on the RH stabilisation, the so-called hygroscopic ratio [158] was calculated as the ratio between the total volume of the hygroscopic materials (i.e., collection and wooden shelves), and the total volume of the library room.

4.2 Modelling library buildings and collections

4.2.1 *Sinusoidal heat and moisture transfer models*

The annual seasonal cycles of temperature and mixing ratio were estimated following an approach described and used in Appendix D. The annual cycles were fitted as generic time-dependent sinusoidal equations, as follows:

$$x(t) = \overline{x} + \Delta x \cdot sin(\omega t - \Phi) \tag{4.5}$$

where x is the variable considered (i.e., T or MR), t is time (in days), $\overline{x}$ is the annual average of x, ω is the angular frequency (i.e., $\omega = 2\pi/P$ where P is the period) and Δx and Φ are the amplitude and the phase shift of the best-fit sine function, respectively.

This method, traditionally used to quantify the attenuation and lag between waves transmitted across homogeneous materials [49], can be applied under certain limits to the case of historical buildings with natural climate and no (or at least negligible) influence of people, thermal bridges, infiltration and openings (i.e., windows and doors). The underlying idea is that the seasonal frequency of the outdoor wave is transmitted across the historical building envelope with a characteristic attenuation (in terms of amplitude) and time lag (in terms of phase shift), whereas its diurnal frequency is entirely cut out by the thick building walls. However, if the outdoor air (advective air flows) and/or people (heat and moisture sources) can enter the building, or if solar radiation (radiative energy) infiltrates it, the possibility to rigorously apply the method will be limited.

The T and MR data collected in Ca' Granda and Delfiniana were used as these libraries had natural free-floating microclimates. However, it should be noticed that the influence of visitors and openings could not be excluded a priori, although it could be relevant particularly in the case of Delfiniana (as it is part of the itinerary of a museum). The hourly hygrothermal observations collected over a year inside the historic libraries and outdoors by the closest weather station were used to derive the indoor (Δx_{in} and Φ_{in}) and outdoor (Δx_{out} and Φ_{out}) coefficients of the fitting curves. The combination of the two sinusoids, i.e., the outdoor T or MR cycles in abscissa and the indoor T or MR cycles in ordinate, gives the annual hysteresis cycle in the building [50].

Outdoor monthly temperature and mixing ratio data were then extracted from the Copernicus Climate Data Store for the 30-year time windows 1981-2010 (Recent Past), 2021-2050 (Near Future) and 2071-2100 (Far Future). A CMIP6 dataset, namely the Sixth phase of the Coupled Model Intercomparison Project (CMIP), was chosen for both the historical climate and for intermediate Shared Socioeconomic Pathway (SSP) future scenarios. Each CMIP6

modelling centre produces repeated runs on the same experiment (e.g., a historical scenarios or a future projection) using the same Global Climate Model (together referred to as an "ensemble") to increase robustness and inform sensitivity of results through statistical information [71]. The CMIP6 ensemble dataset used in this analysis (0.9°×1.25° grid resolution) was produced by Centro Euro-Mediterraneo sui Cambiamenti Climatici (CMCC) [55], providing both historical atmospheric data from 1850 onward (based on ERA5-Land reanalysis dataset [136]) and future predictions following a SSP2-4.5 scenario. Scenario 4.5 is the moderate scenario developed by the Intergovernmental Panel on Climate Change (IPCC) that assumes higher CO_2 emissions until 2050 and their decrease afterwards [120].

The hygrothermal conditions inside the libraries were inversely simulated as described in [37, 50, 156] to estimate the indoor microclimate associated to past and future outdoor scenarios. RH values were computed from T and MR using the formula numbered as 2 in Supplementary equations. Finally, the modelled T and RH conditions were used to qualitatively evaluate the evolution of chemical deterioration risks for paper collections.

4.2.2 *Whole-building dynamic simulation*

A simplified 3D geometrical model of the Collegio Romano library was created in SketchUp based on the 2D drawings of the building levels together with the shapes of the surrounding buildings to consider the shadow they project over the case study (Figure 4.3). Dynamic whole-building simulation was performed using the software IDA Indoor Climate and Energy (IDA ICE) 4.8 developed and distributed by EQUA. IDA ICE was chosen as it has a modular architecture that allows extending his features at advanced level.

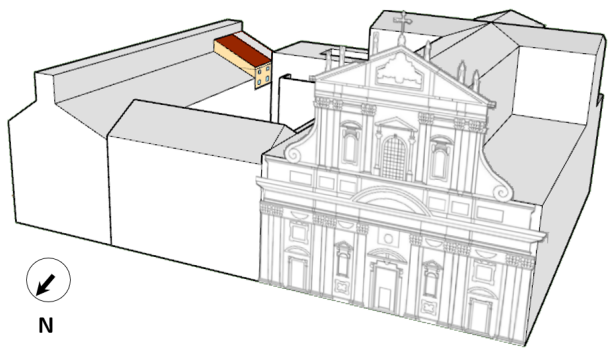

Figure 4.3. 3D geometrical model of the Collegio Romano library (coloured) together with the adjoining baroque Church of St. Ignatius of Loyola in Rome.

The library model has a total internal volume equal to 382 m^3 and an orientation of 100°N. The default thermal model was used for wall modelling. The wall stratigraphy (Table 4.2) was guessed based on the building drawings and on data retrieved from literature on similar masonry constructions of the XVI century in Rome [21, 117, 132], with typical thermal properties of coeval historic building [103]. To take into account the high thermal inertia of historic buildings, the initialisation period was set to start six months before the simulation period.

Table 4.2. Thermal properties of the opaque components in the model of Collegio Romano Library. λ = dry thermal conductivity; ρ = density; C_p = specific heat capacity.

Material	Thickness m	λ W/(m·K)	ρ kg/m³	C_p J/(kg·K)
Internal plaster	0.02	0.8	1400	1000
Historical bricks + mortar (80:20)	0.93	0.6	1480	852
External plaster	0.02	0.9	1800	850
Clay tiles	0.03	1	2000	1000
Insulation panel	0.055	0.05	240	2100
Membrane	0.05	0.17	500	840
Roof brick	0.03	1	1800	840
Mortar	0.05	0.9	1800	900
Wooden board	0.06	0.22	700	1600
Internal plaster	0.02	0.8	1400	1000
Belgian bricks + mortar (80:20)	0.76	0.95	1922	870
Internal plaster	0.02	0.8	1400	1000
Wooden board	0.03	0.22	700	1600
Air gap	0.08	0.59	1.3	1000
Wooden board	0.03	0.22	700	1600
Gypsum	0.01	0.3	850	1000
Ceramic tiles	0.015	1.4	1700	1000
Screed + subfloor+ sand/gravel	0.16	1.28	1625	943.8
Wooden board	0.03	0.22	700	1600
Air gap	0.08	0.59	1.3	1000
Wooden board	0.03	0.22	700	1600
Internal plaster	0.01	0.8	1400	1000

The windows were modelled as single-pane glasses with wooden frames 0.075 m thick and a recess depth of 0.2 m. The glazing system parameters were set with a U-value of 5.830 W/(m^2·K) and solar heat gain coefficient (SHGC) value of 0.870 and solar transmittance – global (Tglobal=0.834) and visible (T-vis=0.899). The wooden frame was set with U-value of 2.3W/(m^2·K). No internal nor external shadings were included in the model of the windows. Infiltrations were initially assumed to be constant with an ACH=0.2h^{-1}, based on the typical values in historical buildings found in literature [22]. Thermal bridges and internal gains due to lighting were neglected. The ACH value in the

above crawl space of the roof was set to be equal to $0.5h^{-1}$ (corresponding to 0.49 l/s·m^2). The two radiators installed in the library were assumed to have a total power of 5000 W based on their model and size. The schedule for heating was set from November 1st to April 15th and operating from 6 a.m. to 6 p.m. Simple fan-coils having power equal to 3500 W were integrated in the model but kept off as they were rarely used in the library. Based on the average use of the library, the occupancy schedule considered two people sit in the library (MET=1) once a week from 12 a.m. to 18 p.m. (excluding holidays).

The weather file used to run the model was determined from the hourly measurements of temperature, relative humidity, pressure, wind speed and direction and global horizontal solar irradiance (GHI) collected on the CREA weather station in the Calandrelli Tower of Collegio Romano (66.4 m a.m.s.l.). GHI was split in the direct and diffuse solar irradiance components by including in the formula in [89] the sun elevation data measured in Rome at the ESTER (Solar Energy TEst and Research) station of Tor Vergata University [62].

A manual calibration was performed adjusting the input parameters to minimise of the discrepancy between measured and modelled data. The mean absolute error (MAE), the root mean square error (RMSE), the coefficient of variation of RMSE (CV-RMSE) and the correlation coefficient (r) were calculated as reported in the equations in section Supplementary equations. Since standardised statistical criteria for calibration are not available in the literature [85], a general criterion to assess the model accuracy can be referring to the instrumental error of the measurements: the closer is the simulations' uncertainty to the sensor's one, the better the building model reproduces the behaviour of the actual building [24, 77]. The model validation was carried out in the same way, but comparing measured and modelled data in a period not included in the calibration. To avoid the uncertainty due to the modelling od the HVAC components, the periods selected for calibration and validation were June and September, respectively.

Finally, the validated model was used to study possible strategies able reduce deterioration risks and energy consumption without compromising the comfort of the occupants by using an *ad hoc* weighted function (Equation 4.15).

4.2.3 Hygrothermal model of paper collections

The HMWall (Heat air and Moisture) model can be coupled with the modular software IDA ICE to provide reliable dynamic hygrothermal simulations in historic buildings, as studied in Appendix B. So far, HMWall has never been tested in modelling the hygrothermal conditions within library and archival repositories. The HMWall model, whose underlying physical laws can be found in [83], is based on the balance equations for heat and moisture transfers. In this

1D fully coupled heat and mass model, the hygrothermal variables are strongly linked to each other since the thermal conductivity, which drives the heat transfer, is moisture-dependent and because the enthalpy flux is a function of both temperature and vapour diffusion flux. In HMWall, the adsorption isotherms are calculated only as a function of relative humidity, since the equilibrium water content (w) is assumed to be little sensitive to temperature changes and the hysteresis between adsorption and desorption is usually considered negligible. The moisture storage curve of the materials is computed as follows:

$$w(\phi) = w_f \cdot \frac{\phi \cdot (b-1)}{b-\phi} \tag{4.6}$$

where w is the equilibrium water content (kg/m^3) corresponding to the relative humidity ϕ (expressed as a fraction from 0 to 1), w_f is the moisture content at free water saturation and b is an approximation factor calculated from the equilibrium water content at $\phi = 0.8$ (w_{80}). The diffusion of the material is expressed as a function of the dry diffusion resistance factor (μ). Capillary liquid water transport is described as a diffusion phenomenon in the material pore spaces regulated by the water absorption coefficient. The thermal conductivity of dry materials (λ) increases linearly with moisture content.

The hygrothermal properties of paper available in literature are measured following various procedures; moreover, as they depend on both the constituent materials and the manufacturing process, modern [67, 68, 98, 144] and historical [98] papers can have rather different hygrothermal properties. Sensitivity Analysis (SA) was used to determine which are the most influential parameters in the computation of the simulation results and to quantify their effect on the variability of the outputs [157]. Since SA results are strongly related to the specific configuration to be tested [119, 139], the analysis was conducted in relation with the modelling goals, carefully choosing the variability of the input parameters (Appendix C).

Sensitivity analysis input	Range
Density (ρ)	600–900 kg/m^3
Specific heat capacity (C_p)	700–1200 J/(kg·K)
Dry thermal conductivity (λ)	0.05–0.10 W/(m·K)
Thermal conductivity supplement (σ)	1.0–5.0
Free water saturation moisture content (w_f)	100–200 kg/m^3
Equilibrium moisture content at RH = 80% (w_{80})	50–100 kg/m^3
Dry vapour diffusion resistance factor (μ)	50–100

Table 4.3. Ranges of the hygrothermal properties of paper tested in the Sensitivity Analysis.

A HMWall single wall model with area equal to 1 m^2, thickness 0.2 m and

divided into N=63 sub-layers, was preconditioned at paper wall temperature Twall=20°C and relative humidity RHwall=50% and connected to identical boundary conditions of T=20°C and RH=70% (Figure 4.4). N was chosen in order to have a detailed model able to describe the heat and moisture transfer phenomena in paper, with thickness of each sub-layers equal to 3 mm.

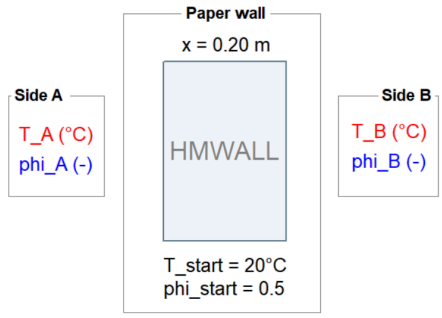

FIGURE 4.4. Paper wall model built by coupling the HMWall model in IDA ICE 4.8.

The sensitivity analysis was performed by using the Elementary Effects (EE) method based on the Morris random sampling method [82]. The Morris random sampling considered 10 EE for each parameter and 4 discretised levels to span within the ranges of the selected hygrothermal parameters summarized in Table 4.3.

The water vapor sorption curves of a cellulose paper sample were measured to refine the values of some of the input parameters in the paper wall model. The measurements were carried out at 15°C, 25°C and 30°C and for a full range of water vapor relative pressures with the aid of the vacuum microbalance (CI Electronics Ltd.) at the laboratory of the Jerzy Haber Institute of Catalysis and Surface Chemistry of the Polish Academy of Sciences (Krakow, Poland) following the experimental procedure in [38, 39, 98].

4.3 CLIMATE-INDUCED RISK ASSESSMENT

4.3.1 Dose-response functions, damage functions and the historical climate

In heritage science, *dose-response functions* are expressions of the relationship between measurable changes in the material properties (response) and quantifiable physical or chemical agents driving the process of change (dose) [26]. Since not all changes in heritage materials can be considered to be damage [25], *damage functions* represent functions where a threshold of unacceptable change was defined through a value-based decision [146].

Mechanical deterioration and the historical climate

Mechanical damage of library objects can occur due to incorrect handling and tensile stresses caused by climate-induced dimensional changes [48].

The average number of large missing pieces that each handling event could develop every 100 pages on paper-based books having DP<800 can be estimated by using the empirical formula in [147]. Table 4.4 shows the time until documents are expected to become unfit for use assuming various scenarios of average frequency of use.

Table 4.4. Years until documents with a given degree of polymerisation (DP) are expected to become unfit for use assuming various scenarios of average frequency of use (times per each interval of years, in columns). One large missing piece per 100 sheets was set as the threshold for damage [147].

DP	average frequency of use			
	30 years	5 years	1 year	5 times per year
200	240	32	8	2
300	686	91	23	5
400	1961	261	65	13
500	5604	747	187	37
600	16014	2135	534	107
700	45761	6102	1525	305
800	130770	17436	4359	872

It is worth noticing that the paper objects already deteriorated will last only few years even if consulted only once a year. Moreover, it should be also taken into account that natural ageing and the other deterioration mechanisms will further reduce DP as time goes by.

The European standard EN 15757:2010 [7] was used to reconstruct the historical climate to which the library objects made in organic hygroscopic materials have acclimatised and adapted. The calculation of the historical climate is based on a 30-day central moving average (MA) of the RH observations, which defines the seasonal variability. The bands of tolerable RH variations are obtained superimposing on the MA the lower and the upper limits, calculated respectively as the 7^{th} and the 93^{rd} percentiles of the distribution of short-term RH fluctuations (i.e., the difference between RH readings and MA). When RH fluctuations depart by less than 10% from the seasonal RH levels, these limits can be considered unnecessarily strict [7] and thus the RH band can be calculated as the MA ±10%. This information can be relevant for library management, e.g., for the relocation/loan/consultation of objects potentially vulnerable to mechanical damage such as composite objects, parchment-bound volumes.

Chemical deterioration

Chemical reactions are influenced by temperature (which exponentially affect the kinetic constant according to Arrhenius equation), and moisture content (which in hygroscopic materials depends on the environmental air relative humidity). Cellulose hydrolysis, considered as the most alarming damage risks for the preservation of vulnerable collections, has been extensively studied by using dose-response functions.

The Preservation Index (PI) was developed by Sebera to account for the chemical deterioration of a wide variety of organic materials based on the Arrhenius equation for the hydrolysis rate of cellulose acetate [118]. The isoperm method (i.e., curves of equal permanence expressed in PI) is based on the idea that an indication of the relative durability of a given material can be estimated as a function of the distance from the standard conditions of 20°C and 50%RH (where PI=1). Equation 3 in Supplementary equations was used to obtain the Sebera's isoperms by dividing the reaction rate at given T and RH conditions to the reaction rate at the standard conditions.

The Lifetime Multiplier (LM) was proposed in [110] to estimate the risk of chemical degradation by taking into account the activation energy of the degradation processes involved in the deterioration of various organic materials (i.e., 70 kJ/mol for yellowing of varnishes and 100 kJ/mol for degradation of cellulose). This index is a multiplier of the time left to an object to remain usable when compared to standard conditions (Equation 4 in Supplementary equations).

A dose-response function for paper was developed in [148] by modelling k, i.e., the rate of paper degradation per year (at the conditions of dark storage), as a function of both the acidity of paper (pH) and the indoor temperature and relative humidity, as follows:

$$\ln(k) = 36.981 + 36.72 \cdot \left(\frac{ln(1-RH)}{1.67 \cdot T - 285.66}\right)^{\frac{1}{2.491-0.012 \cdot T}} + 0.244 \cdot \ln(10^{-pH}) - \frac{14300}{(T + 273.15)} \quad (4.7)$$

Figure 4.5 shows the comparison among the isoperms obtained using the three dose-response functions presented above to assess the chemical deterioration of paper. The graph shows that the divergence in the isoperms is negligible between 20% and 60%RH. This observation implies that, at the typical conditions inside libraries, their alternative use does not lead to any significant difference in the results [19].

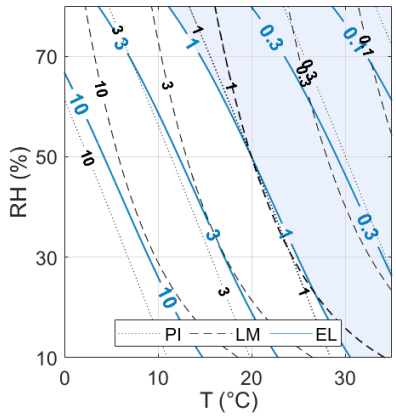

Figure 4.5. Comparison among the curves of equal permanence (isoperms) according to Lifetime Multiplier (LM), Preservation Index (PI) and Expected Lifetime (EL).

Although the Guggenheim-Anderson-deBoer (GAB) fitting function is currently considered as the most adequate to describe the moisture sorption curves of hygroscopic materials [43, 128, 145, 160], the EL function has the advantage of considering an exponential relationship between paper moisture content and relative humidity [122] in the place of the linear dependence used to calculate PI [145]. For this reason, the EL was chosen to assess the chemical risk for paper materials.

Equation 4.7 can be embedded in the Ekenstam's function to obtain a damage function for paper where the expected lifetime, EL (i.e., the time required for objects to become unfit for use), is calculated as a function of the initial degree of polymerisation (DP) and the critical degree of polymerisation, which is typically 300, at which objects are no longer suitable for general access:

$$EL = \left(\frac{1}{300} - \frac{1}{DP}\right) \cdot k^{-1} \tag{4.8}$$

In light of the isochrones (i.e., the curves of equal EL expressed in years), it was noticed that the T and RH values given in EN 16893 [16] are advisable for the preservation of acidic paper collections; conversely, the recommendations by Italian standards [2–4] may not prevent from the chemical decay of acidic paper collections before the planning horizon of 500 years [158]. It has to be borne in mind that, although the 500-year planning horizon was here used as a reference to guide the evaluation, each cultural institution should seek the expected lifetime being more appropriate for its collection given the peculiar contextual factors (e.g., mission, purpose, building performance and climate forcing due to geographic location) [19]. Further detail on this topic can be found in Appendix A.

To account for an average risk of chemical degradation for paper collections due to cellulose hydrolysis,

defined a synthetic index, hereafter named as Time Weighted Expected Lifetime (TWEL). Figure 4.6 shows the workflow for the calculation of the TWEL.

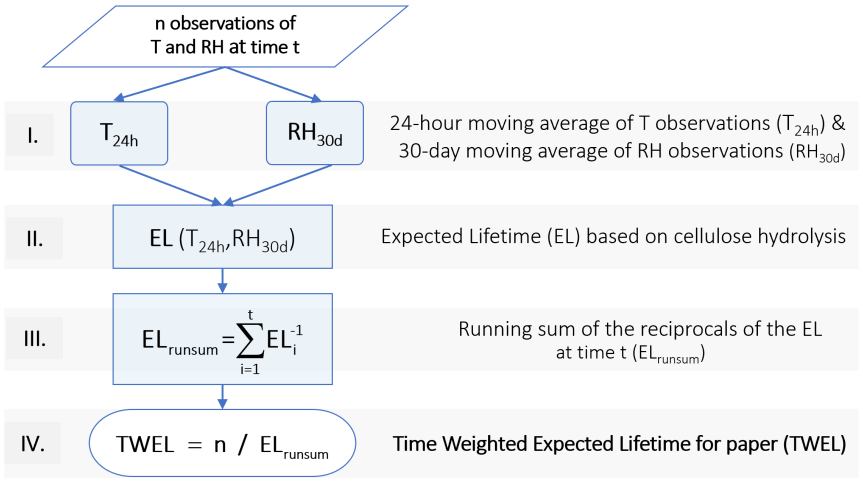

FIGURE 4.6. Workflow of the procedure to calculate the Time Weighted Expected Lifetime (TWEL).

The TWEL index integrates the damage function for paper derived and validated in [148] with the concept of a time-weighted index to quantitatively compare the chemical risk due to the indoor climate conditions over different time windows (e.g., a year or a season). Inspired by the well-established TWPI index formulated for the chemical degradation of organic materials [95], the TWEL is calculated based on the running sum of the multiplicative inverses of EL at each time t. Indeed, we examined various formulations for averaging the EL (e.g., the simple arithmetic mean, the inverse of the arithmetic mean, etc.) and found that the proposed calculation of TWEL was the one giving more weight to the lower values of EL, thus considering the risk underlying the worst-case scenario. In this way, the TWEL emphasises the impact of the most adverse climate conditions (mainly temperature) on the overall chemical deterioration risk for paper collections on a yearly and seasonal basis.

Biological deterioration

Biological deterioration indoors is usually the result of fungal colonisation and insect proliferation. Spore germination is possible when RH>70% for most of the mould species, while insects are more sensitive to temperature, being

basically inactive for T<15°C.

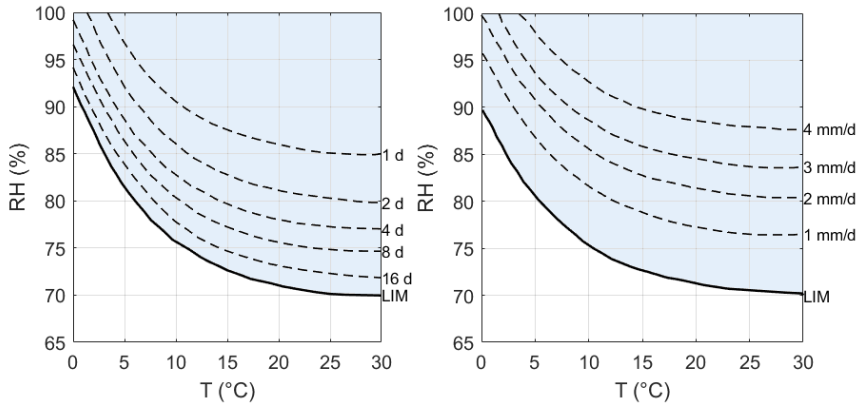

Figure 4.7. Sedlbauer curves of spore germination (left) and mycelial growth (right) for optimal substrate [154]. LIM: Lowest Isopleth for Mould.

A well-established method to evaluate mould risk are the Sedlbauer curves [96], where emphasis was given to the role of the substrate determining the actual availability of nutrients necessary for fungal growth (*Aspergillus versicolor*). The so-called isopleths, shown in Figure 4.7, are the curves having equal time of spore germination or mycelial growth. Although these curves were thought for materials different than cultural heritage, they have been extensively used to assess the risk of spore germination and mould growth for biologically recyclable materials. The risk of mould growth is assessed by comparing T and RH observations to the Sedlbauer isopleths. As recently proposed in [44], the critical RH can be considere as the one associated to the Lowest Isopleth for Mould (LIM) for an optimal substrate [154], thus assuming a worst-case scenario.

The metabolic activity of insects and larvae linearly increases with temperature between 5 and 30°C. The easiest approach to evaluate how much the environmental conditions favour insect growth is based on the calculation of the degree-days, i.e., the number of days in a given time window where temperature observations exceed a given threshold value [26]. The threat of insect pest infestation can be evaluated using an index proposed by P. Brimblecombe and P. Lankester [45] to quantitatively derive the number of eggs laid by webbing cloth moths (*Tineola bisselliella*) as a function of temperature:

$$n_{\text{eggs-laid}} = \text{int}\left(130 \cdot \exp\left(-\left(\frac{\frac{T^2}{30} - 30}{12}\right)^2\right)\right) \tag{4.9}$$

where T is the monthly average of the temperature observations.

4.3.2 NDT measurements

Colorimetry was used to detect colour changes and evaluate the possible impact of solar radiation in the E-oriented side of the Alessandrina repository as described in (Appendix F).

An experimental program following a 4-month schedule was set up and conducted from October 2019 to October 2020 to monitor the cumulative colour changes induced by light on the covers of 5 already discoloured books exposed to solar radiation (Figure 4.8). A digital portable spectrophotometer Konica Minolta (model 2600d) was used to obtain the reflectance spectrum and the CIE colorimetric parameters (L*a*b*). Colorimetric measurements were also performed on an unproofed green target sample of cardboard (made in pure Elemental Chlorine Free cellulose, grammage 200 g/m^2) to empirically derive the magnitude of the luminous exposure in the repository.

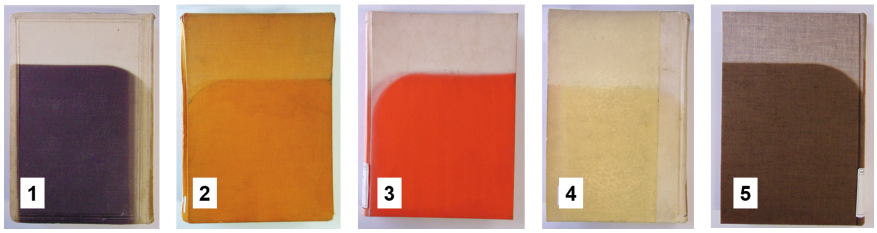

FIGURE 4.8. Book covers monitored over a year in Alessandrina repository though colorimetric measurements repeated on a 4-month basis.

In order to be able to compare the measurements taken at different times, the monitoring required to align the sampled area and to use the same calibration standard, spot area and illumination source. After calibration with the white standard provided by the manufacturer, measurements were repeated 3 times in 3 different sampling points for each sample.

The ΔE^*, i.e., the colour difference, was calculated as:

$$\Delta E^* = \sqrt{(\Delta L^*)^2 + (\Delta a^*)^2 + (\Delta b^*)^2} \tag{4.10}$$

Then, the change of ΔE^* through time was fitted using the following exponential curve [57]:

$$\Delta E^* = \frac{E_\infty \cdot t}{t_s + t} \tag{4.11}$$

where E_∞ is the fitted value of ΔE^* at infinite time and t_s is the time corresponding to $E_\infty/2$.

4.3.3 Trade-off between preservation and sustainability

The trade-off between preservation and sustainability within historic libraries was obtained by combining dynamic simulation and climate-induced risk proxies [102, 140].

A weighted function (Ψ) was proposed in Appendix E and tested to identify appropriate compromise solutions balancing conservation of artworks, energy saving and thermal comfort. The study aimed at finding the model settings that minimise the value of the target function Ψ [78]. Three specific functions for the optimisation were defined to guarantee a high-quality conservation environment (ψ_A), to reduce energy consumption (ψ_B) and to improve thermal comfort of visitors (ψ_C):

$$\psi_A = \sum (C_{proxy} < C_{threshold}) \tag{4.12}$$

$$\psi_B = \int_0^t Q(t) \cdot dt \tag{4.13}$$

$$\psi_C = \text{PDH} \tag{4.14}$$

ψ_A takes into account conservation needs (e.g., the expected lifetime as C_{proxy}, when it is lower than the 500 years horizon, used as $C_{threshold}$); ψ_B is the total energy consumption given by the sum of both heating and cooling demands (Q); ψ_C is the total amount of discomfort hours computed as Predicted Discomfort Hours (PDH). The three targets need to be normalised so that limits range between 0 (best-compromise solution) and 1 (worst-compromise solution).

Then, they are combined into the weighted function Ψ, as follows:

$$\Psi = \min(0.5 \cdot \psi_A + 0.3 \cdot \psi_B + 0.2 \cdot \psi_C) \tag{4.15}$$

The highest coefficient was given to ψ_A in order to assign priority to conservation [78] and here adjusted to the case of historic libraries, where the presence of people inside the library can be reduced to the minimum by consulting the materials in designated reading rooms. Nevertheless, the weights were chosen to keep significant the contribution of ψ_B and ψ_C to the final score.

In the specific application to the whole-building model of Collegio Romano, the insect risk ψ_A was estimated as the total number of eggs laid monthly by the webbing cloth moth; energy consumption ψ_B was calculated as the sum of heating and cooling loads; discomfort of occupants ψ_C was computed as the number of hours where T<18°C or T>27°C over 240 hours of expected presence of people. The weighted function Ψ was used to find a compromise solution in the operation of the HVAC systems in the Library.

Part III

Results

Chapter 5

Microclimate analysis

The following analysis took into account the measurements collected by the RHT probes in Figure 4.1, selecting the periods resulted to be more continuous (CI=1) and complete (CoI=1), which are summarised in (Table 4.1).

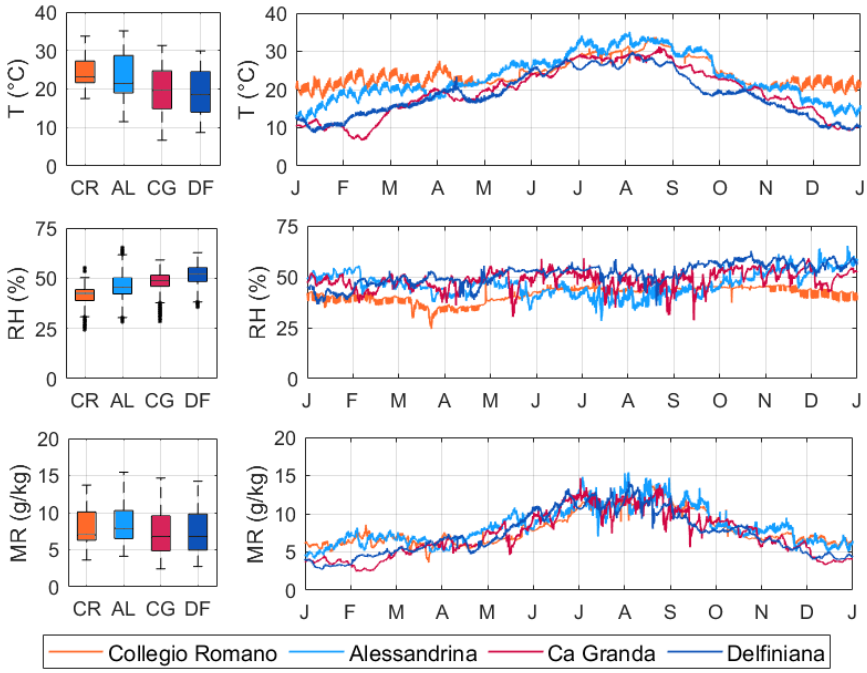

Figure 5.1. Box-and-whisker plots (left graphs) and time plots of indoor temperature (T), relative humidity (RH) and mixing ratio (MR). In the box-and-whisker plots, the medians are indicated as horizontal lines dividing each box and the outliers, i.e., the values above or below 1.5 × IQR (IQR = interquartile range), as black circles beyond the upper and the lower whiskers of each box.

Figure 5.1 shows a synthetic overview on the annual evolution of T, RH and MR values inside the libraries. The box-and-whisker plots (left graphs) highlighted that, on a yearly basis, the indoor median temperatures were higher in

Collegio Romano and Alessandrina than in Ca' Granda and Delfiniana. In cold periods, both the libraries in Rome experienced higher T due to the switching on of the heating systems during the working days (from Monday to Friday). The indoor relative humidity observations in all the libraries were found to have similar behaviour during the year, with values oscillating around the average levels. The few RH drops inside the libraries were mainly caused by outdoor MR drops. In Collegio Romano, short-term RH fluctuations were observed in winter due to the heating systems. Lower RH values in Alessandrina, Ca' Granda and Delfiniana were measured in summer with respect to the rest of the year, whereas the minimum RH levels in Collegio Romano were observed in March-April in relation to a prolonged outdoor MR drop. Although the MR medians in the libraries were similar (MR ≈ 7.0 g/kg), higher MR values were registered in winter in Collegio Romano and Alessandrina, likely because of the moisture release from the hygroscopic collections.

Normalised Diurnal Range

The Normalized Diurnal Range (NDR) index was used to compare the thermal buffering capacity of the buildings housing the libraries (Figure 5.2). Although NDR does not entirely depend from the air exchange rate (AER), it can be considered as a proxy of AER to a certain extent. In Collegio Romano, summer NDR values ranged from -0.1 to +0.1, whereas a higher variability characterised the period with the heaters on (from November until April). The NDR values in Collegio Romano highlighted a relatively higher heat accumulation (NDR<0) due to the use of heaters in winter and the low air exchanges in summer [158]. The NDR values in Alessandrina ranged from -0.2 to +0.2, with a different behaviour in the cold seasons with respect to the warm ones (positive values from March to November and negative values from December to March), likely due to different management of the windows. Ca' Granda had NDR values ranging from -0.1 to +0.1 and the highest frequency of zero values, meaning that the building envelope filtered out most of the largest outdoor thermal variability, probably thanks to massive building envelopes and low air exchange rates [53]. Delfiniana showed NDR values around zero in winter and negative NDR values during summer. The negative NDR values, meaning that $T_{d,22} > T_{d,14}$, were probably due to indoor summer T peaks being delayed after the outdoor T peaks. It was not possible to establish a correspondence between the anomalous NDR values (i.e., those lying outside the coloured band in Figure 5.2) and particular events occurred in the libraries. This latter fact was interpreted as the consequence of the operation of averaging the daily outdoor values over the reference period, that might have smoothed out the real pattern of the outdoor thermal variability occurred in the monitored years [158].

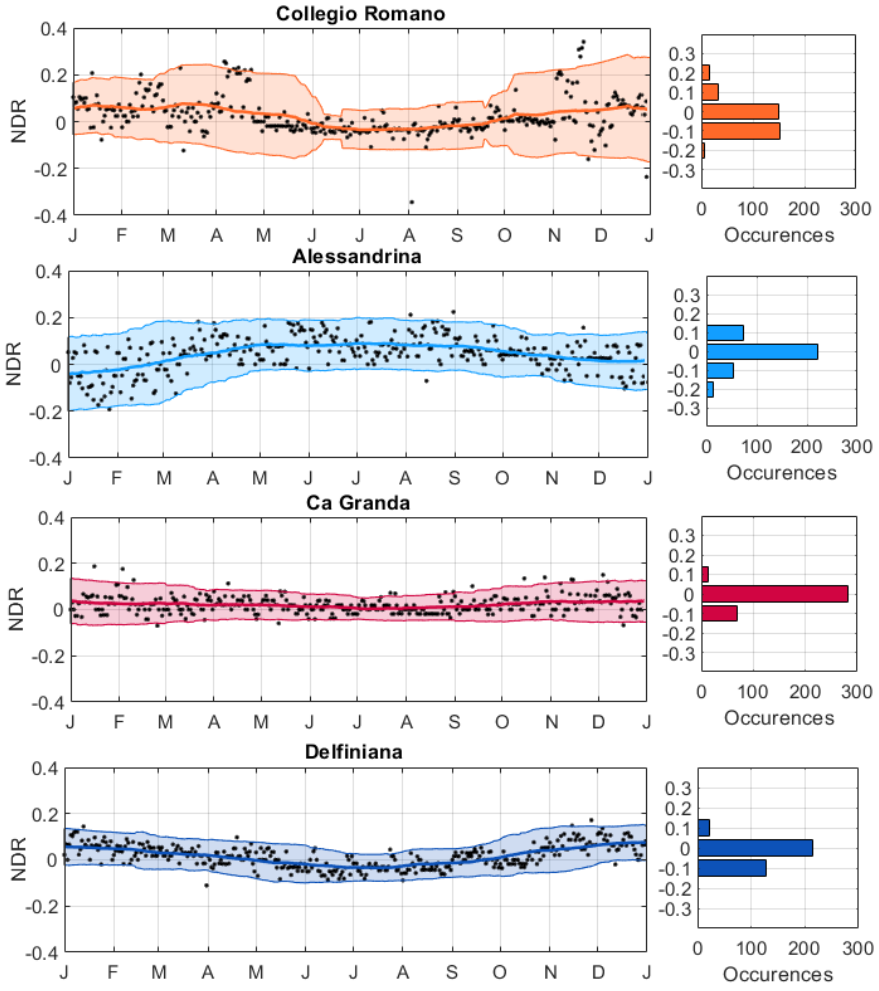

FIGURE 5.2. Normalized Diurnal Range (NDR): time plots (left) and histograms (right). NDR values in time plots (black dots) are shown together with the curves of the 90-day moving average (thick coloured curves) and double moving standard deviation (thin coloured curves).

Thermal vertical gradients

In Figure 5.3 the thermal vertical gradients (ΔT/Δz, where T upper probe - T lower probe) in the high-ceilinged libraries (i.e., Alessandrina, Ca' Granda and Delfiniana) were compared with the adiabatic gradient of vertical temperature for dry air (Γ_d = 0.1°C/10m).

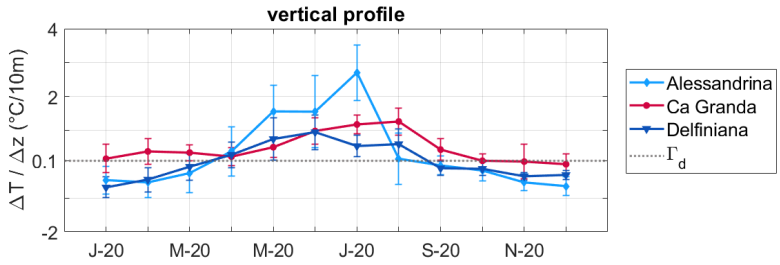

FIGURE 5.3. Thermal vertical gradient ($\Gamma = \Delta T/\Delta z$), shown as monthly averages, together with the adiabatic gradient of vertical temperature for dry air (Γ_d = 0.1°C/10m). When $\Gamma < \Gamma_d$ vertical instability occurs.

Both in Alessandrina and Delfiniana air instability (i.e., favourable conditions for vertical transport) occurred in winter due to the higher T measured by the lower probe with respect to those measured by the upper probe. Since upraising flows of warmer air masses from the floor and descending flows of colder air masses from the ceiling can be responsible for transporting pollutants and other airborne particulate matter, air instability can affect paper conservation by causing soiling and deposition of dust and fungal spores [19, 48]. The lower temperatures collected near the ceiling were interpreted as the possible consequence of heat losses caused by the poorly insulated roof. During the warm season, the air temperatures near the ceiling were higher than those collected at lower levels above the floor, with natural positive values observed from mid-May to mid-June in Ca' Granda and from mid-June to August in Delfiniana. This thermal stratification may affect the conservation of the collections closer to the ceiling because of accelerated rates of chemical deterioration [158].

RH buffering

Figure 5.4 shows the frequency distribution plots of the indoor RH observations. All the libraries were characterized by high RH buffering, with a narrow and almost symmetric spread of the RH observations around the medians. The average RH levels slightly differed among the case studies: the RH medians were equal to 43% in Collegio Romano, 46% in Alessandrina, 48% in Ca' Granda and 52% in Delfiniana. The distances between the 7^{th} and 93^{th} percentiles of the RH distributions were equal to 7% in Collegio Romano, 14% in Alessandrina, 8% in

Ca' Granda and 9% in Delfiniana. The 7th and 93th percentiles were chosen as they correspond to 1.5 standard deviations in a Gaussian distribution [7].

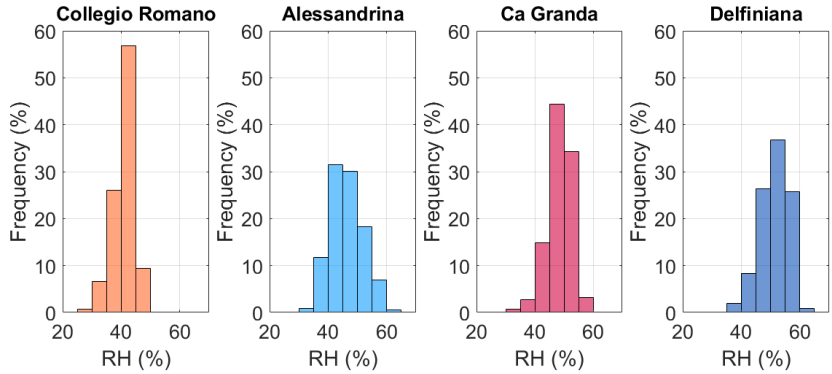

FIGURE 5.4. Frequency distribution plots of the indoor RH observations over a year.

Table 5.1 summarises the results of RH_{ratio}, average annual absolute differences between the indoor MR observations and the outdoor ones ($\overline{\Delta MR}$) and the estimated hygroscopic ratio (calculated as described in Chapter 4). Ca' Granda had the relatively highest RH_{ratio} (i.e., 24.1%), whereas Delfiniana had the relative lowest hygroscopic ratio (i.e., 6.2%). Alessandrina, Ca' Granda and Delfiniana showed comparable values of ($\overline{\Delta MR}$), but the RH_{ratio} in Ca' Granda resulted to be almost doubled with respect to the other two libraries. Collegio Romano had the relatively highest value of $\overline{\Delta MR}$ (i.e., 1.8 g/kg), together with the lowest value of RH ratio (i.e., 9.3%). Since it was not possible to measure the air exchanges, the MR values were used as a tracer of the indoor/outdoor air masses exchanges [9], as already done in literature [37, 86]. For this reason, the relatively higher value of $\overline{\Delta MR}$ in Collegio Romano was interpreted as the possible consequence of reduced indoor/outdoor air masses exchanges with the outdoors [158].

TABLE 5.1. RH_{ratio}, average absolute difference indoor/outdoor MR observations ($\overline{\Delta MR}$), and hygroscopic ratio.

Library	RH_{ratio}	$\overline{\Delta MR}$	Hygroscopic ratio
Collegio Romano	9.3%	1.8 g/kg	7.9%
Alessandrina	15.6%	1.3 g/kg	17.3%
Ca' Granda	24.1%	1.3 g/kg	11.3%
Delfiniana	12.7%	1.2 g/kg	6.2%

Figure 5.4 and Table 5.1 seem to confirm a key aspect of the buffering behaviour of hygroscopic materials in confined environment [68, 99]: when the percentage of storage space occupied by hygroscopic materials (i.e., the

hygroscopic ratio) is high and air exchanges are low, the hygroscopic materials actively contribute to the stabilisation of RH (i.e., lower values of RH_{ratio}) [158]. The same behaviour was observed at small scale in the case of microclimate frames containing paper, as discussed in Appendix D.

Response time of paper-based books

The response time of the paper-based mock-up book in Collegio Romano was estimated from the measurements collected by the RHT probes inside the book by using the formula in Equation 4.3. As the environmental conditions inside the library are rarely perturbed by large and prolonged RH variability, only a single event (occurred on October 15th, 2019) could be used for the analysis. The estimated value of response time for the specific experimental configuration was 37 days, hence compatible with the typical response time of paper-based objects reported in [118]. The difference between the RH values measured and simulated inside the book by using this value of response time in Equation 4.3 was tested between July and November 2020 (i.e., during the unconditioned period without the use of any HVAC system) and found to be equal to RMSE=0.5%.

Chapter 6

Modelling library buildings and collections

Sinusoidal heat and moisture transfer models

The sinusoidal functions to simulate heat and moisture transfer across the historic building envelope were determined as described in Chapter 4 using the outdoor and indoor observations in Ca' Granda and Delfiniana (Figure 6.1).

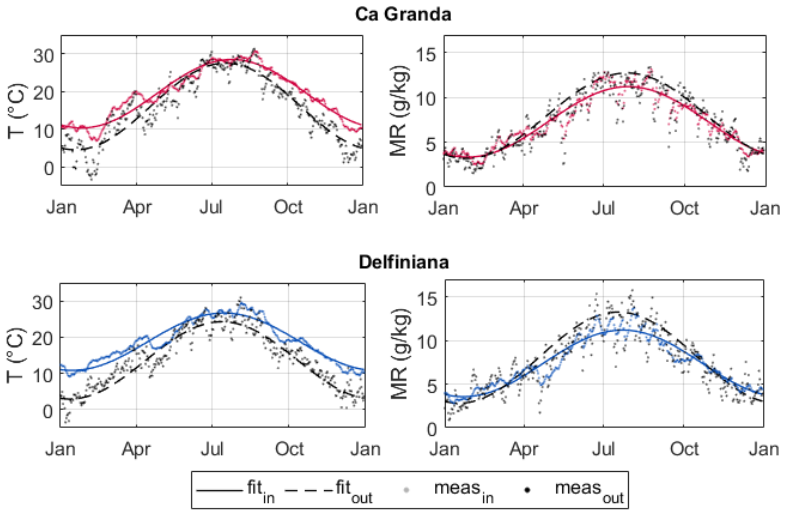

Figure 6.1. Best-fit sinusoidal heat and moisture transfer curves in Ca' Granda (Milan) and Delfiniana (Udine).

The best-fit values of the parameters describing the sinusoidal curves (Table 6.1) were estimated in MATLAB using `fitnlm` function to fit non-linear regression models without any imposed constraints. The goodness-of-fit coefficients were high and significant for both indoor and outdoor fitting curves (R^2>0.7).

The combination of indoor and outdoor sinusoidal fits formed an ellipse during the year (Figure 6.2). The temperature hysteresis cycle in Ca' Granda highlighted the high thermal inertia of the building envelope, whereas it was not clearly detectable in the case of Delfiniana, probably due to the building use (e.g., visitors and openings) and features (e.g., infiltration). In terms of mixing

Table 6.1. Best-fit values of the parameters of the sinusoidal curves for heat and moisture transfer in Ca' Granda and Delfiniana. $\overline{T_{in}}$ (°C) and $\overline{MR_{in}}$ (g/kg) = annual averages; ΔT_{in} and ΔMR_{in} (g/kg) = amplitude; ΦT_{in} and ΦMR_{in} = phase shift.

	Ca' Granda	Delfiniana		Ca' Granda	Delfiniana
$\overline{T_{in}}$	19.4	18.8	$\overline{MR_{in}}$	7.3	7.4
ΔT_{in}	9.1	7.9	ΔMR_{in}	3.9	3.8
ΦT_{in}	8.3	1.8	ΦMR_{in}	2.0	1.9
R^2	0.93	0.92	R^2	0.90	0.90
$\overline{T_{out}}$	16.0	13.6	$\overline{MR_{out}}$	8.0	8.0
ΔT_{out}	11.5	10.7	ΔMR_{out}	4.8	5.2
ΦT_{out}	8.1	8.0	ΦMR_{out}	2.0	1.9
R^2	0.79	0.74	R^2	0.80	0.77

ratio, the annual MR ellipses in the libraries had similar slope and shape (almost a straight line), meaning that the hysteresis on MR was negligible due to the joint effect of air exchanges with the outdoors (e.g., infiltration and openings) and indoor moisture sources/sinks (e.g., visitors and hygroscopic collections).

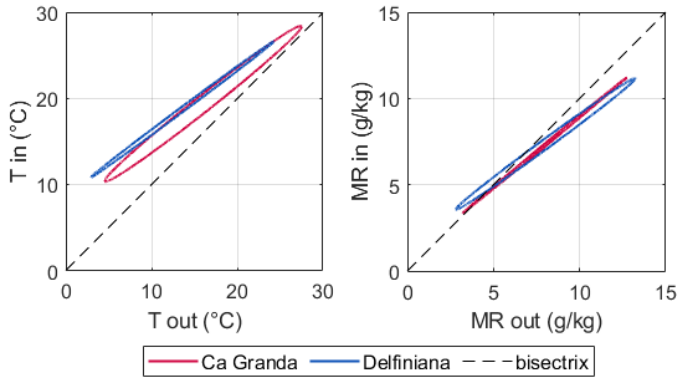

Figure 6.2. Hysteresis cycles of the indoor *versus* outdoor temperature (left) and mixing ratio (right) best-fit sinusoidal curves over the year.

The CMIP6 datasets in the area of Milan and Udine were used to derive the outdoor sinusoidal T and MR curves in the Recent Past (1981-2010), Near Future (2021-2050) and Far Future (2071-2100). In Ca' Granda, the inversely simulated T and MR conditions showed that, with respect to the Recent Past, the indoor temperature could rise up to +1.7°C in the Near Future and up to +4.5°C in the Far Future, while the indoor mixing ratio could increase of approximately +0.3 g/kg in the Near Future and +1.1 g/kg in the Far Future. In Delfiniana, the indoor temperature could rise up to +2°C in the Near Future and up to +5°C in the Far Future with respect to the Recent Past, while the indoor mixing ratio could increase of approximately +0.4 g/kg in the Near Future and +1.3 g/kg in the Far Future. It has to be noticed that the accuracy

of these simulations, particularly in Delfiniana, could have been negatively affected by the combined effect of visitors, thermal bridges, infiltration, and solar radiation, hence they should be regarded as a qualitative estimation of the evolution of indoor T and MR conditions due to the outdoor climate scenarios.

Whole-building dynamic simulation

A whole-building model of the Collegio Romano library was created in IDA ICE 4.8 environment (Figure 4.3) using the thermal properties reported in Table 4.2. On-site measurements of carbon dioxide (CO_2) concentration and heat flux (Figure 6.3) were carried out to refine the initial assumptions and used as an input in the first-guess thermal model.

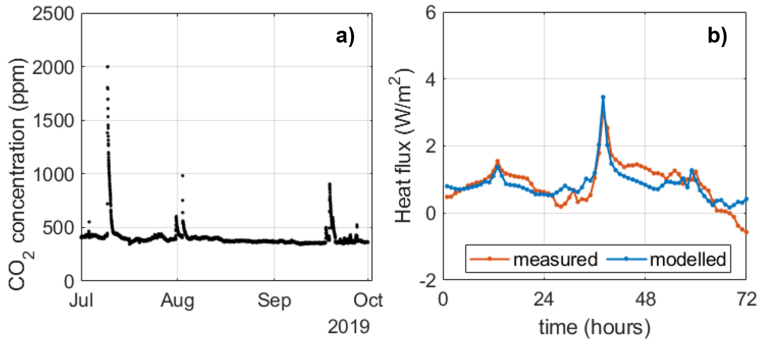

FIGURE 6.3. a) CO_2 concentration values collected in Collegio Romano from July 1st to September 30th, 2019. b) Heat flux measurements from June 3rd to 5th 2021 compared to the simulated values obtained from the thermal model.

The CO_2 concentration values were used to estimate the Air Changes per Hour (ACH) according to Equation 4.2. In Collegio Romano, the peaks of gas concentration due to the presence of people in the library were always associated with the concurrent opening of the windows. For this reason, the ACH value that was estimated based on the fitting decay curves (ACH=2.5h^{-1}) could not be used in the model as it did not reflect the standard conditions in library, which is seldom frequented. The initial guess of ACH=0.2h^{-1} was therefore kept unchanged. The heat flux measured across the external wall of the historic building was compared to the simulated values using the properties given in Table 4.2 together with the indoor and outdoor temperature measured by the thermofluximeter. The comparison showed a reasonably good agreement between measurements and simulations (RMSE = 0.3 W/m^2) and the initial assumptions on the wall stratigraphy were considered sufficiently accurate.

Four configurations of the first-guess model (Table 6.2) were tested to identify the one that better simulates the thermal behaviour of the historic library. In Cases 1 and 3, the wooden shelves full of paper-based books were simulated

as thermal masses having the total area equal to approximately 120 m^2 and composed of a 0.05 m thick layer of wood ($\lambda = 0.14\ W{\cdot}m^{-1}{\cdot}K^{-1}$, $\rho = 500\ kg{\cdot}m^{-3}$, $C_p = 2300\ J{\cdot}kg^{-1}{\cdot}K^{-1}$) and 0.20 m thick layer of paper ($\lambda = 0.06\ W{\cdot}m^{-1}{\cdot}K^{-1}$, $\rho = 690\ kg{\cdot}m^{-3}$, $C_p = 750\ J{\cdot}kg^{-1}{\cdot}K^{-1}$). In Cases 2 and 4, the bookshelves were integrated in the stratigraphy of the internal walls, using the same properties of paper and wood and adding an air layer (0.02 m thickness) between them.

Table 6.2. Tested configurations of the first-guess model of Collegio Romano using the thermal properties given in Table 4.2.

Configuration	Shading	Bookshelves
Case 1	No	Thermal masses
Case 2	No	Wood + paper wall
Case 3	Yes	Thermal masses
Case 4	Yes	Wood + paper wall

The similarity between the given T simulations and the T observations (Case 0) was assessed in the period from June 1st to 30th, 2020 using the Taylor diagram (Figure 6.4) in terms of their correlation coefficient, their centered Root Mean Square Difference (RMSD) and the amplitude of their variations (represented by the Standard Deviation). The configurations where the bookshelves were modelled as thermal masses (Cases 1 and 3) were found to be significantly closer to the measurements. The inclusion of shadings was found to have a negligible effect on the outputs. Case 3 model was chosen for the following calibration.

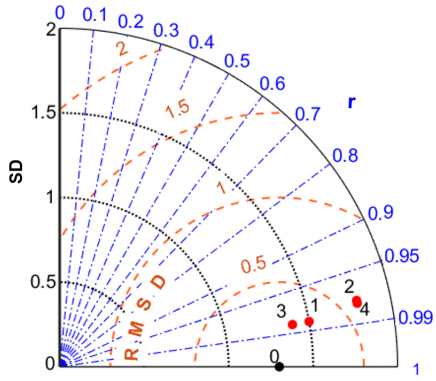

Figure 6.4. Taylor diagram comparing the temperature outputs of four configurations of the first-guess thermal model of Collegio Romano (Table 6.2). Case 0 (black dot): reference T observations; SD: Standard Deviation; r: correlation coefficient; RMSD: centered Root Mean Square Difference [151].

In the manual calibration of the first-guess model, a fine-tuned schedule for windows opening was set up to better in order to better reproduce the increased air exchanges during the weekdays of the warm season. The schedule regulated

the opening of the lower order of windows (up to half aperture). QQplots of modelled *versus* measured values of indoor air T were used to assess the results obtained with the first-guess model (Figure 6.5a) and the calibrated model in the calibration period (June 2020, Figure 6.5b) and in the validation period (September 2020, Figure 6.5c).

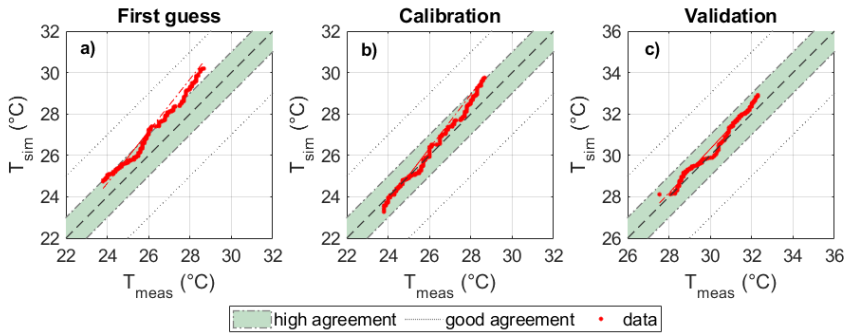

FIGURE 6.5. QQplots of modelled *versus* measured values of indoor air T in the first-guess model (a) and in the calibrated model in the calibration (b) and in the validation (c) periods.

The agreement between modelled and measured temperature is summarised in Table 6.3. The MAE of the first-guess model (MAE = 0.9°C) was improved in the calibrated model up to mean absolute error MAE = 0.3°C and maintained in the validation period; the root mean square error RMSE of the first-guess model (RMSE = 0.9°C) was improved in the calibrated model up to RMSE = 0.4°C and maintained in the validation period; the CV-RMSE of the first-guess model (CV-RMSE = 3.6%) was improved in the calibrated model up to coefficient of variation CV-RMSE = 1.7% in the calibration period and to CV-RMSE = ++1.4% in the validation period. Finally, the Spearman's rank correlation coefficient between modelled and measured data (r_s) was higher than 0.8 for both the models. The building model resulted to be well calibrated, since the discrepancy between modelled and measured data was equal to the instrumental uncertainty (Table 4.1).

TABLE 6.3. Summary statistics of air temperature simulated with the thermal models of Collegio Romano in comparison with the measurements. MAE: mean absolute error; RMSE: root mean square error; CV-RMSE: coefficient of variation of RMSE; r_s: Spearman's rank correlation coefficient.

	First guess	Calibration	Validation
MAE	0.9°C	0.3°C	0.3°C
RMSE	0.9°C	0.4°C	0.4°C
CV-RMSE	3.6%	1.7%	1.4%
r_s	1.0	0.9	0.8

Hygrothermal model of paper collections

A preliminary sensitivity analysis (SA) on the hygrothermal model of a wall made in paper was performed to identify the most relevant hygrothermal parameters in the model influencing the moisture gradients across the paper wall (ΔRH), thus allowing to select among the various hygrothermal properties found in literature (Table 4.3). The SA results (Figure 6.6) showed that the equilibrium moisture content at RH=80% (w_{80}), the equilibrium moisture content at saturation (w_f) and the vapour diffusion resistance factor (μ) can have a significant but low impact on the RH gradient (ΔRH) among the outermost sub-layers of a paper wall (ΔRH L(N/8)); the remaining hygrothermal properties seem to have a negligible effect on the chosen output [158].

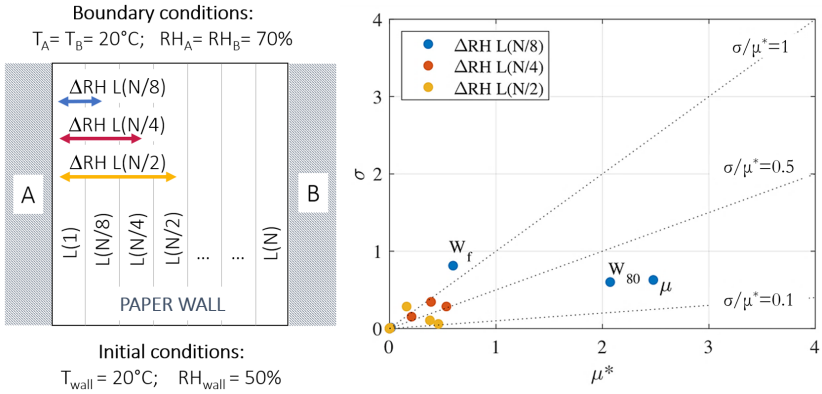

FIGURE 6.6. Scheme of the configuration of a paper wall model divided into N sub-layers (left); results of the sensitivity analysis (right) in terms of the mean (μ^*) and the standard deviation (σ) of the Elementary Effects (EE) calculated on the RH gradients (ΔRH) after one month at the steady-state conditions described in a) with N=63 [156].

In the light of the above considerations, further measurements were conducted to define the sorption isotherms of cellulose paper and to verify the extent of the dependency from temperature on the fitting value of these parameters [74]. Figure 6.7 shows the isotherms obtained at 15°C, 25°C and 30°C on a modern cellulose paper sample taken from the mock-up book. Since the influence of temperature on the adsorption branch of the isotherms of paper can be considered low, it was neglected in the modelling.

The set of hygrothermal parameters given in [67, 68] was used for the simulation because more complete. However, the input values for w_{80} and w_f were adjusted based on the sorption measurement (w_{80}=75 kg/m^3 and w_f=106 kg/m^3). These values were fitted using the HMWall moisture storage curve (Equation 4.6), so that the discrepancy between the measured and simulated equilibrium water content values (w) was minimized at a benchmark value of

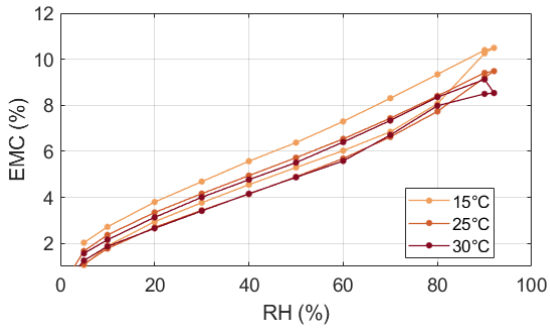

FIGURE 6.7. Sorption isotherms of paper at various temperatures: Equilibrium Moisture Content (EMC) of paper as a function of relative humidity measured on the same pure-cellulose paper used in the mock-up book monitored in Collegio Romano.

RH=40%, i.e., around the annual average RH in Collegio Romano (Figure 5.1). It has to be borne in mind that the HMWall curve (used in our simulation) is an approximating moisture storage function validated for building materials [83, 97]. Although other fitting equations may be able to more accurately reproduce the hygroscopic behaviour of paper [68, 160], the capability of HMWall to simulate moisture exchanges in paper was explored as it can be integrated into whole-building models.

The paper wall model was then tested in the simulation of the RH values inside the mock-up book monitored in Collegio Romano. The paper wall model was preconditioned to RH=44.5%, i.e., the average RH value measured inside the mock-up book over a year (Figure 6.8).

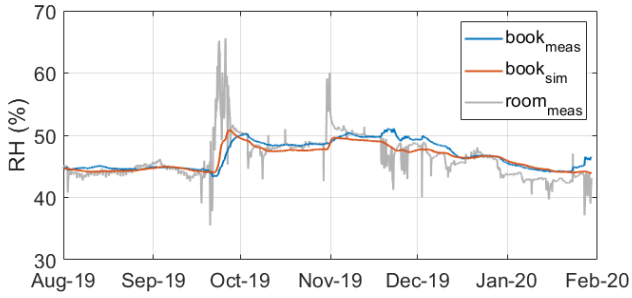

FIGURE 6.8. Observations (book$_{meas}$) *versus* simulated (book$_{sim}$) RH values inside the mock-up book in Collegio Romano modelled using RH conditions collected in the room (room$_{meas}$).

As shown in Figure 6.8, the model satisfactorily simulates the RH conditions inside the mock-up book. The value of A_w, i.e., the water absorption coefficient, was adjusted to the value of 0.007 kg·m^{-2}·s$^{-0.5}$ after having performed a

parametric analysis to fine-tune modelled and measured RH values. Although not significant in terms of the uncertainty associated to the measurements, it is worth to notice that the modelled RH values slightly differed from the RH observations in the second half of November 2019. In this occasion, it is reasonable to assume that paper released moisture to compensate the RH drop occurred in the room.

In Figure 6.9 are shown the RH values obtained across the high-resolution paper wall as a function of the duration of boundary adiabatic conditions (T=20°C) and of a steady-state RH gradient from the preconditioning value (RH=50%) to RH=70%. The RH distribution within the paper wall evolves slowly, showing a significant variation starting from one week of prolonged exposure and reaching the full equilibrium between the bulk and the surfaces only after several years.

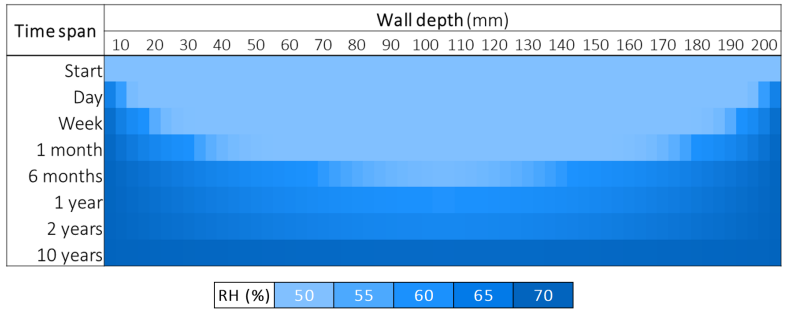

Figure 6.9. Relative humidity values inside the paper wall due to moisture uptake as a function of the duration of the steady-state boundary conditions described in Figure 6.6a [156].

The influence of transient boundary conditions was also investigated for the case of a single paper wall having 63 equally-spaced sub-layers and being initially conditioned to Twall=20°C and RHwall=50% [156]. The configuration was tested at boundary constant temperature T=20°C and RH conditions periodically ranging from 30% to 70% at weekly, monthly and seasonal frequency. The results emphasised that the first 5 sub-layers (corresponding to the first 15 mm from the wall surface) are the most responsive to the external transient forcing. More insight on this investigation is provided in Appendix C.

Even if high-resolution models can provide more accurate results, they would require much computation effort to run the simulation when included in whole-buildings. For this reason, a simplified paper wall model was proposed as schematized in Figure 6.10. The simplified paper wall model has a reduced number of unequally-spaced sub-layers. The first 5 sub-layers located under the surfaces A and B (i.e., L(A) and L(B)) are assigned the same thickness as that of the high-resolution reference sub-layers (3 mm). The impact of the inner

layers' thickness on the outputs was tested and found to be negligible [156]. Hence, the minimum number of 3 was chosen for the inner sub-layers.

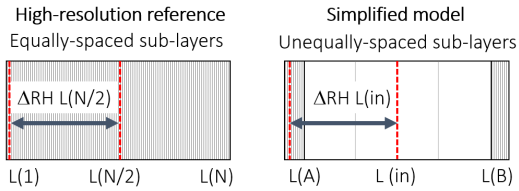

FIGURE 6.10. Scheme of the high-resolution paper wall divided into equally-spaced sub- layers (left) and the simplified paper wall divided into a reduced number of unequally-spaced sub-layers (right) [156].

The simplified model was tested in comparison with the high-resolution reference in terms of the RH gradient between the surface and the centre of the paper wall [156]. As explained in Figure 6.10, the gradient ΔRH L(N/2) of the high-resolution paper wall was calculated as the difference between the RH of the exterior sub-layer L(1) and that of the central sub-layer L(N/2), while the gradient ΔRH L(in) of the simplified paper wall model was calculated as the difference between the RH of the exterior sub-layer L(A) and that of the central sub-layer L(in).

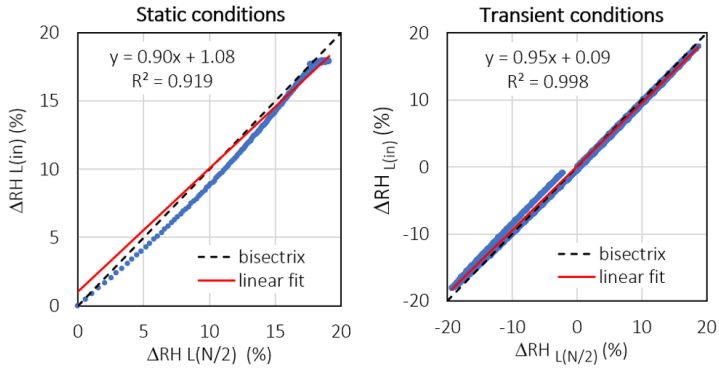

FIGURE 6.11. Scatterplot of hourly relative humidity gradients between the surface and the bulk of a paper wall over a year at the steady-state conditions described in Figure 6.6a (left) and at transient seasonal conditions. ΔRH L(N/2) and ΔRH L(in) refer respectively to the RH gradients of a high-resolution model with N=63 equally-spaced sub-layers and of a simplified model with N=13 unequally-spaced sub-layers [156].

Figure 6.11 shows a scatterplot of the ΔRH L(N/2) *versus* ΔRH L(in) calculated on a hourly basis over a year at both steady-state and transient seasonal conditions. The linear curve fitted on the results points out that the gradients in the simplified paper wall accurately reproduce those obtained with the high-resolution reference, therefore the proposed model can be used as a reliable

alternative to reduce the simulation effort without losing accuracy in the results [156].

The hygrothermal model simulating the behaviour of paper collections can be exploited to evaluate the distribution of RH values inside a paper wall. In this way, it can be used to qualitatively assess the extent of the potential mechanical risk due to RH cycles monitored inside libraries (Chapter 7). Moreover, it can be integrated in whole-building models to take into account the buffering effect of paper collections on the RH conditions in libraries and archives. To this aim, an investigation using exercises at increasing complexity is currently under development to define the most effective method to integrate the hygroscopic collections in the hygrothermal models.

Chapter 7

Climate-induced risk assessment

Mechanical deterioration

The mechanical risk in the libraries was evaluated by reconstructing the historic microclimate according to the European Standard EN 15757:2010 [7]. Since short-term fluctuations departed by less than 10% from seasonal RH levels (calculated as 30-day central moving average), the tolerance RH bands shown in Figure 7.1 were drawn as ±10% of the seasonal RH level.

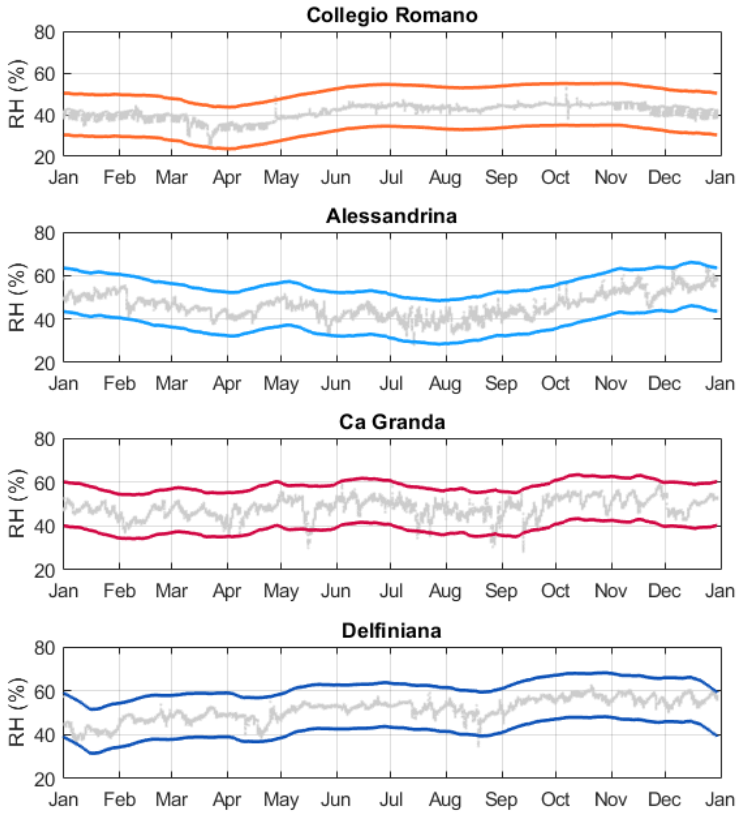

Figure 7.1. Allowable RH bands based on the historical climate [7] in the libraries under study.

The maximum allowable RH span during the year is equal to 31% in Collegio Romano (with RH ranging from 24% to 55%), 38% in Alessandrina (with RH ranging from 28% to 66% RH), 29% in Ca' Granda (with RH ranging from 34% to 63%) and 37% in Delfiniana (with RH ranging from 32% to 68%). Collegio Romano and Delfiniana were extremely stable and the RH observations never approached the limit bands of the standard. Collegio Romano reached the lowest RH values (RH<30%) in the second half of March because of a prolonged MR drop registered outdoor (from 8.7 g/kg on March 12th to 2.1 g/kg on March 22nd). This RH drop (measured in the room) was observed inside the mock-up book as a RH decrease from 40% to 36%. The RH observations in Ca' Granda were found to lay below the lower limit band (but never below 34%) on three single events from May to September, in association with outdoor MR drops.

The information on the historical climate (Figure 7.1) in the libraries can have a relevant impact on the management of the collections. Indeed, it is useful in the case of loan and consultation, supporting the definition of allowable RH fluctuations to avoid mechanical risks to the vulnerable objects when the items are moved to spaces characterised by different hygrothermal conditions.

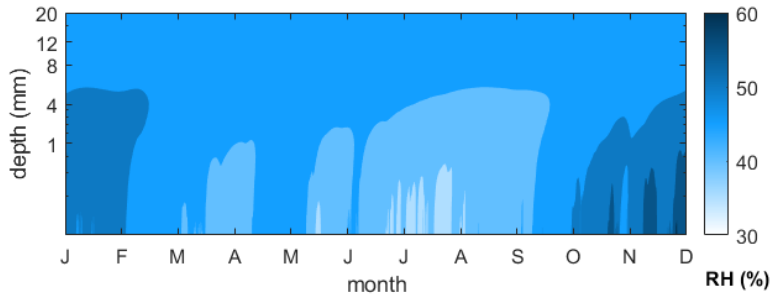

Figure 7.2. Distribution of relative humidity inside a paper wall exposed to the microclimate in Alessandrina over a year (y-axis not equally spaced) .

The hygrothermal model of a paper wall (described in Chapter 6) was used to evaluate the effect of the RH fluctuations registered in Alessandrina on the RH distribution inside the paper collection Figure 7.2, following the same approach proposed in Appendix B. The paper wall was preconditioned for one year to the annual RH of the library (RH=46%) and connected to one face to the RH values registered in 2020 (while keeping the other face constant at the initial value). Both the faces were assumed to be in equilibrium with the T observations in the library. The results showed that only the first 4 mm of paper exposed to the library conditions experienced RH fluctuations, while the deeper paper layers remained stable at the annual RH average value.

According to the statistics on the loans and consultation in Alessandrina in

2019 [114], more than 2500 volumes were moved out from the repository and handled. Based on the average preservation conditions of paper (in terms of the degree of polymerisation), it could be possible to establish the maximum allowable frequency of use for each item as a function of the chosen durability horizon (Table 4.4).

Chemical deterioration

Since it was not possible to measure the acidity and degree of polymerisation of the paper collections (due to technical and budget limitations), an exploratory matrix of TWEL values was calculated from T and RH observations in the historic libraries by combining the typical average values of pH of acidic (pH=5), neutral (pH=7) and basic (pH=8) paper types with the average degree of polymerisation of paper conditions classified as critical (DP=600), fair (DP=1500) and good (DP=2000).

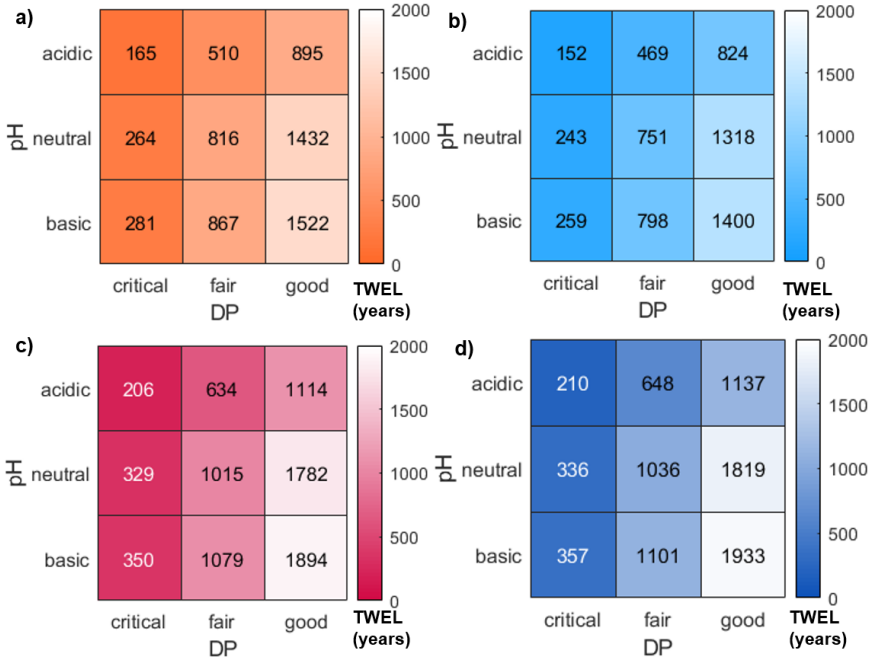

FIGURE 7.3. Exploratory matrix of TWEL values obtained combining typical average values of acidity (pH) and degree of polymerisation (DP) of various paper types at the yearly microclimate conditions in Collegio Romano (a), Alessandrina (b), Ca' Granda (c) and Delfiniana (d).

Figure 7.3 shows the TWEL matrixes to evaluate the risk of cellulose hydrolysis associated with the annual T and RH observations collected in the libraries. The TWEL matrixes highlighted that the chemical risk can be relevant

for all the paper-based objects having DP < 600 (critical), with a reduction of the expected lifetime of the most acidic ones below 200 years in Collegio Romano and Alessandrina. On the contrary, for paper-based objects having DP from fair to good, the chemical risk was found to be compatible with the 500-year horizon typical of preventive conservation strategies.

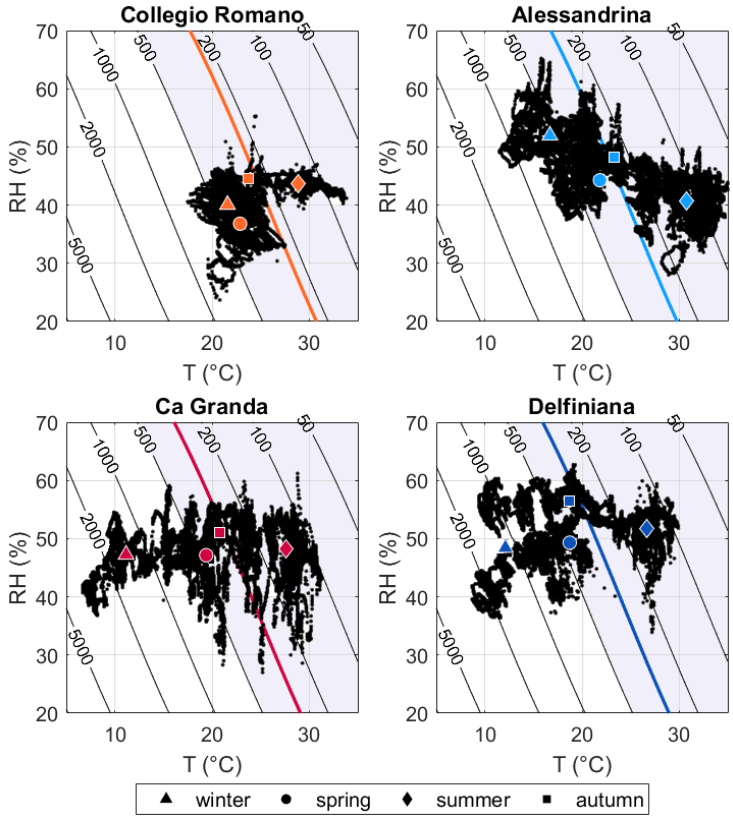

FIGURE 7.4. Temperature and relative humidity observations (black dots) plotted on the isochrones of expected lifetime for acidic paper (pH=5.2, DP=826.3), together with the yearly (coloured curves) and seasonal (coloured markers) TWEL values. Shaded area: T and RH conditions where EL is below the preservation horizon of 500 years.

In Figure 7.4 the temperature and relative humidity observations collected in the libraries were plotted over the isochrones for acidic paper collections to evaluate the expected lifetime associated with the indoor climates. The TWEL index was used to average the overall chemical risk on both a yearly and a seasonal basis. The value of TWEL in winter was equal to 400 years in Collegio Romano and to 566 years in Alessandrina, while it exceeded 1000 years in Ca' Granda and Delfiniana, where the heating systems were not in use. In summer, the durability for acidic collections was less than 150 years in all the libraries.

The TWEL values in spring and autumn spanned approximately between 200 and 400 years. It is worth noticing that, since the calculation of TWEL does not linearly weight the expected lifetime over time, lower values of EL have a higher influence on the final output, thus considering a worst-case scenario [158]. For this reason, although the winter TWEL values in Ca' Granda and Delfiniana were more than three times higher than in Collegio Romano, the yearly TWEL values in all the libraries were below 300 years and comparable in magnitude (235 years in Collegio Romano, 267 years in Alessandrina, 293 years in Ca' Granda and 299 years in Delfiniana). In Ca' Granda, the heat accumulation observed in summer (Figure 5.3) caused the yearly TWEL near the ceiling to be reduced of a further 5% with respect to the TWEL at 1.4 m above floor. These results better highlighted not only that winter heating should be avoided whenever possible as a preventive conservation measure, but also that it is necessary to reduce indoor temperatures exceeding 20°C in order to significantly mitigate the risk of cellulose hydrolysis. Moreover, the comparison among the libraries showed that the natural unconditioned indoor climates within historic buildings are preferable and thus could be suggested as a sustainable and effective preservation strategy for paper collections [158].

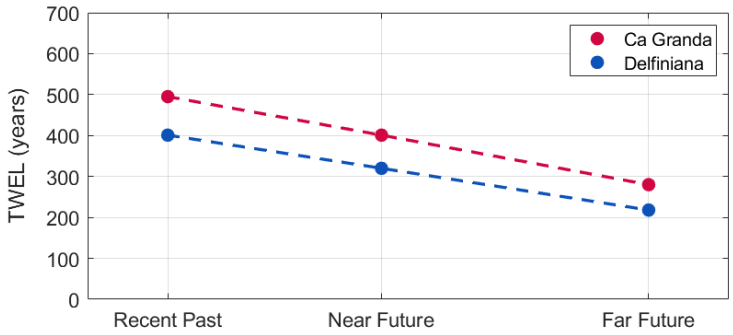

FIGURE 7.5. Potential chemical risk for acidic paper in the Recent Past (1981-2010), Near Future (2021-2050) and Far Future (2071-2100) in terms of the Time Weighted Expected Lifetime (TWEL).

The inversely simulated T and MR conditions were used to qualitatively evaluate the evolution of the potential chemical risk for acidic paper in Ca' Granda and Delfiniana (Figure 7.5) from the Recent Past (1981-2010) to Near Future (2021-2050) and Far Future (2071-2100). Even without considering the years passing between past and future scenarios, the durability of acidic paper could be reduced up to -43% of the initial value in Ca' Granda (TWEL from 495 to 280 years) and -46% in Delfiniana (TWEL from 401 to 218 years).

Biological deterioration

In Figure 7.6 the maximum daily T and RH values collected in the libraries over a year were compared to the lowest isopleths for spore germination and mycelium growth at optimal substrate according to Sedlbauer [154]. Based on the results, the risk of fungal colonisation could be excluded. However, it has to be borne in mind that in microenvironments with low ventilation and on cold metal surfaces (e.g., the shelves used in Alessandrina) could proliferate xerophilic fungal species with high tolerance to water stress [113, 115, 126].

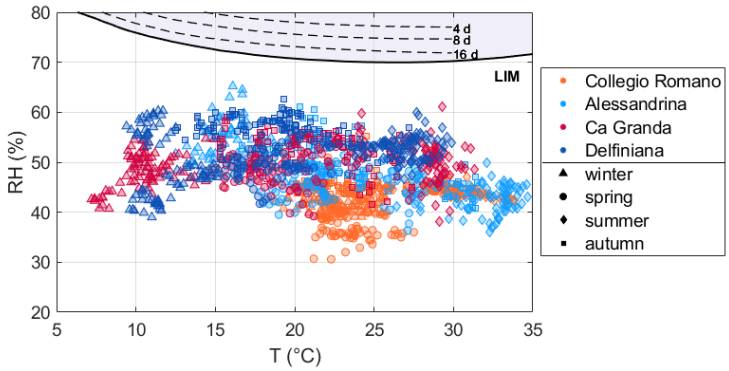

FIGURE 7.6. Daily maximum T and RH observations in the libraries compared to the lowest isopleths for spore germination at optimal substrate [154]. Shaded area: RH conditions exceeding the threshold favourable to fungal decay.

The risk of insect proliferation was estimated in Figure 7.7 as a function of the monthly T average values in the libraries according to Equation 4.9. The expected number of eggs laid by the webbing cloth moth (*Tineola bisselliella*) was found to be higher from May to September and lower from November to April. Only in Collegio Romano insect can potentially proliferate all over the year thanks to T>20°C. In Alessandrina, a slight inversion of the trend was observed in August due to T>30°C (see also Appendix F).

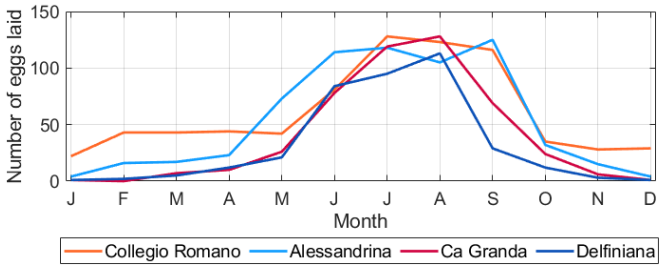

FIGURE 7.7. Number of eggs laid by the webbing cloth moth (*Tineola bisselliella*) as a function of the average monthly temperature values in the libraries [45].

Photodeterioration

In Table 7.1 are summarised the total color difference (ΔE^*) measured on the 5 book covers shown in Figure 4.8 over the experimental program. The ΔE^* did not significantly change after one year, meaning that the discolouration rate was already too low to be observed in such a short time window.

TABLE 7.1. Colour changes (ΔE^*) measured on 5 book covers in Alessandrina from October 2019 to October 2020 (mean ± half maximum spread).

Book cover	ΔE^*
1	128 ± 2
2	32 ± 4
3	34 ± 7
4	94 ± 1
5	78 ± 4

For this reason, the target sample of green cardboard (Figure 7.8) exposed to light in the same position as the monitored book covers from October 2019 to October 2020 was useful to qualitatively estimate the risk of photodeterioration to which the collections were subject.

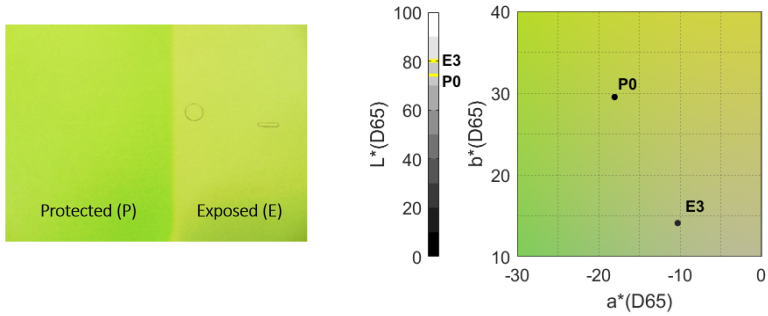

FIGURE 7.8. Colorimetric coordinates of the points measured on the green sample exposed to light in Alessandrina from October 2019 (P0) to October 2020 (E3).

The colour change observed on the green sample followed a typical exponential trend (Figure 7.9), with ΔE^* rapidly drifting from the initial conditions (P0) in the first 4 months of sun exposure (E1) and then slowly decreasing the rate of colour change in the following spring and summer months, even if the sample was likely exposed to a higher dose of sun radiation (E2 and E3). These results highlighted the high dose of solar radiation hitting part of the collection deployed in the E-facing side of the building (Figure 4.1). For this reason, it is advisable to substitute the UV-filter screens applied on the glasses as well as providing curtains to the windows.

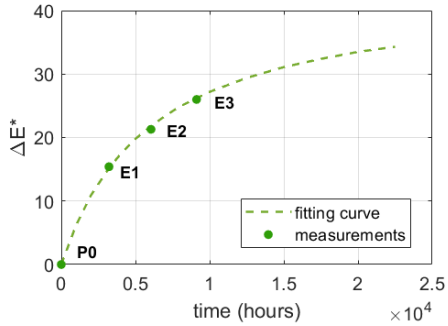

Figure 7.9. Total color difference ΔE^* measured on the green sample as a function of time. The measured data (dots) are fitted using the curve in Equation 4.11. P0=protected area (October 2019) and E1, E2, E3=areas exposed to light (February, June and October 2020, respectively).

Synthetic overview on climate-induced deterioration

The Risk Index (RI) defined in Appendix E was adjusted to the case of historic libraries and used to synthetically visualise climate-induced deterioration risks on a yearly basis. The chemical RI was computed as the percentage of time in which the microclimate conditions caused the expected lifetime for various paper types (i.e., acidic, rag and contemporary) to be less than 500 years [148]. For the risk of insect proliferation, RI was calculated as number of eggs laid by the webbing cloth moths every month compared to the theoretical maximum annual number of eggs according to the model [45]. Finally, the fungal colonisation risk was expressed as the percentage of time in which mould germination could occur [154]. Mechanical deterioration was not taken into account as it is usually considered to be not a priority in library conservation [108].

Figure 7.10 shows the radar plots with the Risk Index obtained in the libraries to compare the overall climate-induced risk in conditioned (Collegio Romano and Alessandrina) and unconditioned (Ca' Granda and Delfiniana) historic buildings. Collegio Romano and Alessandrina were associated to a severe risk of acidic paper hydrolysis (RI=94% and 80%, respectively) and insect proliferation (RI=47% and 41%, respectively). As already discussed, these risks are mainly driven by temperature, which was always higher in winter than in Ca' Granda and Delfiniana. The chemical risk for rag paper was around 30% in all the libraries, while for contemporary paper it was less than 10%. Mould germination was not of concern in the libraries. RI provided a fast and reliable diagnostic evaluation tool to more easily compare the magnitude of chemical and biological risks, providing a global characterisation of potential climate-induced deterioration in library contexts [79].

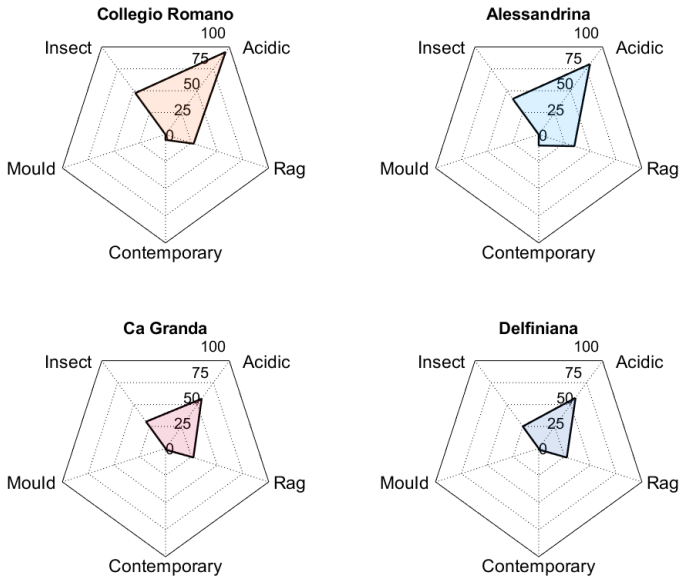

FIGURE 7.10. Radar plot of the Risk Index (%) calculated on a yearly basis for the cellulose hydrolysis of acidic, rag and contemporary paper-based collections and for the biological risk due to mould and insects proliferation.

Trade-off between preservation and sustainability

The thermal model of Collegio Romano was used to study possible strategies to reduce deterioration risks and energy consumption without compromising people's comfort. The weighted function Ψ (Equation 4.15) was used to pinpoint trade-off solutions balancing preservation and sustainability. Since the model was validated only for temperature, the risk of insect proliferation was chosen as the proxy for the deterioration potential. The period from July to December 2020 was considered in the analysis.

Five possible settings were hypothesised (Table 7.2) on the basis of the already installed HVAC systems in the library (i.e., radiators for heating and fan-coils for cooling) and compared to the actual situation (Baseline).

TABLE 7.2. Tested settings of the HVAC systems already existing in Collegio Romano.

Setting	Heating	Cooling
Baseline	5000 W	off
1	5000 W	3500 W
2	2500 W	3500 W
3	2500 W	off
4	off	3500 W
5	off	off

As for heating, the schedule for the radiators was kept the same as in Baseline, but in Setting 2 and 3 one of the two radiators was switched off. As for cooling, the schedule modulated the use of fan-coils in order to have them working during workdays from May to September at increasing power (from 25% at 7 a.m to 90% between 12 a.m and 6 p.m. and from 90% at 6 p.m. to 25% at 8 p.m). Setting 5, where both heating and cooling systems were switched off, was tested to simulate the natural microclimate established in the library in the absence of active climate control systems (i.e., in free-floating conditions) due only to the specific features of the building envelope and the air exchange rate.

Table 7.3. Risks associated with the microclimate simulated in five tested settings compared to the current situation (Baseline). Insect risk was estimated as the total number of eggs laid monthly by the webbing cloth moths. Energy consumption was calculated as the sum of heating and cooling loads. Discomfort of occupants was computed as the number of hours where T<18°C or T>27°C over 240 hours of expected presence of people. The weighted function Ψ was used to find the best-compromise solution, i.e., the one minimising the value of Ψ.

Setting	Insects (eggs)	Energy (kWh)	Discomfort (hours)	Ψ
Baseline	433	557	80	38%
1	211	2504	30	44%
2	204	2204	36	41%
3	407	349	110	35%
4	196	1749	48	36%
5	397	0	121	31%

Settings 1 and 2 obtained higher scores (i.e., a worse compromise) than the Baseline, as they reduce deterioration risks at the cost of increasing the total energy consumption up to 4.5 times (Table 7.3). For this reason, Settings 1 and 2 were considered as incompatible with the sustainability requirement. Setting 3 and 4 could be chosen as acceptable compromise solutions if considering that the climate control systems are not modern. Indeed, although the Setting 3 increased thermal discomfort in winter and Setting 4 energy consumption for cooling, they both slightly reduce the final value of Ψ with respect to the Baseline. It has to be highlighted that these settings would have obtained better scores if more efficient HVAC systems were available. In addition, in the chance of disposing of newer systems, the whole-building dynamic simulation could be used to define the most optimal schedules and setpoints for the climate control strategy. Setting 5 confirmed that the natural microclimate in historic buildings like Collegio Romano, as already observed in Ca' Granda in Milan and Delfiniana in Udine (Figure 7.4), is preferable for library preservation also at lower latitudes (Rome). In this last configuration, preservation and energy savings are improved, but discomfort in winter is intensified. The issue of thermal discomfort could be mitigated by reducing the presence of people inside the library and/or by providing conditioned reading rooms to consult

the materials. If for technical and management reasons this option would not be feasible, Setting 4 is more advisable than Setting 3, as it halves the risk of insects while keeping a reasonably equivalent compromise solution (based on the the obtained score of Ψ). In this latter case, upgrading the currently installed fan-coils with units relying on a more efficient technology is recommended to limit energy consumption.

Similar multi-optimisation approaches can be potentially exploited in other historic libraries, also considering different deterioration proxies (or combining more than one at the same time), thus providing a useful tool to pinpoint trade-off solutions able to balance preservation and sustainability. This synthetic evaluation can be effective only if carried out in combination with a thorough assessment of the current climate-induced risks for the collections. Indeed, the knowledge of the microclimate and its interactions with the objects is a necessary prerequisite to define the specific conservation priorities and to plan rational mitigation and adaptation strategies.

Part IV

Epilogue

Chapter 8

Conclusions and perspectives

Historic libraries require tailored methods to assess the climate-induced risk. Indeed, when it comes to study their microclimate, at least three peculiar features must be considered: 1) they are usually preserved in massive historic buildings; 2) their collections are mainly made of acid paper; 3) they typically conserve large amounts of hygroscopic materials (e.g., paper, cardboard, parchment), which contribute to buffer relative humidity by moisture exchanges.

The approach followed in this thesis integrated microclimate observations and modelling to support rational decision making for the preventive conservation of four historic libraries in Italy (Collegio Romano and Alessandrina in Rome, Ca' Granda in Milan and Delfiniana in Udine).

The comparative study involved a wide-ranging evaluation of the climate-induced risks affecting historic libraries, including mechanical, chemical and biological deterioration mechanisms, as well as colorimetric changes due to light exposure. Temperature was found to be a key microclimate stressor for the durability of paper collections, as it controls the rate of cellulose hydrolysis and favours insect proliferation. In terms of chemical deterioration of paper-based collections, the Time Weighted Expected Lifetime (TWEL) index was defined to quantitatively average the expected lifetime resulting from the indoor climate conditions over different time windows. It was found that the microclimate conditions monitored in all the libraries over an entire year would lead to the loss of their acidic paper in less than 300 years. However, the calculation of TWEL on a seasonal basis highlighted that winter heating, used in Collegio Romano and Alessandrina, markedly reduced the estimated expected lifetime (approximately to 500 years) with respect to the unconditioned climates of Ca' Granda and Delfiniana (where the TWEL values in the same season exceeded 1000 years). Relative humidity, on the contrary, could be considered safe for conservation as RH observations never exceeded 65% and RH fluctuations didn't depart by more than 10% from the seasonal levels. This result was further explored in simulation environment through the use of a hygrothermal model of a paper collection, which showed that moisture exchanges with the surrounding environment would affect only the first layers under the air-surface interface of the collection, showing a low impact on its mechanical deterioration risk. The

discolouration rate monitored on some faded book covers in the Alessandrina repository was already too low to be quantified over a single year; however, the estimated luminous exposure near the windows was found to be incompatible with the conservation of photosensitive materials, thus any deployment of unproofed materials on the shelves would be risky unless protections from direct solar exposure were to be installed.

Heat and moisture transfer functions were used to estimate the possible evolution of the future indoor microclimate in unconditioned historic libraries in view of the predicted climate change. It was found that the expected lifetime of acidic paper in the Far Future (2071-2100) could decrease up to -46% of the initial value in the Recent Past (1981-2010). A validated whole-building model of Collegio Romano allowed to reconstruct the natural climate in the library without the use of heating. The outcomes confirmed that, since historic buildings naturally smooth out the outdoor climate forcing, their natural unconditioned microclimate could be suggested in winter as a sustainable conservation measure (no energy consumption and carbon footprint impact). In addition, the whole-building model was used to investigate five different settings of the climate control systems that currently equip the room (i.e., radiators for winter heating and fan-coils for summer cooling). This study was useful to pinpoint a trade-off preventive conservation strategy balancing conservation needs, energy demand and thermal comfort.

To conclude, the integrated approach enabled to enhance the understanding of the role of climate on the preservation of historic libraries and provided a comprehensive insight on the impact of conditioned and unconditioned microclimates on the durability of paper collections. Although the investigation focussed on specific case studies, a similar approach could be adapted to most library and archival collections made of paper. Nonetheless, some considerations about the limitations of the study can be outlined. First, the limited number of instruments made it unfeasible to analyse the spatial differences in temperature, relative humidity and light intensity in the libraries. Moreover, it was not possible to measure the acidity and degree of polymerisation of paper collections in order to obtain more tailored application of the TWEL index. Finally, the use of the hygrothermal model of paper collections could be more informative if coupled with the whole-building model. This research is currently under development for the case of Collegio Romano by means of exercises with increasing complexity.

References

[1] HERIe 2.0. URL https://herie.pl/.

[2] UNI 10586. Climatic conditions for storage environments of graphic documents and features of the housings, 1997.

[3] UNI 10829. Properties of historical and artistic interest – environmental conservation – measurement and analysis, 1999.

[4] D. Lgs. 112/98 art. 150 comma 6. Guideline on technical and scientific criteria and standards of functioning and development of museum, 2001.

[5] D. Lgs. 42/2004. Codice dei beni culturali e del paesaggio, 2004.

[6] Damage risk assessment, economic impact and mitigation strategies for sustainable preservation of cultural heritage in the times of climate change, 2009-2014. URL https://www.climateforculture.eu/.

[7] EN 15757. Conservation of Cultural Property - Specifications for temperature and relative humidity to limit climate-induced mechanical damage in organic hygroscopic materials, 2010.

[8] Directive 2012/27/EU on energy efficiency, 2012.

[9] EN 16242. Conservation of cultural heritage - Procedures and instruments for measuring humidity in the air and moisture exchanges between air and cultural property, 2012.

[10] List of standards published by CEN/TC 346 on Conservation of Cultural Heritage, 2015. URL https://standards.cencenelec.eu/.

[11] ISO 11799. Information and documentation — Document storage requirements for archive and library materials, 2015.

[12] IFLA - Principles for the Care and Handling of Library Materials, 2016.

[13] BS 4971. Conservation and care of archive and library collections, 2017.

[14] EN 16883. Conservation of Cultural Heritage-Guidelines for Improving the Energy Performance of Historic Buildings, 2017.

[15] Directive 2018/2002/EU on energy efficiency, 2018.

[16] EN 16893. Conservation of cultural heritage - New sites and buildings intended for the storage and use of collections, 2018.

[17] Internet Culturale. Cataloghi e collezioni digitali delle biblioteche Italiane, 2018.

[18] ISO/TR 19815. Information and documentation — Management of the environmental conditions for archive and library collections, 2018.

[19] ASHRAE Handbook—HVAC Applications, Chapter 24. Museums, galleries, archives, and libraries, 2019.

[20] CollectionCare. Innovative and affordable service for the Preventive Conservation monitoring of individual Cultural Artefacts during display, storage, handling and transport, 2019-2022. URL https://www.collectioncare.eu/.

[21] I. Ait, M. V. Piñeiro, and S. Cavaciocchi. Costruire a Roma fra XV e XVII secolo, 2004.

[22] G. G. Akkurt, N. Aste, J. Borderon, A. Buda, M. Calzolari, D. Chung, V. Costanzo, C. Del Pero, G. Evola, H. E. Huerto-Cardenas, F. Leonforte, A. Lo Faro, E. Lucchi, L. Marletta, F. Nocera, V. Pracchi, and C. Turhan. Dynamic thermal and hygrometric simulation of historical buildings: Critical factors and possible solutions. *Renewable and Sustainable*

Energy Reviews, 118:109509, 2020. ISSN 18790690. doi: 10.1016/j.rser.2019.109509.

[23] M. Andretta, F. Coppola, and L. Seccia. Investigation on the interaction between the outdoor environment and the indoor microclimate of a historical library. *Journal of Cultural Heritage*, 2016. ISSN 12962074. doi: 10.1016/j.culher.2015.07.002.

[24] A. Angelotti, M. Ballabio, L. Mazzarella, C. Cornaro, G. Parente, F. Frasca, A. Prada, P. Baggio, I. Ballarini, G. De Luca, et al. Dynamic simulation of existing buildings: considerations on the model calibration. In *Building Simulation 2019 16th IBPSA Conference*, pages 4165–4172, 2020.

[25] J. Ashley-Smith. *Risk assessment for object conservation*. Routledge, 2013.

[26] J. Ashley-Smith. Report on newly gathered knowledge on damage functions. *Climate for Culture: Deliverable 4.1 Report on newly gathered knowledge about damage functions based on the various climate data interpretations existing throughout Europe*, 2013.

[27] C. Balocco and G. Volante. A method for sustainable lighting, preventive conservation, energy design and technology-Lighting a historical church converted into a university library. *Sustainability*, 11(11):1–17, 2019. ISSN 20711050. doi: 10.3390/su11113145.

[28] C. Balocco, G. Petrone, O. Maggi, G. Pasquariello, R. Albertini, and C. Pasquarella. Indoor microclimatic study for Cultural Heritage protection and preventive conservation in the Palatina Library. *Journal of Cultural Heritage*, 22:956–967, 2016. ISSN 12962074. doi: 10.1016/j.culher.2016.05.009.

[29] B. Bartl, L. Mašková, H. Paulusová, J. J. Smolík, L. Bartlová, and P. Vodička. The effect of dust particles on cellulose degradation. *Studies in Conservation*, 61(4):203–208, 2016. ISSN 20470584. doi: 10.1179/2047058414Y.0000000158.

[30] H. E. Beck, N. E. Zimmermann, T. R. McVicar, N. Vergopolan, A. Berg, and E. F. Wood. Present and future Köppen-Geiger climate classification maps at 1-km resolution. *Scientific Data*, 5:1–12, 2018. ISSN 20524463. doi: 10.1038/sdata.2018.214.

[31] N. Bell, M. Cassar, and M. Strlič. Evidence for Informed Preservation Planning and Advocacy: A Synoptic View. *Studies in Conservation*, 63:8–14, 2018. ISSN 20470584. doi: 10.1080/00393630.2018.1475099.

[32] M. C. Beltrano, G. Dal Monte, S. Esposito, and L. Iafrate. The CRA-CMA archive and library for agricultural meteorology and phenology: A heritage to know, preserve and share. *Ital. J. Agrometeorol*, 17(3):15–24, 2012.

[33] M. C. Beltrano, S. Esposito, and L. Iafrate. The archive and library of the former Italian Central Office for Meteorology and Climatology. *Advances in Science and Research*, 8(1): 59–65, 2012. ISSN 1992-0636. doi: 10.5194/asr-8-59-2012.

[34] C. Bertolin. Il ruolo del microclima nella conservazione del patrimonio librario e archivistico. Il caso della Biblioteca Delfiniana nel palazzo Arcivescovile di Udine. In *Proceedings of the International Conference "Clima negli edifici di culto. Esperienze e prospettive" (Venice, 2018). Sovrintendenza di Trieste*. Mimesis.

[35] C. Bertolin. Preservation of cultural heritage and resources threatened by climate change, 2019.

[36] C. Bertolin and A. Loli. Sustainable interventions in historic buildings: A developing decision making tool. *Journal of Cultural Heritage*, 34:291–302, 2018.

[37] C. Bertolin, D. Camuffo, and I. Bighignoli. Past reconstruction and future forecast of domains of indoor relative humidity fluctuations calculated according to EN 15757:2010. *Energy and Buildings*, 2015. ISSN 03787788. doi: 10.1016/j.enbuild.2015.05.028.

[38] C. Bertolin, L. De Ferri, G. Grottesi, and M. Strojecki. Study on the conservation state of wooden historical structures by means of acoustic attenuation and vacuum microbalance. *Wood Science and technology*, 54(1):203–226, 2020.

[39] C. Bertolin, L. De Ferri, and M. Strojecki. Application of the Guggenheim, Anderson, de

Boer (GAB) equation to sealing treatments on pine wood. *Procedia Structural Integrity*, 26: 147–154, 2020.

[40] J. M. Bloom. Papermaking: The Historical Diffusion of an Ancient Technique. pages 51–66. 2017. doi: 10.1007/978-3-319-44654-7_3.

[41] E. Bosco, R. Peerlings, and M. Geers. Hygro-mechanical properties of paper fibrous networks through asymptotic homogenization and comparison with idealized models. *Mechanics of Materials*, 108:11–20, 2017.

[42] E. Bosco, R. Peerlings, B. Lomans, C. van der Sman, and M. Geers. On the role of moisture in triggering out-of-plane displacement in paper: From the network level to the macroscopic scale. *International Journal of solids and Structures*, 154:66–77, 2018.

[43] Ł. Bratasz, A. Kozłowska, and R. Kozłowski. Analysis of water adsorption by wood using the Guggenheim-Anderson-de Boer equation. *European Journal of Wood and Wood Products*, 70(4):445–451, 2012. ISSN 00183768. doi: 10.1007/s00107-011-0571-x.

[44] Ł. Bratasz, T. White, S. Butts, C. Sease, N. Utrup, R. Boardman, and S. Simon. Toward Sustainable Collections Management in the Yale Peabody Museum: Risk Assessment, Climate Management, and Energy Efficiency. *Bulletin of the Peabody Museum of Natural History*, 59(2):249–268, oct 2018. ISSN 0079-032X. doi: 10.3374/014.059.0206.

[45] P. Brimblecombe and P. Lankester. Long-term changes in climate and insect damage in historic houses. *Studies in Conservation*, 58(1):13–22, 2013. ISSN 00393630. doi: 10.1179/2047058412Y.0000000051.

[46] A. Buda, E. J. d. P. Hansen, A. Rieser, E. Giancola, V. N. Pracchi, S. Mauri, V. Marincioni, V. Gori, K. Fouseki, C. S. López, A. L. Faro, A. Egusquiza, F. Haas, E. Leonardi, and D. Herrera-Avellanosa. Conservation-compatible retrofit solutions in historic buildings: An integrated approach. *Sustainability*, 13(5), 2021. ISSN 20711050. doi: 10.3390/su13052927.

[47] A. E. Bülow, B. J. Colston, and D. S. Watt. Preventive Conservation of Paper-Based Collections Within Historic Buildings. *Studies in Conservation*, 47:27–31, 2002. ISSN 0039-3630. doi: 10.1179/sic.2002.47.s3.006.

[48] D. Camuffo. *Microclimate for cultural heritage*. Elsevier, Amsterdam, 2019. ISBN 9780444632968.

[49] D. Camuffo and S. Vincenzi. Thermal structure inside a statue or column under stationary lighting. *Science of The Total Environment*, 53(3):179–191, 1986.

[50] D. Camuffo, C. Bertolin, A. Bonazzi, F. Campana, and C. Merlo. Past, present and future effects of climate change on a wooden inlay bookcase cabinet: A new methodology inspired by the novel European Standard EN 15757:2010. *Journal of Cultural Heritage*, 15 (1):26–35, 2014. ISSN 12962074. doi: 10.1016/j.culher.2012.12.005.

[51] D. Camuffo, A. della Valle, C. Bertolin, and E. Santorelli. Temperature observations in Bologna, Italy, from 1715 to 1815: a comparison with other contemporary series and an overview of three centuries of changing climate. *Climatic Change*, 142(1-2):7–22, 2017. ISSN 15731480. doi: 10.1007/s10584-017-1931-2.

[52] D. Camuffo, V. Fassina, and J. Havermans. *Basic environmental mechanisms: affecting cultural heritage: understanding deterioration mechanisms for conservation purposes*. Nardini, 2017.

[53] F. Cappitelli, P. Fermo, R. Vecchi, A. Piazzalunga, G. Valli, E. Zanardini, and C. Sorlini. Chemical–physical and microbiological measurements for indoor air quality assessment at the ca'granda historical archive, milan (italy). *Water, air, and soil pollution*, 201(1): 109–120, 2009.

[54] M. Carlessi and A. Kluzer. Il cuore dell'antico Ospedale Maggiore di Milano. *I luoghi*, 2011.

[55] A. Cherchi, P. G. Fogli, T. Lovato, D. Peano, D. Iovino, S. Gualdi, S. Masina, E. Scoccimarro, S. Materia, A. Bellucci, et al. Global mean climate and main patterns of variability in the cmcc-cm2 coupled model. *Journal of Advances in Modeling Earth Systems*, 11(1):185–209, 2019.

[56] R. E. Child. Insect damage as a function of climate. *Museum Microclimates*, pages 57–60, 2007.

[57] I. Cianchetta, I. Colantoni, F. Talarico, F. D'Acapito, A. Trapananti, C. Maurizio, S. Fantacci, and I. Davoli. Discoloration of the smalt pigment: Experimental studies and ab initio calculations. *Journal of Analytical Atomic Spectrometry*, 27(11):1941–1948, 2012. ISSN 02679477. doi: 10.1039/c2ja30132f.

[58] G. B. A. Coelho, H. E. Silva, and F. M. A. Henriques. Calibrated hygrothermal simulation models for historical buildings. *Building and Environment*, 142(June):439–450, 2018. ISSN 03601323. doi: 10.1016/j.buildenv.2018.06.034.

[59] R. J. Cole and M. Jose Valdebenito. The importation of building environmental certification systems: international usages of breeam and leed. *Building Research & Information*, 41(6):662–676, 2013.

[60] F. Coppola, N. Brown, F. Amicucci, M. Strlič, and A. Modelli. Non-destructive collection survey of the historical Classense Library. Part II: Conservation scenarios. *Heritage Science*, 8(1):1–10, 2020. ISSN 20507445. doi: 10.1186/s40494-020-00430-y.

[61] C. Cornaro, A. Paravicini, and A. Cimini. Monitoring indoor carbon dioxide concentration and effectiveness of natural trickle ventilation in a middle school in Rome. *Indoor and Built Environment*, 22(2):445–455, 2013. ISSN 1420326X. doi: 10.1177/1420326X11430099.

[62] C. Cornaro, F. Bucci, M. Pierro, F. Del Frate, S. Peronaci, and A. Taravat. Twenty-four hour solar irradiance forecast based on neural networks and numerical weather prediction. *Journal of Solar Energy Engineering*, 137(3), 2015.

[63] C. Cornaro, V. A. Puggioni, and R. M. Strollo. Dynamic simulation and on-site measurements for energy retrofit of complex historic buildings: Villa Mondragone case study. *Journal of Building Engineering*, 6:17–28, 2016. ISSN 23527102. doi: 10.1016/j.jobe.2016.02.001.

[64] R. Cornes, G. van der Schrier, E. van den Besselaar, and P. Jones. An Ensemble Version of the E-OBS Temperature and Precipitation Datasets. *Journal of Geophysical Research: Atmospheres*, 123, 2018. doi: 10.1029/2017JD028200.

[65] T. Coşkun, C. D. Şahin, Ö. Gülhan, Z. D. Arsan, and G. G. Akkurt. Ventilation Strategies for the Preventive Conservation of Manuscripts in the Necip Paşa Library, Izmir, Turkey. *Exergetic, Energetic and Environmental Dimensions*, pages 179–192, 2018. doi: 10.1016/B978-0-12-813734-5.00011-1.

[66] David Ribar in collaboration with the Heritage Science Lab Ljubljana and UCL Institute for Sustainable Heritage. Collections Demography App, 2015. URL https://hsll.shinyapps.io/collections_demography_app/.

[67] H. Derluyn, H. Janssen, J. Diepens, and D. Derome. Can Books and Textiles Help in Controlling the Indoor Relative Humidity? 2007.

[68] H. Derluyn, H. Janssen, J. Diepens, D. Derome, and J. Carmeliet. Hygroscopic behavior of paper and books. *Journal of Building Physics*, 31(1):9–34, 2007. ISSN 17442591. doi: 10.1177/1744259107079143.

[69] A. Di Bernardino, A. M. Iannarelli, S. Casadio, G. Mevi, M. Campanelli, G. Casasanta, A. Cede, M. Tiefengraber, A. M. Siani, E. Spinei, et al. On the effect of sea breeze regime on aerosols and gases properties in the urban area of rome, italy. *Urban Climate*, 37:100842, 2021.

[70] M. Dick, A. M. Rous, V. M. Nguyen, and S. J. Cooke. Necessary but challenging: multiple disciplinary approaches to solving conservation problems. *Facets*, 1(1):67–82, 2016.

[71] V. Eyring, S. Bony, G. A. Meehl, C. A. Senior, B. Stevens, R. J. Stouffer, and K. E. Taylor. Overview of the Coupled Model Intercomparison Project Phase 6 (CMIP6) experimental design and organization. *Geoscientific Model Development*, 9(5):1937–1958, 2016.

[72] K. Fabbri and M. Pretelli. Heritage buildings and historic microclimate without HVAC technology: Malatestiana Library in Cesena, Italy, UNESCO Memory of the World. *Energy and Buildings*, 2014. ISSN 03787788. doi: 10.1016/j.enbuild.2014.02.051.

[73] V. Fassina. CEN TC 346 Conservation of Cultural Heritage- Update of the Activity After a Height Year Period. 8:37–41, 2015. doi: 10.1007/978-3-319-09408-3.

[74] C. Feng, Q. Meng, H. Janssen, and Y. Feng. Effect of temperature on the sorption isotherm and vapor permeability. *2nd Central European Symposium on Building Physics*, (September 2013):71–76, 2013.

[75] J. Ferdyn-Grygierek and K. Grygierek. Proposed strategies for improving poor hygrothermal conditions in museum exhibition rooms and their impact on energy demand. *Energies*, 12(4), feb 2019. ISSN 19961073. doi: 10.3390/en12040620.

[76] F. Frasca, A. M. Siani, G. R. Casale, M. Pedone, Ł. Bratasz, M. Strojecki, and A. Mleczkowska. Assessment of indoor climate of Mogiła Abbey in Kraków (Poland) and the application of the analogues method to predict microclimate indoor conditions. *Environmental Science and Pollution Research*, 24(16):13895–13907, 2017. ISSN 16147499. doi: 10.1007/s11356-016-6504-9.

[77] F. Frasca, C. Cornaro, and A. M. Siani. A method based on environmental monitoring and building dynamic simulation to assess indoor climate control strategies in the preventive conservation within historical buildings. *Science and Technology for the Built Environment*, 25(9):1253–1268, 2019. ISSN 2374474X. doi: 10.1080/23744731.2019.1642093.

[78] F. Frasca, E. Verticchio, C. Cornaro, and A. M. Siani. Optimising Conservation of Artworks , Energy Performance and Thermal Comfort Combining Hygrothermal Dynamic Simulation and On-Site Measurements in Historic Buildings. In *Proceedings of the 16th IBPSA Conference*, pages 2856–2863, 2019.

[79] F. Frasca, E. Verticchio, A. Caratelli, C. Bertolin, D. Camuffo, and A. M. Siani. A comprehensive study of the microclimate-induced conservation risks in hypogeal sites: The mithraeum of the baths of Caracalla (Rome). *Sensors*, 20(11):1–18, 2020. ISSN 14248220. doi: 10.3390/s20113310.

[80] F. Frasca, E. Verticchio, C. Cornaro, and A. M. Siani. Performance assessment of hygrothermal modelling for diagnostics and conservation in an Italian historical church. *Building and Environment*, 193:107672, 2021. ISSN 03601323. doi: 10.1016/j.buildenv.2021.107672.

[81] F.-J. García-Diego, E. Verticchio, P. Beltrán, and A. M. Siani. Assessment of the minimum sampling frequency to avoid measurement redundancy in microclimate field surveys in museum buildings. *Sensors*, 16(8):1291, 2016.

[82] D. Garcia Sanchez, B. Lacarrière, M. Musy, and B. Bourges. Application of sensitivity analysis in building energy simulations: Combining first- and second-order elementary effects methods. *Energy and Buildings*, 68(PART C):741–750, 2014. ISSN 03787788. doi: 10.1016/j.enbuild.2012.08.048.

[83] A. Holm, H. M. Kuenzel, and K. Sedlbauer. The hygrothermal behaviour of rooms: combining thermal building simulation and hygrothermal envelope calculation. In *Eighth international IBPSA Conference*, volume 1, pages 499–505. Eindhoven Netherlands, 2003.

[84] S. H. Hong, M. Strlič, I. Ridley, K. Ntanos, N. Bell, and M. Cassar. Climate change mitigation strategies for mechanically controlled repositories: Thecase of The National Archives, Kew. *Atmospheric Environment*, 49:163–170, 2012. ISSN 13522310. doi: 10.1016/j.atmosenv.2011.12.003.

[85] H. E. Huerto-Cardenas, F. Leonforte, N. Aste, C. Del Pero, G. Evola, V. Costanzo, and E. Lucchi. Validation of dynamic hygrothermal simulation models for historical buildings:

State of the art, research challenges and recommendations. *Building and Environment*, 180 (June):107081, 2020. ISSN 03601323. doi: 10.1016/j.buildenv.2020.107081.

[86] H. E. Huerto-Cardenas, N. Aste, C. Del Pero, and S. Della Torre. Effects of Climate Change on the Future of Heritage Buildings : Case Study and Applied Methodology. 2021.

[87] Z. Huijbregts, M. Martens, A. Van Schijndel, and H. Schellen. Computer modelling to evaluate the risks of damage to objects exposed to varying indoor climate conditions in the past, present, and future. In *Proceedings of the 2nd Central European Symposium on Building Physics*, pages 9–11, 2013.

[88] ICCU. Statistics on library data. URL https://anagrafe.iccu.sbn.it/it/statistiche/statistiche-al-31-12-2020/.

[89] P. Ineichen, R. Perez, R. Seal, E. Maxwell, and A. Zalenka. Dynamic global-to-direct irradiance conversion models. *ASHRAE transactions*, 98(1):354–369, 1992.

[90] Istat. Istituto Nazionale di Statistica. Le biblioteche in Italia. Anno 2019, 2021. URL https://www.istat.it/it/files//2021/04/REPORT_BIBLIOTECHE-IN-ITALIA.pdf.

[91] Istituto Superiore per la Conservazione ed il Restauro. Vincoli in rete. URL http://vincoliinrete.beniculturali.it/.

[92] A. Khalid, G. F. Malik, and K. Mahmood. Sustainable development challenges in libraries: A systematic literature review (2000–2020). *Journal of Academic Librarianship*, 47(3): 102347, 2021. ISSN 00991333. doi: 10.1016/j.acalib.2021.102347.

[93] K. Kompatscher, R. Kramer, B. Ankersmit, and H. Schellen. Intermittent conditioning of library archives: Microclimate analysis and energy impact. *Building and Environment*, 2018. ISSN 03601323. doi: 10.1016/j.buildenv.2018.10.013.

[94] R. Kozłowski, A. Kupczak, A. Działo, Ł. Bratasz, and M. Łukomski. Herie: A decision-supporting tool based on quantitative assessment of damage risk. *The Mechanics of Art Materials and Its Future in Heritage Science*, page 21, 2019.

[95] E. L. Krüger and W. Diniz. Relationship between indoor thermal comfort conditions and the Time Weighted Preservation Index (TWPI) in three Brazilian archives. *Applied Energy*, 2011. ISSN 03062619. doi: 10.1016/j.apenergy.2010.09.011.

[96] M. Krus, R. Kilian, and K. Sedlbauer. Mould growth prediction by computational simulation on historic buildings. In *Museum Microclimates*, pages 185–189, 2007. ISBN 9788776020804.

[97] H. Künzel, A. Holm, D. Zirkelbach, and A. Karagiozis. Simulation of indoor temperature and humidity conditions including hygrothermal interactions with the building envelope. *Solar energy*, 78(4):554–561, 2005.

[98] A. Kupczak, Ł. Bratasz, J. Kryściak-Czerwenka, and R. Kozłowski. Moisture sorption and diffusion in historical cellulose-based materials. *Cellulose*, 25(5):2873–2884, 2018. ISSN 1572882X. doi: 10.1007/s10570-018-1772-9.

[99] A. Kupczak, A. Sadłowska-Sałęga, L. Krzemień, J. Sobczyk, J. Radoń, and R. Kozłowski. Impact of paper and wooden collections on humidity stability and energy consumption in museums and libraries. *Energy and Buildings*, 158:77–85, 2018. ISSN 03787788. doi: 10.1016/j.enbuild.2017.10.005.

[100] B. Library. *British Library Annual Report and Accounts 2020/21*. ISBN 9781528626958.

[101] S. López-Aparicio, J. Smolík, L. Mašková, M. Součková, T. Grøntoft, L. Ondráčková, and J. Stankiewicz. Relationship of indoor and outdoor air pollutants in a naturally ventilated historical building envelope. *Building and Environment*, 46(7):1460–1468, 2011.

[102] E. Lucchi. Multidisciplinary risk-based analysis for supporting the decision making process on conservation, energy efficiency, and human comfort in museum buildings, 2016. ISSN 12962074.

[103] E. Lucchi. Thermal transmittance of historical brick masonries: A comparison among

standard data, analytical calculation procedures, and in situ heat flow meter measurements. *Energy and Buildings*, 134:171–184, 2017. ISSN 03787788. doi: 10.1016/j.enbuild.2016.10.045.

[104] E. Lucchi. Review of preventive conservation in museum buildings. *Journal of Cultural Heritage*, 29:180–193, 2018.

[105] S. Maraghechi, E. Bosco, J. Hoefnagels, and A. Suiker. An in-depth insight of the mechanical response of cellulose fibres by means of optical profilometry techniques. In *Optics for Arts, Architecture, and Archaeology VIII*, volume 11784, page 1178415. International Society for Optics and Photonics, 2021.

[106] M. H. J. Martens. *Climate risk assessment in museums: degradation risks determined from temperature and relative humidity data*. PhD thesis, Technische Universiteit Eindhoven, 2012.

[107] L. Mazzarella. Energy retrofit of historic and existing buildings. the legislative and regulatory point of view. *Energy and Buildings*, 95:23–31, 2015. ISSN 03787788. doi: 10.1016/j.enbuild.2014.10.073.

[108] E. Menart, G. De Bruin, and M. Strlič. Dose-response functions for historic paper. *Polymer Degradation and Stability*, 2011. ISSN 01413910. doi: 10.1016/j.polymdegradstab.2011.09.002.

[109] G. Mergos, N. Patsavos, E. Camatsos, and G. Voulgaridis. Cultural heritage and sustainable development. *Technical University of Crete*, 2017.

[110] S. Michalski. Double the life for each five-degree drop, more than double the life for each halving of relative humidity. *Thirteenth Triennial meeting ICOM-CC*, (3):66–72, 2002.

[111] S. Michalski. The Ideal Climate, Risk Management, the ASHRAE Chapter, Proofed Fluctuations, and Toward a Full Risk Analysis Model. *Contribution to the Experts' Roundtable on Sustainable Climate Management Strategies, held in April 2007, in Tenerife, Spain*, (April 2007):1–19, 2007.

[112] S. Michalski and I. Karsten. The Cost-effectiveness of Preventive Conservation Actions. 2018. ISSN 2047-0584. doi: 10.1080/00393630.2018.1471894.

[113] A. Micheluz, S. Manente, V. Tigini, V. Prigione, F. Pinzari, G. Ravagnan, and G. C. Varese. The extreme environment of a library: Xerophilic fungi inhabiting indoor niches. *International Biodeterioration and Biodegradation*, 2015. ISSN 09648305. doi: 10.1016/j.ibiod.2014.12.012.

[114] Ministero per i Beni e le Attività Culturali e per il Turismo - Ufficio Statistica. Rilevazione biblioteche pubbliche statali 1999-2019. URL http://www.statistica.beniculturali.it/Biblioteche_pubbliche_statali.htm.

[115] M. Montanari, V. Melloni, F. Pinzari, and G. Innocenti. Fungal biodeterioration of historical library materials stored in Compactus movable shelves. *International Biodeterioration and Biodegradation*, 2012. ISSN 09648305. doi: 10.1016/j.ibiod.2012.03.011.

[116] R. Mora, L. J. Sánchez-Aparicio, M. Á. Maté-González, J. García-Álvarez, M. Sánchez-Aparicio, and D. González-Aguilera. An historical building information modelling approach for the preventive conservation of historical constructions: Application to the Historical Library of Salamanca. *Automation in Construction*, 121(May 2020), 2021. ISSN 09265805. doi: 10.1016/j.autcon.2020.103449.

[117] M. F. Nicoletti and P. C. Verde. *Pratiche architettoniche a confronto nei cantieri italiani della seconda metà del Cinquecento*. Officina libraria, 2019.

[118] D. W. Nishimura. Understanding Preservation Metrics. Technical report, Image Permanence Institute, Rochester Institute of Technology, 2011.

[119] I. Othmen, P. Poullain, and N. Leklou. Sensitivity analysis of the transient heat and moisture transfer in a single layer wall. *European Journal of Environmental and Civil*

Engineering, 24(13):2211–2229, 2020.

[120] R. K. Pachauri, M. R. Allen, V. R. Barros, J. Broome, W. Cramer, R. Christ, J. A. Church, L. Clarke, Q. Dahe, P. Dasgupta, et al. *Climate change 2014: synthesis report. Contribution of Working Groups I, II and III to the fifth assessment report of the Intergovernmental Panel on Climate Change*. Ipcc, 2014.

[121] T. Padfield, M. Ryhl-Svendsen, P. Klenz Larsen, and L. Aasbjerg Jensen. A Review of the Physics and the Building Science which Underpins Methods of Low Energy Storage of Museum and Archive Collections A Review of the Physics and the Building Science which Underpins Methods of Low Energy Storage of Museum and Archive Collections. 2018. ISSN 2047-0584. doi: 10.1080/00393630.2018.1504456.

[122] J. Paltakari and M. Karlsson. Determination of specific heat for dry fibre material. In *CPPA 82nd Annual Meeting Week 96, Convention Centre, Montréal, Canada, 30.1.-2.2. 1996*, pages s–B117, 1996.

[123] C. Pasquarella, C. Balocco, G. Pasquariello, G. Petrone, E. Saccani, P. Manotti, M. Ugolotti, F. Palla, O. Maggi, and R. Albertini. A multidisciplinary approach to the study of cultural heritage environments: Experience at the Palatina Library in Parma. *Science of the Total Environment*, 536:557–567, 2015. ISSN 18791026. doi: 10.1016/j.scitotenv.2015.07.105.

[124] D. Pinniger. *Pest Management in Museums, Archives and Historic Houses*. 2001.

[125] S. Piussi. Le Biblioteche del Capitolo cattedrale di Aquileia e del Capitolo collegiato di Udine ora del Capitolo metropolitano. (1753):25–56.

[126] A. Polo, F. Cappitelli, F. Villa, and F. Pinzari. Biological invasion in the indoor environment: the spread of Eurotium halophilicum on library materials. *International Biodeterioration and Biodegradation*, 2017. ISSN 09648305. doi: 10.1016/j.ibiod.2016.12.010.

[127] M. Posani, M. D. R. Veiga, and V. P. de Freitas. Towards Resilience and Sustainability for Historic Buildings: A Review of Envelope Retrofit Possibilities and a Discussion on Hygric Compatibility of Thermal Insulations. *International Journal of Architectural Heritage*, 0(0):1–17, 2019. ISSN 15583066. doi: 10.1080/15583058.2019.1650133.

[128] E. J. Quirijns, A. J. Van Boxtel, W. K. Van Loon, and G. Van Straten. Sorption isotherms, GAB parameters and isosteric heat of sorption. *Journal of the Science of Food and Agriculture*, 85(11):1805–1814, 2005. ISSN 00225142. doi: 10.1002/jsfa.2140.

[129] J. Radoń, P. Sadłowska-Sałęga, K. Wąs, A. Gryc, and A. Kupczak. Energy use optimization in the building of National Library. *IOP Conference Series: Materials Science and Engineering*, 415:012029, 2018. ISSN 1757-899X. doi: 10.1088/1757-899X/415/1/012029.

[130] S. Ramírez, M. Zarzo, A. Perles, and F.-J. García-Diego. Characterization of temperature gradients according to height in a baroque church by means of wireless sensors. *Sensors*, 21(20):6921, 2021.

[131] O. Y. Rieger. *Preservation in the Age of Large-Scale Digitization A White Paper*, volume 2006. 2008. ISBN 9781932326291.

[132] E. Rinaldi. *La fondazione del Collegio Romano: memorie storiche*. Cooperativa tipografica, 1914.

[133] D. Rodwell. The UNESCO world heritage convention, 1972–2012: reflections and directions. *The historic environment: policy & practice*, 3(1):64–85, 2012.

[134] C. Rogerson and P. Garside. Increasing the profile and influence of conservation—an unexpected benefit of risk assessments. *Journal of the Institute of Conservation*, 2017. ISSN 19455232. doi: 10.1080/19455224.2016.1214848.

[135] M. Ryhl-Svendsen, L. A. Jensen, P. K. Larsen, B. Bøhm, and T. Padfield. Ultra low energy museum storage. In *16th Triennial Meeting, ICOM Committee for Conservation, Lisbon*, pages 19–23, 2011.

[136] M. Sabater and Data. Era5-land hourly data from 1950 to 1980. *Copernicus Climate*

Change Service (C3S) Climate Data Store (CDS), 2021.

[137] A. Sadłowska-Sałęga and J. Radoń. Feasibility and limitation of calculative determination of hygrothermal conditions in historical buildings: Case study of st. martin church in wiśniowa. *Building and Environment*, 186:107361, 2020.

[138] C. D. Sahin, T. Coşkun, Z. D. Arsan, and G. Gökçen Akkurt. Investigation of indoor microclimate of historic libraries for preventive conservation of manuscripts. Case Study: Tire Necip Paşa Library, İzmir-Turkey. *Sustainable Cities and Society*, 30:66–78, 2017. ISSN 22106707. doi: 10.1016/j.scs.2016.11.002.

[139] D. G. Sanchez, B. Lacarrière, M. Musy, and B. Bourges. Application of sensitivity analysis in building energy simulations: Combining first-and second-order elementary effects methods. *Energy and Buildings*, 68:741–750, 2014.

[140] E. Schito, P. Conti, and D. Testi. Multi-objective optimization of microclimate in museums for concurrent reduction of energy needs, visitors' discomfort and artwork preservation risks. *Applied Energy*, 224:147–159, 2018. ISSN 03062619. doi: 10.1016/j.apenergy.2018.04.076.

[141] E. Schito, L. Dias Pereira, D. Testi, and M. Gameiro da Silva. A procedure for identifying chemical and biological risks for books in historic libraries based on microclimate analysis. *Journal of Cultural Heritage*, 2018. ISSN 12962074. doi: 10.1016/j.culher.2018.10.005.

[142] M.-A. Serrano, J.-L. Baró Zarzo, J.-C. Moreno Esteve, and F.-J. García-Diego. Spectral Relative Attenuation of Solar Radiation through a Skylight Focused on Preventive Conservation: Museo De L'Almoina in Valencia (Spain) Case Study. *Sensors*, 21(14):4651, 2021.

[143] S. H. Smedemark, M. Ryhl-Svendsen, and J. Toftum. Distribution of temperature, moisture and organic acids in storage facilities with heritage collections. *Building and Environment*, 175:106782, 2020.

[144] M. Steeman, M. De Paepe, A. Janssens, M. D. Paepe, and A. Janssens. Impact of whole-building hygrothermal modelling on the assessment of indoor climate in a library building. *Building and Environment*, 45(7):1641–1652, 2010. ISSN 03601323. doi: 10.1016/j.buildenv.2010.01.012.

[145] T. Strang and D. Grattan. Temperature and humidity considerations for the preservation of organic collections—the isoperm revisited. *E-Preservation Science*, 6:122–128, 2009.

[146] M. Strlič, D. Thickett, J. Taylor, and M. Cassar. Damage functions in heritage science. *Studies in Conservation*, 58(2):80–87, 2013. ISSN 00393630. doi: 10.1179/2047058412Y.0000000073.

[147] M. Strlič, C. M. Grossi, C. Dillon, N. Bell, K. Fouseki, P. Brimblecombe, E. Menart, K. Ntanos, W. Lindsay, D. Thickett, F. France, and G. De Bruin. Damage function for historic paper. Part II: Wear and tear. *Heritage Science*, 3(1):1–11, 2015. ISSN 20507445. doi: 10.1186/s40494-015-0065-y.

[148] M. Strlič, C. M. Grossi, C. Dillon, N. Bell, K. Fouseki, P. Brimblecombe, E. Menart, K. Ntanos, W. Lindsay, D. Thickett, F. France, and G. De Bruin. Damage function for historic paper. Part III: Isochrones. *Heritage Science*, 2015. ISSN 20507445. doi: 10.1186/s40494-015-0062-1.

[149] M. Strlič, Y. Liu, D. A. Lichtblau, G. De Bruin, B. Knight, T. Winther, I. Kralj Cigic, and R. G. Brereton. Development and mining of a database of historic European paper properties. *Cellulose*, 27:8287–8299, 2020. doi: 10.1007/s10570-020-03344-x.

[150] H. A. Taylor. The collective memory: archives and libraries as heritage. *Archivaria*, pages 118–130, 1982.

[151] K. E. Taylor. Summarizing multiple aspects of model performance in a single diagram. *Journal of Geophysical Research: Atmospheres*, 106(D7):7183–7192, 2001.

[152] D. Thickett, R. Soek-Joo, and S. Lambarth. Libraries and archives in historic buildings. *Museum Microclimates, The National Museum of Denmark, Copenhagen*, pages 145–156, 2007.

[153] S. VanSnick and K. Ntanos. On Digitisation as a Preservation Measure. *Studies in Conservation*, 63:282–287, 2018. ISSN 20470584. doi: 10.1080/00393630.2018.1504451.

[154] E. Vereecken and S. Roels. Review of mould prediction models and their influence on mould risk evaluation. *Building and Environment*, 51:296–310, 2012. ISSN 03601323. doi: 10.1016/j.buildenv.2011.11.003.

[155] E. Verticchio. Deliverable model of the BS2019 Student Modelling Competition, 2019. URL http://www.ibpsa.org/downloads/competitions/BS2019/individual.pdf.

[156] E. Verticchio, F. Frasca, F.-J. Garcìa-Diego, and A. M. Siani. Investigation on the Use of Passive Microclimate Frames in View of the Climate Change Scenario. *Climate*, 7(8):98, aug 2019. ISSN 2225-1154. doi: 10.3390/cli7080098.

[157] E. Verticchio, F. Frasca, C. Cornaro, and A. M. Siani. Investigation on the use of hygrothermal modelling for paper collections. *IOP Conference Series: Materials Science and Engineering*, 949(1), 2020. ISSN 1757899X. doi: 10.1088/1757-899X/949/1/012015.

[158] E. Verticchio, F. Frasca, C. Bertolin, and A. M. Siani. Climate-induced risk for the preservation of paper collections: Comparative study among three historic libraries in Italy. *Building and Environment*, 206:108394, 2021. ISSN 03601323. doi: 10.1016/j.buildenv.2021.108394.

[159] A. L. Webb. Energy retrofits in historic and traditional buildings: A review of problems and methods. *Renewable and Sustainable Energy Reviews*, 77:748–759, 2017. ISSN 18790690. doi: 10.1016/j.rser.2017.01.145.

[160] X. X. Zhang, W. Zillig, H. M. Künzel, X. X. Zhang, and C. Mitterer. Evaluation of moisture sorption models and modified Mualem model for prediction of desorption isotherm for wood materials. *Building and Environment*, 92:387–395, 2015. ISSN 03601323. doi: 10.1016/j.buildenv.2015.05.021.

Supporting equations

S.I Microclimate variables

Input parameters air temperature T (°C), relative humidity RH (%) or mixing ratio MR ($g \cdot kg^{-1}$), barometric pressure p (hPa)

Output parameters MR mixing ratio ($g \cdot kg^{-1}$) or relative humidity RH (%)

$$MR = 38.015 \times \frac{10^{\frac{7.65 \times T}{243.12+T}} \times RH}{p - (0.06112 \times 10^{\frac{7.65 \times T}{243.12+T}} \times RH)} \tag{1}$$

$$RH = \frac{MR \times p}{38.015 \times 10^{\frac{7.65 \times T}{243.12+T}} + 0.0612 \times 10^{\frac{7.65 \times T}{243.12+T}} \times MR} \tag{2}$$

S.II Dose-response functions

Input parameters activation energy E_a ($J \cdot mol^{-1}$), air temperature T (°C), relative humidity RH (%), perfect gas constant R ($8.314\ J \cdot mol^{-1} \cdot K^{-1}$)

Output parameters PI Preservation Index (-), LM Lifetime Multiplier (-)

$$PI = \frac{exp\left(\frac{E_a - 134.9 \times RH}{R \cdot T} + 0.0284 \times RH\right)}{365} \tag{3}$$

$$LM = \left(\frac{50\%}{RH}\right)^{1.3} \times e^{\left(\frac{E_a}{R}\left(\frac{1}{T} - \frac{1}{293.15}\right)\right)} \tag{4}$$

S.III Uncertainty indices for simulation accuracy

Input parameters measured data m_i, mean of measured data $\overline{m}$, simulated data s_i, mean of simulated data $\bar{s}$, number of data samples n

Output parameters MAE mean absolute error, RMSE root mean square error, CV-RMSE coefficient of variation of the RMSE (%), R^2 coefficient of determination, r correlation coefficient

$$MAE = \frac{\sum_{i=1}^{n} |m_i - s_i|}{n} \tag{5}$$

$$RMSE = \sqrt{\frac{\sum_{i=1}^{n} (m_i - s_i)^2}{n}} \tag{6}$$

$$CV - RMSE = \frac{1}{\overline{m}} \cdot \sqrt{\frac{\sum_{i=1}^{n} (m_i - s_i)^2}{n}} \cdot 100 \tag{7}$$

$$R^2 = 1 - \frac{\sum_{i=1}^{n} (m_i - s_i)^2}{\sum_{i=1}^{n} (m_i - \overline{m})^2} \tag{8}$$

$$r = \frac{\sum_{i=1}^{n} (m_i - \overline{m})(s_i - \overline{s})}{\sqrt{(m_i - \overline{m})^2} \sqrt{(s_i - \overline{s})^2}} \tag{9}$$

Appendix A

Climate-induced risk for the preservation of paper collections: Comparative study among three historic libraries in Italy

---

Verticchio, E., Frasca, F., Bertolin, C., and Siani, A.M.

Building and Environment **206**, 108394 (2021)

Building and Environment 206 (2021) 108394

Contents lists available at ScienceDirect

Building and Environment

journal homepage: www.elsevier.com/locate/buildenv

Climate-induced risk for the preservation of paper collections: Comparative study among three historic libraries in Italy

Elena Verticchio [a,*], Francesca Frasca [b], Chiara Bertolin [c], Anna Maria Siani [b]

[a] Department of Earth Sciences, Sapienza University of Rome, Rome, Italy
[b] Department of Physics, Sapienza University of Rome, Rome, Italy
[c] Norwegian University of Science and Technology, Trondheim, Norway

ARTICLE INFO

Keywords:
Library collection
Microclimate investigation
Preventive conservation
Historical building
Paper deterioration
Preservation risk assessment

ABSTRACT

The conservation of historic libraries can be referred towards both the ancient book collections and the buildings themselves. Heritage collections made of paper are threaten by climate-induced deterioration risks such as cellulose hydrolysis. Several studies have investigated the microclimate inside historic libraries but comparisons are difficult due to the lack of long-term microclimate observations and uniformity in the use of standards and risk assessment methods. For the first time, the long-term microclimate observations collected in three historic libraries in Italy were comparatively studied to outline differences and similarities of their microclimates in terms of paper preservation. A multidisciplinary approach was applied to assess the building performance (a) and the deterioration risks for the collections (b). As for a), a common feature of the libraries was the high thermal inertia and low indoor-outdoor air exchanges. As for b), the Time Weighted Expected Lifetime (TWEL) was defined to account for an average chemical risk on a seasonal and yearly basis. TWEL allowed to highlight the impact of the most adverse conditions on the overall chemical risk for acidic paper preservation (e.g., temperatures above 20 °C reached naturally in summer/artificially in winter). It resulted that the measured microclimate conditions in the libraries would lead to the loss of their acidic collections in less than 300 years. Demographic plots were finally used to inform about the risk resulting from the synergy between handling and microclimate as well as to explore the effectiveness of possible preservation measures such as the deacidification of 10% of the collections.

1. Introduction

Libraries are unvaluable witnesses of the human knowledge over the centuries [1]. The term library can refer either to a collection of books and other sources of recorded information or to the building where such a collection is conserved. In this sense, the conservation of historic libraries may be referred towards both the ancient collection of books and the buildings themselves (if with cultural value). The importance of public libraries has been acknowledged since classical antiquity (e.g., Pliny wrote on Julius Caesar: *ingenia hominum rem publicam fecit,* "He made men's talents a public possession"). During the Middle Ages and the Renaissance, libraries were assembled in monasteries and universities, that preserved them over many centuries. After the French Revolution, the abolition of monastic orders led to the expropriation and dispersion of several libraries [2]. Some of them were transformed into private collections, which afterwards became the core of today's national libraries. Nowadays, digital libraries have broadened the access to library contents from any place [3], so users do not need any more to visit the library building nor to physically interact with the materials in order to consult their contents. Although the reduced handling undoubtedly favours book conservation [4], the preservation of historic libraries and their buildings still demands to be carefully managed. In fact, their materiality is an irreplaceable testimony of our past for the present and future generations.

Sections 1.1, 1.2 and 1.3 of the Introduction present the state-of-the-art on the preservation of library collections, focusing on the damage risk assessment for paper objects, the international policy framework and the previous microclimate monitoring studies in historic libraries worldwide. Section 1.4 outlines the research aims of this work.

1.1. Damage risk assessment for paper collections

Library collections are made of a wide range of organic and inorganic materials, where paper is the most represented. All library materials undergo a natural and unavoidable ageing process, however the rate of

* Corresponding author.
E-mail address: elena.verticchio@uniroma1.it (E. Verticchio).

https://doi.org/10.1016/j.buildenv.2021.108394
Received 11 June 2021; Received in revised form 9 September 2021; Accepted 23 September 2021
Available online 1 October 2021

Abbreviations

ANSI	American National Standards Institute
ASHRAE	American Society of Heating, Refrigerating and Air-Conditioning Engineers
BSI	British Standards Institution
CEN	European Committee for Standardization
CREA	Consiglio per la Ricerca in Agricoltura e l'Analisi dell'Economia Agraria
HVAC	Heating, Ventilation, and Air Conditioning
IFLA	International Federation of Library Associations and Institutions
ISO	International Organization for Standardization
NISO	National Information Standards Organization
PAS	Publicly Available Specification
PD	Portable Document
TR	Technical Report
UNI	Italian National Unification Institute

Parameters and variables

Γ_d	Adiabatic gradient of vertical temperature for dry air (°C m^{-1})
ΔMR	Absolute difference between outdoor and indoor mixing ratio ($g \cdot kg^{-1}$)
ΔRH_{24h}	Daily relative humidity fluctuation (%)
ΔT	Vertical temperature gradient (°C)
ΔT_{24h}	Daily temperature fluctuation (°C)
Δz	Vertical distance between probes (m)
DP	Paper degree of polymerisation (–)
k	Rate of paper degradation ($years^{-1}$)
MR	Mixing Ratio ($g \cdot kg^{-1}$)
pH	Acidity of paper (–)
RH	Relative Humidity (%)
RH_{30d}	centred 30-day moving mean of relative humidity (%)
RH_{90d}	centred 90-day moving mean of relative humidity (%)
T	Temperature (°C)
T_{24h}	centred 24-h moving mean of temperature (°C)
$T_{d,14}$, $T_{d,22}$	Temperature at 14:00 ($T_{d,14}$) and 22:00 ($T_{d,22}$) of dth calendar day (°C)
$T_{d,Mean}$, $T_{d,max}$	Mean ($T_{d,mean}$) and maximum ($T_{d,max}$) temperature of dth calendar day (°C)

Indexes

CI	Continuity Index (–)
CoI	Completeness Index (–)
EL	Expected Lifetime of historic paper (years)
eLM	equivalent Lifetime Multiplier (–)
LM	Lifetime Multiplier (–)
NDR	Normalized Diurnal Range (–)
PI	Preservation Index (–)
RH ratio	Relative Humidity ratio (%)
TWEL	Time Weighted Expected Lifetime (years)
TWPI	Time Weighted Preservation Index (years)

decay is dependent on the properties of the constituent materials (e.g., acidity of paper and physical strength) and is greatly affected by the indoor climate [5]. Paper can be classified into three types based on their average acidity (pH) and degree of polymerisation (DP): acidic paper (pH = 5.2, DP = 826.3), rag paper (pH = 6.4, DP = 1481.2) and contemporary paper (pH = 7.6, DP = 1526.2) [6].

Cellulose hydrolysis represents the main concern for damage risk of paper collections, being the rate of chemical degradation mainly driven by temperature [7]. This deterioration mechanism has been extensively studied by using the dose-response functions, such as the Lifetime Multiplier (LM) for various materials such as varnishes and cellulose [7] and the Preservation Index (PI) for organic materials (e.g. paper, textiles, plastics, dyes, leather, fur, etc.) [8]. Strlič et al. [9] derived the isochrones for paper (i.e., curves of equal expected lifetime, EL), based on a damage function which relates the DP loss with the pH of paper and the indoor temperature and relative humidity at the reference conditions of dark storage (i.e., without considering natural and artificial light). In this way, the isochrones allow to assess the chemical deterioration risk for the different paper types by taking into account their different vulnerability to cellulose hydrolysis as a function of their pH and DP [9].

Handling is the main responsible for the accumulation of wear and tears of paper [4]. The time required for a library collection to become unfit for use by readers due to the combined effect of handling and cellulose hydrolysis can be estimated through a dose-response function [4] that depends on the percentages of paper types constituting the collection (i.e., its demography) [9].

Thermal stratification may occur in high-ceilinged libraries. Hence, if too high temperatures are experienced, the chemical decay of paper collections located at the upper levels is accelerated based on the vulnerability of the paper types. Moreover, high relative humidity levels might occur in poor ventilated areas in the proximity of cooler surfaces, favouring mould growth [10]. Finally, temperature and relative humidity fluctuations might accelerate paper degradation (e.g., tensile creep of paper), but consensus on their influence on the degradation has not been reached yet among the researchers [5].

Pollutants do not generally represent a significant threat to the overall rate of chemical degradation, as their concentrations are small (e.g., acetic acid<250 $\mu g \cdot m^{-3}$; formic acid<35 $\mu g \cdot m^{-3}$; nitrogen dioxide<15 $\mu g \cdot m^{-3}$; ozone<25 $\mu g \cdot m^{-3}$; sulphur dioxide< 3 $\mu g \cdot m^{-3}$ [11,12]) and their effect on historic paper preservation is limited [13]. Dust particles can affect paper conservation in terms of cellulose degree of polymerisation, thus increasing the vulnerability of paper to the other environmental parameters [14].

Fungal spores, which are ubiquitous, may become a biological risk when RH>65% for a sufficient period of time. This risk is frequently assessed using the Sedlbauer isopleths for spore germination and mould growth for biologically recyclable materials [15].

Digital platforms, such as HERIe [16] and Collection Demography app [17], are freely available for conservation professionals and decision makers to easily and effectively carry out the quantitative assessment of the climate-induced risks for paper collections based on the prevailing environmental conditions where the objects are displayed or stored.

1.2. Standards and guidelines on library conservation

This section describes the international policy framework on the preservation of cultural heritage including library and archive materials. Table 1 summarises standards and guidelines on the library conservation. Standards are published by national or international standards bodies (e.g., UNI, BSI, CEN, ISO), whereas guidelines are usually formulated by unions (e.g., ASHRAE, IFLA). The earlier standards specified temperature (T) and relative humidity (RH) ranges for various types of materials including paper, parchment and leather [18–22]. It is worth noticing that sometimes, for the same classes of materials, these standards provide conflicting recommendations about T and RH ranges, thus arising doubts about which indication has to be followed. The introduction of the concepts of "proofed fluctuations" [23] and "historical climate" [24] led to more flexible T and RH ranges with respect to the target values previously recommended as satisfactory to mitigate

Table 1
Italian and international policy framework on the preservation of cultural heritage including library and archive materials. Remarks' field provides the microclimate specifications indicated in each document. The withdrawn standards (highlighted in footnotes) are here reported to support the interpretation of Table 2.

REF.	YEAR	DOCUMENT	INSTITUTION	TYPE OF DOCUMENT	REMARKS[a]
[18]	1997	UNI 10586	Italian National Unification Institute (UNI)	Standard	T = 14 ÷ 20 °C, RH = 50 ÷ 60% (illustrative documents). T = 18 ÷ 23 °C, RH = 50 ÷ 65% (consultation and reading). Acclimatisation is advised if T and RH in consultation places differ more than ±4 °C and ±5% respectively from storage facilities conditions.
[19]	1999	UNI 10829	Italian National Unification Institute (UNI)	Standard	T = 13 ÷ 18 °C, RH = 50 ÷ 60% (archival document and books); T = 19 ÷ 24 °C, RH = 45 ÷ 55% and ΔT_{24h} = ±1.5 °C, ΔRH_{24h} = ±6% (book bindings in leather and parchment).
[20]	2001	D. lgs. 112/98,art. 150, comma 6	Italian Ministry of Cultural Heritage (MIBAC)	Legislative Decree	T = 19 ÷ 24 °C, RH = 50 ÷ 60% (books and manuscripts). T < 21 °C, RH = 40 ÷ 55% to avoid microbiological attacks on organic materials.
[21]	2001	ANSI/NISO Z39.79[b]	American National Standards Institute (ANSI) – National Information Standards Organization (NISO)	Standard	T < 21 °C ± 3 °C, RH = 35 ÷ 50%±5% (library and archival materials).
[22]	2003	ISO 11799[c]	International Organization for Standardization (ISO)	Standard	T = 2 ÷ 18 °C±1 °C, RH = 30 ÷ 45%±3% (optimum preservation) T = 14 ÷ 18 °C±1 °C, RH = 35 ÷ 50%±3% (staffed stack areas, items in regular use)
[24]	2010	EN 15757	European Committee for Standardization (CEN)	Standard	T = no limits; RH = within safe bands calculated from the historical climate.
[30]	2011	ASHRAE Handbook—HVAC Applications Chapter 23[d]	American Society of Heating, Refrigerating and Air-Conditioning Engineers (ASHRAE)	Guidelines	Class B is the reference for historic buildings (no risk to most books): T = 15 ÷ 25 °C, with seasonal adjustment T+10 °C (but not above 30 °C), and T down as low as necessary to maintain RH control, and RH = 50% ± 10% (or historic annual average for permanent collections); short-term fluctuations T±5 °C, RH±10%.
[25]	2012	PD 5454[e]	British Standards Institution (BSI)	Guidelines	T = 13 ÷ 20 °C, RH = 35 ÷ 60% (mixed collections); T = 5 ÷ 25 °C, RH = 25 ÷ 60% (paper records storage).
[26]	2012	PAS 198[f]	British Standards Institution (BSI)	Publicly Available Specification	Tables on the relative risk of damage and deterioration due to T and RH [26] as a function of the sensitivity to hydrolysis (rag paper = low; wood pulp paper = medium) are reported as an informative appendix.
[27]	2015	ISO 11799	International Organization for Standardization (ISO)	Standard	Recommended T and RH ranges not explicitly specified.
[32]	2016	IFLA - Principles for the Care and Handling of Library Materials	International Federation of Library Associations and Institutions (IFLA)	Guidelines	T < 10 °C to favour paper chemical stability and physical appearance; RH = 50 ÷ 65% to minimise mechanical damage (while reducing the risk of biological attacks).
[28]	2017	BS 4971	British Standards Institution (BSI)	Standard	T = 13 ÷ 23 °C, with annual average T < 18 °C; RH = 35 ÷ 60% (mixed archives).
[29]	2018	EN 16893	European Committee for Standardization (CEN)	Standard	Tables on the relative risk of damage and deterioration due to T and RH [26] as a function of the sensitivity to hydrolysis (rag paper = low; wood pulp paper = medium) are reported as an informative appendix.
[31]	2018	ISO/TR 19815	International Organization for Standardization (ISO)	Standard	Tables on the relative risk of damage and deterioration due to T and RH [26] as a function of the sensitivity to hydrolysis (rag paper = low; wood pulp paper = medium) are reported as an informative appendix.
[10]	2019	ASHRAE Handbook—HVAC Applications Chapter 24	American Society of Heating, Refrigerating and Air-Conditioning Engineers (ASHRAE)	Guidelines	Class B is the reference for historic buildings (no risk to most books): T ≤ 30 °C, RH = 30 ÷ 70%, seasonal adjustment from annual average T+10 °C, T-20 °C) and RH±10%, short-term fluctuations T±5 °C, RH±10%.

[a] The paper types to which microclimatic specifications are suitable for are specified in this column, if mentioned in the document.
[b] Withdrawn in 2013.
[c] Withdrawn and superseded by ISO 11799:2015 (that will be replaced by ISO/AWI 11799, currently under development).
[d] The ASHRAE Handbook —HVAC Application of 2015 did not modify Chapter 23.
[e] Withdrawn and superseded by EN 16893:2018 and BS 4971:2017.
[f] Withdrawn in 2018.

mechanical risks for organic hygroscopic materials. As a result of the above concepts, the standards have evolved along different paths: ISO and BSI updated their documents [22,25,26] with new specifications [27–29], while UNI did not change the original version of the norms [18, 19]. The ASHRAE handbook [30] introduced museum climate classes without prescriptive T and RH specifications, which have been extensively adopted for both environmental design and risk management in museums, galleries, archives and libraries. In the last years, EN 16893:2018 [29], ISO/TR 19815:2018 [31] and the updated ASHRAE guidelines [10] focused on sustainability and greater flexibility in the climate control strategy based on risk management principles and existing literature on best practices in museums as well as the collections' response to the surrounding environment. Although EN 16893:2018 [29] gives useful recommendations for buildings intended for the storage and use of heritage collections (including reading rooms), no European standards exist by CEN/TC 346, i.e. the Technical Committee of the European Committee for Standardization dedicated to the Conservation of cultural property, which specifically deals with the conservation in libraries and archives.

Table 2
Indoor microclimate monitoring studies in historic libraries over the last 20 years.

Ref.	Year	Library (foundation year)	Place	Monitoring period	HVAC	Damage risk assessment	Policy framework
[34]	2002	Guildhall library (1876) Bronte Parsonage Museum library (1778–79)	Leicester (UK) Haworth (UK)	12 months	Yes No		BS 5454
[49]	2007	Audley End House (early 17th-century) Brodsworth Hall (1861) Eltham Palace (1933) Iveagh Bequest (1754) Walmer Castle (1539) Dover Castle (1912)	Saffron Walden (UK) Doncaster (UK) London (UK) London (UK) Walmer (UK) Dover (UK)	not mentio-ned	Yes	Time Weighted Preservation Index [8].	BS 5454
[11]	2011	National Library (1726)	Prague (Czech Republic)	9 months (on monthly basis)	No		
[38]	2014	Malatestiana (1454)	Cesena (Italy)	3 months	No		UNI 10829; MIBAC D. lgs 112/98.
[39]	2016	Palatina (1761)	Parma (Italy)	2 months (spot)	No		UNI 10829; MIBAC D. lgs 112/98; ASHRAE guidelines
[12, 50]	2016	Classense (1513)	Ravenna (Italy)	15 days summer/15 days winter	No	Wear and tear dose–response function [4]; paper isochrones [9].	UNI 10586; UNI 10829
[48]	2017	Tire Necip Pasa (1827)	Izmir (Turkey)	1 year	No	Lifetime Multiplier [7]; Sedlbauer isopleth [15].	ASHRAE guidelines
[47]	2018	Fine Arts Library (1905) Physics Library (1897) Historical Archive of the Presidency of the UNLP (1884) Historical Archive of the Natural Sciences Museum (1877–1884)	La Plata (Argentina)	4 months	Yes Both Yes Yes		UNI 10829
[36]	2018	Baroque Library of the University (1716)	Coimbra (Portugal)	6 months	No	equivalent Lifetime Multiplier; Sedlbauer isopleth [15].	UNI 10829
[51]	2018	National Library (1677)	Warsaw (Poland)	13 months	Yes		
[37]	2020	Library of the National Observatory (1842)	Athens (Greece)	1 month	Yes		ISO 11799:2003; UNI 10586

1.3. Microclimate monitoring in historic libraries

In Italy, almost half of the historic libraries was founded before the XIX century [33]. Historic libraries are frequently conserved in massive buildings characterised by high thermal inertia [12,34–37]. Most of these buildings have natural ventilation and unconditioned indoor climate (i.e., without any HVAC systems) [11,12,36,38,39]. Windows, usually small-sized, were often placed on two sides of the main reading hall [12,35,39] to maintain relatively constant daylight levels for visual comfort. The orientation of the building was chosen to protect from dampness and to take advantage of natural daylighting. To cite but a few, Vitruvius advised that libraries should have an eastern exposure to the morning light useful to dispel dampness [40] and, many centuries after, the Italian Renaissance architect Leon Battista Alberti wrote that private libraries should have western exposure to benefit the reading at twilight [41]. Recently, it has been highlighted that hygroscopic collections act as buffers on air relative humidity fluctuations due to the exchanges of moisture with the surrounding air [42]. The RH buffering, already visible at smaller scale (e.g. in sealed boxes containing paper [43]), can be evaluated at large scale (e.g. in libraries and historical buildings) through microclimate analysis and hygrothermal simulation [44–46].

Table 2 provides a synthetic overview of studies on microclimate monitoring conducted in historic libraries over the last 20 years. A significant variability can be observed in the length of the monitoring period as well as in the policy framework adopted for microclimate analysis and, more in general, in the methods followed for damage risk assessment. The T and RH ranges recommended by standards and guidelines in Table 1 have been frequently used as threshold values to evaluate the quality of the environmental conditions for the conservation of library materials [24,26,28,29,34]. Sedlbauer spore germination isopleths and fungal growth curves have been employed in Refs. [36,48] to evaluate the biological risk for collections. Synthetic indexes, such as the equivalent Lifetime Multiplier (eLM) and the Time Weighted Preservation Index (TWPI), have been used in Refs. [36,49] to account for average values of LM and PI over the monitored period. The damage function for historic paper [9] was used in Ref. [50] for the estimation of the collection expected lifetimes in various conservation scenarios.

1.4. Research aims

Several studies have separately evaluated the microclimate inside historic libraries; however, few of them were based on long-term microclimate observations and there is lack of uniformity in the use of standardised microclimate specifications and risk assessment methods (Table 2). Taking advantage of the availability of annual time series of data collected by the authors, the microclimates of three historic libraries located in different sites of Italy (Milan, Udine and Rome) were analysed. Besides, the collected hygrothermal conditions were compared with respect to those recommended by both Italian and European regulations (Table 1) and used as an input in dose-response functions for paper. Moreover, the comparison allowed us to investigate to what extent the differences in the external climate, building features and library management can affect the climate-induced risk for the preservation of paper collections. The comparison can provide useful insight on the impact on paper collections of conditioned and unconditioned indoor climates to inform preservation strategies within historic buildings.Section 2 deals with the description of the three historic libraries, the microclimate monitoring campaigns and the methods for characterising the indoor climate and assessing the conservation risks. Section 3 is devoted to the presentation and discussion of the results. Finally, section 4 outlines the main conclusions of the work and the future perspectives in the research on library preservation.

2. Materials and methods

2.1. Case studies: the three historic libraries in Italy

The historic libraries under study (Fig. 1), hereafter named Ca' Granda (Milan), Delfiniana (Udine) and Collegio Romano (Rome), are located in different regions of Italy. Milan (Köppen-Geiger climate class Cfa, i.e. temperate climate, fully humid with hot summer [52]) and Udine (Köppen-Geiger climate class Cfb, i.e. temperate climate, fully humid with warm summer [52]) are in northern Italy, whereas Rome is in the central part of the peninsula (Köppen-Geiger climate class Csa, i.e. temperate climate, with dry and hot summer [52]).

2.1.1. Ca' Granda Library (Milan)

The library is hosted in the Ca' Granda Ospedale Maggiore Policlinico (Milan, Lat. 45.5°N and Long. 9.2°E, 120 m a.m.s.l.). The library collection of the IRCC Foundation (Istituto di Ricovero e Cura a Carattere Scientifico) represents a national *unicum* in terms of richness and specialisation on medical sciences, with a patrimony estimated in about 100.000 printed volumes among monographies, periodicals and magazines from XV to XX century [53]. The history of the collection dates back to the foundation of the Hospital (1456), but the main core is from the XIX century and it is continuously updated thanks to private donations. The collection is deployed in a three-level wooden shelf on the perimeter of a room at the ground floor (Fig. 2a).

2.1.2. Delfiniana Library (Udine)

The Library of the Archbishop's Palace (Udine, Lat. 46.1°N and Long. 13.2°E, 113 m a.m.s.l.) was named "Delfiniana" after his founder, Dionisio Delfino, which was the patriarch of the diocese of Aquileia from 1699 to 1734 [54]. The foundation of the library dates back to 1708, when the patriarch commissioned the construction of its building, to be donated to eternal public utility. The collection was organised in a two-level wooden shelf deployed on the perimeter of a hall at the second floor of the patriarchal palace (Fig. 2b). The collection comprises printed volumes, manuscripts (dated from XVI to XIX century) and some illuminated liturgical codices (dated from IX to XIV century). The library is nowadays part of the touristic itinerary of the Diocesan Museum of Udine.

2.1.3. CREA Meteorological Library at the Collegio Romano (Rome)

The Historical Meteorological Library in the monumental complex of Collegio Romano, hereafter called simply Collegio Romano (Rome, Lat. 41.9°N and Long. 12.5°E, 21 m a.m.s.l.), is considered the most important collection in Italy devoted to Atmospheric Sciences, Meteorology and Geophysics of the Modern Age (Fig. 2c). Although its original nucleus, gathered by Jesuits, dates back to the foundation of the building (1584), the current location on its fourth floor was elected in 1879, after the establishment of the first Central Meteorological Office in Italy, so as to become an integral part of it (currently an important sector of CREA, the leading Italian research organization dedicated to the agri-food supply chains). The collection includes several national and international periodicals published by scientific societies, CREA's interesting publications and original books and manuscripts, mostly from the XIX century [55].

The plans of three historic libraries are shown in Fig. 2. Ca' Granda library (Fig. 2a) has the largest volume (approximately 2100 m^3), with rectangular shape and high ceiling (up to 12 m). Delfiniana (Fig. 2b) has similar features as Ca' Granda, but smaller dimensions (approximately 1150 m^3). Collegio Romano (Fig. 2c) has a 4.5 m high ceiling and the smallest volume (approximately 380 m^3). All the libraries are covered by a wooden roof and have SW-W-facing windows on two orders. The windows in Collegio Romano and Ca' Granda have simple glass panes and wooden shadings which are closed most of time during the year. New air-tight windows with UV-IR-filtered glass were mounted in Delfiniana in May 2017 in place of the previous single panes [54]. During the microclimate monitoring campaigns, Ca' Granda and Delfiniana had no HVAC (Heating, Ventilation and Air-Conditioning) system, whereas

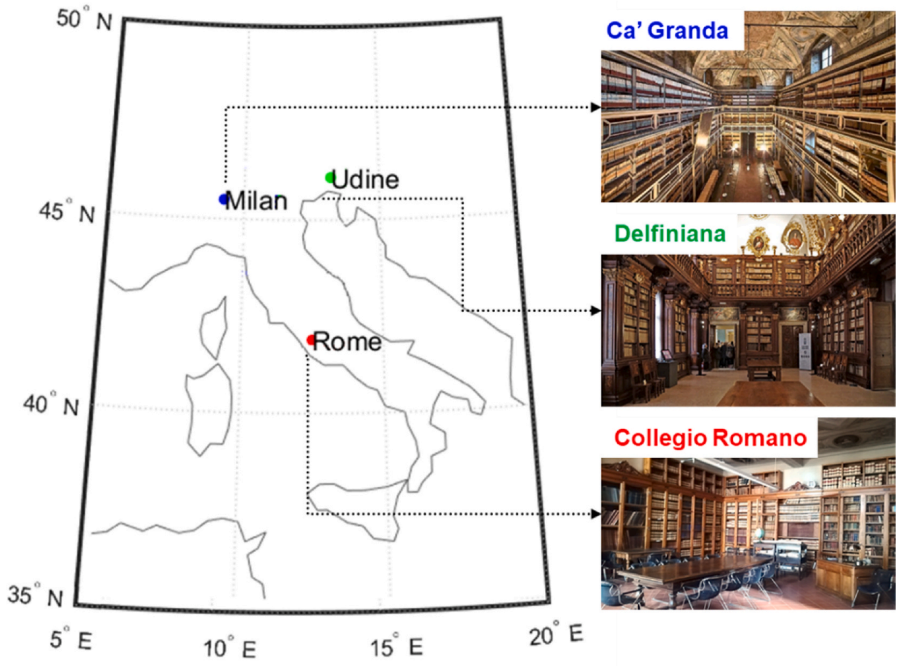

Fig. 1. The geographical position of the three historic libraries (Italy) under study: Ca' Granda in Milan, Delfiniana in Udine and Collegio Romano in Rome.

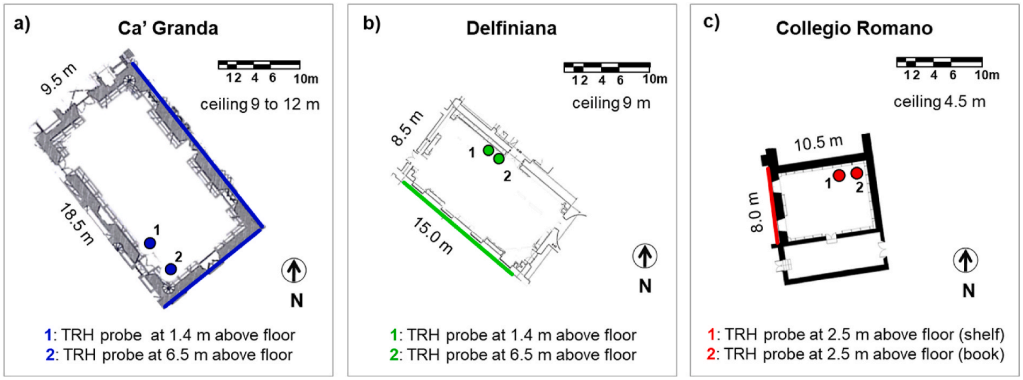

Fig. 2. Plans of the historical libraries with the position of the monitoring system devices (TRH) marked as coloured points. External walls are highlighted with coloured lines.

Collegio Romano was heated by cast iron radiators from November 1st to April 15th (operating from 6 a.m. to 6 p.m. local time) and cooled through fan-coils (switched on when needed). All the libraries were naturally ventilated.

The three library collections are mostly made of mid-19th–mid-20th century paper of Western origin (lignin containing, rosin sized, printed and non-coated), therefore the prevalent composition of the collections was assumed to be acidic. Fig. 3 depicts the percentages of paper types constituting each of the historic collections under study, as estimated on private communication with the library conservators.

2.2. The monitoring campaigns

The indoor climate monitoring campaigns to study the hygrothermal behaviour of the three libraries covered different periods (Table 3), as they were independently planned before this comparative investigation. Two thermo-hygrometers (Fig. 2) were placed inside each library to measure temperature (T) and relative humidity (RH) at local time. In Ca' Granda and Delfiniana, where ceilings are high, TRH probes were deployed at two different heights (1.4 m and 6.5 m above floor) to monitor vertical temperature gradients. In Collegio Romano, one TRH probe was placed on a shelf and the other one inside a mock-up book on the same shelf with the aim to derive the book response time, i.e. the lag between the RH values measured inside the book with respect to those collected in the room. The mock-up book (250 mm × 180 mm × 28 mm) was made using modern rag paper sheets, with cardboard covers and leather spine. The metrological features of the indoor T sensors (Pt100 resistance thermometers) and RH sensors (thin film capacitive sensors), reported in Table 3, were in accordance with the current European Standards on the instruments to be used in cultural heritage conservation [56,57]. Although a higher availability of instruments -also to measure other environmental variables-would have provided a better representativeness of the microclimate behaviour in the libraries, the choice of the instrument number and types was limited due to technical and financial reasons.

2.3. Indoor climate characterisation

The long time series of microclimate data collected in the historic libraries were evaluated for completeness before applying data analysis through the Completeness Index (CoI) and the Continuity Index (CI), two indexes proposed in Ref. [58] and already applied to long-term measurements in other conservation contexts [59,60]. Temperature and relative humidity values collected over the year in the libraries were compared in order to highlight the differences among the sites, if any. Mixing Ratio (MR) was calculated from T and RH values using the formula provided in EN 16242 [57] and used as a proxy to estimate the magnitude of the indoor-outdoor water vapour exchanges through infiltrations and openings [61–63].

The buffering capacity of the building envelopes to smooth out the maximum outdoor temperatures occurring in daylight hours was evaluated using the Normalized Diurnal Range (NDR). NDR is an index defined in Ref. [64] as the ratio between the observed diurnal indoor temperature range (calculated as the difference between the temperatures at 14:00 ($T_{d,14}$) and 22:00 ($T_{d,22}$) of dth calendar day) in the monitored period (MP) with respect to the reference period (RP). $T_{d,14}$ and $T_{d,22}$ were chosen as they are close to the outdoor diurnal maximum and mean temperatures, respectively. Since the NDR value results from the combined effect of building envelope, solar exposure, room ventilation and use [64], this index is not able to distinguish among their

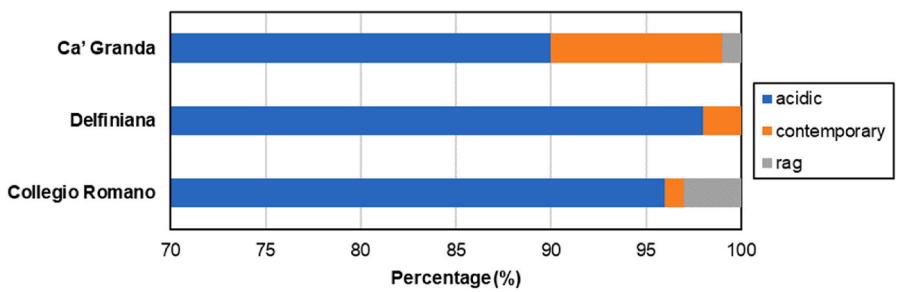

Fig. 3. Paper types constituting the library collections.

Table 3
Microclimate monitoring campaigns in the three historic libraries in Italy.

Library (foundation year)	Place	Monitoring period	Instrument (uncertainty)	Sampling frequency	Outdoor climate	Analysed period
Ca' Granda (1456)	Milan	Sep 2011–Jan 2013	Comet®, model R3121 (0.4 °C for T, 2.5% for RH)	15 min	Weather station (Lat. 45.5°N and Long. 9.2°E)	1st Jan 2012–31st Dec 2012
Delfiniana (1708)	Udine	Oct 2016–Mar 2018	Testo®, model 175H1 (0.4 °C for T, 2% for RH)	15 min	Weather station (Lat. 46.1°N and Long. 13.2°E)	1st Jan 2017–31st Dec 2017
Collegio Romano (1584)	Rome	Jun 2019 – ongoing	Rotronic®, model HC2A-S3 (0.3 °C for T, 1.5% for RH)	10 min (recorded every 30 min as averaged values)	Weather station (Lat. 41.9° N and Long. 12.5° E)	1st Jun 2020–31st May 2021

individual contributions. Nevertheless, although NDR does not entirely depend from the air exchange rate (AER), it can be considered as a proxy of AER to a certain extent. The outdoor temperatures in the 1991–2020 reference period were extracted from the E-OBS v23.1e [65] gridded observational dataset (spatial resolution of 0.1° × 0.25°) via the Climate Data Store (CDS) infrastructure. As E-OBS v23.1e does not include hourly data, the daily maximum temperature ($T_{d,max}$) and the daily mean temperature ($T_{d,mean}$) in the reference period were extracted and used in the place of $T_{d,14}$ and $T_{d,22}$ [64].

The formulation of NDR was here adjusted to enhance its capability to sense the active climate control using heating systems as follows and it was calculated in each site under study:

$$NDR = \frac{\left(T_{d,14} - T_{d,22}\right)_{MP}}{\frac{\left(T_{d,max} - T_{d,mean}\right)_{RP}}{n_{RP}}} \quad (1)$$

where n_{RP} is the total number of days in the reference period (i.e. 30 years). For this reason, if NDR is around zero, the building has a high thermal buffering capacity and low ventilation, while if NDR is close to unity, the indoor and outdoor temperatures are practically identical. The latter condition can be experienced when there is a persistence of sufficient ventilation due, for example, to open windows. Negative NDR can also occur, mainly in summer, when the effect of the highest outdoor temperature values is visible later on the indoor evening temperatures.

In Ca' Granda and Delfiniana libraries, where ceilings are high, the indoor air stability was evaluated by comparing the measured vertical temperature gradient (as the difference between the temperature values measured at 1.4 m and 6.5 m above the floor) with the dry adiabatic gradient of vertical temperature, i.e. $\Gamma_d = \Delta T/\Delta z \cong -0.1$ °C/10 m.

The possible effect of the moisture exchanges between the hygroscopic collections and the surrounding air on the stabilisation on the indoor RH values was explored. Since RH is not an independent variable, it must be studied together with air temperature or mixing ratio, which both influence its behaviour. The RH variability was assessed based on the following approaches: a) analysis of the concurrent time evolutions of indoor T, RH and MR measurements over the year (Fig. 5); b) synthetic visualisation of the frequency distributions of the indoor and outdoor RH observations (Fig. 8); c) calculation of the Relative Humidity ratio (RH ratio, Table 4); d) assessment of the average absolute differences between simultaneous outdoor and indoor MR values (ΔMR, Table 4). The RH ratio was defined as the ratio (in percentage) between the indoor (in) and the outdoor (out) seasonal spreads, i.e., the sum over a year of the absolute differences between the i-th centred 90-day moving average of relative humidity ($RH_{i,90d}$) and the i-th relative humidity observation (RH_i):

$$RH\ \ ratio\ = \frac{\left(\sum_{i=1}^{n}\left|RH_{i,90d} - RH_i\right|\right)_{in}}{\left(\sum_{i=1}^{n}\left|RH_{i,90d} - RH_i\right|\right)_{out}} \cdot 100 \quad (2)$$

When the RH ratio is low, the library has limited air exchanges with the outdoors together with high moisture buffering capacity by the hygroscopic materials (if present); when the RH ratio is close to 100%, the indoor and outdoor RH seasonal spread are practically identical.

Table 4
RH ratio, average absolute difference indoor/outdoor MR observations ($\overline{\Delta MR}$) and hygroscopic ratio.

Library	RH ratio	$\overline{\Delta MR}$	Hygroscopic ratio
Ca' Granda	24.1%	1.3 g/kg	11.3%
Delfiniana	12.7%	1.2 g/kg	6.2%
Collegio Romano	9.3%	1.8 g/kg	7.9%

2.4. Conservation risk assessment

As evaluated by the conservators of the libraries under study, based on their regular and qualitative risk assessment to determine the optimal preservation of their paper collections, the major recognized deterioration risk is cellulose hydrolysis due to the high temperatures occurring in summer. Indeed, since no fungal proliferation was reported to be observed in the case studies before the monitoring campaigns (Dr. Paolo Galimberti for Ca' Granda, Dr. Dania Nobili for Delfiniana and Dr. Luigi Iafrate for Collegio Romano, personal communications), this risk was no further investigated. This investigation was stimulated by the interest of the conservators and managers of the libraries to explore the possible climate-induced deterioration risks by using specific dose-response functions. In fact, it was not possible to ascribe the actual preservation state of the collections over time to the monitored indoor climate, because the previous conditions and arrangement of the collections were not fully known and might have changed through their history. A dose response function for paper was developed in Ref. [9] by modelling k, i.e. the rate of paper degradation per year (at the conditions of dark storage), as a function of both the acidity of paper (pH) and the indoor temperature and relative humidity, as follows:

$$\ln(k) = 36.981 + 36.72 \cdot \left(\frac{\ln(1 - RH)}{1.67 \cdot T - 285.66}\right)^{\frac{1}{2.491 - 0.012 \cdot T}} + 0.244 \cdot \ln\left(10^{-pH}\right) - \frac{14300}{(T + 273.15)} \quad (3)$$

According to Ref. [9], Equation (3) can be embedded in the Ekenstam's function to obtain a damage function for paper where the expected lifetime, EL (i.e. the time required for objects to become unfit for use), is calculated as a function of the initial degree of polymerisation (DP) and the critical degree of polymerisation, which is typically 300, at which objects are no longer suitable for general access [9]:

$$EL = \left(\frac{1}{300} - \frac{1}{DP}\right) \cdot k^{-1} \quad (4)$$

To account for an average risk of chemical degradation for paper collections due to cellulose hydrolysis, we defined a synthetic index, hereafter named as Time Weighted Expected Lifetime (TWEL). The TWEL index integrates the damage function for paper derived and validated in Ref. [9] with the concept of a time-weighted index to quantitatively compare the chemical risk due to the indoor climate conditions over different time windows (e.g. a year or a season). Inspired

by the well-established TWPI index formulated for the chemical degradation of organic materials [8], the TWEL is calculated based on the running sum of the multiplicative inverses of EL at each time t. Indeed, we examined various formulations for averaging the EL (e.g. the simple arithmetic mean, the inverse of the arithmetic mean, etc.) and found that the proposed calculation of TWEL was the one giving more weight to the lower values of EL, thus considering the risk underlying the worst-case scenario. In this way, the TWEL emphasises the impact of the most adverse climate conditions (mainly temperature) on the overall chemical deterioration risk for paper collections on a yearly and seasonal basis.

Fig. 4 shows the workflow for the calculation of the TWEL, which can be summarised in the following steps:

I. Calculation of 24-h moving average of T (T_{24h}) and 30-day moving average of RH (RH_{30d});
II. Calculation of EL from T_{24h} and RH_{30d} according to Equation (4);
III. Calculation of running sum of the reciprocals of EL at each time t (EL_{runsum});
IV. Calculation of seasonal/yearly TWEL value as the ratio between the number of observations in the selected period (n) and the EL_{runsum} value.

The running average over 24 h for temperature and 30 days for relative humidity, chosen according to Ref. [8], were found to be compatible with the response time of paper books as estimated by using the measurements collected in Collegio Romano according to the formula in Ref. [66]. Based on the prevalent composition of the library collections (Fig. 3), in this study we used DP = 826.3 and pH = 5.2 typical of acidic collections [47]. Since it was not experimentally validated yet, the TWEL value expresses only a weighted average of the chemical degradation risk based on the EL.

Demographics of collections were used to investigate the combined effect of paper handling and indoor climate conditions over the time required for objects to become unfit for use. It was estimated that each handling event could develop, on average, at least one large missing piece every 100 pages for objects having DP < 300, thus losing their fitness for use [4,9]. The Collection Demography App [17], was used to run simulations for estimating the accumulation of large missing pieces per number of handlings. To calculate the demographic curves, the yearly average temperature and relative humidity and an average access every 2 years in the library were used. This analysis was based on the percentage of paper typologies constituting each library collection (Fig. 3). The effect of deacidification of 10% of the acidic collection was finally explored by recalculating the demographic curves while modelling the deacidified fraction with DP = 640 and pH = 8.1.

3. Results and discussion

3.1. Indoor climate characterisation

The comparative analysis carried out in this study was based on the periods reported in Table 3. The measurements collected by the TRH probes at 1.4 above floor for Ca' Granda and Delfiniana and TRH probe on the shelf at 2.5 m above floor for Collegio Romano (Fig. 2) were taken into account. The quality of T and RH time series was objectively evaluated before analysing microclimate data in the three libraries and resulted to be complete (CoI = 1) and continuous (CI = 1) for the considered periods.

On a yearly basis, the indoor median temperatures were higher than the outdoor ones (Fig. 5). The outdoor temperatures differed depending on the site, with Udine having cooler average values and larger

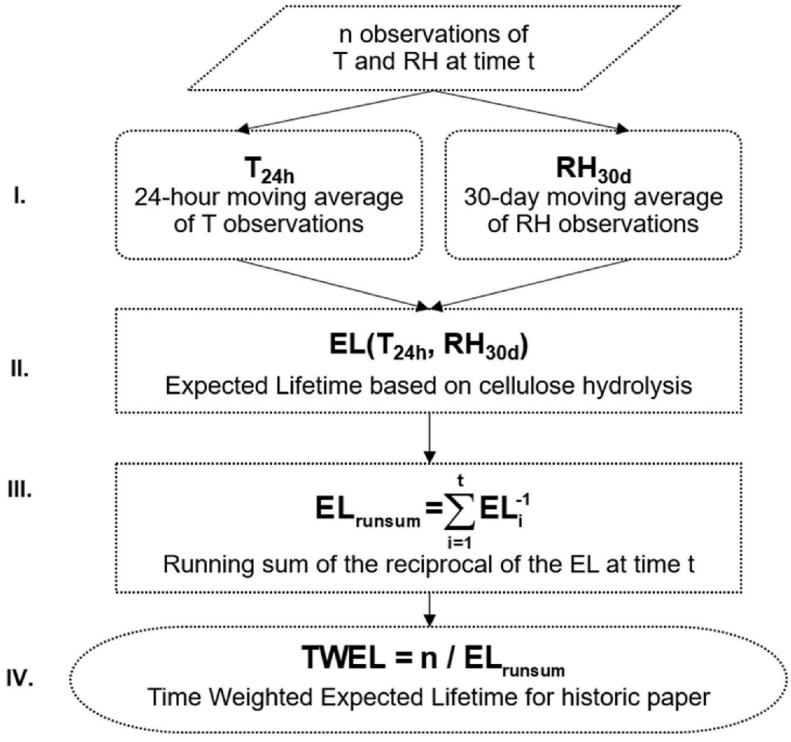

Fig. 4. Workflow of the procedure to calculate the Time Weighted Expected Lifetime (TWEL).

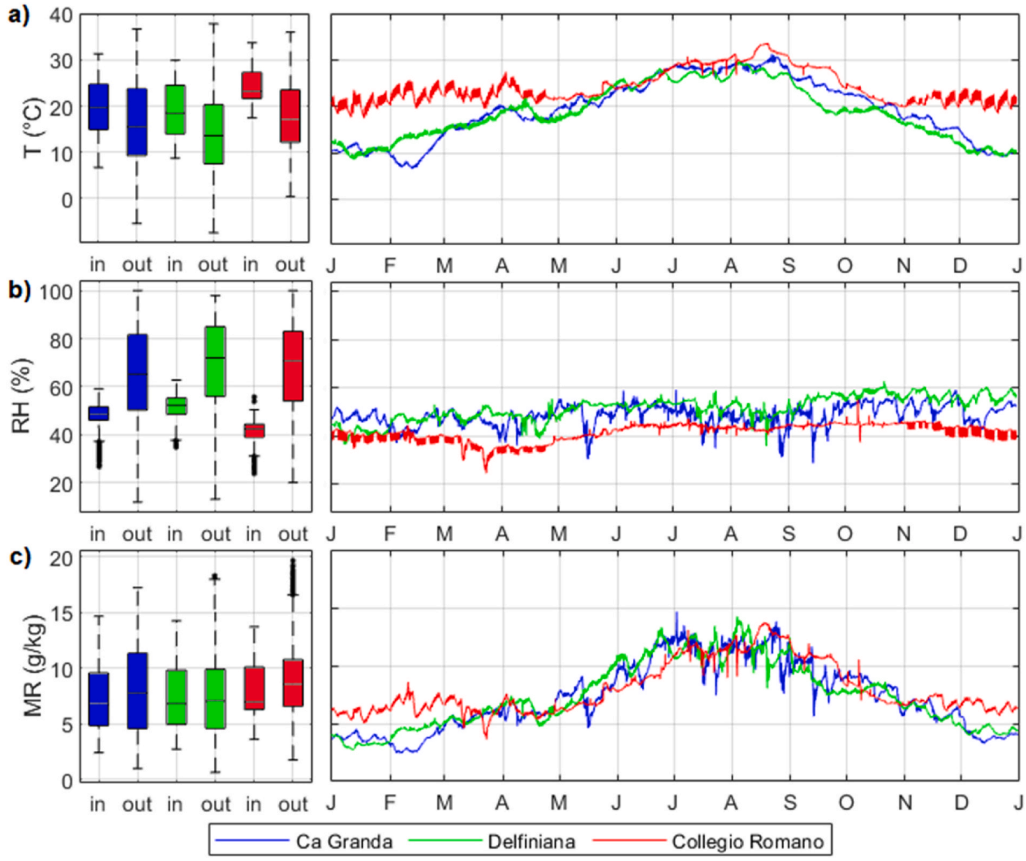

Fig. 5. Left: box-and-whisker plots of indoor (in) and outdoor (out) temperature (a), relative humidity (b) and mixing ratio (c) observations. Right: time plots of indoor T, RH and MR values. In the box-and-whisker plots, the medians are indicated with horizontal lines dividing each box and the outliers, i.e., the values above or below 1.5 × IQR (IQR = interquartile range), with black circles.

variability (from −7.4 °C to 37.8 °C) if compared to Milan (from −5.4 °C to 36.7 °C) and Rome (from 0.4 °C to 36.0 °C). The indoor temperatures in the three libraries showed comparable levels and trends from June to September, except for some sporadic T drops in Collegio Romano (red line) occurred in July/August caused by the cooling system. In cold periods, Ca' Granda and Delfiniana behaved similarly, whereas Collegio Romano experienced higher T due to the switching on of the heating system in the working days (from Monday to Friday).

The indoor relative humidity observations were found to be significantly lower than the outdoor ones (Fig. 5), with medians of indoor relative humidity around 50% in Ca' Granda and Delfiniana and around 40% in Collegio Romano. The outdoor RH variability, ranging from 11.8 to 100% in Ca' Granda, from 13 to 98% in Delfiniana and from 20 to 100% in Collegio Romano, was smoothed out inside the libraries. The drops in the RH observations in the libraries were mainly driven by MR; however, in Collegio Romano the RH drops were also associated with T rises caused by the heating system.

No significant differences in the median of the indoor MR levels (Fig. 5) were observed between Ca' Granda, Delfiniana and Collegio Romano libraries (MR in ≈7.0 g/kg), with outdoor MR medians equal to 7.7 g/kg in Milan, 7.1 g/kg in Udine and 8.6 g/kg in Rome. Although the indoor MR levels in Collegio Romano were only slightly different from those in the other two libraries from spring to autumn, in winter a different MR behaviour was observed, probably due to the moisture release from hygroscopic materials caused by the heating system.

The Normalized Diurnal Range index is shown in Fig. 6 to compare the thermal buffering capacity of the buildings housing the historic libraries. Ca' Granda had NDR values ranging from −0.1 to +0.1 and the highest frequency of zero values, meaning that the building envelope cut off most of the largest outdoor thermal variability, probably due to massive building envelopes and low air exchange rates [67]. The latter assumption could be evaluated by specific methods (e.g. the decay curves of tracer gas), which however are beyond the scopes of this work. The NDR values obtained in Delfiniana showed a different behaviour in the cold seasons with respect to the warm ones, with NDR values around zero in winter and negative NDR values during summer. The negative NDR values, meaning that $T_{n,21} > T_{n,14}$, were probably due to indoor summer T peaks being delayed after the outdoor T peaks. In Collegio Romano, summer NDR values ranged from −0.1 to +0.1 whereas distinct features characterised the heating period (from November until April), with a higher variability of NDR values. The short-term fluctuations caused by the active climate control system could be limited allowing for more relaxed climate targets in winter (e.g. switching off the radiators or lowering their temperature setpoints), with relevant beneficial effects also in terms of energy consumption [68]. The NDR values in Collegio Romano highlighted a higher heat accumulation (NDR<0) due to both the use of the radiators and the low air exchanges in summer. It was not possible to establish a correspondence between

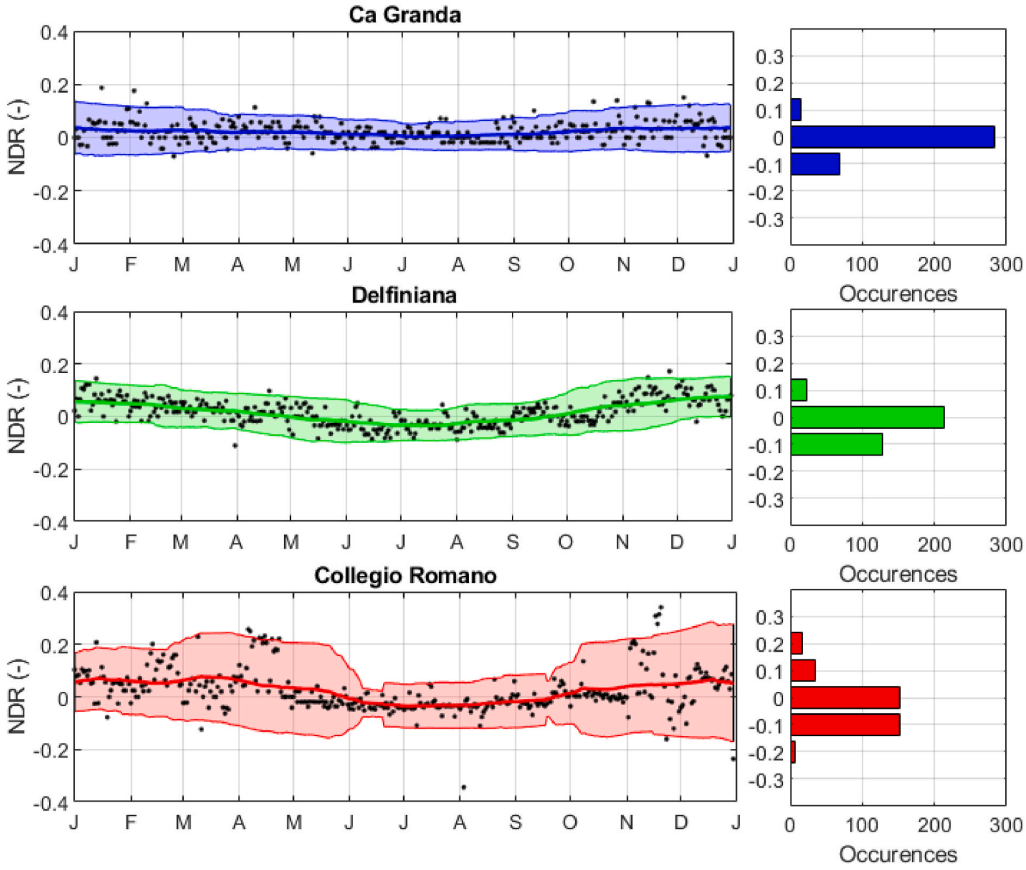

Fig. 6. Normalized Diurnal Range (NDR): time plots (left) and histograms (right). NDR values in time plots (black dots) are shown together with the curves of the 90-day moving average (thick coloured curves) and double moving standard deviation (thin coloured curves).

the anomalous NDR values (i.e. those lying outside the coloured band in Fig. 6) and particular events occurred in the libraries. This latter fact was interpreted as the consequence of the operation of averaging the daily outdoor values over the reference period, that might have smoothed out the real pattern of the outdoor thermal variability occurred in the monitored years.

In Fig. 7 the thermal vertical gradients ($\Delta T/\Delta z$) in Ca' Granda and Delfiniana were compared with the adiabatic gradient of vertical temperature for dry air ($\Gamma_d = -0.05$ °C/5 m). Air instability occurs when $\Delta T/\Delta z > \Gamma_d$. In Delfiniana air instability (i.e. upraising flow of warmer air masses from the floor and descending flow of colder air masses from the ceiling) occurred in winter due to the higher T measured at 1.4 m above floor with respect to those at 6.5 m (Fig. 7). Air instability can affect paper conservation as it could be responsible for transporting pollutants and other airborne particulate matter, thus causing soiling and deposition of dust and fungal spores that are

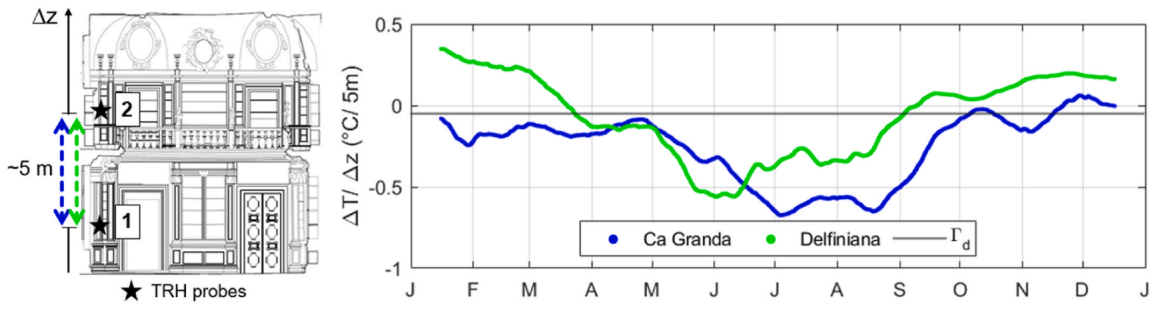

Fig. 7. Thermal vertical gradient ($\Delta T/\Delta z$, where ΔT = T1-T2), shown as 30-day centred moving averages, together with the adiabatic gradient of vertical temperature for dry air ($\Gamma_d = -0.05$ °C/5 m). Thermal vertical gradients exceeding Γ_d indicate vertical instability.

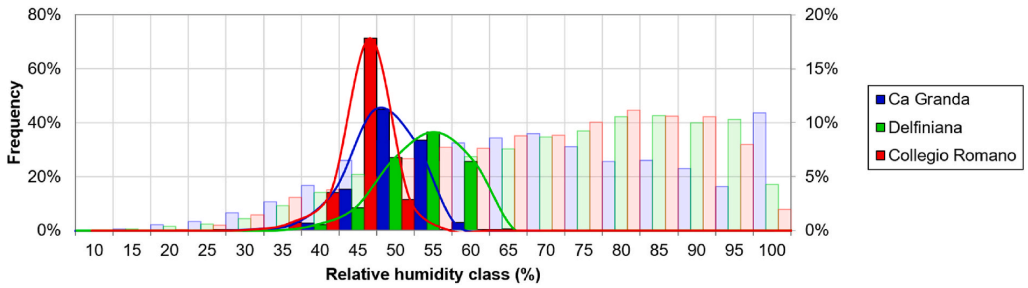

Fig. 8. Frequency distribution plots of the indoor (opaque) and outdoor (transparent) RH observations in a year. The secondary vertical axis refers to the frequency of outdoor RH values in each class.

ubiquitous. The lower temperatures collected near the ceiling were interpreted as the possible consequence of the poorly insulated roof causing heat losses, which were mitigated by the thermal masses in the lower air layers. As expected, during the warm season the air temperatures near the ceiling were higher than those collected at lower levels above the floor. The natural summer negative peaks were observed from mid-May to mid-June in Ca' Granda and from mid-June to August in Delfiniana. Thermal stratification may affect the conservation of the collections closer to the ceiling due to accelerated rates of chemical deterioration.

Fig. 8 shows the frequency distribution plots of the indoor and outdoor RH observations in the three libraries over the selected periods. All the libraries were characterized by high RH stability if compared to the outdoor variability. Indeed, the spread of the indoor RH observations was narrow and almost symmetric around the medians, as opposed to the markedly skewed distributions of the outdoor RH towards the highest values. Ca' Granda had RH observations centred around 48% (median) varying between 44% (7th percentile) and 52% (93rd percentile), Delfiniana RH median = 52% (varying between 48% and 57%) and Collegio Romano RH median = 43% (varying between 39% and 46%). It is worth noticing that, in the case of a Gaussian distribution, 7th and 93rd percentiles correspond to 1.5 standard deviations [24].

The RH ratio results are summarised in Table 4 together with the average absolute differences between the indoor MR observations and the outdoor ones ($\overline{\Delta MR}$) and the estimated hygroscopic ratio, calculated as the ratio between the volume of total hygroscopic materials (i.e. collection and wooden shelves), and the volume of library room. Ca' Granda had the relatively highest RH ratio (i.e., 24.1%), whereas Delfiniana had the relative lowest hygroscopic ratio (i.e., 6.2%). Although the libraries had comparable values of $\overline{\Delta MR}$ (i.e., 1.3 g/kg and 1.2 g/kg, respectively), the RH ratio resulted to be almost doubled in Ca' Granda (RH ratio = 24.1%) with respect to Delfiniana (RH ratio = 12.7%). Collegio Romano showed the relatively highest value of $\overline{\Delta MR}$ (i.e., 1.8 g/kg), together with the lowest value of RH ratio (i.e., 9.3%). Since it was not possible to measure the air exchanges, the MR values were used as a proxy of the indoor/outdoor air masses exchanges [57,61], as already done in literature [62,63]. For this reason, the relatively higher value of ΔMR in Collegio Romano was interpreted as the possible consequence of reduced indoor/outdoor air masses exchanges with the outdoors.

Fig. 8 and Table 4 seem to confirm a key aspect of the buffering behaviour of hygroscopic materials [42,69] in confined environment: when the percentage of storage space occupied by hygroscopic materials (i.e., the hygroscopic ratio) is high and air exchanges are low, the hygroscopic materials actively contribute to the stabilisation of RH (i.e., lower values of the RH ratio). However, even though stable relative humidity values limit the risk of tensile creep of paper [5], it has to be considered that reduced ventilation may favour fungal growth and pollutant accumulation.

3.2. Conservation risk assessment

Fig. 9 shows the temporal difference of the expected lifetime (EL) from the planning horizon of 500 years in the libraries. The conservation risk assessment took into account acidic historic paper, since it was the predominant paper type in the library collections as well as the one needing more attention due to its high sensitivity to indoor climate. From March to December, the EL values resulted to be lower than 500 years, meaning that temperature and relative humidity levels affected the durability of acidic historic paper. In winter, the low temperatures observed in Ca' Granda and Delfiniana (where indoor climate is not controlled) led to a significant increase in the expected lifetime of the collections. In Collegio Romano, in which radiators were active from Monday to Friday during the heating season (from November till April), the paper collection was under risky conditions.

The T and RH observations collected in the libraries are shown in Fig. 10 together with the T and RH ranges recommended by some of the standards in Table 1 (i.e., [18–20,29,31]). The microclimate conditions inside Ca' Granda and Delfiniana fitted the selected specifications for a small amount of the year and substantially never in the case of Collegio Romano.

In Fig. 11 the temperature and relative humidity observations collected in the libraries were plotted over the isochrones for acidic paper collections to evaluate the expected lifetime associated with the indoor climate. The TWEL index was used to average the overall chemical risk on both a yearly and a seasonal basis. The value of TWEL in all the libraries was lower than 350 years in autum, lower than 460 years in spring and only around 135 years in summer. In winter, TWEL was equal to 1540 and 1230 years respectively in Ca' Granda and Delfiniana but only 400 years in Collegio Romano. It is worth noticing that, since the calculation of TWEL does not linearly weight the expected lifetime over time, lower values of EL have a higher influence on the final output, thus considering a worst-case scenario. For this reason, although the winter TWEL values in Ca' Granda and Delfiniana were more than three times higher than in Collegio Romano, the yearly TWEL values in the three libraries were comparable in magnitude (293, 299 and 235 years, respectively). In Ca' Granda, the heat accumulation observed in summer (Fig. 7) caused the yearly TWEL near the ceiling to be reduced of a further 5% with respect to the TWEL at 1.4 m above floor. These results better highlighted not only that winter heating should be avoided whenever possible as a preventive conservation measure, but also that it is necessary to reduce indoor temperatures exceeding 20 °C in order to significantly mitigate the risk of cellulose hydrolysis. Moreover, the comparison among the libraries showed that the natural unconditioned indoor climates within historic buildings are preferable and thus could be suggested as a sustainable and effective preservation strategy for paper collections.

Looking at Fig. 10 in light of the isochrones in Fig. 11, it can be noticed that the T and RH ranges recommended by EN 16893 [29] are advisable for the preservation of acidic paper collections; conversely, the

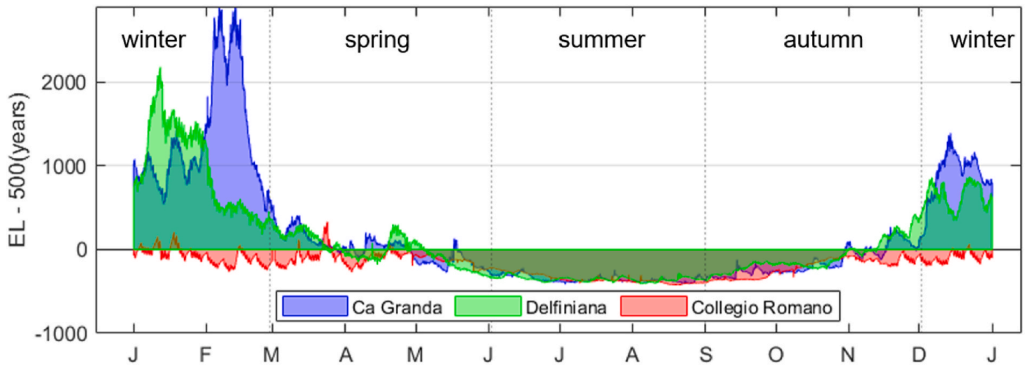

Fig. 9. Expected Lifetime (EL) spread from 500-year planning horizon for acidic paper.

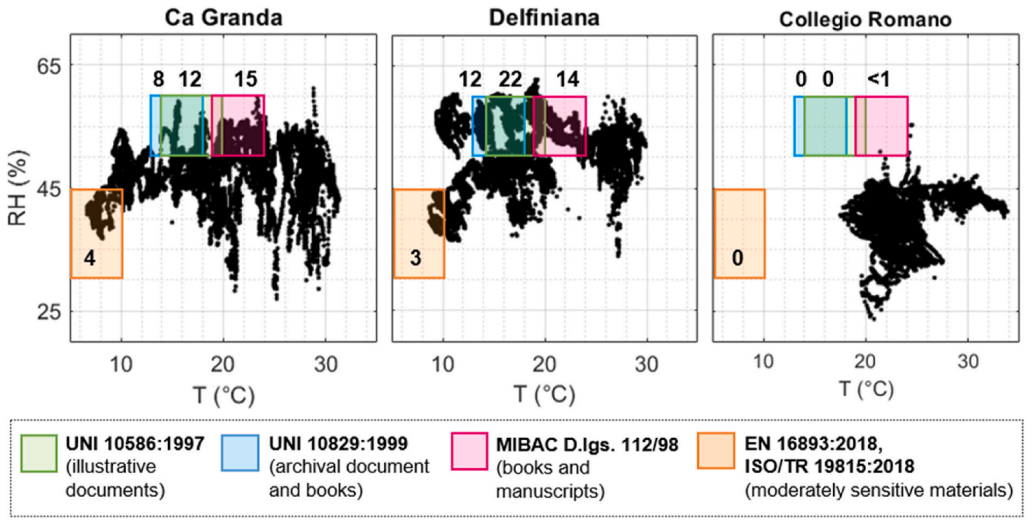

Fig. 10. Temperature and relative humidity observations (black dots) together with the T and RH ranges recommended by some of the standards in Table 1 (coloured boxes). In each box is reported the percentage of observations inside each target.

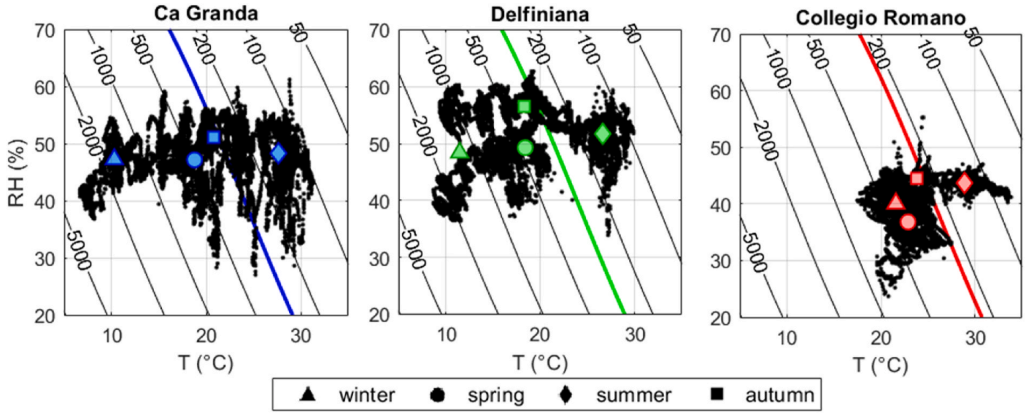

Fig. 11. Temperature and relative humidity observations (black dots) plotted on the isochrones of expected lifetime for acidic paper, together with the yearly (coloured curves) and seasonal (coloured markers) TWEL.

T and RH ranges recommended by Italian standards UNI 10586 [18], UNI 10829 [19] and legislative decree D.lgs. 112/98 [20] may not prevent from the chemical decay of acidic paper collections before the planning horizon of 500 years. It has to be borne in mind that, although the 500-year planning horizon was here used as a reference to guide the evaluation, each cultural institution should seek the expected lifetime being more appropriate for its collection given the peculiar contextual factors (e.g., the mission, the purpose, the building performance and the climate forcing due to its geographic location [10]). In this sense, the use of the TWEL index can be advantageous to inform preventive conservation strategies through an evidence-based criteria.

Fig. 12 shows the current scenario of the time required for the library collections to become unfit for use based on the proportions of paper types in each library (Fig. 3) and the average thermo-hygrometric conditions inside the libraries (Fig. 5). Over the next 200 years, large missing pieces could occur in Ca' Granda and Delfiniana to up to 20% of their collections and in Collegio Romano to up to 40%. If considering the conservation planning horizon of 500 years (vertical dashed black line), Collegio Romano could experience the whole collection being damaged from the combination of handling and chemical decay, while the wear and tear risk in Ca' Granda and Delfiniana could affect more than a half of the collections.

Table 5 summarises the increase in the fraction of collection fit for purpose through the preservation measure scenario of the deacidification of 10% of the acidic collection with respect to the current scenario (Fig. 12). Deacidification is a conventional treatment for the restoration of acidic paper that rises the pH by removing the accumulated acid components as well as introducing an alkaline reserve that protects the material from further acid degradation. In the tested scenario, 10% of the acidic part of collections was replaced by an identical amount of paper having DP = 640 and higher pH = 8.1. Taking into account the high investments and time required to accomplish such an intervention, the expected benefit after the deacidification is low in terms of the increase in the fit-for-use fraction of the total collection if compared to the current scenario (Table 5). For this reason, if the current indoor climate conditions will be maintained, the deacidification of 10% of the collections might be not an effective preservation measure.

Finally, based on the EL definition (Equation (4)), it was possible to explore the effect of mitigation measures -such as climate control and deacidification on the resulting chemical risk for acidic paper preservation. Fig. 13 illustrates some examples of the changes in the EL values of severely deteriorated acidic paper collections (DP = 600) from the initial conditions (where EL = 68 years, at T = 30 °C and RH = 50%) to the final conditions (highlighted in bold on the y-axes), where temperature (T), relative humidity (RH) or paper acidity (pH) were changed. As shown in the graphs, a RH reduction of 20% (Fig. 13a) and a T decrease of 10 °C (Fig. 13b) are not sufficient to make EL > 255 years; deacidification up to pH = 8 (Fig. 13c) increases the EL value up to 369 years; however, only through the concurrent T and RH reduction (Fig. 13d) it is possible to reach the planning horizon of EL = 500 years.

Table 5
Fit-for-use fraction of the total collection before (current scenario in Fig. 12) and after the deacidification of 10% of the acidic collection fraction in 200 and 500 years.

Fit-for-use fraction of collection (%) before (left) and after (right) deacidification						
Time horizon	Ca' Granda		Delfiniana		Collegio Romano	
200 years	83	87	79	81	64	65
500 years	35	42	28	34	6	13

4. Conclusions

The study of the historic libraries can be addressed both to the book collections and the building itself. For the first time, the availability of long thermo-hygrometric series collected in three historic libraries located in northern and central Italy allowed us to comparatively study their indoor climate conditions to provide more insight into the preventive conservation of paper. The study provided the indoor climate characterisation of the historic buildings housing the libraries and the climate-induced risk assessment based on the chemical risks for the preservation of the library collections.

The approach developed in our study enables a wide-ranging investigation on historic libraries. Indeed, the Normalized Diurnal Index (NDR) was used to compare the natural thermal inertia of the unconditioned buildings of Ca' Granda and Delfiniana with respect to that of Collegio Romano where winter heating is active. In addition, the proposed Time Weighted Expected Lifetime (TWEL) index proved to be useful to explore the effect on paper conservation of changes in the indoor climate conditions resulting from climate control strategies, retrofitting measures and/or the possible future climate change.

The results of the investigation highlighted that the historic libraries had high thermal inertia and moisture buffering capacity due to the possible combined effect of the massive building envelopes, low air exchanges and large total volumes of hygroscopic materials (i.e., paper collections and wooden shelves). In terms of paper preservation, it was found that the monitored microclimate conditions in all the libraries would lead to the loss of their acidic collections in less than 300 years, mostly because of the high temperatures typically occurring in summer. Besides, the use of winter heating in Collegio Romano further reduced the expected lifetime with respect to that estimated in the free-floating climates of Ca' Granda and Delfiniana in the same season. For this reason, the natural unconditioned indoor climates within historic buildings could be suggested as a sustainable preservation strategy for paper collections in winter. This can be relevant for library conservation, since nowadays the increased fruition, the extensive use of heating

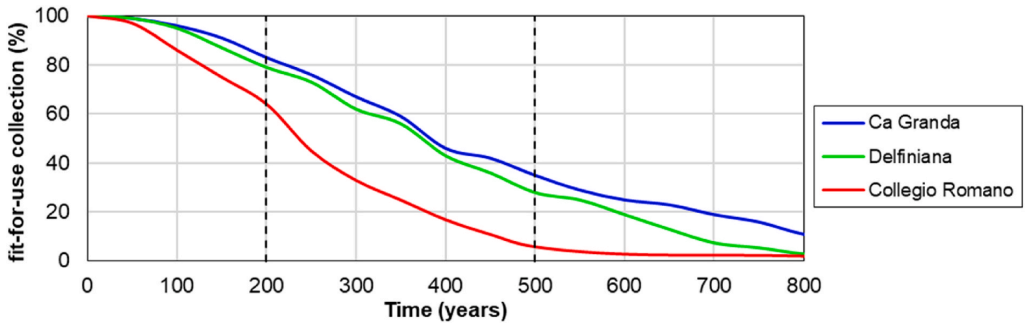

Fig. 12. Scenario of lifetime profiles over time showing the percentage of collection fit-for-use (i.e., items that can be safely handled) if stored at the current average thermo-hygrometric conditions inside the libraries. The vertical dashed lines highlight the current scenario in 200 and 500 years.

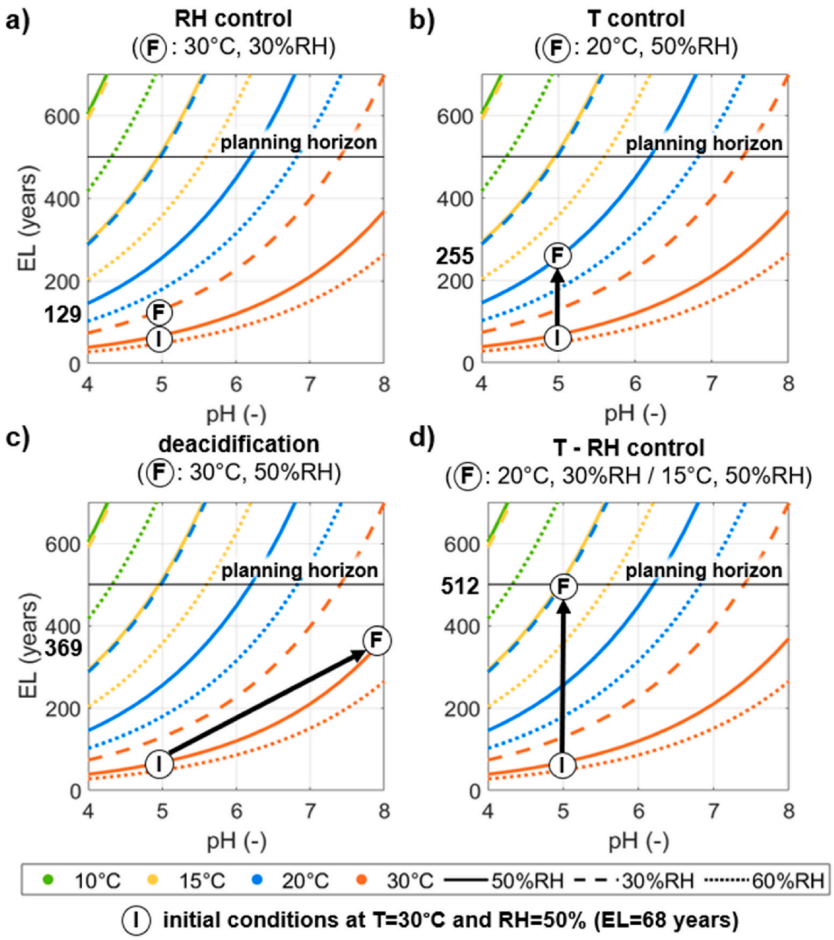

Fig. 13. Examples of mitigation strategies through T/RH reduction (a, b, d) or deacidification (c) by changing temperature (T), relative humidity (RH) or paper acidity (pH): changes in the expected Lifetime (EL) of severely deteriorated acidic paper collections (DP = 600) from the initial condition (I) at T = 30 °C and RH = 50% (EL = 68 years) to the final conditions (F).

systems and the latest climate change scenario [70] are leading the microclimate within historic buildings away from the natural one.

Some considerations about the limitations of our study are here outlined. First, the limited number of thermo-hygrometers per case study made it unfeasible to analyse spatial differences in T and RH values within each library. Moreover, the impact of the solar radiation entering the room and the air exchanges with the outdoors could not be quantitatively assessed because specific instruments for their measurements were not available. Finally, the proposed TWEL has not been experimentally validated yet, hence its value only expresses a weighted average of the chemical degradation risk based on the expected lifetime.

The above reflections stimulate further research on the conservation of historic libraries in view of the climate change predictions.

Funding sources

The APC was funded by CollectionCare project, which has received funding from the European Union's Horizon 2020 research and innovation programme under grant agreement No 814624.

Authors' contribution

All the authors have equally contributed to this study.

Declaration of competing interest

The authors declare that they have no known competing financial interests or personal relationships that could have appeared to influence the work reported in this manuscript.

Acknowledgements

Siani A.M., Frasca F. and Verticchio E. thank the CollectionCare project (European Union's Horizon 2020 research and innovation programme under grant agreement No 814624) for the financial support of the APC. Verticchio E., Siani A.M. and Frasca F. are indebted to Dr Luigi Iafrate for the invaluable support in the data acquisition at Collegio Romano. Bertolin C. is indebted to the project Climate for Culture (European Union's Seventh Framework Programme for Research under Grant Agreement No. 22 6973, Prof. Johanna Leissner and Emeritus Prof. Dario Camuffo) for giving financial support in collecting data for

the Ca' Granda (data are available to CfC partners at http://www.monumenten.bwk.tue.nl/CfC/) and to the Diocesi of Udine for having funded NTNU with a project to monitor the Delfiniana Library. Bertolin C. is indebted with Dr. Paolo Galimberti for the availability demonstrated during the monitoring campaign in the Ca' Granda in Milan; to the whole staff of the Museo Diocesano in Udine and in particular to the director Giuseppe Bergamini, the conservators Dr. Dania Nobili and Arch. Giorgio Della Longa for their continuous and kind availability and to Mr. Marco Birri for the support provided in situ during the campaign. The authors thank Prof. Branko Mitrovic for the support in providing architectural history information. The authors also acknowledge the E-OBS dataset from the EU-FP6 project UERRA (https://www.uerra.eu) and the Copernicus Climate Change Service, and the data providers in the ECA&D project (https://www.ecad.eu).

References

[1] H.A. Taylor, The collective memory: archives and libraries as heritage, Archivaria 15 (15) (1982) 118–130.
[2] D. Beales, Prosperity and Plunder: European Catholic Monasteries in the Age of Revolution, 1650-1815, Cambridge University Press, 2003.
[3] S. VanSnick, K. Ntanos, On digitisation as a preservation measure, Stud. Conserv. 63 (sup1) (2018) 282–287, https://doi.org/10.1080/00393630.2018.1504451.
[4] M. Strlič, et al., Damage function for historic paper. Part II: wear and tear, Herit. Sci. 3 (1) (2015) 1–11, https://doi.org/10.1186/s40494-015-0065-y.
[5] E. Menart, G. De Bruin, M. Strlič, "Dose-response Functions for Historic Paper," *Polymer Degradation And Stability*, 2011, https://doi.org/10.1016/j.polymdegradstab.2011.09.002.
[6] M. Strlič, et al., Development and mining of a database of historic European paper properties, Cellulose 27 (2020) 8287–8299, https://doi.org/10.1007/s10570-020-03344-x.
[7] S. Michalski, Double the life for each five-degree drop, more than double the life for each halving of relative humidity, Thirteen. Triennn. Meet. ICOM-CC 3 (2002) 66–72.
[8] D.W. Nishimura, Understanding Preservation Metrics, 2011.
[9] M. Strlič, et al., Damage function for historic paper. Part III: Isochrones, Herit. Sci. (2015), https://doi.org/10.1186/s40494-015-0062-1.
[10] ", ASHRAE Handbook—HVAC Applications, Chapter 24. Museums, Galleries, Archives, and Libraries, *American Society of Heating, Refrigerating and Air-Conditioning Engineers*, 2019.
[11] S. López-Aparicio, et al., Relationship of indoor and outdoor air pollutants in a naturally ventilated historical building envelope, Build. Environ. 46 (7) (2011) 1460–1468, https://doi.org/10.1016/j.buildenv.2011.01.013.
[12] M. Andretta, F. Coppola, L. Seccia, Investigation on the interaction between the outdoor environment and the indoor microclimate of a historical library, J. Cult. Herit. (2016), https://doi.org/10.1016/j.culher.2015.07.002.
[13] E. Menart, G. de Bruin, M. Strlič, Effects of NO2 and acetic acid on the stability of historic paper, Cellulose 21 (5) (2014) 3701–3713, https://doi.org/10.1007/s10570-014-0374-4.
[14] B. Bartl, L. Mašková, H. Paulusová, J. Smolík, L. Bartlová, P. Vodička, The effect of dust particles on cellulose degradation, Stud. Conserv. 61 (4) (2016) 203–208, https://doi.org/10.1179/2047058414Y.0000000158.
[15] E. Vereecken, S. Roels, Review of mould prediction models and their influence on mould risk evaluation, Build. Environ. (2012), https://doi.org/10.1016/j.buildenv.2011.11.003.
[16] Jerzy haber Institute of catalysis and surface chemistry - polish academy of sciences, HERIe 2.0 (2020) [Online]. Available: https://herie.pl/. Accessed: 10-Aug-2021.
[17] David ribar in collaboration with the heritage science lab ljubljana and UCL Institute for sustainable heritage, "collections demography app [Online]. Available: https://hsll.shinyapps.io/collections_demography_app/, 2015. (Accessed 26 May 2021). Accessed.
[18] Uni 10586, Climatic Conditions for Storage Environments of Graphic Documents and Features of the Housings, Ente Italiano di Normazione, 1997.
[19] UNI 10829, Properties of historical and artistic interest – environmental conservation – measurement and analysis, Ente Italiano di Normazione, 1999.
[20] Dlgs 112/98 Art. 150 Comma 6. Guideline on Technical and Scientific Criteria and Standards of Functioning and Development of Museum, 2001.
[21] ANSI/NISO Z39.79 - Environmental Conditions for Exhibiting Library and Archival Materials, " American National Standards Institute – National Information Standards Organization, 2001.
[22] ISO 11799, Document Storage Requirements for Archive and Library Materials, International Organization for Standardization, 2003.
[23] S. Michalski, The ideal climate, risk management, the ASHRAE chapter, proofed fluctuations, and toward a full risk analysis model, Contrib. to Expert. Roundtable Sustain. Clim. Manag. Strateg. held April 2007 (April 2007) (2007) 1–19. Tenerife, Spain.
[24] EN 15757, Conservation of Cultural Property - Specifications for Temperature and Relative Humidity to Limit Climate-Induced Mechanical Damage in Organic Hygroscopic Materials, " European Committee for Standardization, Brussels, 2010.
[25] PD 5454, Guide for the Storage and Exhibition of Archival Materials, " British Standards Institution, 2012.
[26] PAS 198, Specification for Managing Environmental Conditions for Cultural Collections, " British Standards Institution, 2012.
[27] ISO 11799, Information and Documentation — Document Storage Requirements for Archive and Library Materials, " International Organization for Standardization, 2015.
[28] BS 4971, Conservation and Care of Archive and Library Collections, 2017.
[29] EN 16893, Conservation of Cultural Heritage - New Sites and Buildings Intended for the Storage and Use of Collections, " European Committee for Standardization, Brussels, 2018.
[30] ASHRAE Handbook—HVAC Applications, Chapter 23. Museums, Galleries, Archives, and Libraries, *American Society of Heating, Refrigerating and Air-Conditioning Engineers*, 2011.
[31] "ISO/TR 19815, Information and Documentation — Management of the Environmental Conditions for Archive and Library Collections, International Organization for Standardization, 2018.
[32] IFLA - Principles for the Care and Handling of Library Materials, International Federation of Library Associations and Institutions, 2016.
[33] ICCU, "Statistics on library data," Anagrafe delle Biblioteche Italiane. [Online]. Available: https://anagrafe.iccu.sbn.it/it/statistiche/statistiche-al-31-12-2020/. [Accessed: 22-Apr-2020].
[34] A.E. Bülow, B.J. Colston, D.S. Watt, Preventive conservation of paper-based collections within historic buildings, Stud. Conserv. 47 (2002) 27–31, https://doi.org/10.1179/sic.2002.47.s3.006.
[35] L. Tronchin, K. Fabbri, Energy and microclimate simulation in a heritage building: further studies on the Malatestiana Library, Energies (2017), https://doi.org/10.3390/en10101621.
[36] E. Schito, L. Dias Pereira, D. Testi, M. Gameiro da Silva, A procedure for identifying chemical and biological risks for books in historic libraries based on microclimate analysis, J. Cult. Herit. (2018), https://doi.org/10.1016/j.culher.2018.10.005.
[37] F. Drougka, et al., Indoor air quality assessment at the library of the national observatory of Athens, Greece, Aerosol Air Qual. Res. 20 (4) (2020) 889–903, https://doi.org/10.4209/aaqr.2019.07.0360.
[38] K. Fabbri, M. Pretelli, Heritage Buildings and Historic Microclimate without HVAC Technology: Malatestiana Library in Cesena, Italy, UNESCO Memory of the World, *Energy Build.*, 2014, https://doi.org/10.1016/j.enbuild.2014.02.051.
[39] C. Balocco, G. Petrone, O. Maggi, G. Pasquariello, R. Albertini, C. Pasquarella, Indoor microclimatic study for Cultural Heritage protection and preventive conservation in the Palatina Library, J. Cult. Herit. 22 (2016) 956–967, https://doi.org/10.1016/j.culher.2016.05.009.
[40] M. Mamoli, Towards a Theory of Reconstructing Ancient Libraries, 2014. PhD Diss.
[41] A. Dressen, J. Connors, Biblioteche l'architettura e l'ordinamento del sapere, Rinascim. Ital. e l'Europa 6 (2010) 199–228. Luoghi, Spaz. Archit., vol. 6.
[42] A. Kupczak, A. Sadłowska-Sałęga, L. Krzemień, J. Sobczyk, J. Radoń, R. Kozłowski, Impact of paper and wooden collections on humidity stability and energy consumption in museums and libraries, Energy Build. 158 (2018) 77–85, https://doi.org/10.1016/j.enbuild.2017.10.005.
[43] E. Verticchio, F. Frasca, F.-J. Garcìa-Diego, A.M. Siani, Investigation on the use of passive microclimate frames in view of the climate change scenario, Climate 7 (8) (Aug. 2019) 98, https://doi.org/10.3390/cli7080098.
[44] M. Steeman, M. De Paepe, A. Janssens, Impact of whole-building hygrothermal modelling on the assessment of indoor climate in a library building, Build. Environ. 45 (7) (2010) 1641–1652, https://doi.org/10.1016/j.buildenv.2010.01.012.
[45] E. Verticchio, F. Frasca, C. Cornaro, A.M. Siani, Investigation on the use of hygrothermal modelling for paper collections, IOP Conf. Ser. Mater. Sci. Eng. 949 (1) (2020), https://doi.org/10.1088/1757-899X/949/1/012015.
[46] F. Frasca, E. Verticchio, C. Cornaro, A.M. Siani, Performance assessment of hygrothermal modelling for diagnostics and conservation in an Italian historical church, Build. Environ. 193 (2021) 107672, https://doi.org/10.1016/j.buildenv.2021.107672.
[47] M. de la P. Diulio, P. Mercader-Moyano, A.F. Gómez, The influence of the envelope in the preventive conservation of books and paper records. Case study: libraries and archives in La Plata, Argentina, Energy Build. 183 (2019) 727–738, https://doi.org/10.1016/j.enbuild.2018.11.048.
[48] C.D. Sahin, T. Coşkun, Z.D. Arsan, G. Gökçen Akkurt, Investigation of indoor microclimate of historic libraries for preventive conservation of manuscripts. Case Study: tire Necip Paşa Library, İzmir-Turkey, Sustain. Cities Soc. (2017), https://doi.org/10.1016/j.scs.2016.11.002.
[49] D. Thickett, R. Soek-Joo, S. Lambarth, Libraries and Archives in Historic Buildings, *Museum Microclim. Natl. Museum Denmark*, Copenhagen, 2007, pp. 145–156.
[50] F. Coppola, N. Brown, F. Amicucci, M. Strlič, A. Modelli, Non-destructive collection survey of the historical Classense Library. Part II: conservation scenarios, Herit. Sci. 8 (1) (2020) 1–10, https://doi.org/10.1186/s40494-020-00430-y.
[51] B. Świątkowska, Ł. Skoczeń-Rąpała, D. Okrągła, M. Jędrychowski, J. Czop, Chemical Degradation and Physical Failure: Risk Analysis for a Paper Collection, vol. 3630, 2018, https://doi.org/10.1080/00393630.2018.1504450.
[52] H.E. Beck, N.E. Zimmermann, T.R. McVicar, N. Vergopolan, A. Berg, E.F. Wood, Present and future köppen-geiger climate classification maps at 1-km resolution, Sci. Data 5 (2018) 1–12, https://doi.org/10.1038/sdata.2018.214.
[53] M. Carlessi, A. Kluzer, Il cuore dell'antico Ospedale Maggiore di Milano: i luoghi dell'archivio e la chiesa della B.V. Annunciata, Silvana Ed., Milano, 2011.
[54] C. Bertolin, Il ruolo del microclima nella conservazione del patrimonio librario e archivistico. Il caso della Biblioteca Delfiniana nel palazzo Arcivescovile di Udine,, in: Proceedings of the International Conference "Clima negli edifici di culto. Esperienze e prospettive, in publication, Venice, 2018.

[55] M.C. Beltrano, S. Esposito, L. Iafrate, The archive and library of the former Italian central Office for Meteorology and climatology, Adv. Sci. Res. 8 (1) (2012) 59–65, https://doi.org/10.5194/asr-8-59-2012.
[56] EN 15758:2010. Conservation of Cultural Property - Procedures and Instruments for Measuring Temperatures of the Air and the Surfaces of Objects, Brussels, 2010.
[57] EN 16242. Conservation of Cultural Heritage - Procedures and Instruments for Measuring Humidity in the Air and Moisture Exchanges between Air and Cultural Property, European Committee for Standardization, Brussels, 2012.
[58] F. Frasca, et al., Assessment of indoor climate of Mogiła Abbey in Kraków (Poland) and the application of the analogues method to predict microclimate indoor conditions, Environ. Sci. Pollut. Res. 24 (16) (2017) 13895–13907, https://doi.org/10.1007/s11356-016-6504-9.
[59] F. Frasca, E. Verticchio, A. Caratelli, C. Bertolin, D. Camuffo, A.M. Siani, A comprehensive study of the microclimate-induced conservation risks in hypogeal sites: the mithraeum of the baths of Caracalla (Rome), Sensors (Switzerland) 20 (11) (2020) 1–18, https://doi.org/10.3390/s20113310.
[60] A.M. Siani, F. Frasca, M. Di Michele, V. Bonacquisti, E. Fazio, Cluster analysis of microclimate data to optimize the number of sensors for the assessment of indoor environment within museums, Environ. Sci. Pollut. Res. (2018), https://doi.org/10.1007/s11356-018-2021-3.
[61] D. Camuffo, Microclimate for Cultural Heritage Conservation and Restoration of Indoor and Outdoor Monuments, Elsevier, Amsterdam, 2019.
[62] H.E. Huerto-Cardenas, N. Aste, C. Del Pero, S. Della Torre, Effects of Climate Change on the Future of Heritage Buildings : Case Study and Applied Methodology, 2021.
[63] C. Bertolin, D. Camuffo, I. Bighignoli, Past Reconstruction and Future Forecast of Domains of Indoor Relative Humidity Fluctuations Calculated According to EN 15757:2010, *Energy Build.*, 2015, https://doi.org/10.1016/j.enbuild.2015.05.028.
[64] D. Camuffo, A. della Valle, C. Bertolin, E. Santorelli, Temperature observations in Bologna, Italy, from 1715 to 1815: a comparison with other contemporary series and an overview of three centuries of changing climate, Climatic Change 142 (1–2) (2017) 7–22, https://doi.org/10.1007/s10584-017-1931-2.
[65] R. Cornes, G. van der Schrier, E.J.M. van den Besselaar, P.D. Jones, An ensemble version of the E-OBS temperature and precipitation datasets, J. Geophys. Res. Atmos. 123 (2018), https://doi.org/10.1029/2017JD028200.
[66] M.H.J. Martens, "Climate risk assessment in museums : degradation risks determined from temperature and relative humidity data, Build. Environ. 2005 (2012) (2012) 41–44, https://doi.org/10.6100/IR729797.
[67] F. Cappitelli, et al., "Chemical-physical and microbiological measurements for indoor air quality assessment at the ca' granda historical archive, Milan (Italy)," *Water*, Air. Soil Pollut. 201 (1–4) (2009) 109–120, https://doi.org/10.1007/s11270-008-9931-5.
[68] R.P. Kramer, H.L. Schellen, A.W.M. van Schijndel, "Impact of ASHRAE's museum climate classes on energy consumption and indoor climate fluctuations: full-scale measurements in museum Hermitage Amsterdam, Energy Build. 130 (2016) 286–294, https://doi.org/10.1016/j.enbuild.2016.08.016.
[69] H. Derluyn, H. Janssen, J. Diepens, D. Derome, J. Carmeliet, Hygroscopic behavior of paper and books, J. Build. Phys. 31 (1) (2007) 9–34, https://doi.org/10.1177/1744259107079143.
[70] IPCC, Assessment Report 6 climate change 2021: the physical science basis [Online]. Available: https://www.ipcc.ch/report/ar6/wg1/, 2021.

Appendix B

Performance assessment of hygrothermal modelling for diagnostics and conservation in an Italian historical church

Frasca, F., **Verticchio, E.**, Cornaro C., and Siani, A.M.

Building and Environment **193**, 107672 (2021)

Building and Environment 193 (2021) 107672

Contents lists available at ScienceDirect

Building and Environment

journal homepage: http://www.elsevier.com/locate/buildenv

Performance assessment of hygrothermal modelling for diagnostics and conservation in an Italian historical church

Francesca Frasca [a,*], Elena Verticchio [b], Cristina Cornaro [c], Anna Maria Siani [a]

[a] Department of Physics, Sapienza University of Rome, P.le Aldo Moro 5, Rome, Italy
[b] Department of Earth Sciences, Sapienza University of Rome, P.le Aldo Moro 5, Rome, Italy
[c] Department of Enterprise Engineering, University of Rome Tor Vergata, Via Del Politecnico 1, Rome, Italy

ARTICLE INFO

Keywords:
Historical churches
Hygrothermal modelling
Historical buildings
HAM model
Diagnostics
Conservation risks

ABSTRACT

The hygrothermal modelling of historical churches is a promising approach to study preservation issues and suitable retrofit measures. However, difficulties can arise in the use of Heat, Air and Moisture (HAM) models, which are often customised objects to be integrated into validated building energy simulation (BES). This research outlines a multi-step methodology to investigate the capability of a BES software coupled with a HAM model (BES + HAM) as a technique for diagnostics and conservation in complex settings. The 17th-century church of Santa Rosalia (Italy) was used as a historical site in a real context. As first step, the performance of the simulation tool was analysed through standardised exercises aiming at excluding incorrect assumptions and calculations in the HAM model (HMWall). Secondly, a building model of the church using a 1D heat transfer model (named building model A) was compared with one using HMWall (named building model B) in terms of the accuracy of the indoor climate simulations against hygrothermal measurements. The results showed that building model B enhanced the simulation accuracy by +50% with respect to building model A. Finally, annual simulations inside the church were run to further compare the seasonal trends of indoor climate scenario obtained from the two building models. Building model B allowed to study the water content distribution inside the altarpiece and a wall partition, showing that BES + HAM tools can be used to identify potential moisture-induced conservation risks.

1. Introduction

The number of historical churches is copious throughout Europe and especially in Italy, where churches, abbeys, cloisters, crypts and monastic complexes represent all together approximately the 30% of the total architectural monuments [1]. Historical churches often contain valuable interiors, which need to be adequately preserved; therefore, the development of suitable strategies for their preservation requires a thorough understanding of the climate-induced risks [2]. For example, hygroscopic furnishings and artworks conserved in churches can be severely damaged by relative humidity fluctuations. In addition, moisture condensation in poor ventilated or damp environments (e.g. crypts) may contribute to biological colonisation and crystallisation/dissolution of deliquescent salts [3]. As in the case of any other building, the indoor environment inside churches is influenced by the local climate and features of the building envelope as well as the management of the site (e.g. Ref. [4] for Mediterranean area and [5] for northern European regions). The conservation of churches can be also threatened by uncontrolled use of heating systems, because they adversely affect the indoor historic climate [6]. In the framework of the Friendly Heating project (2002–2005), the most suitable heating systems for churches were thoroughly studied [7]. Currently, the selection of heating strategies and the ventilation management for the protection of churches, chapels and other places of worship is regulated by the European standard EN 15759-1 [8].

In the last decades, the use of mathematical models has attracted a broad interest in the scientific community as a method to diagnose conservation conditions and to study the suitability of retrofit measures in historical buildings, including churches. An approach in indoor climate modelling is the use of transfer functions (TFs) that derive the indoor hygrothermal conditions from the outdoor climate [9]. A more powerful tool is the whole building dynamic simulation, which can provide both energy and hygrothermal assessment. In Climate for

* Corresponding author.
E-mail addresses: f.frasca@uniroma1.it (F. Frasca), elena.verticchio@uniroma1.it (E. Verticchio), cornaro@uniroma2.it (C. Cornaro), annamaria.siani@uniroma1.it (A.M. Siani).

https://doi.org/10.1016/j.buildenv.2021.107672
Received 28 September 2020; Received in revised form 16 January 2021; Accepted 1 February 2021
Available online 8 February 2021

Abbreviations

ΔRH	Daily RH rate (%·day^{-1})
τ_e	Solar light transmittance
τ_v	Visible light transmittance
ACH	Air Change per Hour
BES	Building Energy Simulation
CV-RMSE	Coefficient of Variation of the Root Mean Square Error
D_{ws}	Liquid transport coefficients for suction
D_{ww}	Liquid transport coefficients for redistribution
HAM	Heat Air and Moisture
MAE	Mean Absolute Error
MR	Mixing Ratio (g·kg^{-3})
p_{sat}	Saturated water vapour pressure
p_v	Water vapour partial pressure
Qv	Prediction rate
RMSE	Root Mean Square Error
RH	Relative Humidity (%)
rho	Correlation coefficient
SHGC	Solar Heat Gain Coefficient
T	Temperature (°C)
TF	Transfer function
TRY	Test Reference Year
U-value	Thermal transmittance
w	Water content (kg·m^{-3})

Hygrothermal properties of building materials in HMWall

λ	Thermal conductivity (W·m^{-1}·K^{-1})
ρ	Density (kg·m^{-3})
C	Specific heat (J·kg^{-1}·K^{-1})
w_f	Free water saturation (kg·m^{-3})
w_{80}	Equilibrium water content at RH = 80% (kg·m^{-3})
b	Thermal conductivity supplement (−)
μ	Vapour diffusion resistance (−)
A_w	Water absorption coefficient (kg·m^{-2}·s$^{-0.5}$)

Culture project (2009–2014) [10], the indoor climate conditions inside 35 churches located around Europe were simulated using various simulation software in order to investigate requirements for preventive conservation strategies (e.g. Refs. [11,12]). Coelho et al. [13] modelled a 13th-century church in WUFI Plus to study the accuracy of hygrothermal simulations in complex buildings such as churches. Sadłowska-Sałęga et al. [14] used indoor and outdoor climate data to validate a hygrothermal building model of a 18th-century wooden church in WUFI Plus, paying attention to the effect of input parameters in the accuracy of the results. Muñoz-González et al. [15,16] assessed passive, active and combined environmental conditioning techniques in two Spanish historical churches by means of Energy Plus. Two Estonian churches were modelled in IDA ICE to study the impact of adaptive ventilation strategies [17], dehumidification and heating systems on indoor climate and energy consumption [18]. Semprini et al. [19] evaluated the effect of HVAC system coupled with radiant devices for temperature and relative humidity control on the thermal comfort of visitors/churchgoers. Airing solutions in Sweden historical churches were evaluated by semi-empirical models [20] and IDA ICE [21] as an alternative to mechanical ventilation in removing contaminants threatening painted surfaces. Finally, the effect of future climate change on the preservation of artworks, thermal comfort and energy consumption was investigated in Ref. [22] by means of hygrothermal building models of three historical churches in parallel with on-site measurements.

A proper modelling of the indoor climate conditions is mandatory to take advantage from the simulation of the indoor climate, as it is directly and indirectly involved in all the deterioration processes of materials [23]. Consequently, whole building simulation tools need to accurately model the time behaviour of the key hygrothermal variables (e.g. temperature and relative humidity) responsible for degradation at short- and long-term scale, this being a necessary prerequisite in order to reliably use them for the design of advanced preventive conservation strategies. The main difficulty in the hygrothermal modelling of historical churches is the construction of the building model, which is demanding and time-consuming. In fact, each building has specific peculiarities due to the construction techniques and materials, resulting in a high risk of errors while modelling the building. In the hygrothermal modelling of historical buildings, Akkurt et al. [24] identified four sources of uncertainties: a) the geometrical model, b) the thermo-physical properties of the envelope, c) the schedules of internal gains and occupancy and d) the outdoor climate data. In this study, we focused on (b) source of uncertainty because the modelling of the simultaneous heat and moisture transfer through walls is essential in the dynamic simulation of historical buildings since most building materials are hygroscopic and can contain moisture at different thermodynamic phases. It follows that moisture and its related processes directly affect not only the thermal response of materials and their durability [25,26], but also the overall humidity inside a room (or zone) due to the sorption effect of hygroscopic materials [27].

Advanced and sophisticated models for indoor climate simulations are rarely employed in modelling historical buildings, as it can be difficult to dispose of robust algorithms and databases with the thermophysical and hygric properties of historical materials. Some building energy simulation tools (BES) integrate the heat and moisture flows through the algorithms of energy and mass balances between the air and hygroscopic surfaces [28,29] using HAM models, i.e. Heat, Air and Moisture models. The current approaches to model moisture exchanges in buildings are based on using either the co-simulation [30] or performing the hygrothermal calculations within the architecture of the building energy simulation (BES) software. In the co-simulation, each individual model is run in parallel (e.g. Refs. [31–33]) but two software are needed, i.e. the BES and the hygrothermal transfer model. Conversely, the second option has the main advantage of performing the hygrothermal assessment using a single simulation tool. IDA Indoor Climate and Energy (IDA ICE) extended with the HMWall model, having this advantage, was effectively exploited in several works including the modelling of historical buildings (e.g. Refs. [34,35]). To the best of our knowledge, not many studies have considered the moisture transfer modelling through walls, to cite a few: [11,12,14–16,22].

As all mathematical models are based on simplified parametrisations, the performance of the HAM models needs to be refined at different levels, from the building materials to the whole-building response [36]. This is particularly true when customised models are integrated into validated BES tool, as in the case of HMWall coupled with IDA ICE.

This study aimed to assess the performance of a BES software extended with a HAM model for diagnostics and conservation in historical churches through a multi-step methodology *ad-hoc* conceived. Since there is still no individual software or model nor an agreed method to perform the hygrothermal validation [37], standardised exercises were used to evaluate the performance of BES software coupled with HAM models. *Chiesa di Santa Rosalia* was chosen as a complex site to test the reliability of hygrothermal modelling for the preventive conservation of historical churches.

Sections 2.1 and 2.2 of this paper describe the site, the monitoring campaign and the construction of the building models. Section 2.3 explains the methodology developed to achieve the research objective. In section 3.1 and 3.2, the performance of HMWall (HAM model) into IDA

ICE (BES software) was assessed firstly in standardised exercises and then in the historical church of Santa Rosalia; section 3.3 dealt with the identification of some aspects of climate-induced conservation risks. Finally, section 4 is devoted to outline the main conclusions of the work and future research perspectives. A brief description of HMWall equations is given in Appendix A.

2. Materials and methods

2.1. Chiesa di Santa Rosalia: on-site climate measurements

The *Chiesa di Santa Rosalia* (Palestrina, Italy, Lat. 41.84° N and Long. 12.89° E, 550 m a.s.l.), hereafter simply called church, was chosen as a case study as its features well fit to the aim of this research. The north-east wall, corresponding to the chancel, is embedded in a rocky outcrop, from which liquid water can freely percolate from the soil to the walls. This could have caused the risk of superficial detachments and chromatic alterations of the cladding marble, leading the restorers to replace the original altarpiece with a copy.

The church was built in 17th-century enclosed into the heavy masonries of the prestigious palace of Barberini Family and is an aisleless church with a square-central plan covered by a groined vault. Walls are covered by polychrome marbles that adorn the two tombs of Cardinals Antonio and Taddeo Barberini (Fig. 1a). A reason of concern was the conservation of the *Pietà Barberini,* attributed to Michelangelo Buonarroti, that used to be preserved in the sacristy of the church and was moved to *Galleria dell'Accademia* in Florence (Italy) in 1938.

An indoor and outdoor climate monitoring was carried out to study the indoor hygrothermal behaviour of the church. Technical and financial reasons limited the monitoring period from January 1st till March 31st, 2015 and that period was chosen since climate conditions can favour the condensation on the walls. Two thermo-hygrometers (manufactured by Rotronic®, model HC2–S3) were placed inside the church to measure temperature (T) and relative humidity (RH): one T-RH probe (labelled as "TRH1" in Fig. 1a) was placed in a central position at 3 m height and the other in an empty space behind the altarpiece (labelled as "TRH2" in Fig. 1a). A third thermo-hygrometer of the same model, shielded from solar radiation by a small Stevenson screen, was placed on the terrace of the church to collect the outdoor T and RH conditions needed for the compilation of the climate file used in the simulation. T sensors were Pt100 resistance thermometers with an operating range −40°C-+60 °C and uncertainty of 0.3 °C; whereas RH sensors were thin film capacitive sensors with an operating range 0–100% and uncertainty of 1.5%. Both sensors were in accordance with the current European Standards about the metrological features of the instruments for measuring T and RH in cultural heritage conservation [38,39]. Moreover, a soil moisture sensor (labelled as "M1" in Fig. 1a) (manufactured by Meter Environment model ECH_2O EC-5) provided the measurements of the volumetric water content with an operating range between 0 and 1 $m^3 \cdot m^{-3}$ and an uncertainty of ±2% and was placed in a small crack located to a corner of the north-east wall.

All measurements were sampled every 5 min and recorded every 30 min as averaged values.

Indoor T and RH values do not show significant differences between

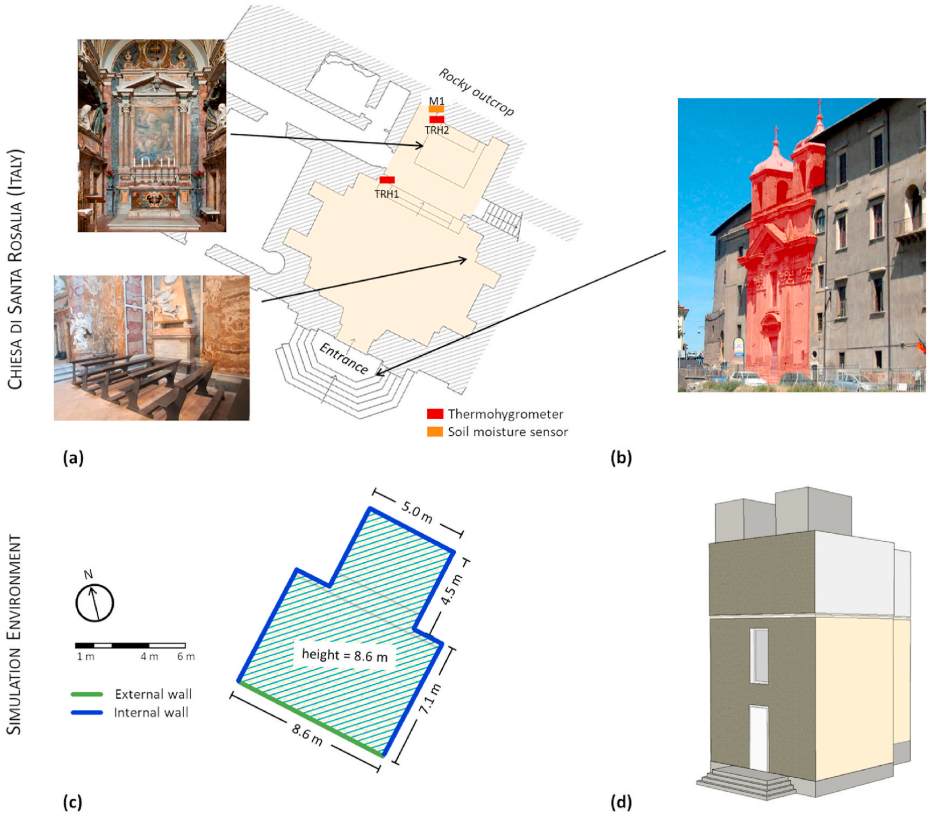

Fig. 1. (a–b) Plan of the Church of Santa Rosalia in Palestrina with the location of internal instruments together with internal [40] and external views; (c–d) floor plan and 3D model of the church in the IDA ICE environment.

the two sampling points. The minimum and maximum T values were 11.0–14.6 °C in "TRH1" and 10.5–18.7 °C in "TRH2", whereas for RH measurements they were 23.0–81.6% in "TRH1" and 21.0–79.5% in "TRH2". These outcomes show that the two areas were in hygrothermal equilibrium. The volumetric water content was constant at 0.114 $m^3 \cdot m^{-3}$ over the monitoring period and was considered as a marker of the moisture level.

2.2. Building model construction of the historical church

The building model of the church was created encompassing (i) indoor and outdoor climate measurements and (ii) architectural surveys carried out by the authors. The former (i) was used to calibrate building model, the latter (ii) to reduce the main uncertainties in the building model as reported in Ref. [24]. The 3D model of the church sketched in IDA ICE is shown in Fig. 1d. The building model consisted of five zones reproducing the church (Fig. 1a,c-d) and the adjoining spaces (not shown in Fig. 1c and d), which were included to estimate both the horizontal and the upward heat transmittance. The total floor area and the total volume of the church were 75.3 m^2 and 608.1 m^3, respectively.

The main difficulties encountered during the construction of a reliable building model regarded the modelling of the rocky outcrop and the simplification of internal geometries as well as walls' orthogonality to keep unchanged the total internal volume (Fig. 1c). The rocky outcrop behind the north-east wall was modelled as ground based on EN ISO 13370:2017 [41] and connected to the wall. This wall was divided in two partitions, the heavy masonry and the wooden altarpiece, due to their considerable thickness (1.06 and 0.05 m, respectively).

First, a thermal building model (hereafter named building model A) was created in IDA ICE environment modelling the walls through a 1D heat transfer model. Then, this wall model was replaced with HMWall (hereafter named building model B) in order to assess whether the building model B may outperform the building model A.

As shown in Fig. 1c, there are six internal walls considered adiabatic due to their considerable thickness, one internal wall adjoining the rocky outcrop and one external wall. When the 1D heat transfer model was replaced with HMWall, moisture connections were added. The moisture connections are identified as RH connections since both moisture flows are driven by the RH gradient. The internal side of walls was connected to the indoor T and RH of the zone. The external side of the external wall was connected to the T and RH values of the climate file. The back side of walls was set to a constant RH values of 50% except for the north-east wall, set to a constant 95% RH, based on the measurements of the water content ("M1"). As for the altarpiece, the back side was set to 80% RH as a compromise between measurements ("TRH2"). The initial conditions of moisture content (w) inside walls were homogeneously set to w values corresponding to RH = 50% in internal/external walls and to a RH gradient from 50% (internal side) to 100% (back side) in the north-east wall to consider the effect of the water infiltrations from the rocky outcrop. The stratigraphy of walls was

Table 1
Hygrothermal and physical properties of the horizontal and vertical opaque components per each partition according to the values obtained after the calibration of the building model with the climate measurements (from internal side to external side).

Input parameters										
Partition	Material (thickness in m)	Total thickness	Thermal conductivity	Density	Specific heat	Equilibrium water content at RH = 80%	Free water saturation	Thermal conductivity supplement	Vapour diffusion resistance	Water absorption coefficient
		s m	λ $W \cdot m^{-1} \cdot K^{-1}$	ρ $kg \cdot m^{-3}$	c $J \cdot kg^{-1} \cdot K^{-1}$	w_{80} $kg \cdot m^{-3}$	w_f $kg \cdot m^{-3}$	b –	μ –	A_w $kg \cdot m^{-2} \cdot s^{-0.5}$
External Wall	marble (0.02)	2.11	3	2300	880	0.9	69	4	530	0.003
	calcareous mortar (0.02)		0.8	1900	850	45	210	4	19	0.03
	tuff (2.0)		0.48	1450	925	75.7	259	4	10.4	0.10
	calcareous mortar (0.02)		0.8	1900	850	45	210	4	19	0.03
	plaster (0.05)		0.7	1600	850	30	250	4	7	0.05
Internal Wall	marble (0.02)	1.06	3	2300	880	0.9	69	4	530	0.003
	calcareous mortar (0.02)		0.8	1900	850	45	210	4	19	0.03
	tuff (1.0)		0.48	1450	925	75.7	259	4	10.4	0.10
	calcareous mortar (0.02)		0.8	1900	850	45	210	4	19	0.03
Altarpiece	gesso (0.01)	0.05	0.3	850	1000	6.3	400	4	8.3	0.29
	wood (0.04)		0.3	685	1500	115	500	4	8	0.01
Floor	cotta brick (0.06)	0.42	0.96	1952	863	123	161	4	19.4	0.14
	calcareous mortar (0.06)		0.8	1900	850	45	210	4	19	0.03
	tuff (0.3)		0.48	1450	925	75.7	259	4	10.4	0.10
Roof	roof brick (0.3)	0.30	1	1800	840	–	–	–	–	–
	calcareous mortar (0.05)		0.9	1800	910	–	–	–	–	–
	tiles (0.05)		1.16	2300	840	–	–	–	–	–

defined during the on-site survey of the church. As the hygrothermal and physical properties of walls could not be measured, those properties were gathered from the *MASEA Datenbank* [42] by choosing the most fitting materials and then adjusting the values of the parameters through the calibration procedure (described in Section 2.3.2). The values of the hygrothermal and physical properties of the opaque components are reported in Table 1.

The only window (1.5 × 3.0 m with a recess depth of 0.3 m) located on the south-west façade was made of a single pane glazing and a steel frame (20% of the total window area) with a thermal transmittance (U-value) of 5.8 and 2.0 $W \cdot m^{-2} \cdot K^{-1}$, respectively. As a layer of fine particles of dust were deposited on the vertical panes of the window, a shading component was added considering 40% of transparency [43]. The Solar Heat Gain Coefficient (SHGC), solar light transmittance (τ_e) and visible light transmittance (τ_v) of the single pane were set at 0.63, 0.50 and 0.45, respectively. In addition, internal thermal masses were added to take into consideration the heat transmittance of wooden furniture (e.g. pews) and other sculptures. Infiltrations were fixed at 0.05 ACH (Air Changes per Hour) mainly due to the door and the window at the façade, whereas thermal bridges were set at 0.04 $W \cdot m^{-1}$ per perimeter of both window and entrance door. Finally, hygrothermal gains and occupancy were set to zero as the number of churchgoers/-visitors was very limited and no hygrothermal sources were present in the church during the climate monitoring.

The climate file was created using hourly T and RH data measured by thermo-hygrometer placed on the terrace of the church. Local measurements are the most representative in whole building dynamic simulation in case of the Test Reference Year (TRY) files that are not suitable for climate model calibration [13]. Hourly wind (intensity and direction) and solar radiation (direct and diffuse) observations collected at *ESTER weather station – University of Rome Tor Vergata* (Lat. 41.86° N and Long. 12.62° E) were included into the climate file, as they were not measured *in situ*. The relatively short distance between the two sites (~21 km) led to similar levels of solar irradiances, especially in winter where weather patterns are mainly controlled by the large-scale air motions.

2.3. Methodology

A multi-step methodology was structured as shown in the schematic workflow of Fig. 2: (a) performance assessment of BES + HAM in standardised exercises (section 2.3.1); (b) performance assessment of BES + HAM in complex settings (section 2.3.2); (c) diagnostics and conservation scenario (section 2.3.3). Step (a) was conceived to pinpoint incorrect assumptions and calculations of HMWall into IDA ICE. Step (c) focused on evaluating the influence of outdoor climate on indoor conditions as well as the climate-induced conservation risks. Depending on results from steps (a) and (b), step (c) can be carried out.

2.3.1. Performance assessment of BES + HAM in standardised exercises

A multi-stage evaluation was conceived to explore the HAM (HMWall) capability in BES (IDA ICE) to model the hygrothermal distribution at wall-level and the influence of wall hygrothermal buffering at zone-level. Three exercises were *ad hoc* designed to understand whether the simulation tool might be able to also address conservation-related issues. Table 2 summarises the main features of the exercises reporting how HMWall is used in IDA ICE, the type of evaluation according to criteria defined in ANSI ASHRAE Standard 140 [47], the investigated process mechanism and the conservation-related issues.

2.3.1.1. Semi-infinite wall (exercise 1). This exercise was chosen to analyse the capability of HMWall to model the hygrothermal distribution inside a wall to estimate more accurately the risk of interstitial condensation. This feature is crucial in the hygrothermal modelling of historical buildings, as it allows to prevent deterioration of walls, such as mechanical damage due to mould infestation, thawing/freeze cycles or crystallisation/dissolution cycles of deliquescent salts, etc.

This exercise is based on the minimisation of hygrothermal curves reported in the European Standard EN 15026:2007 [44], where a detailed description of the exercise is given in Annex A. The modelled distributions of temperature (T) and moisture content (w) inside the material were compared with the range of the T and w values in the Standard. The hygrothermal properties used to run models are listed in Table 3 (first row).

2.3.1.2. Adiabatic building envelope (exercise 2). This exercise was formulated to study the performance of HMWall to estimate the extent of the moisture transfer by itself in the balance of RH inside a room (zone). This feature is useful in the case of historical buildings when there are inaccessible rooms/parts being completely airtight.

The description of this exercise is reported in detail in Ref. [45]. The simulations were performed over 8760 h at 1-h step (i.e. one whole year)

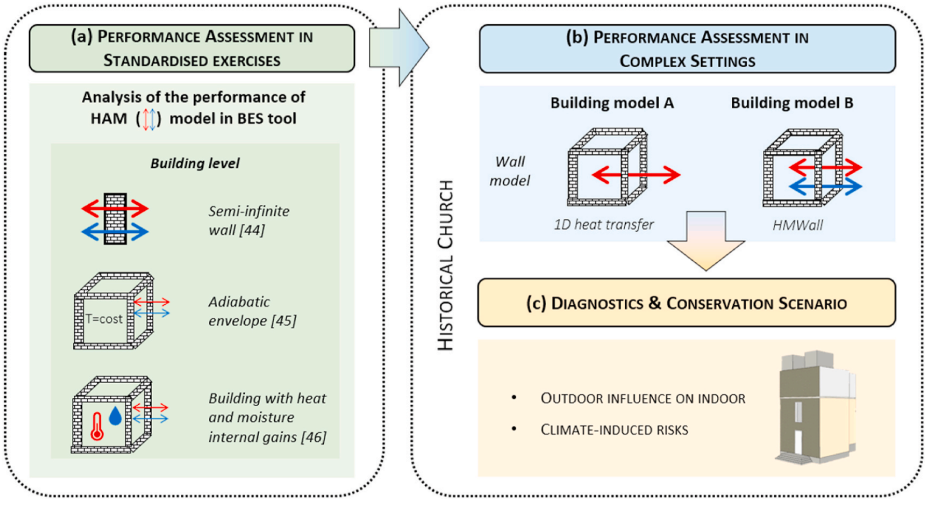

Fig. 2. Workflow of the performance assessment of the hygrothermal modelling (a–b) and diagnostics (c) in historical churches.

Table 2
Summary of the multi-stage evaluation of the BES + HAM performance.

Exercise	Ref	HMWall	Evaluation	Process mechanism	Conservation-related issues
1. semi-infinite wall	[44]	independent wall-object	analytical verification	superficial and/or interstitial condensation	mechanical damage due to thawing/freeze cycles or to crystallisation/dissolution cycles of deliquescent salts, mould infestation
2. adiabatic building envelope	[45]	wall-object of larger system	comparative test	indoor relative humidity solely due to the moisture transfer through walls	hygrothermal conditions in inaccessible rooms/parts completely airtight
3. building envelope with heat and moisture internal gains	[46]		empirical validation	indoor relative humidity affected by the moisture sorption effect of building materials	restoration interventions and retrofit measures

Table 3
List of hygrothermal properties used in HMWall for exercise 1 and used both in HMWall and in WUFI Plus for exercise 2.

Exercise	Input parameters							
	Thermal conductivity	Density	Specific heat	Free water saturation	Equilibrium water content at RH = 80%	Thermal conductivity supplement	Vapour diffusion resistance	Water absorption coefficient
	λ $W \cdot m^{-1} \cdot K^{-1}$	ρ $kg \cdot m^{-3}$	c $J \cdot kg^{-1} \cdot K^{-1}$	w_f $kg \cdot m^{-3}$	w_{80} $kg \cdot m^{-3}$	b –	μ –	A_w $kg \cdot m^{-2} \cdot s^{-0.5}$
1. Semi-infinite wall	1.5	1000.0	1842.0	146.0	87.6	10.5	227.8*	0.10×10^{-2} (*)
2. Adiabatic building envelope	1.0	1830.0	850.0	257.1	27.5	4.0	27.0	0.59×10^{-2}

* Average values referred to those provided by the Standard in the RH range 50–95%.

in an adiabatic building envelope completely airtight. The hygrothermal properties of the walls made of a 0.2 m monolayer of lime silica brick used to run models are listed in Table 3 (second row). It is worth noticing that, in this exercise, the variations of indoor relative humidity (RH_{in}) from initial condition at 50% depend only on the water vapour partial pressure (p_v) gained by the walls, because the saturated pressure (p_{sat}) is set to be constant ($T_{in} = T_{out} = 10$ °C). Three sorption processes driven by the RH indoor-outdoor gradient were considered: 1) moisture adsorption ($RH_{out} = 60\%$); 2) moisture desorption ($RH_{out} = 40\%$); 3) moisture seasonal trends (RH_{out} ranging periodically between 40% and 60%). The evaluation was based on a comparative test with the simulations run by WUFI Plus software, which is one of the most robust and validated hygrothermal simulation tools (e.g. Refs. [48–50]).

2.3.1.3. Two parallel rooms with internal moisture and heat gains (exercise 3). This exercise was chosen to study the performance of HMWall in modelling the moisture sorption effect of hygroscopic materials and hence their influence in the indoor RH values. The capability of a hygrothermal model to accurately reproduce the moisture sorption effect is pivotal in the simulation of historical buildings, as it regulates the short-term fluctuations of RH neither related to the day/night cycle (i.e. temperature) nor external factors (moisture ex/infiltration). This feature is essential for an advanced preventive conservation technique because it can guide restorers to the choice of restoration interventions and retrofit measures in accordance with conservation requirements.

The Common Exercise 3, developed in the framework of the Annex 41 of the International Energy Agency (IEA) Energy Conservation in Buildings and Community Systems program (ECBCS) [46], was used in this exercise as benchmark. It was applied for validating TRNSYS–COMSOL co-simulation tool [33] and for validating WUFI Plus and HAMBase simulation tools in the European project *Climate for Culture* (2010–2014) [51]. The experiments consisted of three tests in two rooms at constant T = 20.0 °C: reference room and test room. While the cladding materials of the reference room were kept unchanged during the tests, those of the test room's walls was changed as follows: Test1- aluminium foils on the walls (from January 17th till February 2nd); Test2- gypsum boards on the walls (from February 14th till March 20th); and Test3- gypsum boards on the walls and roof (from March 27th till April 16th). The indoor RH simulations were compared with RH measurements collected in the three experiments set up for the exercise (data provided by Florian Antretter and Kristin Lengsfeld, 2017).

2.3.2. Performance assessment of BES + HAM in the historical church

The performance of the BES + HAM in complex sites was assessed based on the comparison of the simulations against measurements in the historical church under study.

The building model A (BES + 1D heat transfer model) was calibrated using the indoor T and RH measurements at "TRH1" (Fig. 1a). The calibration was carried out from January 1st till January 31st, 2015 (1488 records), applying an automatic procedure in two steps for fine-tuning the values of: thermo-physical properties of partitions (initial values ± 10%), air infiltration (from 0.05 to 1ACH) and thermal bridges per perimeter of window and entrance door (from 0.00 to 0.10 $W \cdot m^{-2} \cdot K^{-1}$). As first step, a sensitivity analysis based on the Elementary Effect method was carried out identifying air infiltration for both T and RH as the most influencing input. Then, a genetic algorithm was used to minimize the Root Mean Square Error (RMSE) between modelled and measured T-RH data. The fine-tuned input parameters are reported in Section 2.2. The initialisation was set from November till December to take into account the effect of thermal inertia and moisture transfer in old thick masonries.

The validation of the building model was performed from March 1st till March 31st, 2015 (1488 records) with initialisation from January till February. Once building model A was calibrated, HMWall replaced the 1D heat transfer model in building model B so to assess whether it outperformed building model A.

Four statistical metrics were used to assess the accuracy of the hygrothermal simulations: the Mean Absolute Error (MAE), the Root Mean Square Error (RMSE), the Coefficient of Variation of RMSE (CV-RMSE) and the Spearman's correlation coefficient (rho) [52]. The assessment of the accuracy of the building models was extended to mixing ratio (MR, calculated from T and RH values [39]) as moisture mass-related variable. In addition, QQ-plots (quantile-quantile plot) were used to evaluate the agreement between modelled and measured

T-RH [12] and MR values as follows: high agreement, if data are within ±5% for RH and ±1°C for T and ±0.5 $g \cdot kg^{-1}$ for MR, good agreement, if data are within ±10% for RH and ±3°C for T and ±1.5 $g \cdot kg^{-1}$ for MR and poor agreement, if data are beyond ± 10% for RH and ±3°C for T and ±1.5 $g \cdot kg^{-1}$ for MR. Other criteria used to accept the building models as calibrated are CV-RMSE less than 30% [53] and rho higher than 0.8. Furthermore, the prediction rate (Qv) was used to evaluate the accuracy of the simulation in reproducing the daily fluctuations of RH [12].

2.3.3. Diagnostics and conservation in the historical church

It has to bear in mind that the hygrothermal modelling for diagnostics and conservation of historical churches can be pursued only if a reliable hygrothermal software is available and the building model is correctly calibrated with indoor climate measurements. If the performance assessment of the hygrothermal tool fits the requirements of the standardised exercises (section 2.3.1), then we can assume that the simulation of a building model calibrated over a calendar year or at least in different seasons (section 2.3.2) can be transferred to other periods where indoor climate measurements are not available. In this way, the indoor climate scenario from simulations can disclose potentially risky conditions for conservation.

This assumption allowed to further compare the performance of the hygrothermal modelling using 1D heat transfer with respect to HAM transfer through walls. Although calibration and validation were carried out in one season only, the results of the annual simulations can be meaningful for the comparison of the hygrothermal modelling with and without the HAM transfer, even if not fully representative of the actual indoor climate inside the church.

Indoor monthly averages of T and mixing ratio (MR) were plotted against outdoor ones to evaluate the seasonal behaviour of heat and moisture exchanges driven by external conditions.

In addition, building model B (BES + HAM) allowed to assess the moisture content distribution inside the moisture-sensitive partitions. Thus, moisture content distributions inside the north-east wall and the altarpiece were studied to ascertain whether they could threaten the conservation of moisture-sensitive and multi-layered objects.

3. Results and discussion

The preliminary performance evaluation of the heat and moisture transfer model used in this research is presented and discussed in section 3.1. Then, the results obtained using building model A and building model B of the church are analysed in section 3.2.

3.1. Performance assessment of BES + HAM in standardised exercises

3.1.1. Semi-infinite wall (exercise 1)

The hygrothermal profiles of the semi-infinite wall modelled by HMWall (blue dots) and the range of validity limits given in Ref. [44] (red area) are shown in Fig. 3. Both T (Fig. 3a–c) and w (Fig. 3d–f) distributions were satisfactorily reproduced by simulations with HMWall, although after 365 days w tended to diverge from the lower limit of the validity band. Indeed, the profiles were always within the validity limits along the whole wall thickness.

A limitation of HMWall is that discrete function values of hygrothermal curves cannot added. This feature can be pivotal when experimental data are available and when the hygrothermal curves of the materials cannot be adequately described by the HMWall functions.

3.1.2. Adiabatic building envelope (exercise 2)

Fig. 4 shows the scatter diagrams of modelled RH values (HMWall *versus* WUFI Plus) over a whole year for the three sorption processes considered (from Case 1 to Case 3). A strong agreement was found between RH values modelled by the two software. However, when RH_{out} = 40% (Fig. 4b), IDA ICE tended to reach the equilibrium with the outdoor

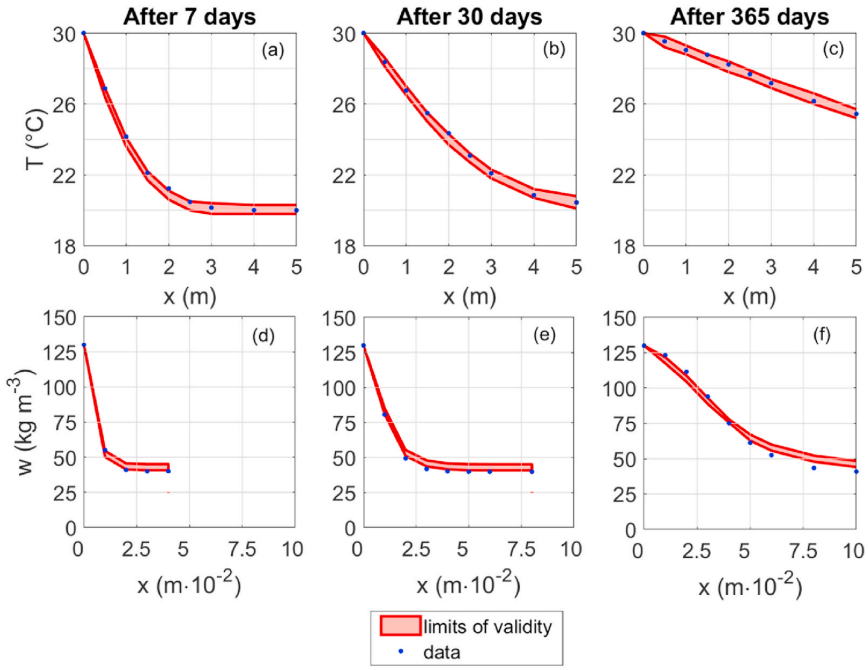

Fig. 3. Temperature (T) and water content (w) distributions along layer thickness (x): data modelled by HMWall (blue dots) and the validity band provided by the EN 15026:2007 (red area). (For interpretation of the references to colour in this figure legend, the reader is referred to the Web version of this article.)

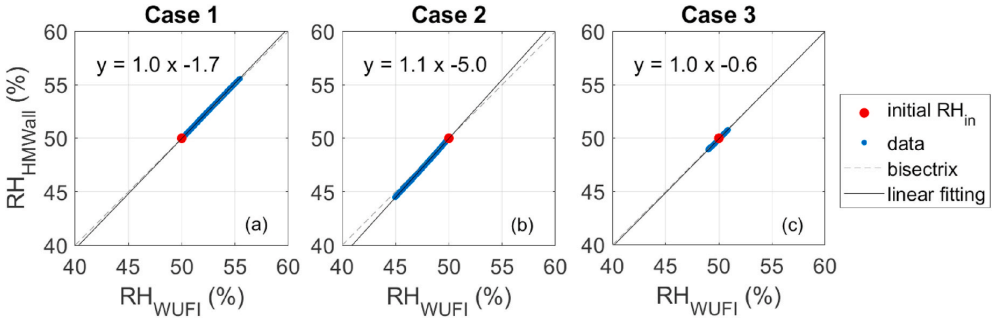

Fig. 4. Scatter diagram of modelled RH values (RH_{HMWall} *versus* RH_{WUFI}) over 8760 h. The indoor initial RH (RH_{in}) is set at 50% (red dot). The linear fitting and its equation are reported. (For interpretation of the references to colour in this figure legend, the reader is referred to the Web version of this article.)

moisture conditions more quickly than WUFI. The difference might be ascribed to the calculation of the liquid transport coefficients for redistribution (D_{ww}): indeed, in HMWall, D_{ww} was always equal to the liquid transport coefficients for suction (D_{ws}), whereas in WUFI, D_{ww} was equal to D_{ws} (equation A.6) except for the water content at RH = 100%, where D_{ww} was set equal to one-tenth of D_{ws}. Refer to Appendix A for a more detailed description of HMWall.

3.1.3. Two parallel rooms with internal moisture and heat gains (exercise 3)

The comparison between the modelled RH values and the experimental measurements is shown in Fig. 5 by means of box-and-whiskers plots for each of the three tests considered (see section 2.3.1).

Left panels of Fig. 5 show a good agreement between modelled and measured RH values in the Reference room in all the tests: the boxes significantly overlapped and the variability of RH values, i.e. the distance between the whiskers, was comparable. RH medians of measurements were 32% (variability of 47%) in Test1, 32% (53%) in Test2 and 48% (49%) in Test3, whereas those of simulations were 32% (variability of 50%), 31% (59%) and 49% (52%), respectively. Concerning the Test room, the building model was able to simulate the RH evolution in accordance with measurements in all tests. Medians were not statistically different (32%, 33% and 46% for measurements and 32%, 33% and 50% for simulation) and the variability differed at most of 5% (60%, 43% and 34% for measurements and 59%, 48% and 36% for simulation). In Test1 of Fig. 5b simulations seem to not perfectly match the RH variability, likely because HMWall was not able to reproduce the poor sorption effect of aluminium foils that coated walls. Conversely, in Test2 (Fig. 5d) and Test3 (Fig. 5f), the sorption effect of gypsum boards on the air RH was well reproduced, although in Test3 the median of modelled

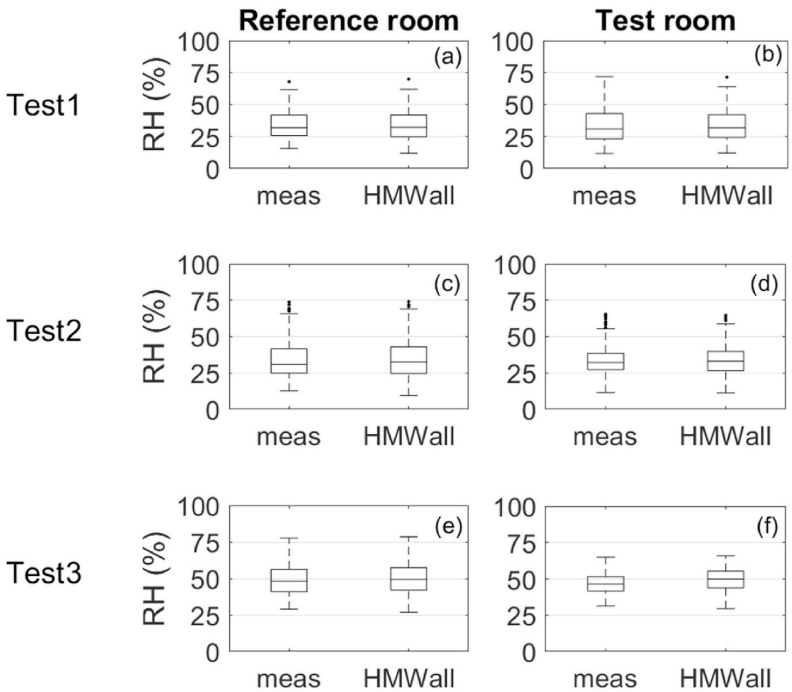

Fig. 5. Box-and-whiskers plots of relative humidity (RH) in Reference room and Test room for test rooms: Test1–aluminium foils on walls; Test2–gypsum boards on walls; Test3–gypsum boards on walls and ceiling.

RH values was slightly higher than the median of measurements.

The Spearman's rank correlation coefficient (rho) was 0.98 in Test1 and 0.96 in Test2, meaning that the building model could reproduce the time evolution of moisture even when moisture peaks and drops occurred. In Test3, rho was slightly lower, although higher than 0.80. In all tests, both MAE and RMSE were found to be less than 4.0%, whereas CV-RMSE was on average 7.6% (never exceeding 11.0%), hence being significantly less than 30%, which is the limit suggested by ASHRAE guideline 14 for hourly calibration [53]. These outcomes make it possible to consider the building model as highly representative of the real site.

As a result, the hygrothermal tool was thoroughly evaluated, encouraging its application also in complex settings.

3.2. Performance assessment of BES + HAM in the historical church

To assess the accuracy of building model B (BES + HAM) with respect to building model A (BES+1D heat transfer), simulations were compared against measurements considering the whole monitoring period from January 1st till March 31st, 2015, as validation outcomes confirmed those of calibration.

QQ plots of modelled *versus* measured values of indoor air T and RH are shown in Fig. 6. The agreement between modelled and measured temperature (Fig. 6a,d) was high for building models. In building model B, all T values within the green band corresponding to ±1 °C were closer to the bisector than those of building model A, meaning that data were equally distributed. MAE and RMSE decreased from 0.3 to 0.4 °C (building model A) to 0.2 °C (building model B), whereas rho was equal to 0.95 (Table 4). The CV-RMSE slightly decreased from building model A (3.0%) to building model B (1.8%), indicating a less residual variance of modelled T values by including the moisture transfer with respect to measurements.

The agreement of modelled RH values with respect to measurements widely changed from building model A to building model B (Fig. 6b,e). If the modelling of walls did not consider the moisture transfer (Fig. 6b), the distribution of modelled RH data highly underestimated the measurements in the range of RH_{meas} between 35 and 60%. Conversely, if the modelling of walls included the simultaneous heat and moisture transfer (e), the agreement between modelled and measured RH values was high in 71% of time (green band, RH = ±5%) and good in 95% of time (dotted band, RH = ±10%). The agreement between modelled and measured data decreased from high to good at the beginning of the simulation (RH_{meas}<30%), as shown in Fig. 7. The enhanced accordance obtained with HMWall was also evident by comparing the statistical metrics: MAE, RMSE and CV-RMSE resulted to be halved with respect to the building model A and rho was equally higher than 0.90 (Table 4).

Finally, the agreement between modelled and measured MR values was evaluated (Fig. 6c,f). MR values were always within the band of good agreement (white-dotted band) with both building models, but a better agreement was found with building model B (MR values were within green band more than 95% of time).

In Fig. 7, the time evolution of T (a), RH (b) and MR (c) measurements inside and outside the church is plotted together with the T, RH and MR values modelled by both building models. Indoor T values were smoothed out and less fluctuating than outdoor ones as the result of the high inertia of the building envelope (Fig. 7a). T values modelled by building model A (Fig. 7a, red line) slightly overestimated

Table 4
Comparison between building model A (BES+1D heat transfer) and building model B (BES + HAM) in the simulation of the hygrothermal condition inside the church (MAE = mean absolute error; RMSE = root mean square error; CV-RMSE = coefficient of variation of RMSE; rho = Spearman's rank correlation coefficient).

Statistical parameter	Building model A			Building model B		
	T	RH	MR	T	RH	MR
MAE	0.3 °C	8.0%	0.7 $g \cdot kg^{-1}$	0.2 °C	3.6%	0.3 $g \cdot kg^{-1}$
RMSE	0.4 °C	9.3%	0.8 $g \cdot kg^{-1}$	0.2 °C	4.7%	0.4 $g \cdot kg^{-1}$
CV-RMSE (%)	3.0	15.4	14.4	1.8	8.0	8.1
rho	0.95	0.90	0.91	0.95	0.90	0.89

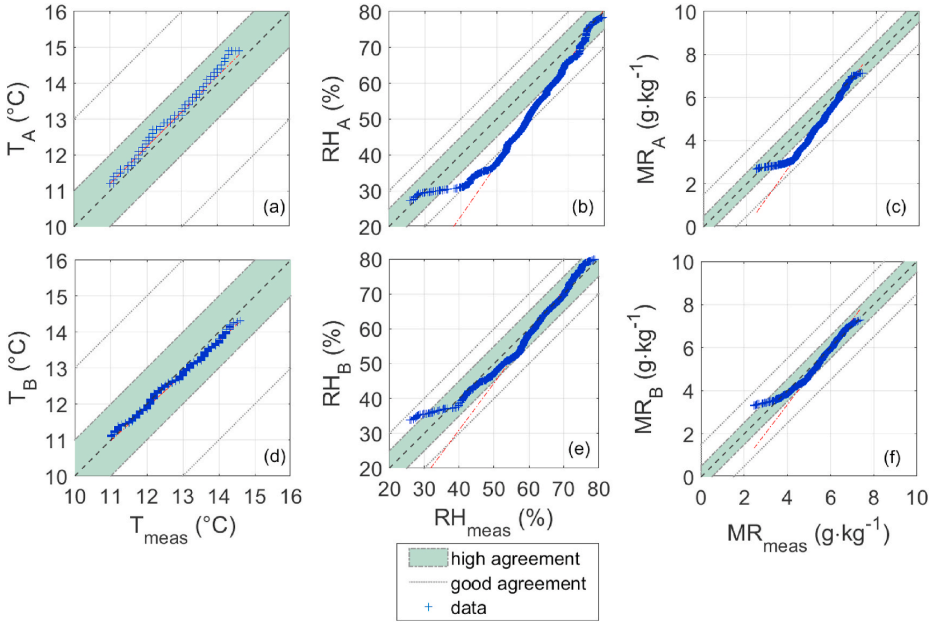

Fig. 6. QQ-plots for temperature (T), relative humidity (RH) and mixing ratio (MR) simulated by building model A (a,b,c) and building model B (d,e,f).

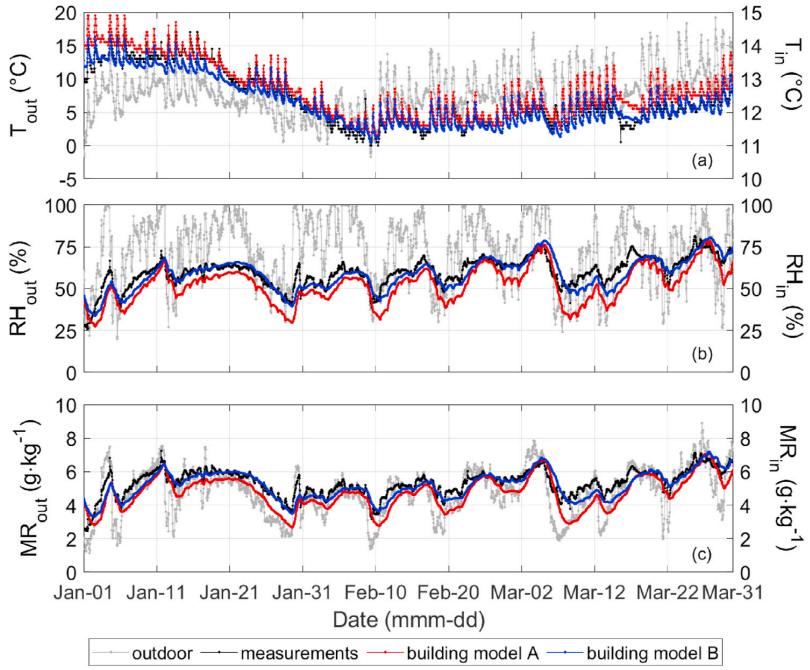

Fig. 7. Time evolution of (a) Temperature, (b) Relative Humidity and (c) Mixing Ratio: indoor and outdoor measurements (black and grey lines), building model A (red line) and building model B (blue line). (For interpretation of the references to colour in this figure legend, the reader is referred to the Web version of this article.)

measurements (Fig. 7a, black line) at the beginning of the simulation and between March 15th-18th, 2015, while T values modelled by building model B (Fig. 7a, blue line) were highly similar to the measurements over the entire simulation. Although the outdoor RH values (Fig. 7b, grey line) strongly influenced the indoor ones (Fig. 7b, black line), it is visible the moisture buffering effect due to the building envelope. As already pointed out, RH values modelled by the two building models were highly correlated with the measurements. However, building model B (Fig. 7b, blue line) simulated the measured RH drops better than building model A (Fig. 7b, red line), because it was able to better reproduce the combined effect of the infiltrations of outdoor air masses and the moisture exchanges between wall surfaces and indoor air masses. This behaviour was also confirmed in MR plot (Fig. 7c), where it is clear that building model B was better able to simulate moisture-mass flows than building model A.

The prediction rate (Qv) for building model A and B was within the ranges in Ref. [12] most of the time, although the results of building model A were slightly better than building model B for $\Delta RH \leq 5\% \cdot day^{-1}$ and $10\% \cdot day^{-1} < \Delta RH \leq 15\% \cdot day^{-1}$ (Table 5). The low rate of compliance of the two building models at $\Delta RH > 15\% \cdot day^{-1}$ was interpreted as related to the moisture internal gains that were not included in the simulations because unknown.

The results showed that the behaviour of RH values inside the church was affected by the combined effect of the air infiltrations, that modulated the relative humidity trend, and the moisture exchanges between air and walls, that governed the short-term variability (RH peaks and drops). Building model B, being able to encompass all the essential features to simulate indoor climate, can be used to investigate preventive conservation measures in the historic church.

Table 5
Evaluation of the prediction rate (Qv) *versus* ΔRH ($\%\cdot day^{-1}$).

ΔRH ($\%\cdot day^{-1}$)	Qv	
	building model A	building model B
≤5	1.00	1.43
>5 and ≤ 10	1.24	0.80
>10 and ≤ 15	0.63	0.06
>15	0.00	0.00
Rate of compliance	high: 0.95≤ Qv ≤ 1.10 good: 0.75≤ Qv < 0.95 and 1.10<Qv ≤ 1.50 low: 0<Qv < 0.75; 1.50<Qv	

3.3. Diagnostics and conservation in the historical church

In this step, the hygrothermal simulations of building model A (BES + 1D heat transfer) were compared with those of building model B (BES + HAM) over a calendar year. The aim was to outline an indoor climate scenario that allowed to evaluate the seasonal effect of the outdoor conditions on the indoor ones and to identify potentially risky conditions using both building models A and B.

Fig. 8 shows the seasonal trends of T and MR values modelled inside the church and calculated as monthly averages.

Although the two building models used the same input parameters and boundary conditions, the results in Fig. 8 showed different indoor climate conditions. This difference was due to the integration of the HAM transfer through walls. Both modelled conditions were the indoor climate scenarios inside the church. However, as building model B outperformed building model A both in the calibration and validation periods (section 3.2), it was reasonable to assume that its associated scenario may have more realistically represented the actual indoor climate in the remaining period.

Looking at T plots (Fig. 8a–b), a pattern typical of heavy-masonry buildings is visible: winter and spring values, on average, were above the bisector and summer and autumn values were above the bisector or

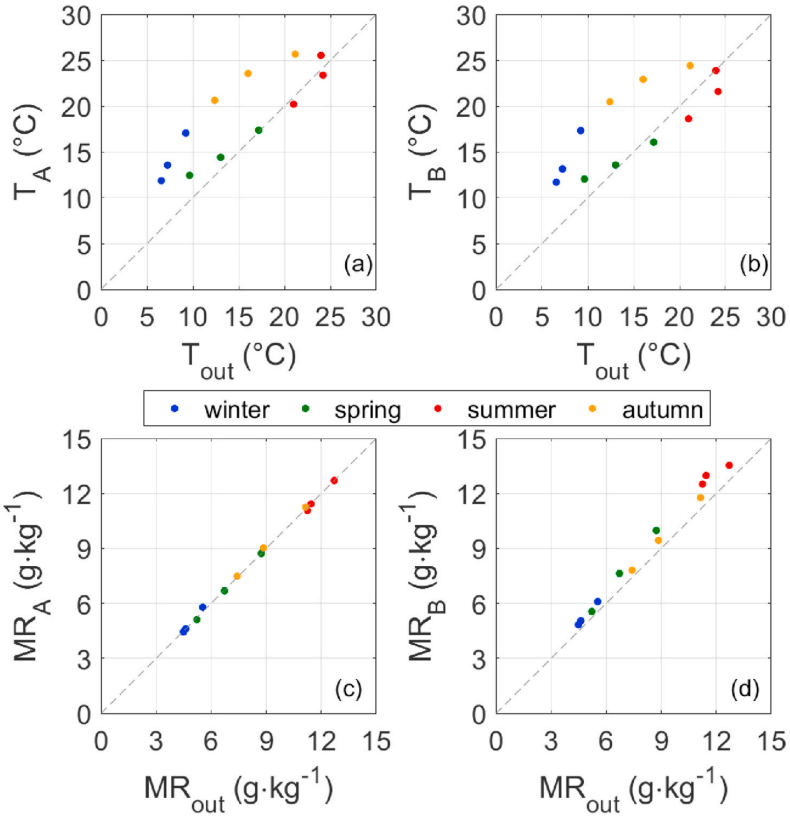

Fig. 8. Outdoor and indoor monthly averages of modelled air temperatures (T) and mixing ratio values (MR) in building model A and building model B.

lie on it. The distribution of T values formed an ellipse as a result of the high thermal inertia of the envelope. Moreover, as the heat flow through walls was computed taking into account the moisture flow (influencing the heat loss), in summer T_B values tended to be lower than T_A.

Looking at MR plots (Fig. 8c-d), data were distributed along the bisector, clearly showing the dependence of the modelled hygric conditions on outdoors. MR_B values (Fig. 8d) were up to 2 $g \cdot kg^{-1}$ higher than the outdoor ones, especially in summer. This behaviour could have been caused by walls releasing moisture or by moisture accumulation due to the poor sorption features of the marble coatings or by the

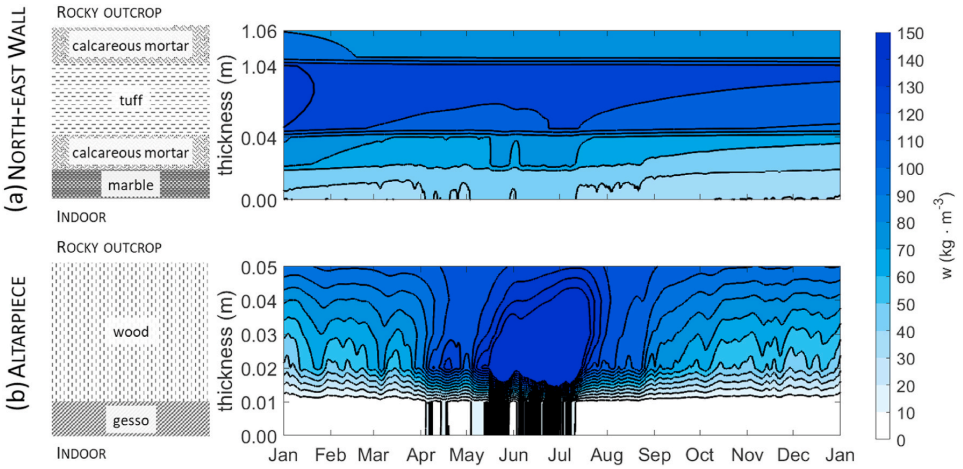

Fig. 9. Water content distribution (w) inside (a) the wall (not equally spaced) and (b) the altarpiece from internal (0.00 m) to external side (rocky outcrop).

combination of the above-mentioned mechanisms.

The north-east wall of the church could be threatened by the damp conditions due to water infiltrations from the rocky outcrop. The back side of the north-east wall and altarpiece (detailed stratigraphy of the partitions are reported in Table 1 and shown in Fig. 9) were set to a constant RH = 95% and RH = 80%, respectively; whereas the front sides were connected to indoor climate conditions of the church. For this reason, the distribution of water content (w) inside the northern wall and the altarpiece was simulated as shown in upper and lower panels of Fig. 9, respectively. This analysis allowed to diagnose the formation of a moisture gradient within the wall components, thus providing a better evaluation of the potential moisture-induced degradation.

Fig. 9a clearly shows that one year of simulation could not be representative of the moisture content (w) distribution inside the wall since different conditions in the middle of the stratigraphy are visible at the beginning and at the end of simulation. This behaviour is typical of ancient thick masonries, in which moisture flows are slower than those in thinner partitions. As expected, the thin stratigraphy of the panel paintings (Fig. 9b) did not show the same behaviour.

Moreover, this analysis demonstrated that two months of initialisation were not enough to capture the slow moisture transfer in thick masonries. In addition, if only one year of simulation is considered, the moisture content distribution across the wall can be also affected by the initial values set in the simulation.

The most critical period was found to be between April and July, when a higher w gradient occurred in both partitions. In the case of the masonry, a w gradient of 60 $kg \cdot m^{-3}$ could trigger crystallisation/dissolution cycles of soluble salts, causing the risk of mechanical degradation of the wall coatings (e.g. detachments of marble layers). In addition, higher w values occurring in the inner layers could favour interstitial condensation, detrimental for the conservation of walls. In the case of the altarpiece, simulated w values were stable between 0 $kg \cdot m^{-3}$ and 10 $kg \cdot m^{-3}$ in the first 0.01 m, whereas a gradient of 40 $kg \cdot m^{-3}$ occurred between 0.01 and 0.02 m and up to 150 $kg \cdot m^{-3}$ in summer due to higher indoor MR values (Fig. 8d).

The behaviour described above could be responsible for stresses to moisture-sensitive and multi-layered artworks, such as the altarpiece, jeopardizing their conservation.

4. Conclusions

The hygrothermal modelling of historical churches is a promising approach to study preservation issues and appropriate strategies for mitigating climate-induced conservation risks. In this context, difficulties can arise in the use of Heat, Air and Moisture (HAM) models into building energy simulation (BES) and the performance of the hygrothermal tool has to be properly assessed to accurately model indoor climate conditions.

This research aimed to investigate the capabilities of BES extended with a HAM model (HMWall) for diagnostics and conservation of historical buildings. To this purpose, a multi-step methodology was conceived and used to assess the performance of the simulation tool from standardised exercises to a complex site. The methodology was thus applied to the historical church of the 17th-century *Chiesa di Santa Rosalia* (Italy), allowing to explore climate-induced conservation risks based on simulations.

The first step of the methodology allowed to exclude incorrect assumptions and calculations in HMWall encompassing the criteria defined in ANSI ASHRAE Standard 140 (section 3.1). This result was preparatory to the hygrothermal modelling of the historical site. The second step compared indoor climate simulations from the hygrothermal modelling of *Chiesa di Santa Rosalia* using BES with either a 1D heat transfer only (building model A) or a HAM transfer (building model B). Building model B improved the simulation accuracy by +50% with respect to building model A. Moreover, building model B proved to be able to reproduce the indoor moisture balance depending simultaneously on infiltrations and on vapour mass flow exchanges with the walls, otherwise left out by the 1D heat transfer model (section 3.2). Finally, annual simulations allowed to compare the indoor climate scenarios resulting from the hygrothermal modelling with and without the HAM transfer (section 3.3). The analysis also explored the capability of hygrothermal modelling with HAM transfer to describe deterioration. For example, the distribution of moisture content in partitions affected by water infiltrations was studied as potentially responsible for mechanical stresses to moisture-sensitive and multi-layered artworks.

This study highlighted some relevant aspects of the hygrothermal modelling of the indoor climate conditions in historical churches. First, standardised exercises are useful to objectively evaluate the performance of BES + HAM tools. Second, hygrothermal models with HAM give the chance to study moisture-induced deterioration risks through the simulation of the moisture content distribution in partitions. Furthermore, this analysis put in evidence the importance of the initialisation period, which should be long enough to cover the period representing the slow moisture flow in thick masonries. A penalty of our work was that the calibration was carried out only in winter; therefore, the hygrothermal simulation over the period without measurements might be not fully representative of the actual indoor climate inside the church. If a calendar year of measurements had been available, the building model would have been more accurate becoming a more robust tool for the simulation of indoor climate inside the church.

Although this study does not exhaust the topic, the conceived methodology could be exploited also for the performance assessment of other hygrothermal simulation tools in other application fields.

Declaration of competing interest

The authors declare that they have no known competing financial interests or personal relationships that could have appeared to influence the work reported in this paper.

Acknowledgement

Frasca F. thanks Dr Florian Antretter (Hygrothermics Department of Fraunhofer Institute for Building Physics - IBP) for his technical advices during her visiting period in the IBP in 2017. Authors are thankful to Principe Don Benedetto Barberini for giving consent for the case study to be used in this research, Arch. Nicoletta Marconi for the historical support and Serena Contardi for the acquisition of indoor climate data. Finally, authors are grateful to Tecno.El S.r.l. for the indoor climate monitoring system. The authors also thank the anonymous reviewers for the valuable comments to improve the manuscript. Frasca F., Siani A.M. and Verticchio E. thank for the financial support of the APC the CollectionCare project (European Union's Horizon 2020 research and innovation programme under grant agreement No 814624).

Appendix A. The HMWall model: a HAM model in IDA ICE

IDA Indoor Climate and Energy (IDA ICE 4.7.1) software, distributed by EQUA simulation AB, can be extended with HMWall, which simulates the 1D heat and moisture transfer through walls. HMWall can be used in IDA ICE either as a single independent wall-object or as a wall-component of a larger building system [44,54].

The moisture storage curve (equation A.1) is calculated as a function of relative humidity as follows:

$$w(\phi) = w_f \times \frac{(\beta - 1) \times \phi}{\beta - \phi} \tag{A.1}$$

where w is the water content ($kg \cdot m^{-3}$), w_f is the free water saturation ($kg \cdot m^{-3}$), ϕ is the relative humidity (−) and β is the approximation factor (−) [55].

The simultaneous heat (equation A.2) and moisture (equation A.3) transport equations are:

$$\frac{dH}{dT} \times \frac{\partial T}{\partial t} = \nabla(\lambda \times \nabla T) - h_v \times \nabla g_v \tag{A.2}$$

$$\frac{dw}{d\phi} \times \frac{\partial \phi}{\partial t} = \nabla(\nabla g_v + \nabla g_w) \tag{A.3}$$

where dH/dT is the heat storage capacity of the moist material ($J \cdot m^{-3} \cdot K^{-1}$); $\partial T/\partial t$ is the rate of temperature (T) ($K \cdot s^{-1}$); λ is the thermal conductivity of the wet material ($W \cdot m^{-1} \cdot K^{-1}$) (equation A.4); $h_v \times \nabla g_v$ is the latent heat source where h_v is the evaporation enthalpy of water ($J \cdot kg^{-1}$) and ∇g_v is the vapour diffusion flux ($kg \cdot m^{-2} \cdot s^{-1}$). In eq. A.3, dw/dϕ is the moisture storage capacity ($kg \cdot m^{-3}$); $\partial\phi/\partial t$ is the rate of relative humidity (−); ∇g_w is the capillary moisture flux ($kg \cdot m^{-2} \cdot s^{-1}$) and is expressed as $D_\phi \times \nabla\phi$ with D_ϕ as the liquid conduction coefficient of water ($kg \cdot m^{-1} \cdot s^{-1}$) (equation A.5); ∇g_v is the vapour diffusion flux ($kg \cdot m^{-2} \cdot s^{-1}$) and is expressed as $(\delta_a/\mu) \times \nabla(\phi \times p_{sat})$ with δ_a the water vapour permeability of air [56], μ the dimensionless vapour resistance factor of material and p_{sat} as the saturated vapour pressure (Pa). The model considers μ as a constant value in the RH range.

$$\lambda(w) = \lambda_d \times \frac{1 + b \times w}{\rho} \tag{A.4}$$

where λ_d is the dry thermal conductivity ($W \cdot m^{-1} \cdot K^{-1}$); b the thermal conductivity supplement and ρ the material density ($kg \cdot m^{-3}$).

The liquid conduction coefficient (D_ϕ) is calculated assuming no difference between suction and redistribution [55].

$$D_\phi = D_{ws} \times \frac{dw}{d\phi} \tag{A.5}$$

where D_{ws} -liquid transport coefficient for suction- is calculated as equation A.6:

$$D_{ws} = 3.8 \times \left(\frac{A_w}{w_f}\right)^2 \times 1000^{\frac{w}{w_f}-1} \tag{A.6}$$

where A_w is the water penetration coefficient and w_f is the free water saturation ($kg \cdot m^{-3}$).

Funding sources

The APC was funded by CollectionCare project, which has received funding from the European Union's Horizon 2020 research and innovation programme under grant agreement No 814624.

Authors' contribution

All the authors have equally contributed to this study.

References

[1] Vincoli in rete. http://vincoliinrete.beniculturali.it/VincoliInRete/vir/statistics/redirectReport3. (Accessed 31 July 2020).

[2] A. Mleczkowska, M. Strojecki, Ł. Bratasz, R. Kozłowski, Particle penetration and deposition inside historical churches, Build. Environ. 95 (2016) 291–298, https://doi.org/10.1016/j.buildenv.2015.09.017.

[3] F. Frasca, E. Verticchio, A. Caratelli, C. Bertolin, D. Camuffo, A.M. Siani, A comprehensive study of the microclimate-induced conservation risks in hypogeal sites: the Mithraeum of the baths of caracalla (Rome), Sensors 20 (11) (2020) 3310, https://doi.org/10.3390/s20113310.

[4] M.J. Varas-Muriel, R. Fort, M.I. Martínez-Garrido, A. Zornoza-Indart, P. López-Arce, Fluctuations in the indoor environment in Spanish rural churches and their effects on heritage conservation: hygro-thermal and CO2 conditions monitoring, Build. Environ. 82 (2014) 97–109, https://doi.org/10.1016/j.buildenv.2014.08.010.

[5] T. Kalamees, A. Väli, L. Kurik, M. Napp, E. Arümagi, U. Kallavus, The influence of indoor climate control on risk for damages in naturally ventilated historic churches in cold climate, Int. J. Architect. Herit. 10 (4) (2016) 486–498, https://doi.org/10.1080/15583058.2014.1003623.

[6] F. Frasca, A.M. Siani, G.R. Casale, M. Pedone, M. Strojecki, A. Mleczkowska, Assessment of indoor climate of Mogiła Abbey in Kraków (Poland) and the application of the analogues method to predict microclimate indoor conditions, Environ. Sci. Pollut. Control Ser. 24 (16) (2017) 13895–13907, https://doi.org/10.1007/s11356-016-6504-9.

[7] D. Camuffo, E. Pagan, S. Rissanen, Ł. Bratasz, R. Kozłowski, M. Camuffo, A. della Valle, An advanced church heating system favourable to artworks: a contribution to European standardisation, J. Cult. Herit. 11 (2) (2010) 205–219, https://doi.org/10.1016/j.culher.2009.02.008.

[8] EN 15759-1, Conservation of Cultural Property - Indoor Climate - Part 1: Guidelines for Heating Churches, Chapels and Other Places of Worship, European Committee for Standardization (CEN), Brussels, 2011.

[9] E. Verticchio, F. Frasca, F.J. García-Diego, A.M. Siani, Investigation on the use of passive microclimate frames in view of the climate change scenario, Climate 7 (8) (2019) 98, https://doi.org/10.3390/cli7080098.

[10] J. Leissner, R. Kilian, L. Kotova, D. Jacob, U. Mikolajewicz, T. Broström, J. Ashley-Smith, H.L. Schellen, M. Martens, J. van Schijndel, F. Antretter, M. Winkler, C. Bertolin, D. Camuffo, G. Simeunovic, T. Vyhlídal, Climate for Culture: assessing the impact of climate change on the future indoor climate in historic buildings using simulations, Heritage Science 3 (1) (2015) 1–15, https://doi.org/10.1186/s40494-015-0067-9.

[11] H.L. Schellen, A.W.M. Van Schijndel, Setpoint control for air heating in a church to minimize moisture related mechanical stress in wooden interior parts, Building Simulation 4 (1) (2011, March) 79–86, https://doi.org/10.1007/s12273-011-0026-7.

[12] V. Rajčić, A. Skender, D. Damjanović, An innovative methodology of assessing the climate change impact on cultural heritage, Int. J. Architect. Herit. 12 (1) (2018) 21–35, https://doi.org/10.1080/15583058.2017.1354094.

[13] G.B. Coelho, H.E. Silva, F.M. Henriques, Calibrated hygrothermal simulation models for historical buildings, Build. Environ. 142 (2018) 439–450, https://doi.org/10.1016/j.buildenv.2018.06.034.
[14] A. Sadłowska-Sałęga, J. Radoń, Feasibility and limitation of calculative determination of hygrothermal conditions in historical buildings: case study of st. Martin church in Wiśniowa, Build. Environ. 186 (2020) 107361, https://doi.org/10.1016/j.buildenv.2020.107361.
[15] C.M. Muñoz-González, A.L. León-Rodríguez, J. Navarro-Casas, Air conditioning and passive environmental techniques in historic churches in Mediterranean climate. A proposed method to assess damage risk and thermal comfort pre-intervention, simulation-based, Energy Build. 130 (2016) 567–577, https://doi.org/10.1016/j.enbuild.2016.08.078.
[16] C.M. Muñoz-González, A.L. León-Rodríguez, M. Campano-Laborda, C. Teeling, R. Baglioni, The assessment of environmental conditioning techniques and their energy performance in historic churches located in Mediterranean climate, J. Cult. Herit. 34 (2018) 74–82, https://doi.org/10.1016/j.culher.2018.02.012.
[17] M. Napp, M. Wessberg, T. Kalamees, T. Broström, Adaptive ventilation for climate control in a medieval church in cold climate, Int. J. Vent. 15 (1) (2016) 1–14, https://doi.org/10.1080/14733315.2016.1173289.
[18] M. Napp, T. Kalamees, Energy use and indoor climate of conservation heating, dehumidification and adaptive ventilation for the climate control of a mediaeval church in a cold climate, Energy Build. 108 (2015) 61–71, https://doi.org/10.1016/j.enbuild.2015.08.013.
[19] G. Semprini, C. Galli, S. Farina, Reuse of an ancient church: thermal aspect for integrated solutions, Energy Procedia 133 (2017) 327–335, https://doi.org/10.1016/j.egypro.2017.09.395.
[20] A. Hayati, M. Mattsson, M. Sandberg, Single-sided ventilation through external doors: measurements and model evaluation in five historical churches, Energy Build. 141 (2017) 114–124, https://doi.org/10.1016/j.enbuild.2017.02.034.
[21] A. Hayati, Measurements and modeling of airing through porches of a historical church, Sci. Technol.Built. Environ. 24 (3) (2018) 270–280, https://doi.org/10.1080/23744731.2017.1388132.
[22] Muñoz-González, C.M.M. González, A.L. Rodríguez, R.S. Medina, J.R. Jaramillo, Effects of future climate change on the preservation of artworks, thermal comfort and energy consumption in historic buildings, Appl. Energy 276 (2020) 115483, https://doi.org/10.1016/j.apenergy.2020.115483.
[23] D. Camuffo, Microclimate for Cultural Heritage 3rd Edition Measurement, Risk Assessment, Conservation, Restoration, and Maintenance of Indoor and Outdoor Monuments, Elsevier, Amsterdam, 2014.
[24] G.G. Akkurt, N. Aste, J. Borderon, A. Buda, M. Calzolari, D. Chung, F. Leonforte, Dynamic thermal and hygrometric simulation of historical buildings: critical factors and possible solutions, Renew. Sustain. Energy Rev. 118 (2020) 109509, https://doi.org/10.1016/j.rser.2019.109509.
[25] M. Barclay, N. Holcroft, A.D. Shea, Methods to determine whole building hygrothermal performance of hemp–lime buildings, Build. Environ. 80 (2014) 204–212, https://doi.org/10.1016/j.buildenv.2014.06.003.
[26] T. Colinart, P. Glouannec, Temperature dependence of sorption isotherm of hygroscopic building materials. Part 1: experimental evidence and modeling, Energy Build. 139 (2017) 360–370, https://doi.org/10.1016/j.enbuild.2016.12.082.
[27] M. Andreotti, D. Bottino-Leone, M. Calzolari, P. Davoli, L. Dias Pereira, E. Lucchi, A. Troi, Applied research of the hygrothermal behaviour of an internally insulated historic wall without vapour barrier: in situ measurements and dynamic simulations, Energies 13 (13) (2020) 3362, https://doi.org/10.3390/en13133362.
[28] A. Holm, H.M. Kuenzel, K. Sedlbauer, The hygrothermal behaviour of rooms: combining thermal building simulation and hygrothermal envelope calculation, in: Eighth International IBPSA Conference, vol. 1, 2003, August, pp. 499–505 (Eindhoven Netherlands).
[29] H.L. Hens, Combined heat, air, moisture modelling: a look back, how, of help? Build. Environ. 91 (2015) 138–151, https://doi.org/10.1016/j.buildenv.2015.03.009.
[30] C. Gomes, C. Thule, D. Broman, P.G. Larsen, H. Vangheluwe, Co-simulation: a survey, ACM Computing Surveys (CSUR) 51 (3) (2018) 1–33, https://doi.org/10.1145/3179993.
[31] M. Steeman, M. De Paepe, A. Janssens, Impact of whole-building hygrothermal modelling on the assessment of indoor climate in a library building, Build. Environ. 45 (7) (2010) 1641–1652, https://doi.org/10.1016/j.buildenv.2010.01.012.
[32] L. Havinga, H. Schellen, Applying internal insulation in post-war prefab housing: understanding and mitigating the hygrothermal risks, Build. Environ. 144 (2018) 631–647, https://doi.org/10.1016/j.buildenv.2018.08.035.
[33] M.Y. Ferroukhi, R. Djedjig, K. Limam, R. Belarbi, Hygrothermal behavior modeling of the hygroscopic envelopes of buildings: a dynamic co-simulation approach, In Building Simulation 9 (5) (2016, October) 501–512, https://doi.org/10.1007/s12273-016-0292-5. Tsinghua University Press.
[34] M. Napp, T. Kalamees, T. Tark, E. Arumägi, Integrated design of Museum's indoor climate in medieval episcopal castle of haapsalu, Energy Procedia 96 (2016) 592–600, https://doi.org/10.1016/j.egypro.2016.09.105.
[35] F. Frasca, C. Cornaro, A.M. Siani, A method based on environmental monitoring and building dynamic simulation to assess indoor climate control strategies in the preventive conservation within historical buildings, Sci. Technol.Built. Environ. 25 (9) (2019) 1253–1268, https://doi.org/10.1080/23744731.2019.1642093.
[36] T. Busser, M. Pailha, A. Piot, M. Woloszyn, Simultaneous hygrothermal performance assessment of an air volume and surrounding highly hygroscopic walls, Build. Environ. 148 (2019) 677–688, https://doi.org/10.1016/j.buildenv.2018.11.031.
[37] J. Straube, E.F.P. Burnett, Overview of hygrothermal (HAM) analysis methods, in: H.R. Trechsel (Ed.), ASTM Manual 40 - Moisture Analysis and Condensation Control in Building Envelopes, 1991, pp. 81–89 [chapter 5].
[38] EN 15758, Conservation of Cultural Property - Procedures and Instruments for Measuring Temperatures of the Air and the Surfaces of Objects, European Committee for Standardization (CEN), Brussels, 2010.
[39] EN 16242, Conservation of Cultural Heritage - Procedures and Instruments for Measuring Humidity in the Air and Moisture Exchanges between Air and Cultural Property, European Committee for Standardization (CEN), Brussels, 2012.
[40] N. Marconi, E. Eramo, La chiesa di Santa Rosalia nel palazzo dei principi Barberini a Palestrina: committenza e cantiere,» Studi e Ricerche di Storia dell'Architettura, Rivista dell'Associazione Italiana Storici dell'Architettura (2017) 46–65.
[41] EN ISO 13370, Thermal Performance of Buildings – Heat Transfer via the Ground – Calculation Methods, European Committee for Standardization (CEN), Brussels, 2017.
[42] MASEA certified database, Available: https://www.masea-ensan.de/. (Accessed 25 June 2020).
[43] A.A. Hegazy, Effect of dust accumulation on solar transmittance through glass covers of plate-type collectors, Renew. Energy 22 (4) (2001) 525–540, https://doi.org/10.1016/S0960-1481(00)00093-8.
[44] EN 15026, Hygrothermal Performance of Building Components and Building Elements - Assessment of Moisture Transfer by Numerical Simulation, International Organization for Standardization, Geneva, 2007.
[45] F. Frasca, C. Cornaro, A.M. Siani, Performance assessment of a heat and moisture dynamic simulation model in IDA ICE by the comparison with WUFI Plus, IOP Conf. Ser. Mater. Sci. Eng. 364 (2018), 012024, https://doi.org/10.1088/1757-899X/364/1/012024.
[46] M. Woloszyn, C. Rode, Tools for performance simulation of heat, air and moisture conditions of whole buildings, Building Simulation 1 (1) (2008) 5–24, https://doi.org/10.1007/s12273-008-8106-z.
[47] R. Judkoff, J. Neymark, Model validation and testing: the methodological foundation of ASHRAE Standard 140, Build. Eng. 112 (2) (2006) 367–376.
[48] A.A. Hamid, P. Wallentén, Hygrothermal assessment of internally added thermal insulation on external brick walls in Swedish multifamily buildings, Build. Environ. 123 (2017) 351–362, https://doi.org/10.1016/j.buildenv.2017.05.019.
[49] Z. Pasztory, P.N. Peralta, S. Molnar, I. Peszlen, Modeling the hygrothermal performance of selected North American and comparable European wood-frame house walls, Energy Build. 49 (2012) 142–147, https://doi.org/10.1016/j.enbuild.2012.02.003.
[50] J. Maia, N.M. Ramos, R. Veiga, Evaluation of the hygrothermal properties of thermal rendering systems, Build. Environ. 144 (2018) 437–449, https://doi.org/10.1016/j.buildenv.2018.08.055.
[51] Climate for culture. WP 3. Hygrothermal building simulation, Available: https://www.climateforculture.eu/index.php?inhalt=project.workpackages. (Accessed 10 December 2020).
[52] H.E. Huerto-Cardenas, F. Leonforte, N. Aste, C. Del Pero, G. Evola, V. Costanzo, E. Lucchi, Validation of Dynamic Hygrothermal Simulation Models for Historical Buildings: State of the Art, Research Challenges and Recommendations, Building and Environment, 2020, https://doi.org/10.1016/j.buildenv.2020.107081, 107081.
[53] ASHRAE Guideline 14, Measurement of Energy and Demand Savings, American Society of Heating and Air-Conditioning Engineers, Inc., Atlanta, 2002.
[54] J. Kurnitski, M. Vuolle, Simultaneous Calculation of Heat, Moisture, and Air Transport in a Modular Simulation Environment, Estonian Academy Publishers, 2000, pp. 25–47.
[55] H.M. Künzel, Simultaneous Heat and Moisture Transport in Building Components. One-And Two-Dimensional Calculation Using Simple Parameters, IRB-Verlag, Stuttgart, 1995.
[56] P. Slanina, Š. Šilarová, Moisture transport through perforated vapour retarders, Build. Environ. 44 (8) (2009) 1617–1626, https://doi.org/10.1016/j.buildenv.2008.10.006.

Appendix C

Investigation on the use of hygrothermal modelling for paper collections

---

Verticchio, E., Frasca, F., Cornaro, C., and Siani, A.M.

IOP Conference Series: material science and engineering **949** (1), 015604 (2020).

Investigation on the use of hygrothermal modelling for paper collections

IOP Conf. Series: Materials Science and Engineering **949** (2020) 012015 doi:10.1088/1757-899X/949/1/012015

Investigation on the use of hygrothermal modelling for paper collections

E. Verticchio[1], F. Frasca[2], C. Cornaro[3], A.M. Siani[2]

[1]Department of Earth Sciences, Sapienza Università di Roma, Italy
[2]Department of Physics, Sapienza Università di Roma, Italy
[3]Department of Enterprise Engineering, Università degli Studi di Roma "Tor Vergata", Italy

elena.verticchio@uniroma1.it

Abstract. Dynamic simulation is increasingly adopted in the preventive conservation of cultural heritage as an advanced method to investigate strategies for mitigating the climate-induced degradation. The conservation of paper collections is strongly interrelated with the relative humidity of the air, as organic-hygroscopic materials act as buffers on relative humidity fluctuations while being vulnerable to moisture-induced damage. In the dynamic simulation of the microclimate within library and archival storage facilities, it is thus fundamental to include the hygrothermal interaction between the building and its hygroscopic content. The hygroscopic behaviour of paper collections can be modelled by hygrothermal tools such as those of the HAM-family (Heat, Air and Moisture), used to simulate simultaneous heat and mass transfers through porous envelope materials. This research aims at investigating the use of the HMWall model coupled with the software IDA ICE (Indoor Climate and Energy) to simulate of the 1-D heat and moisture transfer through a single wall made of paper. A literature survey was carried out to collect the available hygrothermal properties of modern and historical papers. Sensitivity analysis was used to identify the most relevant hygrothermal parameters in the simulation of moisture gradients across the paper wall. Moreover, the number of sub-layers in the paper wall model was found to significantly affect the internal distribution of moisture gradients. The use of the HMWall model was then tested in the simulation of the hygroscopic behaviour of a single paper wall in both steady-state and transient conditions. Finally, a simplified model able to preserve the accuracy of the results was proposed with the purpose of reducing the computation effort that a high-resolution model could involve if implemented in whole buildings. This study represents the first step towards the application of the HMWall model for the simulation of the indoor climate of library repositories.

1. Introduction

The conservation of library collections is strongly interrelated with the air relative humidity (RH) of the environment in which they are stored. In fact, organic hygroscopic materials are particularly vulnerable to moisture-induced damage due to chemical, biological and physical deterioration processes such as hydrolytic degradation, metabolic reactions and RH fluctuations affecting some properties of paper (e.g. pH and physical strength) [1]. Moreover, a reduction in the degree of polymerization and mechano-sorptive creep of paper can be accelerated under cycling humidity [2,3].

Whole-building dynamic simulation is being increasingly adopted in the preventive conservation of cultural heritage to study indoor environmental conditions and to investigate mitigation strategies of the climate-induced damages [4]. Hygroscopic materials effectively act as buffers on RH fluctuations [5−6] because they continuously exchange moisture with their surrounding environment. In modelling the environmental conditions within library and archival repositories, it is thus fundamental to include the hygrothermal interactions between the building and its hygroscopic content (i.e. the paper collections) [6−9]. Hence, a degradation scenario related to the microclimate conditions experienced by the library collections can be estimated using dose-response functions for paper [1].

The simulation of moisture transport through materials is complex as the properties of materials (particularly the historical ones) are frequently not fully known. The moisture buffering behaviour of paper collections is usually simplified by using the effective moisture capacity (EMC) approach, where the moisture buffering capacity of the indoor air is integrated with that of the books [6,9]. However, the hygrothermal response of cellulose-based objects can be more effectively modelled by means of tools commonly used for the simulation of the simultaneous heat and moisture transfer through porous envelope materials such as those of the HAM-family (Heat, Air and Moisture) [7,8,10,11]. In the simulation of moisture buffering effects, the HAM models are indicated as the most appropriate to account for moisture exchange in hygroscopic materials [12]. Steeman et al. [8] used a HAM model to simulate the hygrothermal conditions within a library repository and found the obtained results to be more accurate and reliable with respect to those obtained with the EMC approach. More recently, Kupczak et al. [7] have proposed a way to accurately model the water vapour diffusion in 3-D objects using 1-D moisture transport equations so that the buffering effects of paper collections can be precisely integrated. One must bear in mind that most of these studies focussed on the impact of the RH stabilization in terms of energy savings [7] and in the design of the air-conditioning systems [10] rather than on the implications on the conservation of paper collections. Furthermore, none of the above-mentioned studies investigated the uncertainties to be associated to the simulation outputs.

The HMWall model (hereafter called HMWall), based on Künzel equations [13] can be coupled with the modular software IDA ICE (Indoor Climate and Energy) to provide reliable dynamic hygrothermal simulations in historic buildings [4]. In Frasca et al. [14], the simulation performance of HMWall in IDA ICE was assessed through the comparison with the validated software WUFI Plus [15,16] and improved in its hygric part. To the authors' knowledge, HMWall has never been tested so far in modelling the hygrothermal conditions within library and archival repositories.

The hygrothermal properties of paper available in literature are measured following various procedures; moreover, as they depend on both the constituent materials and the manufacturing process, modern [6,7,9,20] and historical [19] papers can have rather different hygrothermal properties. Sensitivity Analysis (SA) can be used to determine which are the most influential parameters in the computation of the simulation results and to quantify their effect on the variability of the outputs. Since SA results are strongly related to the specific configuration to be tested, the analysis must be performed in relation with the modelling goals, carefully choosing the variability of the input parameters [17]. A recent work conducting a sensitivity analysis on the Künzel model found that thermal conductivity in a single layer wall of concrete can influence the water content distribution [18].

This paper aims at investigating for the first time the capability of HMWall coupled with IDA ICE 4.8 to simulate the dynamic moisture transport across a single wall made in paper at both steady-state and transient boundary conditions. A satisfactory performance of this coupled model will allow to move forward to the modelling of the whole-building hygrothermal behaviour of paper storage environments and to the implementation of methods for the preventive conservation of library and archival collections.

2. Materials and methods

The approach followed in this study includes five main steps:

- literature survey on the available hygrothermal properties of modern and historical paper;
- minimization of the discrepancy between the hygrothermal curves calculated by HMWall and those provided in literature;

- sensitivity analysis on the influence of the variability of the hygrothermal properties found in literature on the simulation outputs of a single paper wall;
- study of the effect of the number of sub-layers in the paper wall model on the computation of moisture gradients;
- investigation on the use of HMWall to simulate the hygroscopic behavior of a paper wall both in steady-state and in transient conditions.

2.1. Background information on HMWall

The HMWall model, whose underlying physical laws are thoroughly discussed in the PhD dissertation of Künzel [13], is based on the balance equations for heat and moisture transfers. In this 1-D fully coupled heat and mass model, the hygrothermal variables are strongly linked to each other since the thermal conductivity, which drives the heat transfer, is moisture-dependent and because the enthalpy flux is a function of both temperature and vapour diffusion flux.

In HMWall, the adsorption isotherms are calculated only as a function of relative humidity (φ), since the equilibrium water content (w) is assumed to be little sensitive to temperature changes and the hysteresis between adsorption and desorption is usually considered negligible. The moisture storage curve of the material is computed as follows:

$$w(\varphi) = w_f \cdot \frac{\varphi \cdot (b-1)}{b-\varphi} \qquad (1)$$

where w is the equilibrium water content (kg/m^3) corresponding to the relative humidity φ, w_f is the moisture content at free water saturation and b is an approximation factor calculated from the equilibrium water content at φ = 0.8 (w_{80}).

The diffusion of the material is expressed as a function of the dry diffusion resistance factor (μ). Capillary liquid water transport is described as a diffusion phenomenon in the material pore spaces regulated by the water absorption coefficient. The thermal conductivity of dry materials (λ_0) increases linearly with moisture content and is expressed as a function of the moisture-induced conductivity supplement (s), i.e. the fractional increase of λ_0 per percentage of moisture mass, which is mostly independent of the bulk density in the case of hygroscopic materials.

2.2. Hygrothermal properties of paper from literature

A literature survey was conducted to obtain an overview of the available experimental hygrothermal properties of common types of paper in library and archival repositories.

Table 1. Hygrothermal properties of modern* and historic** paper according to literature references.

References	ρ	C_p	λ_0	μ	w_f	w_{80}
	kg/m^3	J/(kg·K)	W/(m·K)	-	kg/m^3	kg/m^3
* [6,9]	690	750	0.06	87	165	95
* [7]	618	-	-	-	61	52
** [19]	-	-	-	-	105	76
* [20]	839	1150	0.09	-	-	-

Table 1 summarizes the values of bulk density (ρ), specific heat capacity of dry material (C_p) and dry thermal conductivity (λ_0) according to recent experimental works about paper. The value for water vapour diffusion resistance factor in dry conditions (μ) was obtained at RH=50% applying the formula in [6,9]; the values of w_{80} and w_f refer to the parameters of the HMWall moisture storage curve (Equation 1) fitted on literature data as will be described in the next paragraph. The hygrothermal properties of modern paper were measured on telephone-book paper [6,9], contemporary book paper [7] and offset uncoated paper [20], while the moisture coefficients in [19] are specific for historical cellulose-based paper. References [6,9] considered standard values for C_p and λ_0, whereas [7,19] did not provide any value for these parameters; therefore, reference [20] was introduced and used as a benchmark for the thermal properties of modern paper.

2.3. Modelling the hygroscopic behaviour of a paper wall with HMWall

The moisture storage curve of the various types of paper were first reconstructed according to the literature fitting equations and parameters. Then, the approximating parameters of the HMWall moisture storage curve in Equation 1 were chosen so that the discrepancy between the equilibrium water content values (w) in literature and those computed with HMWall was minimized at a benchmark value of ϕ=0.5 (Figure 1). The benchmark value was chosen as it encompasses the recommended conditions for the preservation of library collections, i.e. those targeting to avoid the risk of paper becoming brittle (at low ϕ) and the risk of mould growth (at high ϕ) [1].

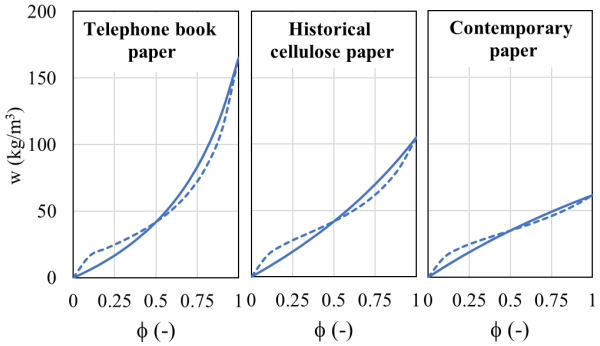

Figure 1. Moisture storage curves of paper from literature data (dashed lines) *versus* those computed by HMWall (solid lines). The discrepancy is minimized at ϕ = 0.5.

A preliminary sensitivity analysis (SA) was considered necessary to identify the most relevant hygrothermal parameters in the model influencing the moisture gradients across the paper wall (ΔRH), thus allowing to select among the various hygrothermal properties found in literature. For example, since the heat and moisture fluxes are balanced, the thermal properties driving the heat transfer could have an impact on the water content distribution in hygroscopic materials [18].

3. Results and discussion

The sensitivity analysis was conducted by using the Elementary Effects (EE) method based on the Morris random sampling method [17]. A HMWall single wall with area equal to 1 m^2, thickness 0.2 m and divided into N=63 sub-layers, was preconditioned at paper wall temperature T_{wall}=20°C and relative humidity RH_{wall}=50% and connected to identical boundary conditions of T=20°C and RH=70% (Figure 2). N was chosen in order to have a detailed model able to describe the heat and moisture transfer phenomena in paper, with thickness of each sub-layers equal to 3 mm.

The Morris random sampling considered 10 EE for each parameter and 4 discretized levels to span within the ranges of the selected hygrothermal parameters summarized in Table 1. Water liquid transport was assumed to be negligible for the scopes of this investigation and thus the vapour absorption coefficient was set to the minimum.

Table 2. Ranges of the selected hygrothermal properties of paper tested in the sensitivity analysis.

Sensitivity analysis inputs	Range
Density (ρ)	600−900 kg/m^3
Specific heat capacity (C_p)	700−1200 J/(kg·K)
Dry thermal conductivity (λ_0)	0.05−0.10 W/(m·K)
Thermal conductivity supplement (s)	1.0–5.0
Free water saturation moisture content (w_f)	100−200 kg/m^3
Equilibrium moisture content at RH = 80% (w_{80})	50−100 kg/m^3
Dry vapour diffusion resistance factor (μ)	50−100

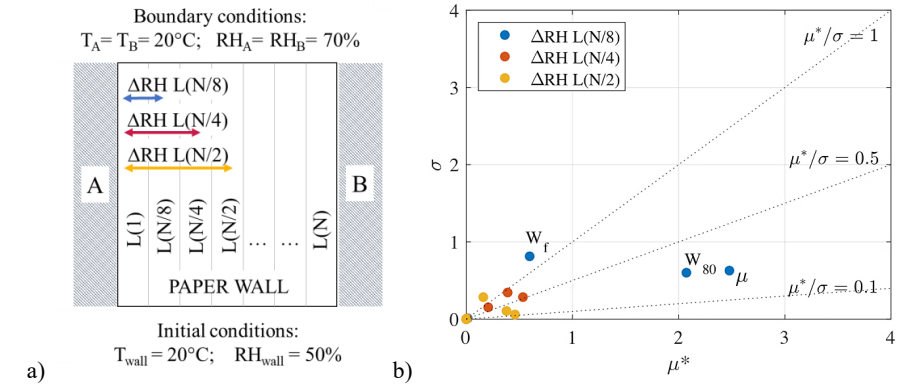

Figure 2. Scheme of the configuration of a paper wall model divided into N sub-layers (a); results of the sensitivity analysis (b) in terms of the mean (μ*) and the standard deviation (σ) of the Elementary Effects (EE) calculated on the RH gradients (ΔRH) after one month at the steady-state conditions described in a) with N=63.

The results of the sensitivity analysis showed that only the equilibrium moisture content at RH=80% (w_{80}) and the vapour diffusion resistance factor (μ) have a significant but low impact on the RH gradient (ΔRH) among the outermost sub-layers of a paper wall (ΔRH L(N/8) in Figure 2a); the remaining hygrothermal properties seem to have a negligible effect on the chosen output. In the light of the above considerations, for the simulation in HMWall it was reasonable to choose the set of parameters given in [6,9] because more complete (Table 3).

Table 3. Hygrothermal properties of paper used in this study.

Hygrothermal properties of paper	Value
Density (ρ)	690 kg/m^3
Specific heat capacity (C_p)	750 J/(kg·K)
Dry thermal conductivity (λ_0)	0.06 W/(m·K)
Thermal conductivity supplement (s)	1.0
Free water saturation moisture content (w_f)	165 kg/m^3
Equilibrium moisture content at RH = 80% (w_{80})	95 kg/m^3
Dry vapour diffusion resistance factor (μ)	87
Liquid water absorption coefficient (A)	1.0×10^{-11} kg/(m^2·s$^{0.5}$)

The influence of the number of N sub-layers in a single paper wall preconditioned to T_{wall}=20°C and RH_{wall}=50% was explored after one month of prolonged exposure to boundary steady-state conditions of T=20°C and RH=70%. Figure 3 shows a comparison among the RH values obtained at the same wall sub-layers as a function of the number N of equally-spaced sub-layers. The thicknesses (t) associated to N=63,31,15,7 sub-layers are t=3,6,13,29 mm, respectively. The high-resolution paper wall (N=63, t=3 mm) was chosen as reference. The results highlighted that a significant underestimation can be introduced in the computation of the internal RH gradients if the simulation is run using a paper wall model with a too low number of sub-layers because of the averaging over a too large sub-layer thickness.

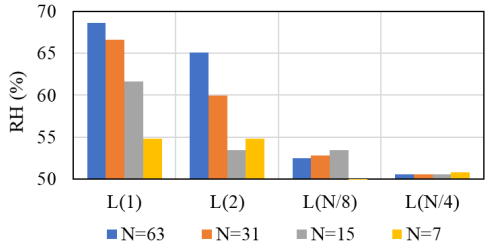

Figure 3. Relative humidity values (RH) after one month at the conditions described in Figure 2a obtained in correspondence with the same wall node as a function of the number of sub-layers (N). The sub-layer thickness (t) associated to N=63,31,15,7 sub-layers is t=3,6,13,29 mm.

In Figure 4 are shown the RH values obtained across the high-resolution paper wall as a function of the duration of boundary adiabatic conditions (T=20°C) and of the steady-state RH gradient from the preconditioning value (RH=50%) to RH=70%. The RH distribution within the paper wall evolves slowly, showing a significant variation starting from one week of prolonged exposure and reaching the full equilibrium between the bulk and the surfaces only after several years.

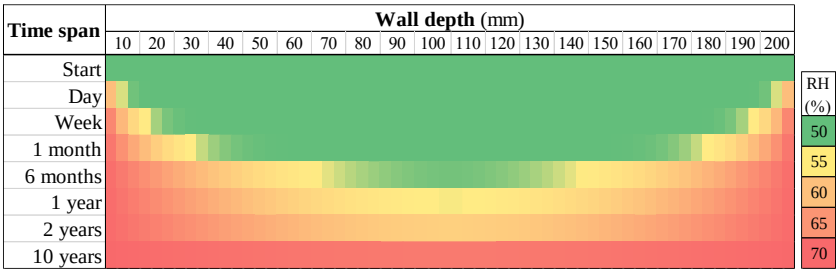

Figure 4. Relative humidity values (RH) within the paper wall as a function of the duration of the steady-state boundary conditions described in Figure 2a.

The influence of transient boundary conditions was also investigated for the case of a single paper wall having 63 equally-spaced sub-layers and being initially conditioned to T_{wall}=20°C and RH_{wall}=50%. The configuration was tested at boundary constant temperature T=20°C and RH conditions periodically ranging from 30% to 70% at weekly, monthly and seasonal frequency. The results in Figure 5 emphasised that the first 5 sub-layers (corresponding to the first 15 mm from the wall surface) are the most responsive to the external transient forcing. For the seasonal cycle, only RH variations above the threshold of +10% and below the threshold of −10% from the preconditioning value of RH_{wall} are shown.

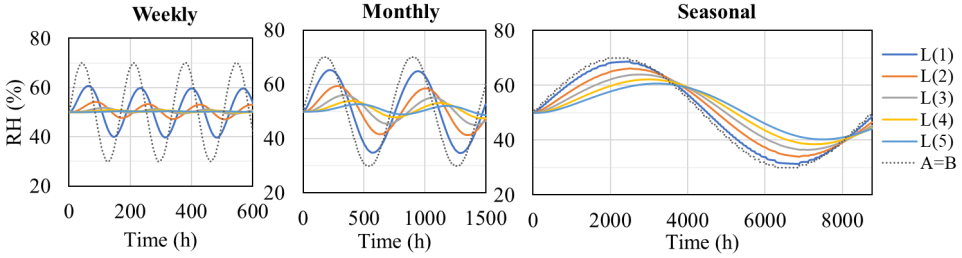

Figure 5. Relative humidity values across a paper wall divided into N=63 equally-spaced sub-layers at constant T=20°C and boundary RH conditions periodically ranging from 30% to 70% at weekly, monthly and seasonal frequency (grey dotted lines).

Even if high-resolution models can provide more accurate results, they may increase too much the computation effort needed to run the simulation when included in whole-buildings. For this reason, a simplified paper wall model was proposed as schematized in Figure 6. The simplified paper wall model has a reduced number of unequally-spaced sub-layers. The first 5 sub-layers located under the surfaces A and B (i.e. L(A) and L(B)) are assigned the same thickness as that of the high-resolution reference sub-layers (3 mm). The impact of the inner layers' thickness on the outputs was tested and found to be negligible. Hence, the minimum number of 3 was chosen for the inner sub-layers.

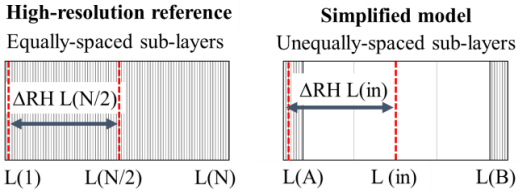

Figure 6 Scheme of the high-resolution paper wall divided into equally-spaced sub-layers (left) and the simplified paper wall divided into a reduced number of unequally-spaced sub-layers (right).

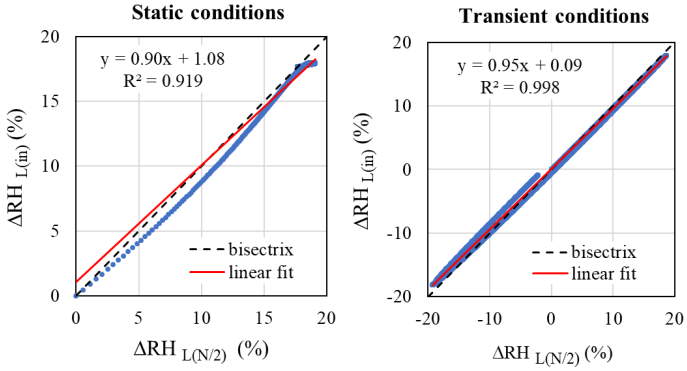

Figure 7. Scatterplot of hourly relative humidity gradients between the surface and the bulk of a paper wall over a year at the steady-state conditions described in Figure 2a (left) and at the transient seasonal conditions described in Figure 5c (right). $\Delta RH_{L(N/2)}$ and $\Delta RH_{L(in)}$ refer respectively to the RH gradients of a high-resolution model with N=63 equally-spaced sub-layers and of a simplified model with N=13 unequally-spaced sub-layers (see Figure 6).

The simplified model was tested in comparison with the high-resolution reference in terms of the RH gradient between the surface and the centre of the paper wall. As explained in Figure 6, the gradient $\Delta RH_{L(N/2)}$ of the high-resolution paper wall was calculated as the difference between the RH of the exterior sub-layer L(1) and that of the central sub-layer L(N/2), while the gradient $\Delta RH_{L(in)}$ of the simplified paper wall model is the difference between the RH of the exterior sub-layer L(A) and that of the central sub-layer L(in). Figure 7 shows a scatterplot of the $\Delta RH_{L(N/2)}$ *versus* $\Delta RH_{L(in)}$ calculated on a hourly basis over a year at both steady-state and transient seasonal conditions. The linear curve fitted on the results points out that the gradients in the simplified paper wall accurately reproduce those obtained with the high-resolution reference, therefore the proposed model can be used as a reliable alternative to reduce the simulation effort without losing accuracy in the results.

4. Conclusions

This paper aimed at investigating for the first time the capability of the HMWall model coupled with IDA ICE 4.8 in the simulation of the 1-D moisture transport across a single paper wall at both steady-state and transient boundary conditions. An initial literature survey has provided the available hygrothermal properties measured in paper. The results of a sensitivity analysis on a single paper wall exposed to an increase of the boundary relative humidity showed that paper thermal properties have a negligible impact on the water content distribution, whereas the equilibrium moisture content and the vapor diffusion resistance factor resulted to be the most influencing parameters on the tested output. The number of sub-layers used in the model significantly affect the relative humidity outputs at various depths within the paper wall. Nevertheless, since high-resolution models involve substantial computation effort when integrated in whole buildings, a simplified model able to keep the accuracy in the results was proposed. This preliminary investigation will be useful for an "informed use" of HMWall in the hygrothermal simulation of the indoor climate of library and archival repositories.

References

[1] Menart E, de Bruin G, and Strlič M 2011 *Polym. Degrad. Stab.* Dose-response functions for historic paper **96** 2029-2039

[2] Bogaard J and Whitmore P M 2002 *Stud Conserv* Explorations of the role of humidity fluctuations in the deterioration of paper **47** 11−15

[3] Alfthan J 2004 *MTDM* The effect of humidity cycle amplitude on accelerated tensile creep of paper **8**(4), 289-302

[4] Frasca F, Cornaro C and Siani A M 2019 *Sci Technol Built En* A method based on environmental monitoring and building dynamic simulation to assess indoor climate control strategies in the preventive conservation within historical buildings **25**(9) 1253–1268

[5] Verticchio E, Frasca F, Garcìa-Diego F J and Siani A M 2019 *Climate* Investigation on the use of passive microclimate frames in view of the climate change scenario **7** 98

[6] Derluyn H, Janssen H, Diepens J, Derome D and Carmeliet J 2007 *JBP* Hygroscopic behavior of paper and books **31.1** 9-3

[7] Kupczak A, Sadłowska-Sałęga A, Krzemień L, Sobczyk J, Radoń J, and Kozłowski R 2018 *Energy Build* Impact of paper and wooden collections on humidity stability and energy consumption in museums and libraries **158** 77–85

[8] Steeman M, de Paepe M and Janssens A 2010 *Build Environ* Impact of whole-building hygrothermal modelling on the assessment of indoor climate in a library building **45**(7) 1641–1652

[9] Derluyn H, Janssen H, Diepens J and Derome D 2007 *Proceedings of Performance of the Exterior Envelopes of Whole Buildings X International Conference* Can Books and Textiles Help in Controlling the Indoor Relative Humidity?

[10] Kompatscher K, Kramer R P, Ankersmit B A and Schellen H L 2018 *Build Environ* Intermittent conditioning of library archives: Microclimate analysis and energy impact **147** 50-66

[11] Radoń J, Sadłowska-Sałęga P, Wąs K, Gryc A and Kupczak A 2018 *IOP Conference Series: Materials Science and Engineering* Energy use optimization in the building of National Library **415** 012029

[12] Akkurt G G, Aste N, Borderonc J, Buda A, Calzolari M, Chunge D, Costanzo V, Del Pero C, Evola G Huerto-Cardenas H E, Leonforte F, Lo Faro A, Lucchi E, Marletta L, Nocera F, Pracchi V, Turhani G 2020 *Renew Sust Energ Rev* Dynamic thermal and hygrometric simulation of historical buildings: Critical factors and possible solutions **118** 109509

[13] Künzel H M 1995 Simultaneous Heat and Moisture Transport in Building Components One-and two-dimensional calculation using simple parameters (PhD dissertation)

[14] Frasca F, Cornaro C and Siani A M 2018 *IOP Conference Series: Materials Science and Engineering* Performance assessment of a heat and moisture dynamic simulation model in IDA ICE by the comparison with WUFI Plus **364**(1)

[15] Antretter F, Sauer F, Schöpfer T and Holm A 2011 *12th IBPSA Conference Proceedings, Sydney* Validation of a hygrothermal whole building simulation software **14** 16

[16] Mundt-Petersen S and Harderup L 2013 *Proceedings of the Thermal Performance of the Exterior Envelopes of Whole Buildings XII-International Conference Florida USA* Validation of a one-dimensional transient heat and moisture calculation tool under real conditions

[17] Garcia Sanchez D, Lacarriere B, Musy M and Bourges B 2014 *Energy Build* Application of sensitivity analysis in building energy simulations: combining first- and second-order elementary effects methods **68** 741–750

[18] Othmen I, Poullain P, and Leklou N 2018 *European Journal of Environmental and Civil Engineering* Sensitivity analysis of the transient heat and moisture transfer in a single layer wall 1–19

[19] Kupczak A, Bratasz Ł, Kryściak-Czerwenka J, and Kozłowski R 2018 *Cellulose* Moisture sorption and diffusion in historical cellulose-based materials **25**(5) 2873-2884

[20] Lavrykov S A and Ramarao B 2012 *Drying Technology* Thermal Properties of Copy Paper Sheets **30(**3) 297–311

Appendix D

Investigation on the use of passive microclimate frames in view of the climate change scenario

---

Verticchio, E., Frasca, F., García-Diego, F.-J., and Siani, A.M.

Climate 7 (8), 98 (2019)

climate

MDPI

Article

Investigation on the Use of Passive Microclimate Frames in View of the Climate Change Scenario

Elena Verticchio [1,*], Francesca Frasca [2] and Fernando-Juan Garcìa-Diego [3] and Anna Maria Siani [2]

[1] Department of Earth Sciences, Sapienza Università di Roma, P.le A. Moro 5, 00185 Rome, Italy
[2] Department of Physics, Sapienza Università di Roma, P.le A. Moro 5, 00185 Rome, Italy
[3] Department of Applied Physics, Centro de Investigación Acuicultura y Medio Ambiente ACUMA, Universitat Politècnica de València, 46022 Valencia, Spain
* Correspondence: elena.verticchio@uniroma1.it; Tel.: +39-06-4991-3479

Received: 28 June 2019; Accepted: 5 August 2019; Published: 9 August 2019

Abstract: Passive microclimate frames are exhibition enclosures able to modify their internal climate in order to comply with paintings' conservation needs. Due to a growing concern about the effects of climate change, future policies in conservation must move towards affordable and sustainable preservation strategies. This study investigated the hygrothermal conditions monitored within a microclimate frame hosting a portrait on cardboard with the aim of discussing its use in view of the climate expected indoors in the period 2041–2070. Its effectiveness in terms of the ASHRAE classification and of the Lifetime Multiplier for chemical deterioration of paper was assessed comparing temperature and relative humidity values simultaneously measured inside the microclimate frame and in its surrounding environment, first in the Pio V Museum and later in a residential building, both located in the area of Valencia (Spain). Moreover, heat and moisture transfer functions were used to derive projections over the future indoor hygrothermal conditions in response to the ENSEMBLES-A1B outdoor scenario. The adoption of microclimate frames proved to be an effective preventive conservation action in current and future conditions but it may not be sufficient to fully avoid the chemical degradation risk without an additional control over temperature.

Keywords: microclimate frame; preventive conservation; risk assessment; Sorolla painting; climate change

1. Introduction

The environment surrounding the objects is one the main driver of their deterioration. Long-term microclimate monitorings, through the identification of risk factors, play a key role in the implementation of preventive conservation actions [1]. Temperature and relative humidity are fundamental physical parameters, as materials adapt themselves to the continually changing hygrothermal conditions to reach a thermodynamic equilibrium. Strict microclimate targets for preservation [2,3] have fostered the use of expensive HVAC (Heating, Ventilation and Air-Conditioning) systems. However, these highly sophisticated systems may be risky in the case of a potential failure and hardly possible for all museums, which, with the increase of cultural tourism, might incur raised costs for the maintenance of adequate conditions for conservation [4]. Furthermore, due to a growing concern about the effects of the expected climate change, future policies in conservation must move towards affordable and sustainable preservation strategies [5]. Passive methods, based on the understanding of the material properties and of its interaction with the environment, might provide a reliable support in this direction.

Among preventive conservation tools, showcases aim at creating an internal micro-environment different from the external macro-environment [6]: this "box-in-box" configuration allows locally fine-tuning the control over various environmental parameters (temperature, relative humidity, pollutants and light), thus reducing the risk of physical and chemical damage to cultural heritage objects [7]. The employment and optimization of passive low-cost devices can be highly effective to provide relative humidity control in less than ideal environments, particularly in the case of mixed collections with different conservation needs. Since their response to temperature fluctuations is usually poor [6,8], panels of materials containing PCMs (Phase Change Materials) have been proposed to be placed inside showcases to keep the internal temperature stable [9].

Microclimate frames are showcases specifically designed for paintings and able to modify their internal conditions in order to comply with tolerability targets for specific typologies of materials. This kind of exhibition enclosures is considered among the safest systems for keeping relative humidity stable and is increasingly being used to protect paintings against indoor hazards [10]. Passive microclimate frames usually take advantage of the inclusion of a buffering agent in combination with the reduction of the air exchange rate [11–13]. A buffering agent is generally an extremely absorbent material which is able to smooth out abrupt changes by releasing moisture when relative humidity decreases and absorbing moisture if it increases. An economical microclimate frame can be produced in-house using the picture's frame as the primary case [14]. As in showcases, every microclimate frame is characterized by a peculiar response to the environmental forcing [8]. Their effectiveness depends on the specific features and can be assessed as a function of the improvement of the surrounding microclimate in terms of the fulfilment of the artwork conservation needs.

The most recent standards in conservation avoid recommending ideal temperature and relative humidity intervals and have evolved towards the concepts of proofed fluctuations [15], i.e., the largest hygrothermal levels experienced by the objects in the past, and historic fluctuations [16], i.e., the environmental conditions to which artworks have acclimatized and adapted during their conservation history. Both these concepts imply methodological indications rather than prescriptive ones [3] and thus a more flexible approach, allowing for the short-term fluctuations and seasonal changes that can be considered safe for the collections. The ASHRAE (American Society of Heating, Air-Conditioning and Refrigerating Engineers) guidelines [17] suggest five classes of quality control, defined on the basis of seasonal and daily hygrothermal fluctuations. The possible risks for collections gradually increase from Class AA, associated with no risk to most objects, to Class D, that protects only from dampness. These guidelines have been effectively applied to quantify the damage potential of environments already actively controlled [18] and those of future climate scenarios [19]. Thanks to the enhanced knowledge of the properties of the materials and of the mechanisms of interaction with the surrounding environment, damage functions can be used to assess the possible risks for various typologies of materials [18]. For paper, one of the most alarming degradation processes is the chemical decay (e.g., yellowing of paper and fading of colors) [20]. The Lifetime Multiplier is an index extensively used to assess the time span in which varnishes and paper objects remain usable if compared to standard reference conditions [21,22].

To extend the microclimate assessment over the effects of the expected climate change, simplified heat and moisture transfer equations through the building envelope can be derived from monitored outdoor and indoor data and employed to simulate the future conditions indoors [23,24]. This methodology was developed within the European project Climate for Culture (2009–2014) [25,26], which focused its attention to the future conservation risks with the aim to suggest possible mitigation actions and inform stakeholders and policy makers.

Simultaneous measurements of temperature and relative humidity collected inside and outside a microclimate frame were used in this study to investigate the quality of its internal environment, making it possible to evaluate the buffering properties over time. The hygrothermal observations were recorded from May 2014 to February 2017, first in the Sorolla room of the Pio V Museum of Fine Art in

Valencia (Spain) [27] and, later on, in a residential building in the same area. The effectiveness of the passive microclimate frame was expressed in terms of the ASHRAE classification and the Lifetime Multiplier index for chemical deterioration. Moreover, a methodology based on heat and moisture transfer functions through the building envelope was applied to derive projections over the future indoor hygrothermal conditions as a function of the ENSEMBLES-A1B outdoor scenario in the area of Valencia [28]. An increased awareness of the potential conservation risks in view of the expected climate change has given the possibility to suggest appropriate preventive conservation strategies.

2. Materials and Methods

2.1. The Microclimate Frame

A long-term hygrothermal monitoring was conducted inside a microclimate frame housing a portrait of the Valencian painter Joaquín Sorolla (1863–1924). The painting, titled "Portrait of a lady with a red flower in her hair" (Figure 1a), measures 64 cm × 49 cm and is enclosed in a hand-crafted microclimate frame (69 cm × 54 cm ×8 cm) made of an external aluminium case and a frontal glass. The specific layout of the components of the microclimate frame under study is shown in Figure 1b. A sheet of cardboard (i.e., the same material supporting the portrait) of the same size of the paintings was used as back plate for the frame and put in direct contact with the painting support in order to offset changes in external relative humidity acting as a buffer [14]. The cardboard was preconditioned to the relative humidity level of 40% according to an extensive literature review on paper degradation [20] with the aim of reducing the impact of deterioration risk factors acting on the painting.

Figure 1. Portrait on cardboard titled "Portrait of a lady with a red flower in her hair" by J. Sorolla (**a**); and schematic cross section of the microclimate frame used and layout of its components (**b**).

The painting by Sorolla was realized on cardboard in 1916 with the gouache technique and donated as a gift to the Traver family. Since then, it used to be conserved in the house of the owners being enclosed within an unbuffered frame. Conservation surveys performed by the Valencian Institute of Conservation and Restoration (IVACOR) detected the presence of dust deposits both on the front and on the back, craquelures and loss of material on the painting layer together with a massive fungal attack visible in the form of dark circular stains. The gum arabic, frequently used as binding media [29], is responsible for its sensitivity to hygrothermal variations as it is particularly vulnerable to mold growth and chemical degradation. In the final report of the surveys, the Institute warned that the deterioration could have been caused by adverse environmental conditions in conjunction with the vulnerability of the materials used [30]. The artwork underwent restoration from 2012 to 2014 in the IVACOR laboratories and at the end of the intervention was enclosed in a passive microclimate frame *ad hoc* designed and provided with internal temperature and relative humidity sensors.

2.2. The Monitoring Campaign

Temperature (T) and relative humidity (RH) data were monitored from May 2014 to February 2017. Over this period, the painting was exposed to different environments: first, the Sorolla room in the Pio V Museum of Fine Art in Valencia from May 2014 to February 2016 and, later on, a residential building located in a city near Valencia. Since the private owners do not want to reveal the new location of the painting for safety reasons, in this investigation were used the climate data of the area of Valencia. The Pio V Museum is housed in a historical building of the XVII century where an active HVAC system of temperature control was in operation, with a variable T set-point ranging from 20 °C to 24 °C and RH left uncontrolled [27]. In the residential building, where the painting continued to be monitored with the same T and RH probes, an intermittent heating system was active only in winter and temperatures exceeded 30 °C during summer.

The microclimate monitoring system was developed by the Department of Applied Physics of the Polytechnic University of Valencia [31]. Two probes, each with coupled T and RH sensors, were assembled and installed within and outside the microclimate frame. Some of the technical features of the sensors are reported in Table 1: the temperature sensors (Maxim Integrated DS18B2) are in accordance with the instrumental metrological characteristics recommended in EN 15758:2010 [32], while the uncertainty of the RH sensors (Honeywell HIH 4030) is slightly higher than that recommended by EN 16242:2012 (3%) [33]. When using multiple sensors for RH, they must be carefully calibrated in advance in order to have no significant difference in their accuracy. For this reason, the RH sensors were calibrated with aqueous solutions of two salts (lithium chloride and sodium chloride) in accordance with the ASTME 104-02 standard [34]. The time interval between consecutive observations was set to 1 h, following the results of a previous study [27] where the sampling frequency was found to be reliable in the application of recent standards and therefore can be considered a good compromise between the priority of disposing of detailed series of observations and the necessity of avoiding redundancy in museum surveys.

The mixing ratio (MR) was derived from simultaneous T and RH data using the formula in [33].

Table 1. Technical features of the T and RH sensors used in the monitoring.

	T	RH
Response time	750 ms	5 s
Uncertainty	±0.5 °C	±3.5%

The outdoor hygrothermal data were obtained from the meteorological hourly dataset of the area of Valencia [35] distributed by the National Agency of Meteorology of the Spanish Government (AEMET) and available on the UPV website.

2.3. The Environmental Risk Assessment

The environmental risk assessment was based on the application of the ASHRAE guidelines and on the computation of the Lifetime Multiplier, an index used to quantify the risk of chemical degradation for paper.

In the ASHRAE guidelines [17], the classification in classes of quality of environmental control is based on the combination of the T and RH seasonal cycles and short-term fluctuations. The maximum and minimum seasonal shift is calculated by adding and subtracting to the annual mean the seasonal changes allowed for each class. The width of the final bands is finally determined shifting the curve of a 91-day central moving average by the short-term fluctuations indicated for the same class [18]. The ASHRAE classes of quality for conservation range from Class D, which prevents only from dampness, to Class AA, which is associated to no risk of mechanical damage to most artifacts and paintings. Class B is considered the reference for most of museums [2], since mechanical damage is proved to be avoided for RH values not exceeding the range of 50 ± 15%.

The Lifetime Multiplier (LM) considers the risk of chemical degradation taking into account the activation energy of the degradation processes involved in the deterioration of the organic materials (i.e., 70 kJ/mol for yellowing of varnishes and 100 kJ/mol for degradation of cellulose). This index is a multiplier of the time left to an object to remain usable when compared to standard conditions of T = 20 °C and RH = 50%. Since the instantaneous values of LM exponentially depend on temperature (Equation (1)), the influence on chemical degradation of T variations is greater than that exerted by RH variations of the same magnitude [36]:

$$LM_i = \left(\frac{50\%}{RH_i}\right)^{1.3} \cdot e^{\left(\frac{E_a}{R}\left(\frac{1}{T_i} - \frac{1}{293.15}\right)\right)} \quad (1)$$

where RH_i is the instantaneous measured value of relative humidity at time i, T_i is the instantaneous measured value of temperature (expressed in K) at time i, E_a is the activation energy for the degradation of paper (100 kJ $\cdot$ mol^{-1}) and R is the perfect gas constant (8.314 J $\cdot$ mol^{-1} $\cdot$ K^{-1}). The level of risk associated to the Lifetime Multiplier values can be defined as follows [18]: safe when LM > 1, medium risk when $0.75 <$ LM ≤ 1 and high risk if LM ≤ 0.75.

2.4. The Hygrothermal Conditions Expected Indoors in the Period 2041–2070

As a consequence of the climate change scenario, the southern European regions will probably increase their need for summer cooling (while decreasing winter heating) in order to keep the environmental conditions suitable for artwork conservation [26]. To evaluate the effects of the climate change scenario in the residential building near Valencia and on the effectiveness of the microclimate frame, we followed the approach applied in [23,24] to forecast the expected indoor T and RH levels.

The principal steps of the methodology can be summarized as follows:

1. monitoring of the simultaneous indoor (a) and outdoor (b) climate over at least one year;
2. derivation of the outdoor/indoor heat and moisture transfer functions (TFs) through the building;
3. extraction of the outdoor climate in the interested area from a simulated scenario;
4. inverse modeling of the future indoor climate based on the derived TFs; and
5. evaluation of the expected changes for artwork conservation by means of damage functions.

The annual hygrothermal data monitored in the residential building (Step 1a) and outdoor (Step 1b) were used to derive the seasonal cycles of temperature and mixing ratio of moist air. The observations collected in 2016 during the heating period were discarded in the analysis in order to consider only the environmental conditions not affected by the HVAC systems.

The annual cycles of temperature and mixing ratio were fitted as generic time-dependent sinusoidal equations as follows:

$$x(t) = \bar{x} + \Delta x \cdot sin(\omega t - \Phi) \quad (2)$$

where x is the variable considered (i.e., T or MR), t is time (in days), $\bar{x}$ is the annual average of x, ω is the angular frequency (i.e., $\omega = 2\pi/P$ where P is the period, equal to 365 days) and Δx and Φ are the amplitude and the phase shift of the best-fit sine function, respectively.

The measured indoor and outdoor data were used to fit the annual cycles (Equation (2)) that regulate heat and moisture exchanges across the building envelope on a seasonal basis, obtaining the indoor coefficients, Δx_{in} and Φ_{in}, and the outdoor ones, Δx_{out} and Φ_{out}. The combination of the two sinusoids, i.e., the outdoor T or MR cycles in abscissa and the indoor T or MR cycles in ordinate, gives the annual hysteresis cycle in the building [23]. During the annual cycle, the capability of the building to accumulate or release heat and moisture is an important factor that influences the transfer functions (TFs) and can be expressed in terms of the gain of the building (A_B), defined as the ratio between Δx_{in} and Δx_{out}, and the phase shift (Φ_B), defined as the difference between Φ_{in} and Φ_{out} (Step 2).

Temperature and relative humidity daily data in the area of Valencia for the 30-year time window from 2041 to 2070 (Step 3) were extracted from the ENSEMBLES dataset [28]. The ENSEMBLES simulation model was developed within the ENSEMBLES European project (2004–2009) [37] to produce regional dynamic projections. The high-resolution projections used in this study were generated by the Max Plank Institute for Meteorology using the IPCC emission Scenario A1B [35]. Scenario A1B was developed by the Intergovernmental Panel on Climate Change (IPCC) and was chosen as it is a moderate scenario that assumes higher CO_2 emissions until 2050 and their decrease afterwards. The ENSEMBLES data were used to obtain the fitting coefficients Δx_E and Φ_E from the annual cycles (Equation (2)). To evaluate the effects of the outdoor climate scenario inside the residential building, the future hygrothermal conditions indoors were inversely simulated using derived T and MR transfer functions (Step 4) based on the same sinusoidal equations in Equation (2) with Δx and the Φ calculated using the gain A_B and the phase shift Φ_B of the residential building computed as described in Equations (3) and (4) and with indoor annual mean $\bar{x}$ estimated as described in Equation (5):

$$\Delta x = A_B \cdot \Delta x_E \tag{3}$$

$$\Phi = \Phi_B + \Phi_E \tag{4}$$

$$\bar{x} = \frac{\bar{x}_{in}}{\bar{x}_{out}} \cdot \bar{x}_E = \bar{x}_B \cdot \bar{x}_E \tag{5}$$

where A_B and Φ_B are the gain and the phase shift of the building, respectively; $\bar{x}_E$, Δx_E and Φ_E are the mean, the amplitude and the phase shift of the best-fit sine function calculated from the ENSEMBLES dataset (2041–2070), respectively.

The indoor RH values were computed after the simulated indoor T and MR data by applying the formula in [33]. The T and RH conditions expected in the residential building were finally used to determine the possible changes in the future risk of chemical deterioration for paper in terms of the Lifetime Multiplier index (Step 5).

3. Results and Discussion

The internal response of the microclimate frame to the external forcing of the room was explored by taking into account annual time series of observations of T and RH values collected in two different sites: the first series was registered in the Pio V Museum from 1 June 2014 to 31 May 2015 (hereafter called Museum) and the second from 15 February 2016 to 14 February 2017 in a residential building near Valencia (hereafter called Private).

The box-and-whiskers plots of the T observations (Figure 2a) show that the values inside the microclimate frame fully overlap the room ones in both the sites. The Wilcoxon–Mann–Whitney test was performed for each pair of microclimate frame (MF) and room (R) temperature and relative humidity series, both in Museum and in Private. The test assumes the samples are not normally distributed and the significance level was set to 5%. No significant difference was found between R and MF temperature series collected in the same site ($p > 0.05$); conversely, at both sites, the RH medians inside the microclimate frame significantly diverge from the room ones ($p < 0.0001$). The medians of the rooms are consistent and equal to 22.7 °C in Museum and 22.8 °C in Private; on the contrary, the variability associated to each dataset is significantly different, i.e less than ±2 °C from the median in Museum and ranging from 16.5 °C to 31.0 °C in Private. While internal MF temperatures have the same variability as the external room, the internal RH levels are kept extremely stable throughout the year thanks to the buffering agent preconditioned to RH = 40% before being enclosed within the microclimate frame. The box-and-whiskers plots of RH values (Figure 2b) show a significant difference between the external (R) and internal (MF) distributions of data: in the rooms the range of the RH values registered is roughly between 20% and 60% with RH medians equals to 47%, while in both the sites the internal RH values are tightly kept around 40 ± 3% throughout the year. The few outliers found in the datasets (less than 1% of the total) were not discarded in the following analysis.

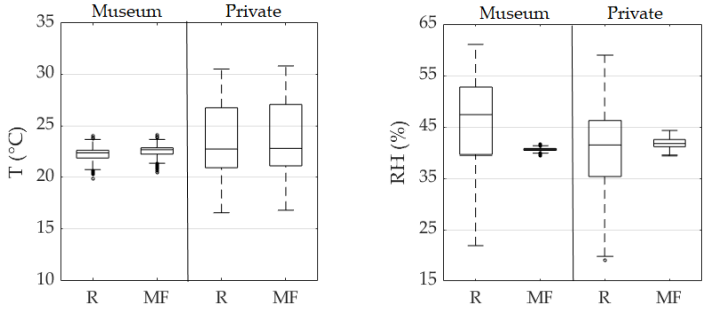

(**a**) Temperature (**b**) Relative humidity

Figure 2. Box-and-whisker plot of temperature (**a**) and relative humidity (**b**) inside the microclimate frame (MF) and in the surrounding room (R) throughout a solar year. Outliers are indicated as points.

The hygrothermal response of the microclimate frame was further explored by comparing their internal conditions to the simultaneous room ones, as shown in the scatterplots in Figure 3. The two indoor environments are thermally controlled by active systems: in Museum, a HVAC system continuously controls temperature maintaining thermal stability with a minimal setpoint adjustment from winter to summer; in Private, an intermittent heating system is active only during the cold season, without any cooling in summer. Both in Museum and in Private, the internal MF temperatures closely follow the surrounding room conditions with a minor delay. In Private, when the heating system is switched off, the internal MF temperatures perfectly match those external, meaning that the thermal cycle is transferred unchanged inside the microclimate frame. The performance of the buffer is examined by relating the internal RH values to the external R temperatures: in Museum, where T is kept almost stable, the considerable RH variability of the room is tightly controlled inside the MF; in Private, as a consequence of the variability of the R temperatures, the internal RH values show a minor drift despite being below significance (Figure 3, lower panels).

Table 2 shows the results of the ASHRAE classification. Both Museum and Private rooms are associated to ASHRAE Class D, which protects only from mold growth with RH $< 75\%$ [17]. The employment of microclimate frame in Museum made it possible to reach Class AA, providing the best possible microclimate for the preventive conservation of the paintings (Table 2); in Private only Class B could be achieved, which however is considered the reference to prevent from mechanical damage [2] as it provides no risk for many artifacts and most books even if a moderate risk for high vulnerability artifacts and paintings remains. Analyzing the T and RH data collected in the Private, the amount of observations overcoming the tolerance bands of Class AA is significantly reduced, passing from 55% of the R values fitting into the required specifications to 90% of the MF ones.

Table 2. Attribution of the ASHRAE class of climate control in the four locations.

ASHRAE Class		
Position	**Museum**	**Private**
Room	D	D
Microclimate frame	AA	B

In Figure 4, the bands of tolerance for ASHRAE Class AA are plotted together with the measured hourly data, better explaining the conditions established inside the microclimate frame in comparison to the surrounding room. Class AA considers a seasonal adjustment of ± 2 °C respect to the annual mean with short-term fluctuations from the seasonal 91-day central moving average smaller than ± 5 °C for temperature and no seasonal adjustment respect to the annual mean of relative humidity with short-term fluctuations below $\pm 5\%$. Both in Museum and in Private, in the room environments,

the observed RH fluctuations reach up to ±20%; however, simultaneous RH values inside the MF are kept reliably around 40%. In Private (Figure 4b), temperatures exceed 30 °C in summer and are occasionally below the lower tolerance band in winter. These values, being transferred inside the microclimate frame, are responsible for the impossibility to achieve ASHRAE Class AA as they are not compatible with conservation.

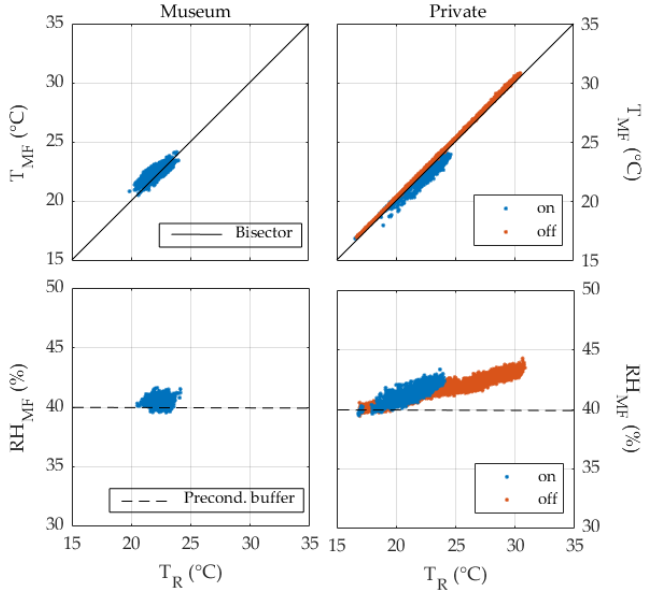

Figure 3. Scatter diagram of simultaneous temperature (T_R) and relative humidity values (RH_R) in the rooms versus values inside the microclimate frame (T_{MF} and RH_{MF}) during a solar year. In Private, the data points are grouped based on whether the intermittent heating system is active (on) or not (off).

The risk of chemical deterioration in the two sites was assessed through the Lifetime Multiplier, as shown in Figure 5. During winter, the LM values associated to both the rooms are higher as a consequence of the considerable drop in RH. However, it has to be highlighted that RH values below 30% may be dangerous for paper conservation (particularly when handling is foreseen) because at low moisture content the flexibility decreases while the brittleness increases [20]. In Museum, where temperature is controlled, an improvement in the duration expectancy of paper objects was observed inside the MF thanks to the buffering in RH values. In Private, the hot summer temperatures account for the almost unchanged average LM values obtained inside the devices. This result is justified by the the greater effect exerted by a drop in temperature on the increase in the life expectancy of an object with respect to the beneficial effect due to an equal drop in relative humidity [36].

The heat and moisture sinusoidal transfer functions in Private were determined as described in Section 2.4. The T and RH data monitored in the residential building were chosen as it is unconditioned for most of the year as well as being the conservation site when the study was conducted. The observations collected during the heating period were discarded in the following analysis. Two sinusoidal equations were fitted to the outdoor data in the area of Valencia [35] and the indoor values monitored in the room. Figure 6 shows the combination of the outdoor T and MR data (i.e., T_{out} and MR_{out}) in abscissa, with the indoor ones (i.e., T_{in} and MR_{in}) in ordinate. The coupled indoor and outdoor sinusoidal fits form the hysteresis cycle during the year. For temperature, it has the shape of an ellipse due to the thermal inertia of the building envelope and the building use and the T phase shift ($\Phi_{B,T}$) is 0.27. For mixing ratio, the yearly cycle is a straight line, meaning that the indoor MR conditions reach a rapid equilibrium with the outdoor ones; indeed, the MR phase shift is

$\Phi_{B,MR} = 0.01$, equal to a delay of about half a day for moisture transfer. It is worth noticing that the results could have been partially affected by the derivation of the transfer functions from the reduced dataset (i.e., including only the period not affected by the heating).

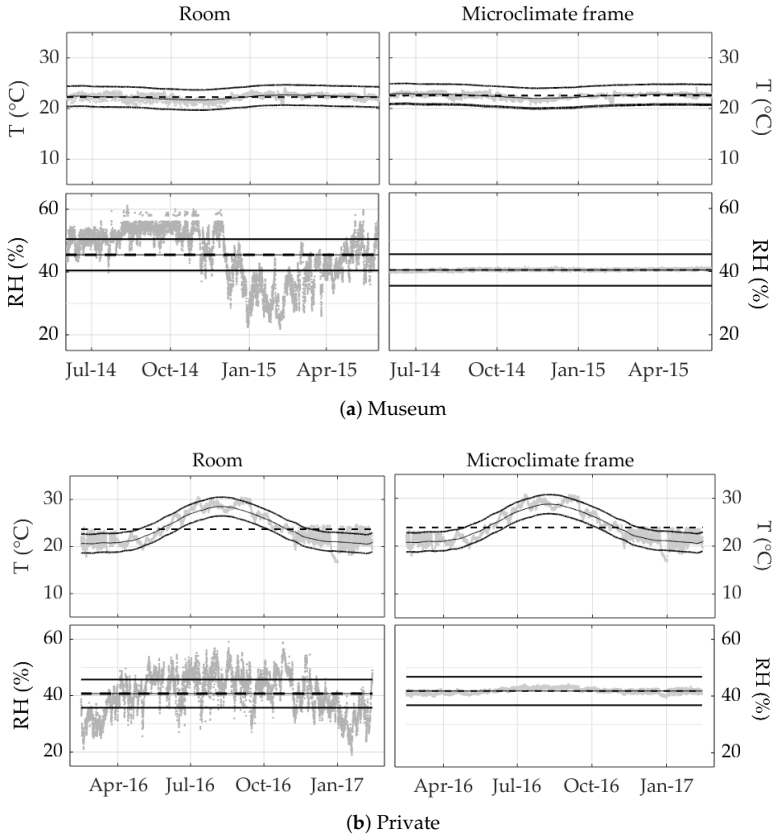

Figure 4. Temperature and relative humidity the bands of tolerance for ASHRAE Class AA (thick lines) together with the values measured in Museum (**a**) and Private (**b**) during a year (grey points). The thin lines indicate the seasonal moving average, the dashed lines the annual mean of the measured values.

The ENSEMBLES scenario for the period 2041–2070 in the area of Valencia forecasts an increase in the outdoor temperature of about +3.5 °C and an increase in the outdoor mixing ratio of about +0.7 g/kg, resulting in an average decrease of 7% in the outdoor RH. The heat and moisture transfer functions allowed simulating the indoor T and MR conditions inside the residential building: in the same 30-year window, the annual average levels are expected to be 27.5 °C for temperature and 37.5% for relative humidity. The potential chemical risk associated to these hygrothermal conditions was assessed through the Lifetime Multiplier values. As shown in Figure 7, the expected change in the indoor climate would lead to augmented chemical risk for cellulose during spring and to improved environmental quality of conservation in autumn. In the hypothesis of the maintenance of the use of the passive microclimate frame with a stable internal RH around 40%, the expected thermal level within the MF would keep the risk of chemical deterioration constant at LM = 1.3, meaning an extended lifetime expectancy for the painting if compared to the standard conditions (T = 20 °C, RH = 50%).

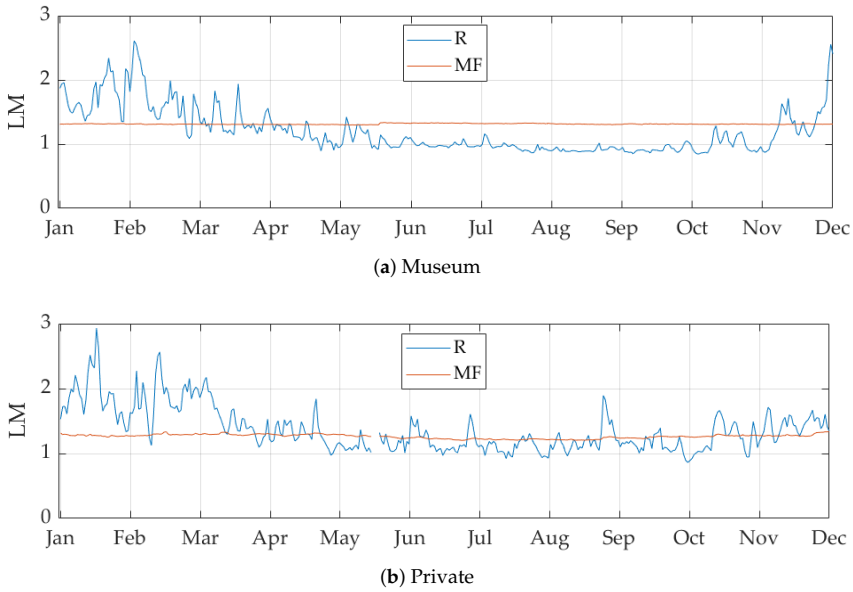

Figure 5. Lifetime Multiplier values (LM) associated to the hygrothermal conditions over a solar year in Museum (**a**) and Private (**b**), in the room (R, blue) and inside the microclimate frame (MF, orange).

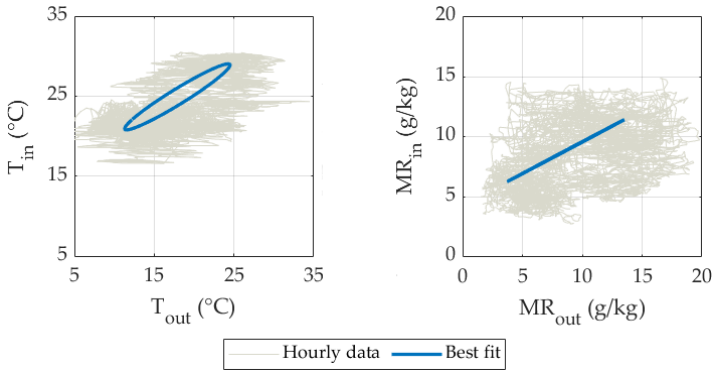

Figure 6. Indoor versus outdoor temperature (**left**) and mixing ratio (**right**) daily data over the solar year monitored (grey dots). The best fit lines (in blue) describe the yearly cycle inside the building.

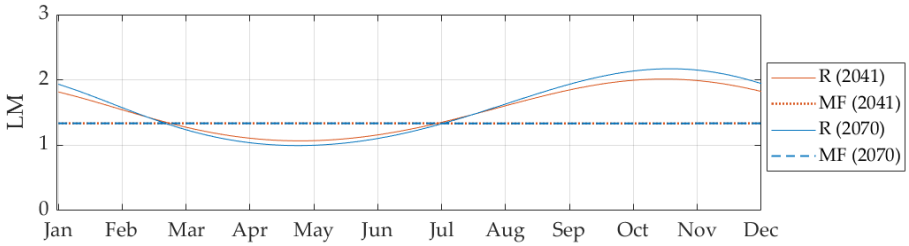

Figure 7. Lifetime Multiplier (LM) associated to the expected climate in Private in 2041 (orange) and 2070 (blue) in the room (R, solid lines) and inside the microclimate frame (MF, dotted/dashed lines).

4. Conclusions

The hygrothermal response of a passive microclimate frame hosting a portrait on cardboard by Sorolla was investigated by analyzing its internal T and RH conditions in response to the surrounding room environment. Its behavior was monitored in two different sites, i.e., the Pio V Museum of Valencia (Museum), with temperatures kept almost stable during the year, and a residential building (Private) in the same area, with a heating system active only in winter. The microclimate frame (MF) proved to be highly effective in controlling the internal RH levels but to be strongly influenced by the boundary thermal variability of the room. The ASHRAE classification of climate quality for conservation pointed out that the hygrothermal conditions in both Museum and Private would have prevented the painting only from the risk of dampness (Class D). On the contrary, within the microclimate frame, since the most dangerous seasonal RH cycles and short-term RH fluctuations were filtered out, the internal MF conditions were found to be compatible with ASHRAE Class B in Private and with ASHRAE Class AA in Museum, ensuring the best possible protection for the artifact. Moreover, the risk of chemical degradation for cellulose was assessed through the Lifetime Multiplier index, which confirmed that the microclimate frame is capable of better mitigating the risks in environments where temperature levels are adequate for conservation (Museum).

To extend our analysis to the application of the microclimate frame in the future, this study showed an example of how the indoor climate can be simulated in unconditioned buildings. In view of the climate ENSEMBLES-A1B scenario for the period 2041–2070 in the area of Valencia, this approach provided insight of the future hygrothermal conditions in Private. Even if the outdoor climate scenario is likely to be beneficial to the conservation of paper indoors in autumn, an increased risk of cellulose degradation would probably be observed during spring. The adoption of passive microclimate frames in the future expected conditions indoors would thus be an effective preventive conservation measure but it is yet important to be aware that these passive enclosures may not be sufficient to fully avoid the chemical degradation risk if an additional mitigation of the unsuitable temperatures is not provided. Considerable improvements on the current and future indoor climate might be provided by implementing some beneficial practices in the management of the environment. For example, the windows' opening might be rescheduled in order to enhance natural ventilation and a cooling device might be helpful to reduce the summer temperature peaks. In addition, passive retrofit intervention on the building envelope may be considered in order to relieve the expected effects of the climate change scenario in a sustainable manner. Notwithstanding the fact that the microclimate frames do not affect the user experience in terms of their overall dimensions and appearance, the adoption of these devices should imply that the ordinary management is adjusted according to their specific features. Indeed, large temperature fluctuations in the surrounding space may cause the absorption/release of considerable amounts of moisture by the buffering agent, determining the possibility of moisture exchanges with the painting itself. This means that it is fundamental to be aware of the effect over moisture exchanges exerted by temperature, which is not controlled within these passive enclosures. Moreover, since buffers are susceptible to ageing and loss of their buffering properties, it is fundamental to recondition and/or replace them on a regular basis in order to preserve their effectiveness.

Author Contributions: All authors helped to develop the manuscript. Conceptualization, Formal analysis and Writing—original draft, E.V. and F.F.; Supervision, Writing—review and editing, A.M.S.; and Resources and Data curation F.-J.G.-D.

Funding: This project received funding from the European Union's Horizon 2020 research and innovation programme under grant agreement No. 814624. This research was partially supported by the Plan Nacionalde I+D, Comisión Interministerial de Ciencia y Tecnología (FEDER-CICYT) under project HAR2013-47895-C2-1-P.

Acknowledgments: The authors thank CollectionCare for the funds for the publication, the Museum Pio V of Valencia, the staff of the IVACOR and the owners of the paintings. E.V. thanks Sapienza Università di Roma for the internship mobility grant.

Conflicts of Interest: The authors declare no conflict of interest. The funders had no role neither in the design of the study, in the collection, analyses, or interpretation of data, nor in the writing of the manuscript or in the decision to publish the results.

Abbreviations

The following abbreviations are used in this manuscript:

AEMET	National Agency of Meteorology of the Spanish Government
ASHRAE	American Society of Heating, Air-Conditioning and Refrigerating Engineers
CO_2	Carbon dioxide
HVAC	Heating, Ventilation and Air-Conditioning
IPCC	Intergovernmental Panel on Climate Change
IVACOR	Valencian Institute of Conservation and Restoration
LM	Lifetime Multiplier
MF	Microclimate Frame
MR	Mixing ratio of humid air (g/kg)
RH	Relative humidity (%)
T	Temperature (°C)
TF	Transfer Function
UPV	Polytechnic University of Valencia

References

1. Camuffo, D. *Microclimate for Cultural Heritage. Conservation, Restoration, and Maintenance of Indoor and Outdoor Monuments*, 2nd ed.; Elsevier: Amsterdam, The Netherlands, 2014; ISBN 9780444632968.
2. Bratasz, Ł. Allowable microclimatic variations in museums and historic buildings: Reviewing the guidelines. In *Climate for Collections: Standards and Uncertainties*; Ashley-Smith, J., Burmester A., Eibl, M., Eds.; Doerner Institut: Munich, Germany, 2013; pp. 11–19.
3. Luciani, A. Evolution of thermo-hygrometric standards. In *Indoor Environment and Preservation Climate Control in Museums and Historic Buildings*; Nardini: Florence, Italy, 2011; ISBN 9788840443393.
4. EN 15999-1:2014. *Conservation of Cultural Heritage - Guidelines for Design of Showcases for Exhibition and Preservation of Objects—Part 1: General Requirements*; European Committee for Standardization: Brussels, Belgium, 2014.
5. Bickersteth, J. IIC and ICOM-CC 2014 declaration on environmental guidelines. *Stud. Conserv.* **2016**, *61*, 12–17. [CrossRef]
6. Perino, M. Air tightness and RH control in museum showcases: Concepts and testing procedures. *J. Cult. Herit.* **2018**, *34*, 277–290. [CrossRef]
7. Shiner, J. Trends in microclimate control of museum display cases. In Proceedings of the Museum Microclimates: Contributions to the Copenhagen Conference, Copenhagen, Denmark, 19–23 November 2007; pp. 19–23.
8. Camuffo, D.; Sturaro, G.; Valentino, A. Showcases: A really effective mean for protecting artworks? *Thermochim. Acta* **2000**, *365*, 65–77. [CrossRef]
9. Bernardi, A.; Becherini, F.; Romero-Sanchez, M.D.; Lopez-Buendia, A.; Vivarelli, A.; Pockelé, L.; De Grandi, S. Evaluation of the effect of phase change materials technology on the thermal stability of Cultural Heritage objects. *J. Cult. Herit.* **2014**, *15*, 470–478. [CrossRef]
10. Dahalin, E. (Ed.) Improved Protection of Paintings during Exhibition, Storage and Transit. In *PROPAINT-Final Activity Report*; Norwegian Institute for Air Research: Kjeller, Norway, 2010.
11. Richard, M. Further Studies on the Benefits of Adding Silica Gel to Microclimate Packages for Panel Paintings. In *Facing the Challenges of Panel Painting Conservation: Trends, Treatments, and Training, Proceedings of the a Symposium at the Getty Centre, Phenix, Los Angeles, CA, USA, 17–18 May 2009*; Getty Conservation: Los Angeles, CA, USA, 2011.
12. Ferreira, C.; de Freitas, V.P.; Ramos, N.M.M. Influence of hygroscopic materials in the stabilization of relative humidity inside museum display cases. *Energy Procedia* **2015**, *78*, 1275–1280. [CrossRef]

13. Thickett, D.; Fletcher, P.; Calver, A.; Lambarth, S. The effect of air tightness on RH buffering and control. In Proceedings of the Museum Microclimates: Contributions to the Copenhagen Conference, Copenhagen, Denmark, 19–23 November 2007; pp. 245–251.
14. Sozzani, L. An economical design for a microclimate vitrine for paintings using the picture frame as the primary housing. *J. Am. Inst. Conserv.* **1997**, *36*, 95–107. [CrossRef]
15. Michalski, S. The ideal climate, risk management, the ASHRAE chapter, proofed fluctuations, and towards a full risk analysis model. In *Experts Roundtable on Sustainable Climate Management Strategies*; Getty Conservation: Los Angeles, CA, USA, 2007; pp. 1–19.
16. EN 15757:2010. *Conservation of Cultural Property—Specifications for Temperature and Relative Humidity to Limit Climate-Induced Mechanical Damage in Organic Hygroscopic Materials*; European Committee for Standardization: Brussels, Belgium, 2010.
17. American Society of Heating, Refrigerating and Air-Conditioning Engineers (ASHRAE). *ASHRAE Handbook—HVAC Applications: Chapter 24—Museums, Galleries, Archives and Libraries*; ASHRAE: Atlanta, GA, USA, 2019.
18. Martens, M. Climate Risk Assessment in Museums: Degradation Risks Determined from Temperature and Relative Humidity Data. Ph.D. Thesis, Eindhoven University of Technology, Eindhoven, The Netherlands, 2012.
19. Huijbregts, Z.; Kramer, R.P.; Martens, M.H.J.; Van Schijndel, A.W.M.; Schellen, H.L. A proposed method to assess the damage risk of future climate change to museum objects in historic buildings. *Build. Environ.* **2012**, *55*, 43–56. [CrossRef]
20. Menart, E.; De Bruin, G.; Strlič, M. Dose–response functions for historic paper. *Polym. Degrad. Stab.* **2011**, *96*, 2029–2039. [CrossRef]
21. Kompatscher, K.; Kramer, R.P.; Ankersmit, B.; Schellen, H.L. Intermittent conditioning of library archives: Microclimate analysis and energy impact. *Build. Environ.* **2018**, *147*, 50–66. [CrossRef]
22. Rajčić, V.; Skender, A.; Damjanović, D. An innovative methodology of assessing the climate change impact on cultural heritage. *Int. J. Archit. Herit.* **2018**, *12*, 21–35. [CrossRef]
23. Bonazzi, A.; Merlo, C.; Campana, F.; Bertolin, C.; Camuffo, D. Past, present and future effects of climate change on a wooden inlay bookcase cabinet: A new methodology inspired by the novel European Standard EN 15757:2010. *J. Cult. Herit.* **2013**, *15*, 26–35. [CrossRef]
24. Bertolin, C.; Camuffo, D.; Bighignoli, I. Past reconstruction and future forecast of domains of indoor relative humidity fluctuations calculated according to EN 15757: 2010. *Energy Build.* **2015**, *102*, 197–206. [CrossRef]
25. CORDIS. CLIMATE FOR CULTURE—Damage Risk Assessment, Economic Impact and Mitigation Strategies for Sustainable Preservation of Cultural Heritage in the Times of Climate Change. Available online: https://cordis.europa.eu/project/rcn/92906/factsheet/en (accessed on 28 June 2019).
26. Leissner, J.; Kilian, R.; Kotova, L.; Jacob, D.; Mikolajewicz, U.; Broström, T.; Ashley-Smith, J.; Schellen, H.L.; Martens, M.; van Schijndel, J.; et al. Climate for Culture: Assessing the impact of climate change on the future indoor climate in historic buildings using simulations. *Herit. Sci.* **2015**, *3*, 38. [CrossRef]
27. García-Diego, F.J.; Verticchio, E.; Beltrán, P.; Siani, A.M. Assessment of the minimum sampling frequency to avoid measurement redundancy in microclimate field surveys in museum buildings. *Sensors* **2016**, *16*, 1291. [CrossRef] [PubMed]
28. AEMET. Climate Projections for the XXI Century: Dynamic Regional Projections Based on the MPI-REMO Model Using the IPCC Emission Scenario A1B. Available online: http://www.aemet.es/es/serviciosclimaticos/cambio$_$climat/datos$_$diarios (accessed on 28 June 2019).
29. Roldán, C.; Juanes, D.; Ferrazza, L.; Carballo, J. Characterization of Sorolla's gouache pigments by means of spectroscopic techniques. *Radiat. Phys. Chem.* **2016**, *119*, 253–263. [CrossRef]
30. IVACOR. Institut Valenciá de Conservació i Restauració de Béns. Dos dibujos de Joaquin Sorolla de la Familia Traver. 2014. Available online: http://www.ivcr.es/media/descargas/monografia-sorolla-familia-traver-w.pdf (accessed on 28 June 2019).
31. Diego, F.J.; Esteban, B.; Merello, P. Design of a hybrid (wired/wireless) acquisition data system for monitoring of cultural heritage physical parameters in smart cities. *Sensors* **2015**, *15*, 7246–7266. [CrossRef] [PubMed]
32. EN 15758:2010. *Conservation of Cultural Property—Procedures and Instruments for Measuring Temperatures of the Air and the Surface of Objects*; European Committee for Standardization: Brussels, Belgium, 2010.

33. EN 16242:2012. *Conservation of Cultural Property – Procedures and Instruments for Measuring Humidity in the Air and Moisture Exchanges Between Air and Cultural Property*; European Committee for Standardization: Brussels, Belgium, 2012.
34. ASTME 104-02. *Standard Practice for Maintaining Constant Relative Humidity by Means of Aqueous Solutions*; ASTM International: West Conshohocken, PA, USA, 2012.
35. Universitat Politècnica de València (UPV). Historical weather observations in Valencia. Available online: http://dataupv.webs.upv.es/datos-historicos-de-la-observacion-meteorologica-en-valencia/ (accessed on 28 June 2019).
36. Michalski, S. Double the life for each five-degree drop, more than double the life for each halving of relative humidity. In Proceedings of the Preprints of the ICOM-CC 13th Triennial Meeting, Rio de Janeiro, Brazil, 22–27 September 2002; James and James (Science Publishers) Ltd.: London, UK, 2002; pp. 66–72.
37. CORDIS. ENSEMBLES-Based Predictions of Climate Changes and Their Impacts. Available online: https://cordis.europa.eu/project/rcn/74001/factsheet/en (accessed on 28 June 2019).

Appendix E

Optimising Conservation of Artworks, Energy Performance and Thermal Comfort Combining Hygrothermal Dynamic Simulation and On-Site Measurements in Historic Buildings

---

Frasca, F., **Verticchio, E.**, Cornaro, C., and Siani, A.M.

IBPSA 2019 Conference (2-4 September 2019) (2019)

Optimising Conservation of Artworks, Energy Performance and Thermal Comfort Combining Hygrothermal Dynamic Simulation and On-Site Measurements in Historic Buildings

Francesca Frasca[1], Elena Verticchio[2], Cristina Cornaro[3], Anna Maria Siani[1]
[1]Department of Physics, Sapienza Università di Roma, Rome, Italy
[2]Department of Earth Sciences, Sapienza Università di Roma, Rome, Italy
[3]Department of Enterprise Engineering, Università degli Studi di Roma "Tor Vergata", Rome, Italy

Abstract

The indoor climate conditions being suitable for the conservation of cultural heritage can be conflicting with energy saving and thermal comfort. Moreover, the moisture dynamics have not been studied enough in the simulation of the indoor environment, even though its interaction with artworks is crucial in deterioration phenomena. This research aims at defining a strategy, based on experimental data and dynamic simulation of hygrothermal behaviour, in order to design a HVAC system able to simultaneously satisfy conservation, thermal comfort and energy requirements. A weighted function for the multi-objective optimization has been proposed and effectively used to pinpoint the combination of temperature and relative humidity set-points.

Introduction

A thorough diagnosis of the interactions between indoor climate and materials is crucial to define efficient climate control strategies for the preventive conservation of Cultural Heritage.

Indoor climate measurements combined with the whole-building dynamic simulation, have been proven effective in the in-depth understanding of the indoor climate and of the object-environment and building-environment interactions (Lucchi et al., 2018). Measurements of temperature and relative humidity allow to investigate the current indoor climate, to understand the on-going deterioration processes, if any, and to define the associated empirical dose-response functions. Dynamic simulation can be employed to plan conservation actions with the aim to reduce the damage risk induced by inadequate temperature and relative humidity conditions. Testing new climate control strategies is particularly important in historic buildings, as it is usually not possible to refurbish the envelope due to their historic value and aesthetic aspect (Mazzarella, 2015). So far, the dynamic simulation of temperature, relative humidity and moisture content within multi-layered building elements (O'Leary et al., 2015) has been mainly carried out to investigate on the effect of humidity on the building materials' durability, the energy consumption and human health (e.g. Barclay et al., 2014; Vereecken et al., 2015; Hansen et al., 2018). On the contrary, few studies have been conducted using the hygrothermal analysis to assess the conservation of materials, such as artworks. A comprehensive overview of the problems and methods in the energy retrofitting of historic/traditional buildings is given by Webb (2017).

The relative humidity plays a key role in all the deterioration phenomena affecting vulnerable hygroscopic materials, such as wood, paper, textile, etc. (Camuffo, 2014). Therefore, simulation models, for humidity cycles and condensation processes, can effectively improve conservation strategies.

The capability to predict the indoor microclimate offers the chance to investigate on integrated solutions that concurrently fulfil different needs. So far, only Schito et al. (2018) have proposed a multi-objective optimisation of the HVAC (Heating Ventilation and Air-Conditioning) system combining the minimisation of the energy cost and the visitors' discomfort with the accomplishment of conservation requirements. In that study, a damage function based on Michalski (2002) was used to prevent the future chemical damage to the collections. Kompatscher et al. (2018) have compared the impact on conservation risks of various climate control strategies recommended by technical standards and guidelines. Neither of the two above studies have focused on the identification of adequate hygrothermal conditions with the aim of mitigating the observed deterioration in the material.

The purpose of this research is to investigate on a possible control climate configuration of the HVAC system using a multi-objective function, which can synthetize conflicting issues in a weighted function. The function is multi-objective as it integrates the concomitant minimisation of the damage risk, the thermal discomfort and the energy consumption in historic buildings.

The hygrothermal analysis was used to thoroughly study the indoor climate by coupling climate measurements and the whole-building dynamic simulation. The latter includes a one-dimensional transfer model of heat air and moisture across opaque components in order to accurately simulate the hygrometric response of the environment over time.

The mechanical risk assessment of the wooden artefacts was based on an empirical dose-response relationship derived from experimental data on climate-induced cracks observed on the objects.

The proposed methodology was applied to the Archaeological Museum of Priverno with the aim to test

https://doi.org/10.26868/25222708.2019.210423

the summer climate control strategy. The preliminary results are presented and discussed in this paper.

The case study

This paper concerns with the Archaeological Museum of Priverno (Lat. 41.5° and Long. 13.2°), housed in a three-floored historic building (13th century) located at about 70 km SE far from Rome (Italy). The building is oriented in the SW-NE direction with respect to the main entrance and consists of thirteen exhibition rooms and three other rooms (the total number of zones is sixteen) deployed between the first and second floor, with an internal courtyard and a terrace in the north-west side. A HVAC system only for temperature control is turned on during the opening hours by staff from November till April (heating) and from June till August (cooling). However, low temperatures in winter and unpleasant warm temperatures in summer are often experienced indoors by visitors and staff. This site preserves valuable wooden ceilings decorated with oil paintings and a collection of sculptures, jewellery and pottery excavated in the close archaeological area. The wooden ceilings were restored in 2012 as they suffered mechanical degradation (i.e. swelling and shrinkage due to moisture absorption and desorption) visible in terms of panels' deformations, detachments of the painted-layer and cracks along the tangential direction of wood panels (Figure 1). However, since cracks and deformations have been visible, they were monitored over the period of this study.

Figure 1: Detail of the wooden ceiling decorated with oil paintings on the second floor (picture taken in 2016). Cracks are visible along the tangential direction of wood panels.

For the above purpose, a monitoring campaign of indoor and outdoor climate and of crack-width in the wooden ceiling was conducted for 15-months (August 2016 – November 2017).

A preliminary analysis, based on the dynamic simulation of the building and the HVAC system, has shown that switching from the current setting to a continue temperature control over the year would improve visitors' comfort and reduce the occurrences of seasonal and daily crack-width fluctuations (i.e. stress-and-strain cycles). Nevertheless, it was found that due to the absence of control over RH the allowable T-RH limits suggested by the American guidelines ASHRAE 2011 for the conservation of artworks were not met (Frasca et al., 2019).

Therefore, a HVAC system equipped with a humidity control device was proposed to further reduce mechanical degradation risks.

Methods

The research was conducted using both on-site measurements and whole-building dynamic simulation. The workflow of the research can be schematised in three steps as shown in Figure 2:

1. the derivation of a empirical dose-response relationship from long-term measurements of indoor climate and identification of the degradation marker;
2. the hygrothermal assessment through the whole building dynamic simulation;
3. the definition of a single-weighted function for the multi-objective optimization of the indoor climate combining artworks' conservation needs, the energy saving and the thermal comfort.

The monitoring campaign of the indoor climate and the damage marker

The monitoring campaign of the main indoor climate variables was carried out from August 2016 to November 2017. The measurement system in room 9 consisted of two temperature (T) and relative humidity (RH) probes, an air-surface thermometer (T_s) and a crack-width (C) meter installed on a panel of the wooden ceiling. Other two T-RH probes were installed in room 4 and 10 with the aim to characterise the microclimate in different sites of the building. Moreover, a T-RH probe was placed outside in order to study the influence of outdoor climate on the indoors and to build a custom weather file to be used in the simulation environment.

The list of sensors and their technical features are reported in Table 1. The metrological features of T and RH sensors are in accordance with the uncertainties suggested by the European standards EN 15758:2010 and EN 16242:2012.

Table 1: The technical features of sensors used within the monitoring campaign.

	T	RH	T_s	C
Sensor	Resistance Pt100 1/3 DIN	Film capacitor Rotronic C94	Thermistor NTC	Potentiometer in conductive plastic
Operating range	-40 °C to +60 °C	0 to 100 %	-30 °C to +150 °C	10 mm
Uncertainty	±0.3 °C	+1.5 %	±0.1 °C	+0.025 mm

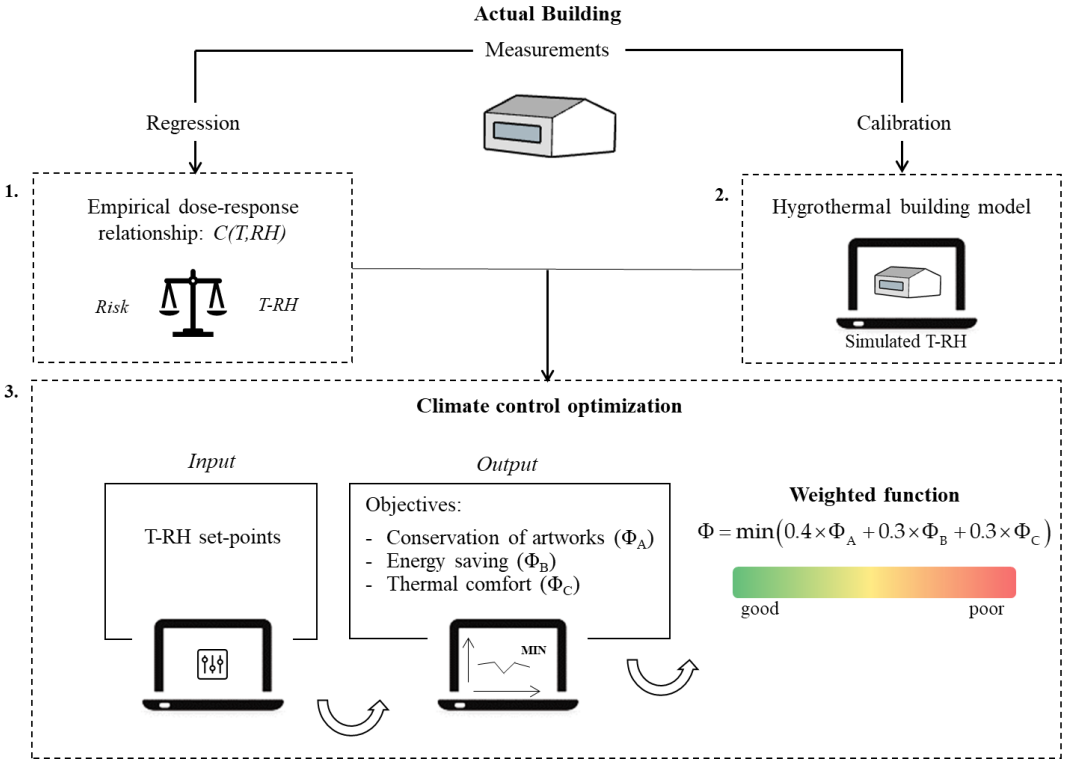

Figure 2: Schematic flow chart of the multi-objective optimization proposed in this paper.

The parameter C was used as damage marker for the mechanical degradation of the wooden ceilings. An empirical dose-response relationship was derived from a production function based on a non-linear multiple regression between the modelled crack (C_m) behaviour and the hygrothermal conditions at the air-surface interfaces:

$$C_m = a \times RH_s^b \times T_s^c \quad (1)$$

where a = 6.5 mm×(100^{-b})×($°C^{-c}$), b = -5.4×10^{-2} and c = -4.0×10^{-5}. RH_s is the relative humidity at the interface between the surface and the air layer computed from mixing ratio (MR) of moist air and surface temperature (T_s). MR was calculated from T and RH readings using the equation reported in the EN 16242:2012 and taking into account the standard value of the atmospheric pressure (1013 hPa).

The uncertainty associated to the derived variables (MR and RH_s) was estimated by applying the propagation of error (Cohen, 1998) based on the uncertainties of experimental measurements. The MR uncertainty was 0.3 g/kg, computed from T and RH uncertainties; the uncertainty of RH_s was 4.6 % derived from the MR uncertainty and the air-surface thermometer uncertainty. Finally, the uncertainty of C_m was 0.024 mm, calculated from T_s and RH_s uncertainties.

The coefficient of determination (R^2) was 0.89, showing the goodness of C_m fit on the experimental C data; the root-mean-square-error (RMSE) was 0.014 mm, i.e. less than the uncertainty of the crack-width meter.

The simulation environment

Dynamic building simulation of the indoor climate was performed using the IDA Indoor Climate and Energy 4.8 (IDA ICE) developed and distributed by EQUA simulation AB. For the modelling of room 9, IDA ICE was extended with the HMWall model, that implements a one-dimensional heat air and moisture transfer model across porous materials. The HMWall model was meticulously tested by the authors using exercises at increasing complexity and the preliminary results are reported in (Frasca et al., 2018).

Our purpose was to calibrate the building envelope when the HVAC system was not in operation. Thus, the calibration was performed in May and the validation procedures were carried out in September/October. Since the thresholds of the statistical parameters for the calibration with hourly T-RH data were not available in the literature, the uncertainty of T-RH measurements was assumed as rejection criteria. The closer is the parameter to the sensor uncertainty, the better the building model reproduces the actual building. The calibration procedure consisted of:

- a first automatic step for the thermal behaviour of the whole building model;
- a second manual step integrating the moisture transport across the walls (HMWall) of room 9.

The geometry of the building model of the Museum was created starting from the architectural survey and using a wall composition comparable to the construction techniques used in lower Latium in the Middle Age. The wall composition was assumed to be unchanged over time except for the ceilings. The building model included sixteen zones but only room 9 (Figure 3) was considered for the hygrothermal assessment with the HMWall model.

The weather file used to run the model was created from outdoor T and RH values measured outside the building. The weather file also included global horizontal solar irradiance and wind speed and direction measured at the ARSIAL (Agenzia Regionale per lo Sviluppo e l'Innovazione dell'Agricoltura del Lazio) meteorological station in Maenza (Lat. 41.5° and Long. 13.2°).

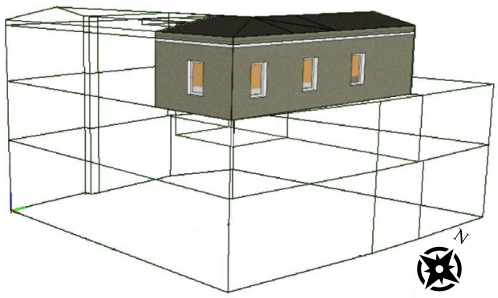

Figure 3: 3D model of the room 9 sketched in IDA ICE.

The automatic calibration of the whole building was carried out to fine-tune the input parameters of the envelope, such as the wall thermal transmittance (U-value), thermal bridges and the infiltration rate, which were unknown. The Sensitivity Analysis (SA) based on the Elementary Effect method (EEs) demonstrated that thermal bridges and infiltration highly affected modelled T and RH data. Then, the Particle Swarm Optimization – General Pattern Search of Hooke-Jeeves (PSO-GPSHJ) genetic algorithm, implemented by GenOpt®, was used to minimise the RMSE between modelled and measured indoor climate data. The PSO-GPSHJ is a hybrid algorithm, that combines a global search method (PSO) with a local search method (GPSHJ). The Parametric Run extension was used to communicate GenOpt® with IDA ICE. A RMSE of 0.4 °C for T and of 2.0 % for RH was found.

The second step of calibration was manually performed on room 9 to fine-tune the hygrothermal properties of opaque components, such as the thermal conductivity (λ), the equilibrium water content at 80 % of relative humidity (w_{80}) and the water absorption coefficient (A_w). Table 2 summarises the main statistic parameters about the calibration and validation performed to model room 9.

It was found that room 9 is well calibrated with the following features:

- a floor area of 62 m^2 and a volume area of 185 m^3;
- three external walls of 0.6 m;
- a thermal transmittance (U-value) of 1.4 W m^{-2} K^{-1};
- an adiabatic internal wall of 0.6 m with a U-value of 1.1 W m^{-2} K^{-1};
- an adiabatic floor with a U-value of 2.7 W m^{-2} K^{-1};
- an internal wooden ceiling of 0.08 m with a U-value of 3.5 W m^{-2} K^{-1};
- thermal bridges higher than 0.5 W m^{-1} K^{-1};
- a fixed infiltration at 0.02 ACH;
- a glazing system with wooden-framed low-emission double panes (6-12-6 mm filled with air) characterised by a U-value of 1.6 W m^{-2} K^{-1} and a solar heat gain coefficient (SHGC) of 0.4. All windows have an area of 1.5 m^2 and are covered by black interior roller shades.

The internal opaque components were modelled assuming to be in dynamic equilibrium with air at RH = 50 % (adjacent room) and RH = 55 % (crawl space).

Table 2: Summary of the calibration and validation statistics of air temperature (T) and relative humidity (RH) in room 9. MAE = mean absolute error; RMSE = root mean square error; CV-RMSE = coefficient of variation of RMSE with respect to the average; r_s = Spearman's rank correlation coefficient.

	Calibration			
	MAE	*RMSE*	*CV-RMSE*	r_s
T	0.2 °C	0.3 °C	1.2 %	1.0
RH	0.8 %	1.0 %	2.0 %	0.9
	Validation			
	MAE	*RMSE*	*CV-RMSE*	r_s
T	0.2 °C	0.3 °C	1.2 %	1.0
RH	1.0 %	1.2 %	2.4 %	0.7

The multi-objective optimization

The optimization aimed at finding the T and RH set-points of a generic HVAC system able to control both the parameters in summertime. July was chosen as the summer reference month, when the artwork preservation, the energy saving and the human comfort may be strongly conflicting (Schito et al., 2018).

Three specific quantities were defined in order to estimate the quality of the environment in terms of conservation needs (Φ_A), energy consumptions (Φ_B) and thermal comfort of people (Φ_C).

$$\Phi_A = \frac{\sum(\Delta C > \Delta C_{risk})}{N_d} \quad (2)$$

$$\Phi_B = \frac{\int_0^t Q(t)\,dt}{\int_0^t Q_{max}(t)\,dt} \quad (3)$$

$$\Phi_C = \frac{PDH}{h_{occ} \times n_{occ}} = \frac{PDD \times h_{occ} \times n_{occ}}{h_{occ} \times n_{occ}} \quad (4)$$

Φ_A (Eq. 2) takes into account Eq. 1 to evaluate the daily stress-and-strain cycle of the wooden ceiling. Φ_A is defined as the ratio between the occurrences of the maximum daily span of C ($\Delta C = C_{max} - C_{min}$) exceeding ΔC_{risk} (= 0.03 mm) and the total number of days (N_d) under study. Since the stress-and-strain cycle is cumulative, ΔC_{risk} was defined so that the maximum daily fluctuations of C were kept at the minimum, assumed close to the sensor's uncertainty. This meant that Φ_A is

zero when ΔC is less than ΔC_{risk} over N_d and is equal to unity when ΔC is always higher than ΔC_{risk}.

Φ_B (Eq. 3) is the ratio between the total energy consumption (Q, i.e. sum of both heating and cooling demands) and the maximum total energy consumption (Q_{max}, estimated as the nominal power of the system multiplied by the total number of hours under study). It is zero when the system is always turned off and is equal to the unity when it is always turned on at the maximum power.

Φ_C (Eq. 4) is the predicted total amount of discomfort hours (PDH), computed as the product among PPD (Percentage of Person Dissatisfied), the number of occupants (n_{occ}) and the occupancy hours (h_{occ}). Ten visitors were considered during the opening hours (10-13 and 14-18) from Wednesday till Sunday (about 22 days in July). The metabolic activity value was set to 1.5 MET, i.e. equivalent to 87 W m^{-2} and corresponding to a standing-walking activity (EN 15251:2007); whereas, the clothing factor was set to 0.5 clo (~ 0.08 m^2 K W^{-1}). Φ_C is zero when PDH = 0 h and is equal to unity when the discomfort is always experienced, i.e. PDH = 1540 h.

The three quantities were linearly combined in a weighted function Φ (Eq. 5) so that limits range between 0 (best-compromise solution) and 1 (worst-compromise solution).

$$\Phi = min(0.4 \times \Phi_A + 0.3 \times \Phi_B + 0.3 \times \Phi_C) \quad (5)$$

The highest coefficient was given to Φ_A in order to assign priority to conservation as recommended by the Italian Legislative Decree 192/2005 for historic buildings. Nevertheless, the weights were chosen to keep significant the contribution of Φ_B and Φ_c to the final score.

The control strategies for T and RH were defined in order to combine different T and RH set-points, by running a total of 30 simulations. T and RH set-points were selected starting from the recommendations given by the American guidelines ASHRAE (2011). T set-points ranged from 21 °C to 26 °C at step of 1 °C; whereas RH set-points ranged from 40 % to 60 % at step of 5 %. The HVAC system was modelled with the following components: an economizer, a pre-heating coil, an adiabatic evaporative humidifier, a cooling coil, a post-heating coil and exhaust/supply fans. The economizer was introduced to mix fresh (outdoor) and exhaust (indoor) air depending on the carbon dioxide (CO_2) concentration with the aim of guaranteeing an acceptable indoor air quality (CO_2 < 1000 ppm). The system was set with a variable air volume (VAV) to adjust the airflow depending on the actual T-RH condition and their distance from the selected set-points within ±1 °C and ±5 % tolerances. The minimum and maximum values of airflows ranged between 55 litres/s and 431 litres/s. This allowed both to limit energy consumption and to not turn off the system, avoiding any abrupt change in the indoor climate related to the system on/off. The nominal power of the HVAC system was set to 20 kW per day.

Results and discussion

The three quantities (Eqs. 2-4) were calculated from the outcomes of 30 simulations in July, as shown in Figure 4 by using carpet plots based on a colour code scale, from green (best condition) to red (worst condition). It can be noticed that the green conditions are experienced for each quantity in different T-RH set-points, so that an adequate compromise among them is not trivial to be found.

Φ_A is equal to zero when the RH set-point is 45 % and the T set-point is below 24 °C, meaning that ΔC values are less than ΔC_{risk}. Besides, low Φ_A values occur when the RH set-point is 40 % or above 55 % for the T set-point > 23 °C. This confirms the importance of controlling both T-RH parameters when the risk of conservation is one of the objectives of the retrofitting or the climate control strategy.

Φ_B is green when the T set-point is closer to the outdoor thermal conditions. The minimum delivered energy of 890 kWh occurs at set-points T = 26 °C and RH = 55 %; whereas the maximum delivered energy of 4500 kWh is found at set-points T = 21 °C and RH = 40 %. In this case, the energy demands are mainly driven by T set-points.

Green Φ_C values related to the thermal comfort occur when the T set-point is less than 23 °C, in accordance with the European standard EN 15251:2007. Indeed, the PDH value is less than 15 h out of a total of 154 h of occupancy per person. The PDH value is tripled up to 46 h per person when the T set-point exceeds 25 °C.

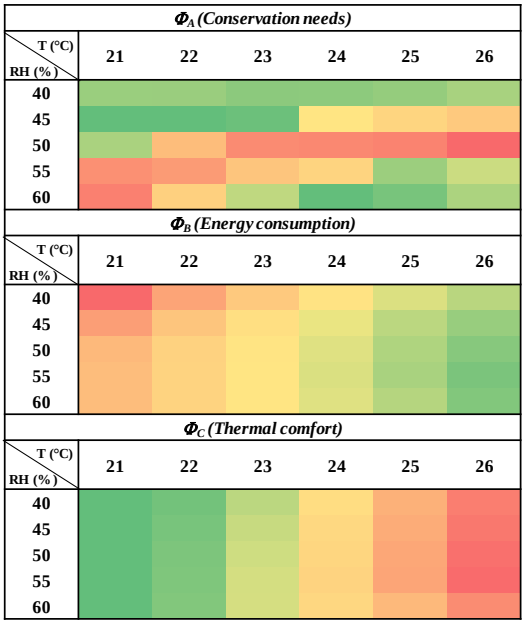

Figure 4: Carpet plots of the three quantities used as objectives for the optimization of the T-RH set-points in the HVAC system. The colour code scale ranges between the minimum (green) and the maximum (red) values.

At this point, the weighted function Φ (Eq. 5) helps to find a compromise among these conflicting needs and, hence, to design a possible climate control strategy by means of the HVAC system. Figure 5 shows the carpet plot for Φ outcomes also including the percentage values. The best-

compromise solutions are found when the T set-point is 22 or 23 °C and the RH set-point is 45 % or when set-point are T = 24 °C and RH = 60 %. On the contrary, the worst case is associated to T set-point of 26 °C and RH set-point of 50 %. It is worth to notice that Φ exceeds 25 % when Φ_A is maximum in conjunction with higher values of Φ_B or Φ_C.

Φ (Weighted function)						
T (°C) / RH (%)	21	22	23	24	25	26
40	14%	12%	10%	10%	12%	15%
45	8%	7%	7%	18%	22%	26%
50	12%	23%	31%	32%	34%	40%
55	30%	28%	22%	21%	13%	18%
60	33%	20%	12%	7%	9%	14%

Figure 5: Carpet plots of the weighted function (Eq. 5) used for the optimization of the T-RH set-points in the HVAC system. The colour code scale ranges between the best-compromise solution (green) and the worst-compromise solution (red). The values are reported on the plot as percentages.

The maximum daily span of the simulated T-RH and C were calculated as the difference between the maximum and minimum value of the day (i.e. ΔT, ΔRH and ΔC, respectively) and are shown in Figure 6.

In the worst-compromise solution (Φ = 40 %), ΔC is on average slightly higher than ΔC_{risk}, even though indoor T-RH values are within the tolerable limits of the HVAC system (26 ± 1 °C and 50 ± 5 %) and the daily spans are less than 2 °C and 6 %, respectively (Figure 6a). These hygrothermal conditions might be very risky for the conservation of the wooden ceiling, because the HVAC system introduces daily T-RH fluctuations to handle with the set-points. The response to the stress-and-strain cycle is a cumulative process and, although small, might induce an irreversible damage.

In the best configuration (Φ = 7 %), ΔC is always less 0.02 mm because indoor T-RH daily spans are less than 0.6 °C and 4 % over the period, respectively (Figure 6b). Here, the delivered energy is 2500 kWh and the PDH is 9 h per person.

Finally, ΔC calculated from the two selected T-RH scenarios (Φ_{max} = 40 % and Φ_{min} = 7 %) were compared with the measured ΔC in order to assess the effectiveness of the new climate control configurations. Figure 7 shows the ΔC values as box-and-whiskers plots and the ΔC_{risk} threshold as dashed horizontal line. In the current hygrothermal conditions (blue box), the maximum ΔC value is 0.04 mm, i.e. slightly above ΔC_{risk}. The hypothesised climate control system would result to be riskier when Φ_{max} is 40 % (red box), as the average behaviour of the modelled ΔC is significantly higher than that of the measured ΔC. On the contrary, when the Φ target reaches the minimum (green box), the modelled ΔC values show an improvement. This hypothesis shows that the average behaviour of ΔC is less than 0.01 mm, suggesting that cumulative mechanical degradation processes have been potentially reduced.

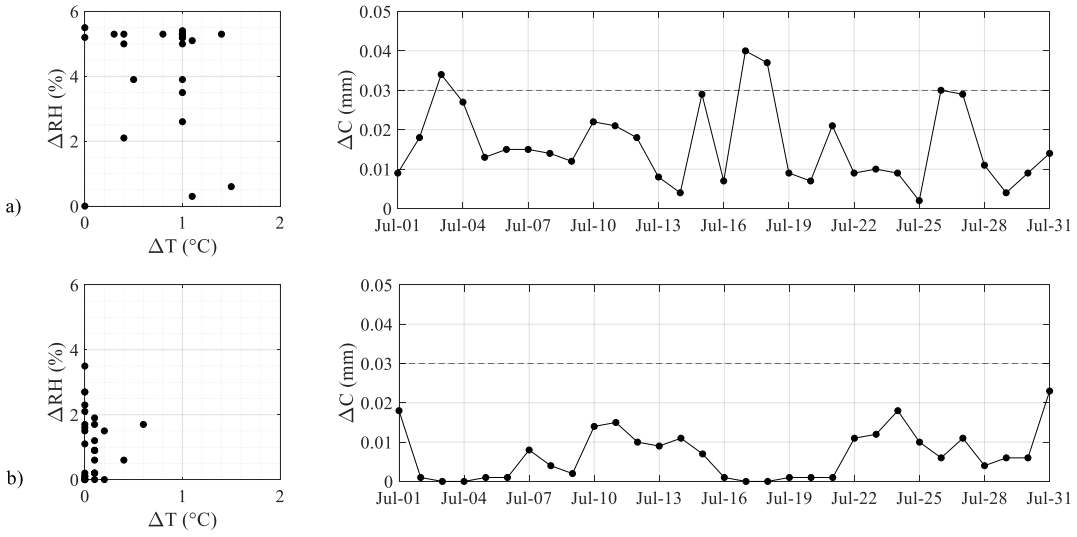

Figure 6: Scatter plot of the maximum daily spans (ΔRH vs ΔT) of simulated T and RH and temporal behaviour of the maximum spans of cracks (ΔC): a) the worst-compromise solution of the weighted function (Φ = 40 %) and b) the best-compromise solution (Φ = 7 %).

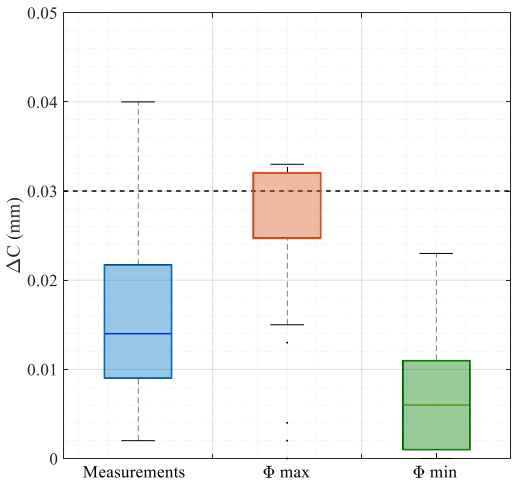

Figure 7: Box-and-whiskers plots of the daily fluctuations of cracks (ΔC): measurements (blue), the maximum of the weighted function Φ max (red) and the minimum of weighted function Φ min (green). The dashed line is the ΔC_{risk} threshold (0.03 mm).

Conclusions

For the first time, a multi-objective optimization of a HVAC system within a historic building has been carried out by combining dynamic simulation with measurements of indoor climate parameters, and the damage marker of the wooden ceilings. In this study, the whole-building dynamic simulation software IDA ICE has the advantage to be integrated with a one-dimensional heat and moisture transfer model, the HMWall model, in order to thouroughly simulate the indoor moisture dynamics.

A weighted function (Φ) has been proposed and tested to identify an appropriate compromise solution between conservation of artworks, energy saving and thermal comfort requirements by comparing different combinations of temperature and relative humidity set-points. These preliminary outcomes support the importance to carefully choose the T-RH set-points. Even though the current hygrothermal conditions seem to not be risky for the conservation of the wooden ceiling, the proposed weighted function Φ has pinpointed a HVAC configuration able to further reduce the conservation risk along with the energy saving and the thermal comfort of visitors.

The methodology can be effective only if a thorough knowledge of the indoor climate and its interaction with the objects is reached. Even if the method has been applied to a specific case study, the Archaeological Museum of Priverno (Italy), it can be potentially exploited for other sites in which also other types of degradation are experienced providing that an empirical does-response relationship is available or can be derived from experimental data.

Acknowledgement

We thank Sapienza University of Rome for funding the multidisciplinary project “Preservation, conservation and valorisation of archaeological sites: The case of the ancient site Privernum”. This research has been carried out within the “Renovation of existing buildings in NZEB vision (nearly Zero Energy Buildings)” Project of National Interest (Progetto di Ricerca di Interesse Nazionale - PRIN) funded by the Italian Ministry of Education, Universities and Research (MIUR).

References

ASHRAE (2011) ASHRAE handbook — HVAC applications. Chapter 23: Museums, galleries, archives, and libraries. American Society of Heating, Refrigerating and Air-Conditioning Engineers, Inc., Atlanta

Barclay, M., Holcroft, N., Shea, A.D. (2014). Methods to determine whole building hygrothermal performance of hemp–lime buildings. *Building and environment 80*, 204-212.

Camuffo D. (2014). *Microclimate for Cultural Heritage-Conservation, Restoration, and Maintenance of Indoor and Outdoor Monuments*. Elsevier. Amsterdam (NL).

Cohen, E.R. (1998). *An introduction to error analysis: The study of uncertainties in physical measurements*. IOP Publishing.

European Committee for Standardization (2007). *Indoor environmental input parameters for design and assessment of energy performance of buildings addressing indoor air quality, thermal environment, lighting and acoustics (EN 15251:2007).*

European Committee for Standardization (2010). *Conservation of cultural property—procedures and instruments for measuring temperatures of the air and the surfaces of objects (EN 15758:2010).*

European Committee for Standardization (2012). *Conservation of cultural property—procedures and instruments for measuring humidity in the air and moisture exchanges between air and cultural property (EN 16242:2012).*

Frasca F., Cornaro C., Siani A.M. (2018). Performance assessment of a heat and moisture dynamic simulation model in IDA ICE by the comparison with WUFI Plus. *IOP Conference Series: Materials Science and Engineering 364*, 012024. Florence (IT), 16-18 May 2018.

Frasca, F., Cornaro, C., Siani, A.M. (2019). A method based on environmental monitoring and building dynamic simulation to assess indoor climate control strategies in the preventive conservation within historical buildings. *Science and Technology for the Built Environment 25(9)*, 1253-1268.

Hansen, T.K., Bjarløv S., Peuhkuri R.H., Harrestrup M. (2018). Long term in situ measurements of

hygrothermal conditions at critical points in four cases of internally insulated historic solid masonry walls. *Energy and Buildings 172*, 235-248.

Kramer R., van Schijndel J., Schellen H. (2017). Dynamic setpoint control for museum indoor climate conditioning integrating collection and comfort requirements: Development and energy impact for Europe. *Building and Environment 118*, 14-31.

Kompatscher, K., Kramer, R.P., Ankersmit, B., Schellen, H.L. (2019). Intermittent conditioning of library archives: Microclimate analysis and energy impact. Building and Environment, 147, 50-66.

Legislative Decree 192/2005. *Attuazione della direttiva 2002/91/CE relativa al rendimento energetico nell'edilizia* pubblicato nella Gazzetta Ufficiale n. 222 del 23 settembre 2005 - Supplemento Ordinario n. 158.

Lucchi, E. (2018). Review of preventive conservation in museum buildings. *Journal of Cultural Heritage 29*, 180-193.

Martens, M.H.J. (2012) *Climate risk assessment in museums: degradation risks determined from temperature and relative humidity data.* Doctoral dissertation. Technische Universiteit Eindhoven. Eindhoven (NL).

Mazzarella L. (2015). Energy retrofit of historic and existing buildings: the legislative and regulatory point of view. *Energy and Buildings 95*, 23-31.

Michalski, S. (2002). Double the life for each five-degree drop, more than double the life for each halving of relative humidity. In *Preprints of 13th Meeting of ICOM-CC* (pp. 66-72).

O'Leary, T.P., Menzies, G., Duffy, A. (2015). The design of a modelling, monitoring and validation method for a solid wall structure. *Energy Procedia 78*, 243-248.

Schito, E., Conti, P. and Testi, D. (2018). Multi-objective optimization of microclimate in museums for concurrent reduction of energy needs, visitors' discomfort and artwork preservation risks. *Applied Energy 224*, pp.147-159.

Webb, A.L. (2017). Energy retrofits in historic and traditional buildings: A review of problems and methods. *Renewable and Sustainable Energy Reviews 77*, 748-759.

Vereecken E., Van Gelder L., Janssen, H., Roels S. (2015). Interior insulation for wall retrofitting - A probabilistic analysis of energy savings and hygrothermal risks. *Energy and Buildings 89*, 231-244.

Appendix F

Conservation risks for paper collections due to the microclimate in the repository of the Alessandrina Library in Rome (Italy)

Verticchio, E., Frasca, F., Cavalieri, P., Teodonio, L., Fugaro, D., and Siani, A.M.

Under review

Research article

Conservation risks for paper collections induced by the microclimate in the repository of the Alessandrina Library in Rome (Italy)

Elena Verticchio [1,*], Francesca Frasca [2], Patrizia Cavalieri [3], Lorenzo Teodonio [3], Daniela Fugaro [4] and Anna Maria Siani [2]

[1] Department of Earth Sciences, Sapienza Università di Roma, P.le A. Moro 5, 00185 Rome, Italy;
[2] Department of Physics, Sapienza Università di Roma, P.le A. Moro 5, 00185 Rome, Italy;
F.F. f.frasca@uniroma1.it; A.M. annamaria.siani@uniroma1.it
[3] Istituto Centrale per la Patologia degli Archivi e del Libro ,Via Milano 76, 00184, Rome, Italy;
P.C. patrizia.cavalieri@beniculturali.it; L.T. lorenzo.teodonio@beniculturali.it
[4] Biblioteca Universitaria Alessandrina, P.le A. Moro 5, 00185 Rome, Italy; daniela.fugaro@beniculturali.it
* Correspondence: elena.verticchio@uniroma1.it Tel.: +39-06-4991-3479

Abstract: The Alessandrina Library, founded in 1667 by pope Alexander VII Chigi and nowadays hosted in the Campus of Sapienza University of Rome (Italy), contains more than one million volumes. In 2019, six thermo-hygrometers were installed in its multi-storey repository to monitor temperature (T) and relative humidity (RH). The collected T and RH data allowed us to evaluate thermo-hygrometric spatial and temporal distributions and carry out a comprehensive climate-induced risk assessment considering mechanical, chemical and biological deterioration mechanisms. The possible departure of RH from the "historical climate" tolerance band was investigated to suggest indications to avoid mechanical stress in case of loans, relocation and consultation. The Time Weighted Expected Lifetime (TWEL) index was used to evaluate the chemical risk for different paper-based collections as a function of their intrinsic vulnerability (i.e., acidity and degree of polymerisation) and considering the typical response time of paper books to T and RH changes. Finally, the biological threats were estimated by using Sedlbauer curves and the Brimblecombe model for potential insect egg production. Measurements of colour change on selected book covers were also performed to evaluate the photo-deterioration rate over a year.

Keywords: Microclimate monitoring; historic library repository; paper collections; risk assessment; preventive conservation.

1. Introduction

The durability of library collections can be threatened by deterioration processes driven by the environmental conditions in which they are preserved. Hence, the management strategies for preserving historical libraries must entail the mitigation of climate-induced deterioration risks. Although digitisation of the collections can reduce to a certain extent the risks due to handling [1], it is however pivotal to guarantee the material preservation of historic libraries, as they are non-renewable resources from our past. The assessment of the climate-induced risks allows an objective evaluation of the deterioration risks, with a view to planning tailored preventive conservation actions [2].

Library collections are made of a wide range of hygroscopic organic materials (e.g., paper, leather, parchment, cloth), which are climate-sensitive and, therefore, vulnerable to deterioration. As the hygroscopic materials continuously exchange moisture with the air, the time needed for them to reach equilibrium with the environmental temperature and humidity changes (i.e., their response time) must be considered while performing the climate-induced risk assessment. In the case of paper materials, attention should be paid to moisture exchanges both in small boxes (e.g., in microclimate frames [3]) and inside libraries [4,5].

Paper is usually the most widely occurring material in libraries in the Mediterranean region, as it has been extensively used since its diffusion from the XI-XII century [6]. Paper typically contains cellulose, a natural polymer forming long chains (i.e., fibres) and can be classified into three main types —rag, acidic and contemporary— as a function of their different acidity (pH) and degree of polymerisation (DP). Rag paper is a high-quality paper made from cotton (originally from cotton rags and nowadays from cotton linters) characterised, on average, by pH = 6.4 and DP = 1481.2 [7,8]. Acidic machine-made paper (produced from the XIX century due to the growing demand for printing media) is a poor-quality paper with short wood fibres and usually containing lignin and acidic chemicals, with an average pH = 5.2 and DP = 826.3 [7,8]. Contemporary paper is made from highly processed wood pulp with alkaline reserves, with average pH = 7.6 and DP = 1526.2 [7,8].

The principal risks affecting the durability of library collections include mechanical, chemical, biological and photodeterioration mechanisms. Several recent studies, summarised in [9], have investigated the microclimate data collected in libraries considering various standards and guidelines for heritage conservation, as well as using different methods to assess the deterioration risks.

Mechanical risk

Library materials can shrink/swell as they lose/gain moisture. Temperature and relative humidity fluctuations (being mechanical stressors) might induce differential dimensional changes in library objects, leading to tensile stresses [10] in tightly and/or layered bound objects [11]. Handling is frequently responsible for the accumulation of wear and tear on paper [12], thus reducing the durability of the collections [13].

Chemical risk

Cellulose hydrolysis is among the main climate-induced risks for paper collections. This mechanism is largely driven by temperature and is usually estimated by using dose-response functions [14] [15]. Strlič *et al.* [13] derived the isochrones for historic paper (i.e., curves of equal expected lifetime, namely the time until an object is expected to reach the

state of threshold fitness-for-use), based on a damage function which relates the loss rate of degree of polymerisation to both the intrinsic paper properties (i.e., pH and DP) and the temperature and relative humidity at dark storage (i.e., without considering natural and artificial light). The Time Weighted Expected Lifetime (TWEL) index was recently proposed to synthesise the expected lifetime of paper collections on a seasonal and a yearly basis [9]. The effect of pollutants on historic paper preservation is generally negligible [16]. However, dust particles may increase paper vulnerability to cellulose hydrolysis by reducing their DP [17].

Biological risk

Fungal spores, which are ubiquitous, become a biological risk when RH>65% for a prolonged time [18]. The risk of mould is frequently estimated using the Sedlbauer isopleths for spore germination and mould growth for biologically recyclable materials [19].
Insect development is directly related to temperature (i.e., insects rapidly proliferate in warm conditions) and relative humidity (e.g., eggs and young larvae can be sensitive to dehydration) [20]. However, the risk of insect infestation is relatively less studied in terms of dose-response functions [21].

Photodeterioration

Visible light, and particularly UV radiation (if not filtered out), can accelerate embrittlement of poor-quality paper and cause yellowing [22] and colour fading of most dyes, inks and colourants [23]. Colorimetry is frequently used in the field of conservation to objectively assess colorimetric changes [24].

Research aims

The aim of this work is to investigate the principal climate-induced deterioration risks for paper collections in the repository of the Alessandrina Library (Rome, Italy). To this end, the microclimate observations collected for two years were analysed. Section 2 deals with the site description, the microclimate monitoring campaign and the observations collected. The methods for characterising the indoor climate and assessing the conservation risks are also described here. Section 3 is devoted to presentation and discussion of the results. Section 4 outlines the main conclusions of the work.

2. Materials and Methods

2.1 *Case study: collection and building metadata*

The Alessandrina Library is among the 46 prestigious libraries belonging to the Italian Ministry of Culture and preserves one of the most important university collections in Italy. The Library was founded in 1667 by Pope Alexander VII Chigi as the Library of the *Studium Urbis,* the University of Rome. Originally housed in the Roman Baroque church of Sant'Ivo alla Sapienza (designed by the architect Francesco Borromini from 1642 to 1660), its historical nucleus includes duplicates from the Chigiana Library, the Vatican Library and the valuable library of the Dukes of Urbino. From 1935, the Alessandrina Library was relocated in the upper floors (from third to fifth) of the Rectorate building (**Figure 1**a) within the Campus of Sapienza University in Rome (Lat. 41.9°N and Long. 12.5°E, 21 m a.m.s.l.). The Library also includes the pre-existing libraries of the Faculties of Humanities, Law and Political Science, as well as important donations. Nowadays, Alessandrina was elected as the

legal repository for all the documents of cultural interest destined to public use and published by editors from the province of Rome. High-resolution digital pictures and metadata of some of the most valuable documents in the Alessandrina collection are available on the web [25,26].

Figure 1 Front (**a**) and back (**c**) view of the Rectorate building of Sapienza University of Rome; west-oriented (**b**) and east-oriented (**d**) windows in the Alessandrina library repository.

The Alessandrina repository is divided into two main blocks (**Figure 2**a). The multi-storey repository has a total volume of more than 4000 m^3, with a ceiling at about 7 m and a floor area wider than 500 m^2. Windows are located on both the east and west walls of the repository and have single-pane glasses with UV-filters, which have severely deteriorated over time. The west-oriented windows (total area of approximately 30 m^2) face the façade of the Rectorate building and are shaded under the Rectorate prostyle (**Figure 1**a-b). These windows are frequently open during the warmer months. On the back of the Rectorate building, larger east-oriented windows (total area of approximately 85 m^2) are exposed to direct natural light during the diurnal hours (**Figure 2**c-d). These windows are mostly closed during the year. The repository is naturally ventilated and equipped with fan coils for both heating and cooling. However, the air conditioning system is obsolete and scarcely effective in temperature control over the year.

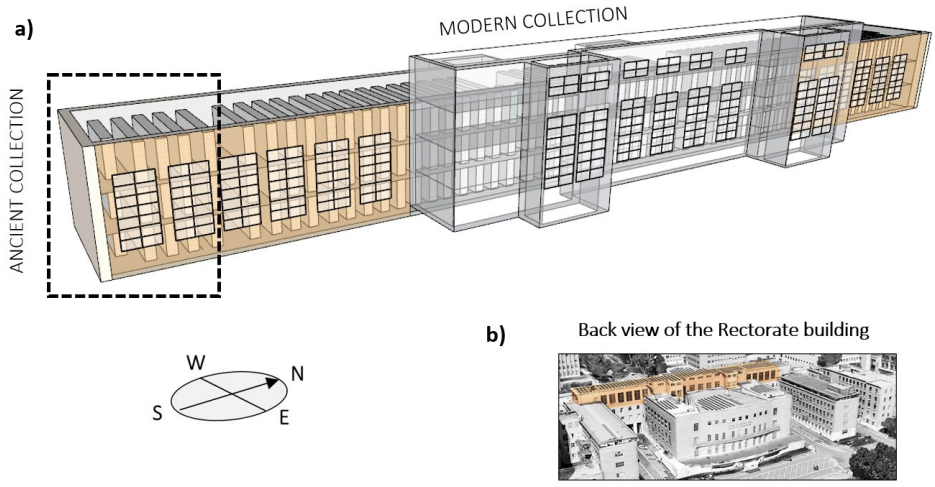

Figure 2 (**a**) Sketch of the Rectorate building portion where the Alessandrina library repository is housed, (**b**) rear aerial view of the building (the major repository block is highlighted in orange).

The Alessandrina collection includes two major assets based on the period of production of the volumes: the hereafter called Ancient collection, deployed on three floors in the south-facing part of the repository (**Figure 2**a, dashed rectangle), and the hereafter called Modern collection, which occupies the rest of the repository space (**Figure 2**). Paper is the prevalent material in both the Ancient and the Modern collection assets. The Ancient collection is mostly made in rag paper produced from XVI to XIX century and around 3% in parchment. The Modern collection is mostly made of XX-XXI century contemporary paper, with small amounts of cardboard, plastics and canvas.

2.2 *Monitoring campaign*

The microclimate conditions were monitored only in the major block (**Figure 2**a, orange volume), where the climate-induced risk assessment was carried out. The indoor climate was monitored for two full years, from 1st August 2019 until 31st July 2021, to study the hygrothermal behaviour of the library.

Two microclimate field campaigns were planned during different times of the day (morning/afternoon) to identify representative sampling points for six microclimate sensors. The field campaigns were conducted on the horizontal cross-sections of the repository on a 4m x 4m regular grid at 1.5 m above the floor using portable instruments (Rotronic Hygropalm thermo-hygrometer, uncertainty ±0.2°C for T and 1.0% for RH at 23±5°C). The spatial distributions of air temperature (T) and mixing ratio (MR) were interpolated from T and RH measurements collected at the nodes of the horizontal grid. MR was calculated from T and RH values using the formula provided in EN 16242:2013 [27] and used as a proxy to estimate the magnitude of the indoor-outdoor water vapour exchanges through infiltrations and openings [28].

Figure 3 shows an example of the spatial representation of the heat and moisture distribution in the repository in the form of contour maps of T and MR observations. The distribution of T turned out to be affected by the solar radiation entering from the east-facing windows during the morning, which locally increased the temperatures up to +2°C (**Figure**

3a). On the contrary, the MR distribution was homogeneous along the horizontal section (**Figure 3**b).

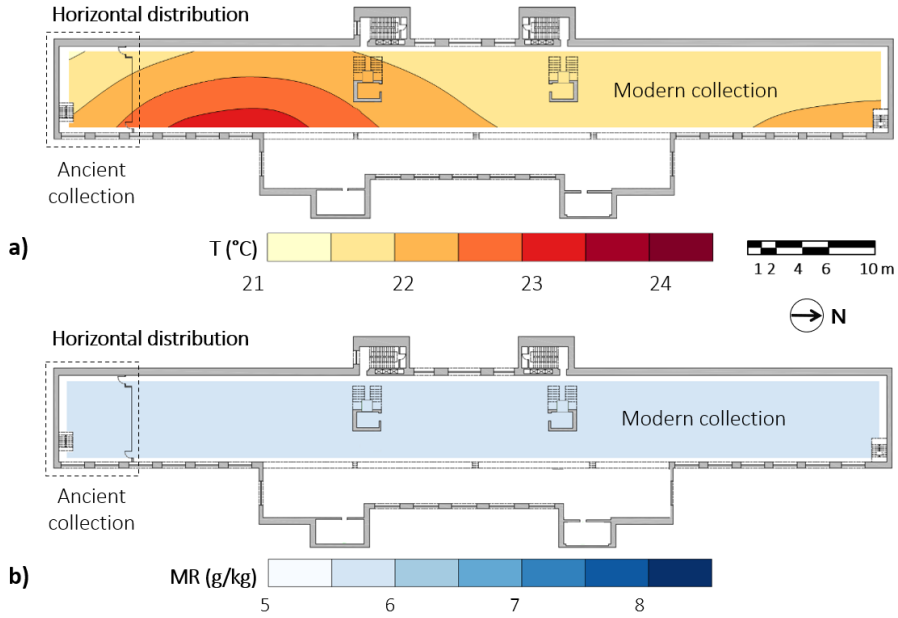

Figure 3 Spatial distributions of air temperature (**a**) and mixing ratio (**b**) in the repository on April 15th, 2019, at 11:30 a.m. (local time).

Six thermo-hygrometers (hereafter called RHT probes), model Rotronic HygroLog (Pt100 resistance thermometers for T and thin film capacitive sensors for RH), were deployed in the repository (Figure 4) to measure T and RH at local time. The uncertainties of the sensors, equal to 0.3°C for T and 0.8% for RH (from 10% to 60%), were in accordance with the current European Standards on the instruments recommended in cultural heritage conservation [28,29]. The RHT probes were positioned on the shelves at about 1.8 m above the floor. RHTs numbered from 1 to 4 were deployed in the area preserving the Ancient collections on three levels (to also monitor vertical T and RH gradients), while RHT5 and RHT6 were installed in the area preserving the Modern collection on the middle level along the major axis of the repository. The sampling frequency was set to 15 minutes to catch the short-term fluctuations due to consultation and management.

A HOBO U12-012 datalogger was used in the week from July 27th to August 3rd 2020 to measure the illuminance near the shelves opposite the east-facing windows (**Figure 4**).

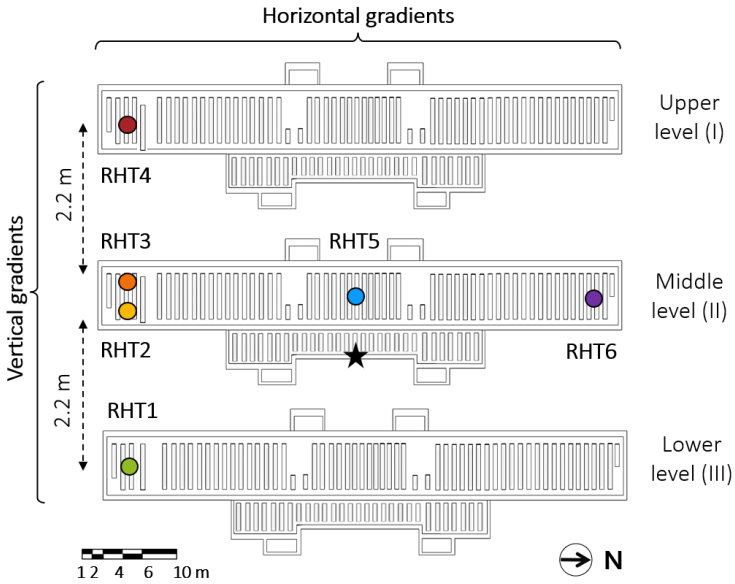

Figure 4 Position of the six thermo-hygrometers (RHT), indicated as coloured markers, and of the light sensor, indicated as a black star. The dashed arrows show the vertical step used to calculate vertical gradients.

The outdoor T and RH data used in this analysis were provided by a meteorological station installed on the roof of Fermi building of the Physics department (27.6 m above ground) within the Sapienza University campus [30]. The ground-based meteorological station (Vaisala Weather Transmitter WXT520), managed by the OMD Foundation (Fondazione Osservatorio Milano Duomo), belongs to the national private network of certified quality urban weather stations "Climate Network".

2.3 *Indoor climate characterisation*

The quality of the long time series of microclimate data collected in the Alessandrina repository was assessed through the Completeness Index (CoI) defined in [31] before performing data analysis.

Spatial gradients were calculated to evaluate whether relevant differences existed among the hygrothermal conditions detected in the various monitoring positions of the repository. The vertical gradient between the air temperatures measured by RHT3 and RHT4 was rescaled with respect to the distance of 10 m to evaluate the indoor air stability by comparing it to the dry adiabatic gradient of vertical temperature, i.e., $\Gamma_d \cong -0.1°C/10$ m. If the vertical temperature gradient ($\Gamma=\Delta T/\Delta z$) is higher than Γ_d, the air parcel tends to rise (unstable condition) and vice versa.

The short-term fluctuations of T (i.e., ΔT_{24h}) were evaluated as the differences between the T readings and the centred 24-hour T moving average (T_{24h}). The short-term fluctuations of RH (i.e., ΔRH_{30d}) were evaluated as the differences between the RH readings and the centred 30-day RH moving average (RH_{30d}). The sliding time windows used to calculate the moving averages are consistent with the typical response time of paper books to T and RH changes, i.e., 24 hours for T and 30 days for RH [15].

2.4 *Conservation risk assessment*

Mechanical risk

European standard EN 15757:2010 [10] was used to reconstruct the historical climate in the Alessandrina repository, i.e., the climatic conditions to which organic hygroscopic collections have become acclimatised. The calculation of the historical climate is based on the centred 30-day moving average of the RH observations (RH_{30d}). The bands of tolerable RH variations are obtained superimposing on RH_{30d} the lower and the upper limits, calculated respectively as the 7th and the 93rd percentiles of the distribution of the short-term fluctuations ΔRH_{30d}. When RH fluctuations depart by less than 10% from the seasonal RH levels, these limits can be considered unnecessarily strict and thus the RH band can be calculated as the RH_{30d}±10%.

Chemical risk

The validated dose-response function for paper derived in [13] was used to model the rate of paper degradation per year as a function of pH and DP and the indoor T and RH values. Then, based on Ekenstam's equation, the expected lifetime (EL) of paper (i.e., the time in years required for objects to become unfit for use) was derived as a function of the initial degree of polymerisation (DP0) and the critical DP at which objects are no longer suitable for handling [13]. It is worth considering that the EL refers to the conditions of dark storage, so the results might underestimate the chemical risk to the collections in the Alessandrina repository exposed to natural and artificial light.

The Time Weighted Expected Lifetime (TWEL) index was used to estimate the risk of chemical degradation for paper collections due to cellulose hydrolysis on both a yearly and a seasonal basis [9]. As the well-established Time Weighted Preservation Index (TWPI) defined in [15], the TWEL index integrates the damage function for historic paper together with the concept of a time weighted index to quantitatively compare the chemical risk due to the indoor climate conditions over different time windows (e.g., yearly or seasonally). The detailed description of the procedure followed to calculate the TWEL is provided in [9], where the TWEL was defined as:

$$TWEL = \frac{n}{\sum_{i=1}^{t} EL_i^{-1}} \quad (1)$$

where n is the total number of observations in the selected time window and the denominator is the cumulative sum of the i-th reciprocals of EL. Since the calculation of the TWEL was purposely based on T_{24h} and RH_{30d} (corresponding to the typical response time of paper books), it takes into account the time needed for paper books to reach the equilibrium with the hygrothermal conditions measured in the environment. Moreover, as the TWEL calculation is based on the reciprocals of EL, its value is clearly more influenced by lower values of EL, thus considering the risk underlying the worst-case scenario.

Biological risk

The risk of mould growth was assessed by comparing T and RH observations to the Sedlbauer diagram with the curves describing the times for spore germination and mycelial growth (known as isopleths) of *Aspergillus versicolor* [19]. As recently proposed in [21], the critical RH is the one associated with the Lowest Isopleth for Mould (LIM), i.e., the lowest

curve where mould activity is assumed to cease, for an optimal substrate [32], thus assuming a worst-case scenario.

The threat of insect pest infestation was evaluated through an index defined in [33] to quantitatively estimate the number of eggs laid (e) by webbing cloth moths (*Tineola bisselliella*) as a function of T:

$$e = \text{int}\left\{130*\exp\left(-\left(\frac{\frac{T^2}{30}-30}{12}\right)^2\right)\right\} \quad (2)$$

Webbing cloth moths very rarely damage books and papers, although a few species of moth can attack and cause damage to textiles, such as those used for book covers. In addition, the larvae may occasionally tunnel into leather book bindings [20].

Although no recent fungal colonisation or insect proliferation has been reported by the library staff, this evaluation was also performed to provide a holistic overview on the climate-induced deterioration risks.

Photodeterioration

In addition to the climate-induced risk assessment based on dose-response and damage functions, colorimetric measurements were performed to detect colour changes and evaluate the possible impact of solar radiation in the east-facing side of the repository.

A digital portable spectrophotometer Konica Minolta (model CM-2600d) was used to obtain the reflectance spectrum and the CIE colorimetric parameters. This instrument is based on the physical measurement of reflected light, through an integrating sphere, at specific wavelengths (400–700 nm at 10 nm steps) corresponding to the visible light spectrum. The CIE coordinates on the L*a*b* (CIELAB) colour space —i.e., the luminance L*, on a scale from 0 (black) to 100 (white), the chromatic dimension a*, on a scale from +60 (red) to –60 (green) and the chromatic dimension b*, on a scale from +60 (yellow) to –60 (blue)— were used to derive the colorimetric difference ΔE*, calculated as the Euclidean distance between the points in the CIELAB space [34]. The temporal change time of ΔE* was finally fitted using the exponential curve given in [24]:

$$\Delta E^* = \frac{E_\infty \cdot t}{t_s + t} \quad (3)$$

where E_∞ is the fitted value of ΔE* at infinite time and t_s is the time corresponding to $E_\infty/2$.

A field campaign following a 4-month schedule was carried out from October 2019 until October 2020 to monitor the cumulative colorimetric changes induced by light on the covers of five already discoloured books exposed to solar radiation. The five books monitored were selected to estimate the residual rate of discolouration affecting the covers that were already photodeteriorated. In this sense, colour changes were used to check whether photodeterioration was still possible on these specimens rather than to quantify the risk for the collection. After calibration with the white standard provided by the manufacturer (white calibration plate Minolta CM-A145), measurements on the book covers were repeated 3 times in 3 different sampling points for each sample and then averaged.

Colorimetric measurements were also performed on an unproofed green target sample of cardboard (made in pure Elemental Chlorine Free cellulose, grammage 200 g/m^2) to estimate the effect of the luminous exposure in the same position as the discoloured books. In order to compare the colorimetric measurements taken at different times on the green target, the same sampling area and calibration standard were used over the monitoring.

Risk Index

The Risk Index (RI), defined in [35] as the percentage of time for which RH and T values are out of the safe ranges for selected risks, was adjusted to the case of the library repository by including the specific climate-induced risks affecting paper collections and used to synthetically express the overall deterioration risks on a yearly basis. The mechanical RI was estimated as the percentage of time in which RH observations are beyond the tolerable RH band. It is worth noticing that, according to the procedure suggested by EN 15757:2010 [10], this value will never exceed 14%. The chemical RI was computed as the percentage of time in which the microclimate conditions are responsible for values of expected lifetime lower than 500 years [13]. The insect proliferation RI was calculated as the total number of eggs laid monthly by the webbing cloth moths over a year compared to theoretical maximum number of eggs in a year (i.e., 1560 eggs, corresponding to 130 eggs per months). The fungal colonisation risk was expressed as the yearly percentage of time in which hygrothermal conditions are favourable to mould germination [32].

3. Results and Discussion

3.1 *Indoor climate characterisation*

The quality of T and RH data collected by all sensors over the two years of monitoring was objectively evaluated before performing the microclimate data analysis. The time series collected over the period from August 1st, 2019, to July 31st, 2020 was found to be the most complete (CoI=1) and was used in the following analysis.

On a yearly basis, the medians of the indoor T were significantly higher than the outdoor ones (**Figure 5**a) and showed comparable levels and trends. Nonetheless, a higher short-term variability can be noticed for RHT5 when looking at the time plot (**Figure 5**b) due to the closer proximity to the entrance door, the fan coils, and the west-facing windows (frequently open during the warm season). The indoor RH observations were found to be significantly lower than the outdoor ones (**Figure 5**c), with medians of indoor relative humidity between 40-50% as observed in other libraries [9]. The outdoor RH variability, ranging from 20% to 100%, was markedly smoothed out inside the repository (**Figure 5**d). The relatively higher variability of the RH observations collected in RHT5 during the warm months was probably caused by the opening of the west-facing windows (**Figure 5**e-f).

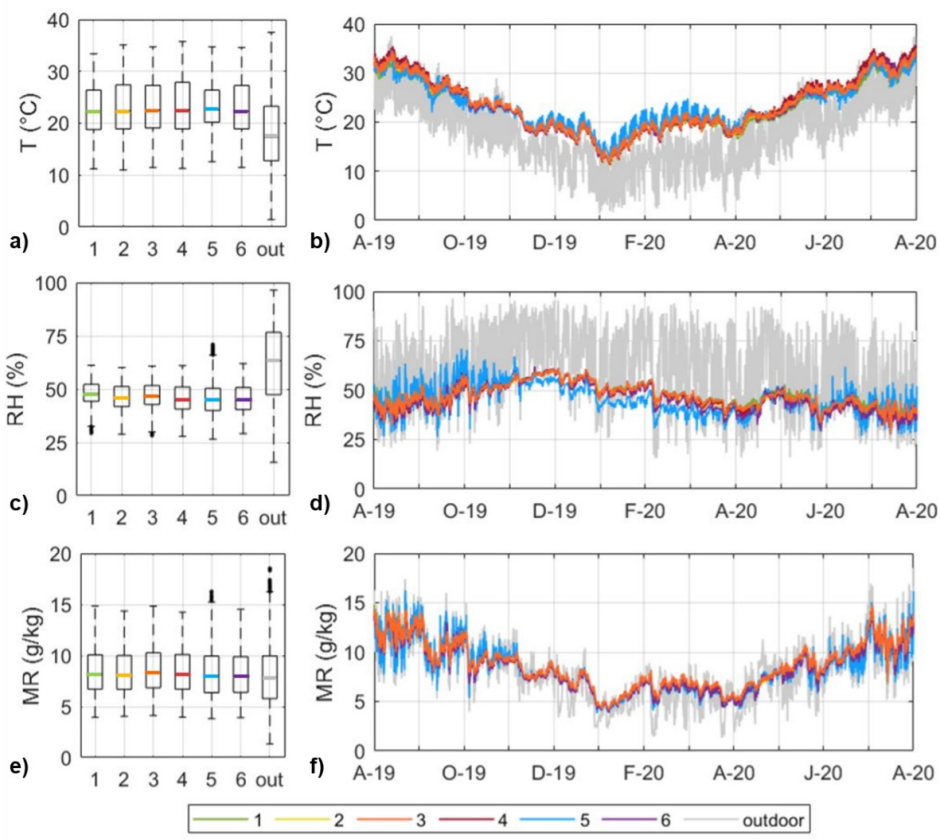

Figure 5 Box-and-whisker plots of indoor (1-6) and outdoor (out) temperature (**a**), relative humidity (**c**) and mixing ratio (**e**) data collected by the six RHT probes and time plots of indoor T (**b**), RH (**d**) and MR (**f**) data. In the box-and-whisker plots, the medians are indicated with horizontal lines dividing each box and the whiskers are set to lowest and the highest value when they are not outliers (i.e., the values above or below 1.5×IQR, indicated as black dots).

Analysis of the vertical temperature gradients ($\Delta T/\Delta z$) highlighted that unstable conditions occurred in winter (red areas in **Figure 6**), mainly caused by the cooler temperatures observed near the ceiling (T4) due to the poorly insulated roof causing heat losses. This effect was partly compensated by the combined effect of heating systems and solar exposure from January to March during weekdays (approximately from 10 a.m. to 7 p.m., visible as white-blue areas), but positive temperature gradients occurred during weekends, when the heating systems were turned down (red areas). Unstable conditions determine that air gains buoyancy and forms an upward current, thus tending to increase soiling and transport of dust and fungal spores. As expected, the air temperatures near the ceiling (blue areas in **Figure 6**) were higher during the warm season, likely due to the combined effect of the increase in outdoor temperature caused by the strong radiative exchange and indoor heat accumulation. This latter condition, being responsible for accelerated rates of chemical deterioration, might affect the conservation of the collections on the upper level. It might be useful to note that the temperature gradient related to stable conditions was steeper than the one related to unstable conditions.

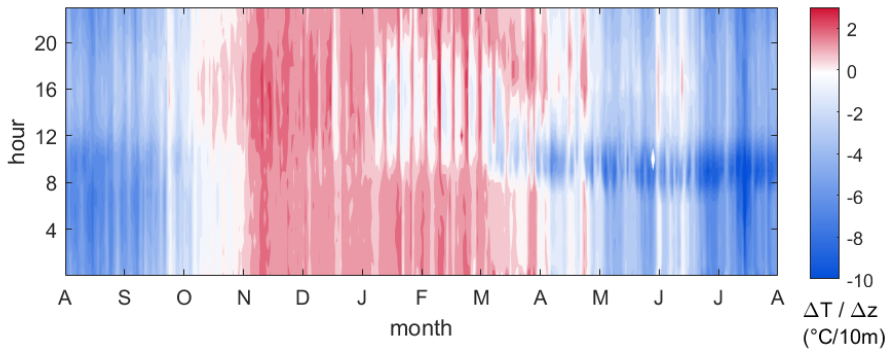

Figure 6 Hourly distribution of vertical temperature gradients ($\Delta T/\Delta z$, where ΔT = T3-T4) compared with the dry adiabatic gradient of temperature (Γ_d=−0.1°C/10m): unstable (red), neutral (white) and stable (blue) conditions.

The differences among T and RH data collected by RHT2, RHT3 and RHT6 (deployed on the middle level of the repository) were found to be lower than instrumental uncertainties. Therefore, we focussed the following analysis on the comparison between the observations collected by RHT3 and RHT5, which were taken as representative respectively of the average conditions surrounding the Ancient collection and the central area of the repository housing the Modern collection.

The T and MR data collected by RHT3 and RHT5 were used to investigate the influence of the external climate on the indoor hygrothermal conditions. Looking at the scatter plots reported in **Figure 7**, the slopes of the solid lines relating indoor and outdoor T and RH monthly averages at the two sites of the repository were similar. It can be noticed that indoor T values were higher than the outdoor ones, while MR values were mostly identical. If compared to the average T conditions collected by RHT3, the monthly T averages measured in the central area of the repository by RHT5 were higher in winter (due to the proximity of the fan coils) and slightly lower in summer (being less affected by solar radiation).

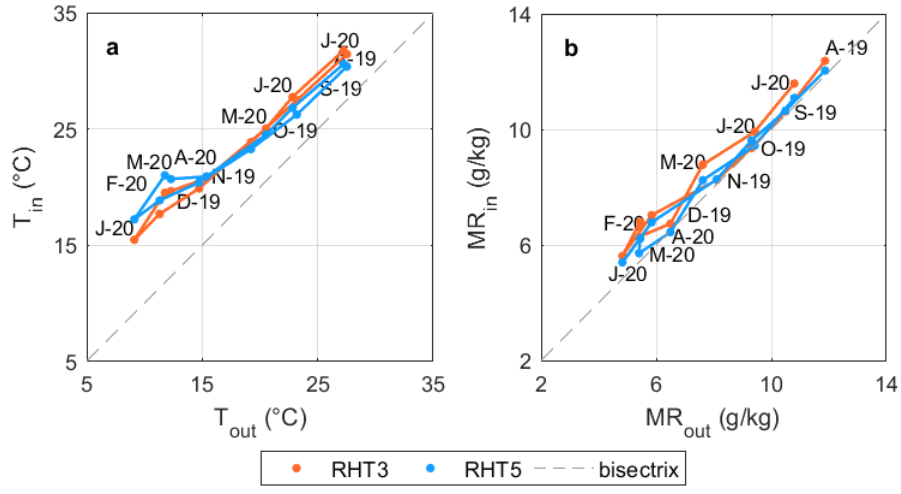

Figure 7 Indoor *versus* outdoor monthly averages of air temperature (**a**) and mixing ratio (**b**) values.

Figure 8 shows the frequency distribution plots of the short-term fluctuations ΔT_{24h} and ΔRH_{30d}. Both ΔT_{24h} and ΔRH_{30d} showed high stability, symmetrically spreading around the zero by about ±1°C for T and ±5% for RH in the case of data collected by RHT3 (**Figure 8**a) and by about ±2°C for T and ±10% for RH in the case of data collected by RHT5 (**Figure 8**b).

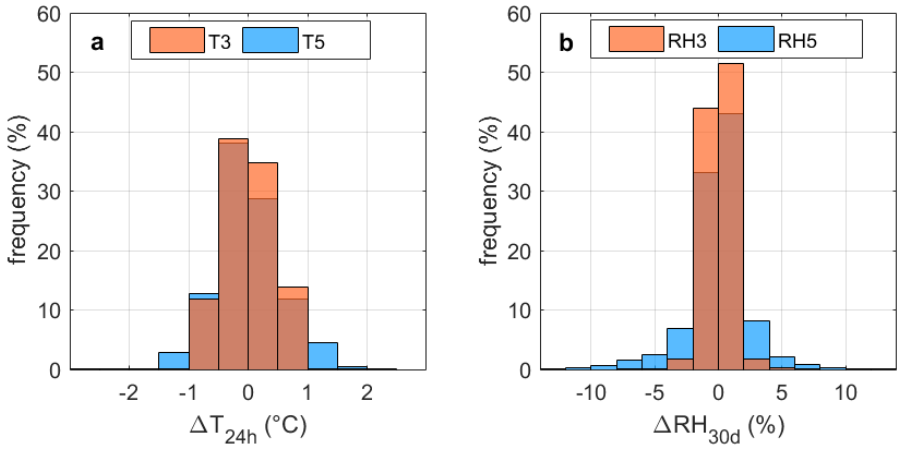

Figure 8 Frequency distribution of differences between T observations and the running average over 24 hours (**a**) and between RH observations and the running average over 30 days for RH (**b**).

3.2 *Conservation risk assessment*

The observations collected by RHT3 and RHT5 were used to estimate the principal conservation risks for the Ancient collection and the Modern collection, respectively.

The mechanical risk was evaluated reconstructing the historical microclimate according to EN 15757:2010 [10]. Since RH short-term fluctuations did not exceed the tolerance bands of ±10% from RH_{30d}, the upper and lower limits for Ancient and Modern collections were drawn as RH_{30d}±10%. The peaks of the two tolerance RH bands in **Figure 9** were slightly shifted by a time lag of one month; as of May 2020 they fully overlapped, probably thanks to a reduced fruition of the repository imposed by the COVID-19 pandemic situation.

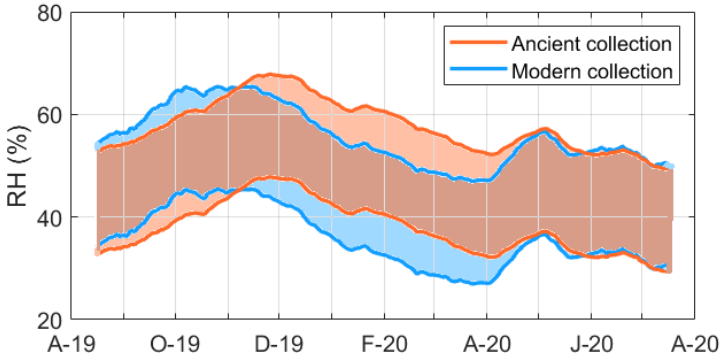

Figure 9 Tolerance RH bands based on the historical climate in the repository. The two 15-day periods at the beginning and the end of the year were cut due to calculation of RH_{30d}.

The information on the historical climate (**Figure 9**) can be used in management of the collections. Indeed, it was found that any relocation of moisture-vulnerable objects (e.g., composite objects, parchment-bound volumes) within the repository area can be considered safe from the physical damage induced by strain-stress cycles [10]. This information can be also beneficial in the case of loan and consultation, as it supports the definition of the target tolerance band of RH fluctuations when library items need to be moved to spaces characterised by different hygrothermal conditions.

To explore the effect of the microclimate on the chemical deterioration risk for various paper types, the annual TWEL associated with the T and RH conditions surrounding Ancient and Modern collections was calculated combining typical average values of pH and DP0 paper types (**Table 1**).

Table 1 TWEL values (in years) in relation with T and RH values surrounding Ancient and Modern collections obtained for various paper types by combining their typical average values of acidity (pH) and initial degree of polymerisation (DP0).

TWEL	pH	DP0		
		critical (600)	fair (1500)	good (2000)
Ancient collection	acidic (5)	219	677	1188
	neutral (7)	351	1083	1902
	basic (8)	373	1151	2021
Modern collection	acidic (5)	204	631	1107
	neutral (7)	327	1009	1772
	basic (8)	348	1072	1882

On a yearly basis, the exploratory evaluation (**Table 1**) highlighted that the risk due to cellulose hydrolysis can be relevant for all the paper-based objects having DP0 < 600 (critical), with a reduction of the expected lifetime of the most acidic ones up to approximately 200 years. On the contrary, for paper-based objects with a DP0 from fair (1500) to good (2000), the chemical risk in both the sites was found to be compatible with the 500-year planning horizon typical of conservation strategies for historic libraries. Overall, the chemical risk associated with the T and RH values surrounding the Modern collection was slightly higher for all the explored paper types.

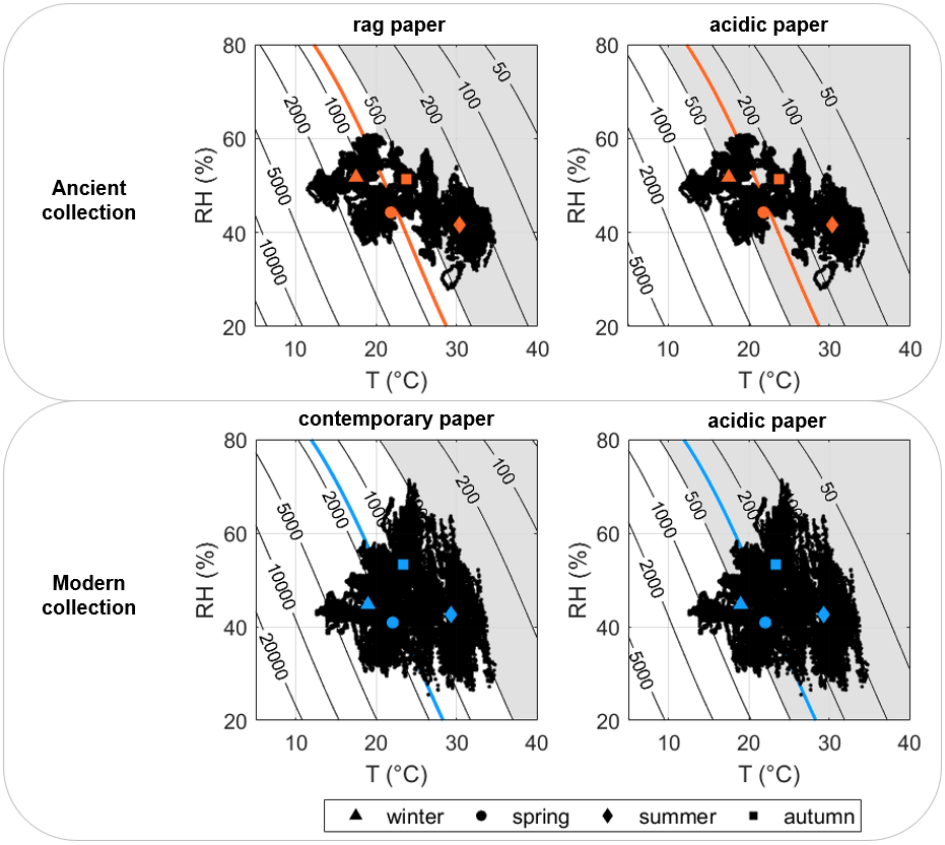

Figure 10 Temperature and relative humidity observations (black dots) plotted on the isochrones of expected lifetime, together with the yearly (coloured curves) and seasonal (coloured markers) TWEL values (in years). Shaded area: T and RH conditions favourable to chemical decay.

To further investigate the riskiest period of the year in terms of chemical deterioration, the T and RH observations at the two sites of the repository were compared to the isochrones for acidic, rag and contemporary paper types (**Figure 10**). A prevalence of rag paper in the Ancient collection and of contemporary paper in the Modern collection was assumed based on the production period of the books. The chemical risk for the acidic items in the collections was also evaluated, as they are the most vulnerable to cellulose hydrolysis. The seasonal TWEL (coloured markers in **Figure 10**) highlighted that, although the annual values (coloured curves in **Figure 10**) exceeded the 500-year planning horizon for conservation [13], the T and RH conditions in summer and autumn were favourable to the chemical decay of rag paper in the Ancient collection. In contrast, acidic paper can be subjected to cellulose hydrolysis throughout most of the year, with winter as the only exception. Contemporary paper is at no risk on a seasonal basis, but the high temperatures (i.e., T > 25°C) occurring in summer could threaten its durability, particularly when associated with high relative humidity values (i.e., RH > 60%).

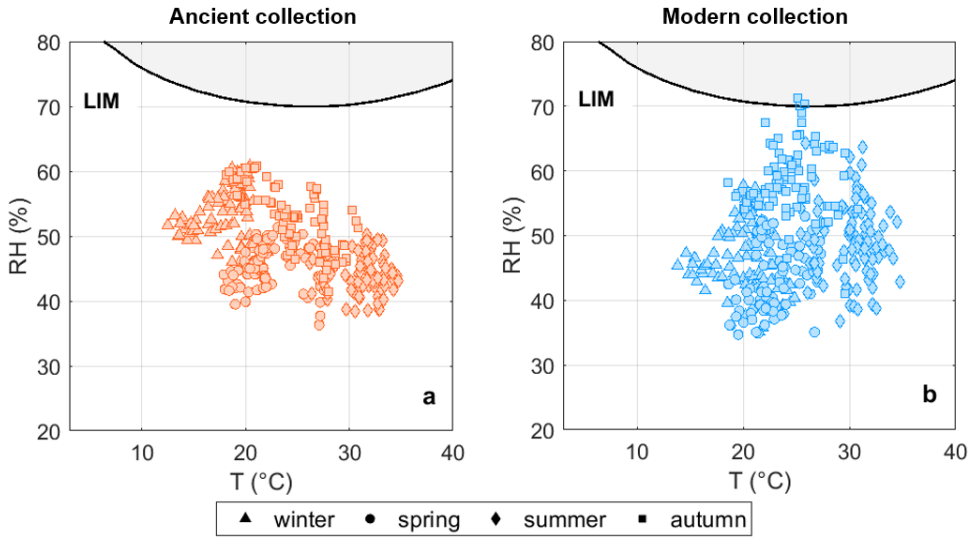

Figure 11 Lowest isopleths for spore germination and mycelium growth (LIM) for optimal substrate according to Sedlbauer [32] and maximum daily T and RH values. Shaded area: RH conditions exceeding the threshold favourable to fungal decay.

In **Figure 11** the maximum daily T and RH values experienced by Ancient (**Figure 11**a) and Modern (**Figure 11**b) collections were compared to the lowest isopleths for spore germination and mycelium growth for optimal substrate [32]. The results highlighted that on a few cases during autumn the risk of fungal colonisation was possible for the Modern collection, should conditions of low ventilation and water vapour condensation occur on cold metal surfaces (such as those of the repository shelves).

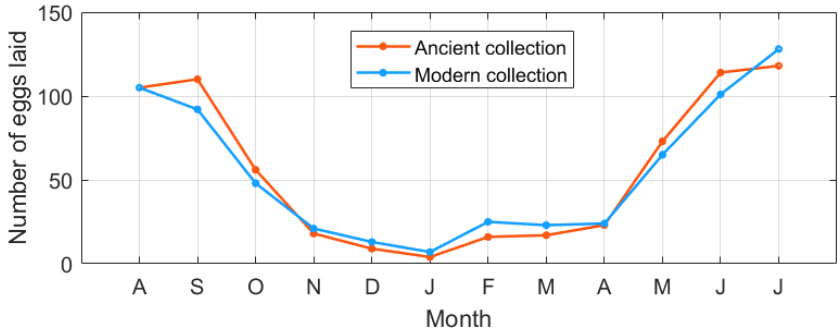

Figure 12 Number of eggs laid by the webbing cloth moth (*Tineola bisselliella*) as a function of the average monthly temperature values in the repository.

The risk of insect proliferation was estimated in **Figure 12** as a function of the monthly T average values in the repository. The expected number of eggs laid by the webbing cloth moth (*Tineola bisselliella*) was found to be practically equal for Ancient and Modern collections. During the monitored year, it was higher than 50 from May to October, with a slight inversion of the trend in August due to T>30°C; in January, the expected amount of moth eggs decreased up to the minimum value of 4 eggs due to T means below 20°C.

The illuminance measured in the proximity of the book covers in August 2020 during the morning hours exceeded 32000 lux (i.e., the upper measurement limit of the light sensor). The total luminous exposure measured within a single week, higher than 5.2 Mlx, was approximately ten times higher than the maximum annual luminous exposure recommended by CEN/TS 16163:2014 [36] for low sensitivity materials (i.e., 0.6 Mlx ·h per year).

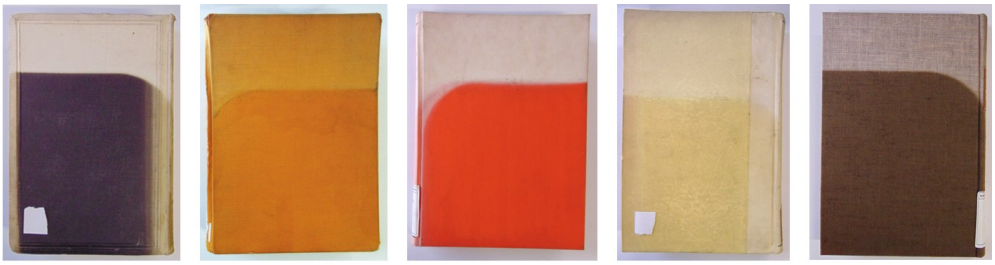

Figure 13 Colour changes (ΔE*) measured on 5 book covers from October 2019 to October 2020 (mean ± half maximum spread).

Figure 13 shows the total colorimetric difference (ΔE*) measured on the 5 book covers over the field campaign. As expected for visibly photodeteriorated samples, ΔE* was found to be always considerably higher than 6 (i.e., perceptible and non-acceptable colorimetric difference from the original colour [37]). The ΔE* did not change significantly after one year, meaning that the discolouration rate was already too low to be observed in such a short time window.

The results of the colorimetric measurement campaign carried out over the period from October 2019 to October 2020 on the target sample of green cardboard are shown in **Figure 14**. The colorimetric change observed on the sample followed a typical exponential trend, with the slope of ΔE* rapidly changing from the initial conditions (P0) to those measured after the first 4 months of luminous exposure (E1) and then slowly decreasing in the following spring and summer (E2 and E3) even if associated with a higher dose of solar radiation.

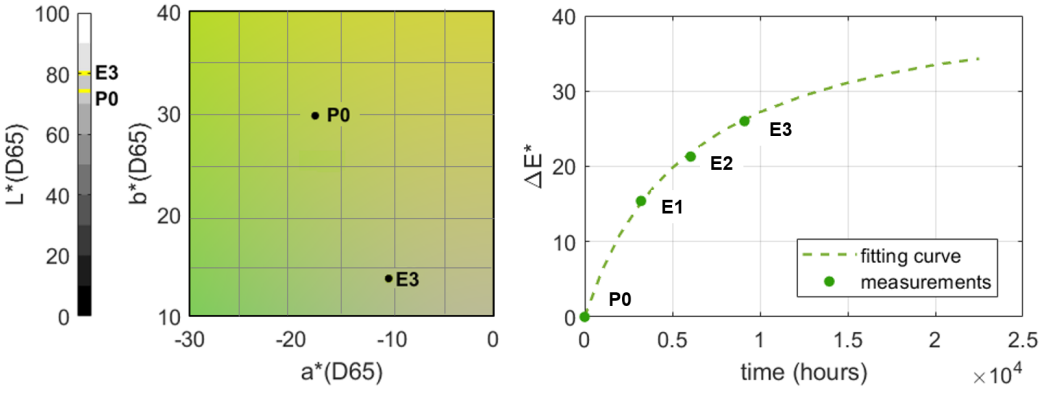

Figure 14 Colorimetric coordinates of the points measured on the green mock sample (**a**) and total colorimetric difference ΔE* as a function of time (**b**). The measured data (dots) are fitted by the curve obtained using Equation 3. P0 = protected area (October 2019) and E1, E2, E3 = areas exposed to light (February, June and October 2020, respectively).

Figure 15 shows the radar plots with the Risk Index to compare the climate-induced risk for the Ancient and Modern collections. The coloured area indicates the magnitude (in percentage of time) of the total mechanical, chemical and biological risk over a year. The risk of cellulose hydrolysis for acidic paper associated with the hygrothermal conditions surrounding the Ancient and Modern collections was consistently high (RI=86% and 84%, respectively), while for less vulnerable paper types it was equal to RI=38% for rag paper in the Ancient collection and to RI=6% for contemporary paper in the Modern collection. Insect proliferation in the repository was favoured during approximately 42% of the year. In contrast, the risk of mechanical deterioration and mould germination was negligible for both collections.

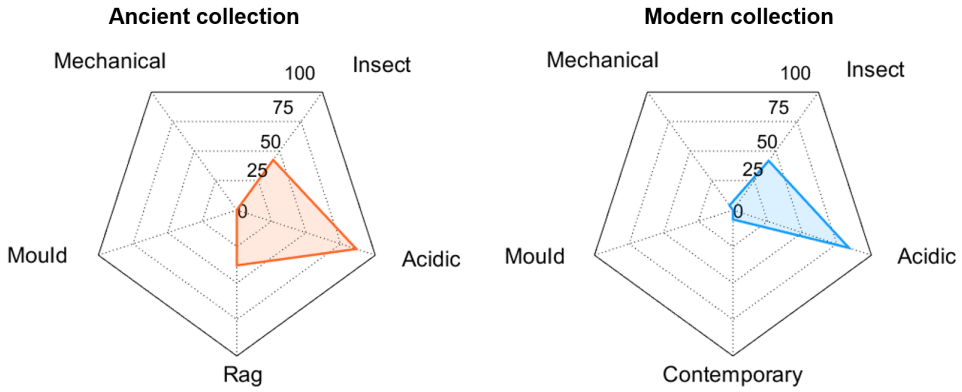

Figure 15 Radar plot of the Risk Index (%) calculated on a yearly basis for the mechanical (EN 15757:2010), chemical (cellulose hydrolysis of acidic, rag and contemporary paper) and biological risks (mould and insects proliferation).

4. Conclusions

A global characterisation of the main climate-induced deterioration risks for paper collections (mechanical stress, cellulose hydrolysis, mould and insect proliferation) was carried out in the repository of the Alessandrina Library (Rome, Italy).

Temperature (T) was found to be the key microclimate stressor to be monitored for preventive conservation of paper collections, as it controlled the rate of cellulose hydrolysis while favouring insect proliferation. The study of the vertical T gradients highlighted that unstable conditions occurred in winter, whereas heat accumulated on the upper levels of the repository during the rest of the year. Relative humidity (RH) in the repository was below 60% for most of the year, although fungal colonisation might occur during autumn in poorly ventilated microenvironments due to water vapour condensation on cold surfaces of the metal shelves. The tolerable RH conditions were defined based on "historical climate" to reduce the mechanical deterioration risk of moisture-vulnerable objects in the event of loans, relocation and consultation. The estimated luminous exposure in the repository was found to be incompatible with conservation of materials sensitive to photodeterioration. In the case of some faded book covers, the monitored discolouration rate was already too low to be quantified over a single year; however, any deployment of unaltered photosensitive materials on the shelves near the windows would be risky unless protections from direct exposure to solar radiation were to be installed.

The study highlighted that high temperatures and solar exposure are responsible for the major deterioration risks affecting the collections. For this reason, two passive retrofit measures could be suggested: 1) improving roof insulation to mitigate summer temperature peaks and winter vertical gradients causing unstable conditions; 2) adopting shading devices to reduce solar radiation entering from the large east-facing windows.

Although the research focussed on a specific case study, a similar approach could be effectively adapted to most library and archival repositories conserving paper-based collections.

Availability of data and materials: The datasets used and/or analysed during the current study are available from the corresponding author on reasonable request.

Funding: The APC was funded by CollectionCare project, which has received funding from the European Union's Horizon 2020 research and innovation programme under grant agreement N^{o} 814624.

Author Contributions: All authors contributed to the development of this study in the framework of the research agreement stipulated in 2019 among Sapienza Università di Roma, Biblioteca Universitaria Alessandrina and Istituto Centrale per il Restauro e la Conservazione del Patrimonio Archivistico e Librario (today Istituto Centrale per la Patologia degli Archivi e del Libro). All authors have read and agreed to the current version of the manuscript.

Acknowledgements: A.M.S., F.F. and E.V. thank the CollectionCare project (European Union's Horizon 2020 research and innovation programme under grant agreement No 814624) for the financial support of the APC.

Competing interests: The authors declare that they have no competing interests.

Abbreviations and symbols

Γ_d	Dry adiabatic vertical gradient of temperature (°C m^{-1})
Δa^*	Colorimetric difference in red and green (-)
Δb^*	Colorimetric difference in yellow and blue (-)
ΔE^*	Total colorimetric difference (-)
ΔL^*	Colorimetric difference in lightness and darkness (-)
ΔRH_{30d}	Difference between T reading and RH_{30d} (%)
ΔT	Vertical temperature gradient (°C)
ΔT_{24h}	Difference between T reading and T_{24h} (°C)
Δz	Vertical distance between two probes (m)
CIE	Commission Internationale de l'Eclairage
CoI	Completeness Index (-)
D65	CIE standard illuminant for the average midday light in Western Europe
DP	Paper degree of polymerisation (-)
DP0	Initial DP (-)
e	Number of eggs laid by webbing cloth moths (-)
EL	Expected Lifetime of paper (years)
E_∞	Fitted value of □E* as time approaches infinity
HVAC	Heating, Ventilation, and Air Conditioning
IQR	Interquartile Range
LIM	Lowest Isopleth for Mould
MR	Mixing Ratio ($g \cdot kg^{-1}$)
pH	Acidity of paper (-)
RH	Relative Humidity (%)
RH_{30d}	centred 30-day moving average of relative humidity (%)
RHT	Probes measuring T and RH
t	Time (hours)
T	Air Temperature (°C)
t_s	time corresponding to $E_\infty/2$ (hours)
T_{24h}	centred 24-hour moving average of temperature (°C)
TWEL	Time Weighted Expected Lifetime (years)
TWPI	Time Weighted Preservation Index (-)

References

1. VanSnick, S.; Ntanos, K. On Digitisation as a Preservation Measure. *Stud. Conserv.* **2018**, *63*, 282–287, doi:10.1080/00393630.2018.1504451.

2. Sahin, C.D.; Coşkun, T.; Arsan, Z.D.; Gökçen Akkurt, G. Investigation of indoor microclimate of historic libraries for preventive conservation of manuscripts. Case Study: Tire Necip Paşa Library, İzmir-Turkey. *Sustain. Cities Soc.* **2017**, *30*, 66–78, doi:10.1016/j.scs.2016.11.002.

3. Verticchio, E.; Frasca, F.; Garcìa-Diego, F.-J.; Siani, A.M. Investigation on the Use of Passive Microclimate Frames in View of the Climate Change Scenario. *Climate* **2019**, *7*, 98, doi:10.3390/cli7080098.

4. Steeman, M.; De Paepe, M.; Janssens, A. Impact of whole-building hygrothermal modelling on the assessment of indoor climate in a library building. *Build. Environ.* **2010**, doi:10.1016/j.buildenv.2010.01.012.

5. Kupczak, A.; Sadłowska-Sałęga, A.; Krzemień, L.; Sobczyk, J.; Radoń, J.; Kozłowski, R. Impact of paper and wooden collections on humidity stability and energy consumption in museums and libraries. *Energy Build.* **2018**, *158*, 77–85, doi:10.1016/j.enbuild.2017.10.005.

6. Bloom, J.M. Papermaking: The Historical Diffusion of an Ancient Technique. In; 2017; pp. 51–66.

7. Strlič, M.; Liu, Y.; Lichtblau, D.A.; De Bruin, G.; Knight, B.; Winther, T.; Kralj Cigic, I.; Brereton, R.G. Development and mining of a database of historic European paper properties. *Cellulose* **2020**, *27*, 8287–8299, doi:10.1007/s10570-020-03344-x.

8. David Ribar in collaboration with the Heritage Science Lab Ljubljana and UCL Institute for Sustainable Heritage Collections Demography App Available online: https://hsll.shinyapps.io/collections_demography_app/ (accessed on May 26, 2021).

9. Verticchio, E.; Frasca, F.; Bertolin, C.; Siani, A.M. Climate-induced risk for the preservation of paper collections: Comparative study among three historic libraries in Italy. *Build. Environ.* **2021**, *206*, 108394, doi:10.1016/j.buildenv.2021.108394.

10. EN 15757. Conservation of Cultural Property - Specifications for temperature and relative humidity to limit climate-induced mechanical damage in organic hygroscopic materials 2010.

11. Bogaard, J.; Whitmore, P.M. Explorations of the Role of Humidity Fluctuations in the Deterioration of Paper. *Stud. Conserv.* **2002**, *47*, 11–15, doi:10.1179/sic.2002.47.s3.003.

12. Strlič, M.; Grossi, C.M.; Dillon, C.; Bell, N.; Fouseki, K.; Brimblecombe, P.; Menart, E.; Ntanos, K.; Lindsay, W.; Thickett, D.; et al. Damage function for historic paper. Part II: Wear and tear. *Herit. Sci.* **2015**, *3*, 1–11, doi:10.1186/s40494-015-0065-y.

13. Strlič, M.; Grossi, C.M.; Dillon, C.; Bell, N.; Fouseki, K.; Brimblecombe, P.; Menart, E.; Ntanos, K.; Lindsay, W.; Thickett, D.; et al. Damage function for historic paper. Part III: Isochrones. *Herit. Sci.* **2015**, doi:10.1186/s40494-015-0062-1.

14. Michalski, S. Double the life for each five-degree drop, more than double the life for each halving of relative humidity. *Thirteen. Trienn. Meet. ICOM-CC* **2002**, 66–72.

15. Nishimura, D.W. *Understanding Preservation Metrics*; 2011;

16. Menart, E.; de Bruin, G.; Strlič, M. Effects of NO_2 and acetic acid on the stability of historic paper. *Cellulose* **2014**, *21*, 3701–3713, doi:10.1007/s10570-014-0374-4.

17. Bartl, B.; Mašková, L.; Paulusová, H.; Smolík, J.J.; Bartlová, L.; Vodička, P. The effect of dust particles on cellulose degradation. *Stud. Conserv.* **2016**, *61*, 203–208, doi:10.1179/2047058414Y.0000000158.

18. EN 16893. Conservation of cultural heritage - New sites and buildings intended for the storage and use of collections 2018.

19. Krus, M.; Kilian, R.; Sedlbauer, K. Mould growth prediction by computational simulation on historic buildings. In Proceedings of the Museum Microclimates; 2007; pp. 185–189.

20. Pinniger, D. *Pest Management in Museums, Archives and Historic Houses*; 2001.

21. Bratasz, L.; White, T.; Butts, S.; Sease, C.; Utrup, N.; Boardman, R.; Simon, S. Toward Sustainable Collections Management in the Yale Peabody Museum: Risk Assessment, Climate Management, and Energy Efficiency. *Bull. Peabody Museum Nat. Hist.* **2018**, *59*, 249–268, doi:10.3374/014.059.0206.

22. Mosca Conte, A.; Pulci, O.; Del Sole, R.; Knapik, A.; Bagniuk, J.; Lojewska, J.; Teodonio, L.; Missori, M. Experimental and theoretical study of the yellowing of ancient paper. *e-Journal Surf. Sci. Nanotechnol.* **2012**, *10*, 569–574, doi:10.1380/ejssnt.2012.569.

23. Ghelardi, E.; Degano, I.; Colombini, M.P.; Mazurek, J.; Schilling, M.; Khanjian, H.; Learner, T. A multi-analytical study on the photochemical degradation of synthetic organic pigments. *Dye. Pigment.* **2015**, *123*, 396–403, doi:10.1016/j.dyepig.2015.07.029.

24. Cianchetta, I.; Colantoni, I.; Talarico, F.; D'Acapito, F.; Trapananti, A.; Maurizio, C.; Fantacci, S.; Davoli, I. Discoloration of the smalt pigment: Experimental studies and ab initio calculations. *J. Anal. At. Spectrom.* **2012**, *27*, 1941–1948, doi:10.1039/c2ja30132f.

25. digitALE ver. 3.0 Available online: http://digitale.alessandrina.librari.beniculturali.it/ (accessed on Dec 22, 2021).

26. Internet Culturale. Cataloghi e collezioni digitali delle biblioteche Italiane Available online: https://www.internetculturale.it/ (accessed on Dec 22, 2021).

27. EN 16242. Conservation of cultural heritage - Procedures and instruments for measuring humidity in the air and moisture exchanges between air and cultural property 2012.

28. Huerto-Cardenas, H.E.; Aste, N.; Del Pero, C.; Della Torre, S. Effects of Climate Change on the Future of Heritage Buildings : Case Study and Applied Methodology. **2021**.

29. EN 15758. Conservation of Cultural Property - Procedures and instruments for measuring temperatures of the air and the surfaces of objects 2010.

30. Di Bernardino, A.; Iannarelli, A.M.; Casadio, S.; Mevi, G.; Campanelli, M.; Casasanta, G.; Cede, A.; Tiefengraber, M.; Siani, A.M., Spinei, E.; Cacciani, M. On the effect of sea breeze regime on aerosols and gases properties in the urban area of Rome, Italy. *Urban Climate* **2021**, *37, 100842*, doi:10.1016/j.uclim.2021.100842.

31. Frasca, F.; Siani, A.M.; Casale, G.R.; Pedone, M.; Bratasz; Strojecki, M.; Mleczkowska, A. Assessment of indoor climate of Mogiła Abbey in Kraków (Poland) and the application of the analogues method to predict microclimate indoor conditions. *Environ. Sci. Pollut. Res.* **2017**, *24*, 13895–13907, doi:10.1007/s11356-016-6504-9.

32. Vereecken, E.; Roels, S. Review of mould prediction models and their influence on mould risk evaluation. *Build. Environ.* **2012**, *51*, 296–310, doi:10.1016/j.buildenv.2011.11.003.

33. Brimblecombe, P.; Lankester, P. Long-term changes in climate and insect damage in historic houses. *Stud. Conserv.* **2013**, *58*, 13–22, doi:10.1179/2047058412Y.0000000051.

34. *CIE 157. Control of damage to museum objects by optical radiation.*; Vienna, 2004;

35. Frasca, F.; Verticchio, E.; Caratelli, A.; Bertolin, C.; Camuffo, D.; Siani, A.M. A comprehensive study of the microclimate-induced conservation risks in hypogeal sites: The mithraeum of the baths of Caracalla (Rome). *Sensors (Switzerland)* **2020**, *20*, 1–18, doi:10.3390/s20113310.

36. CEN/TS 16163. Conservation of cultural heritage–guidelines and procedures for choosing appropriate lighting for indoor exhibitions. 2014.

37. Hardeberg, J. Y. Acquisition and reproduction of color images: colorimetric and multispectral approaches. Universal-Publishers, 2001.

Acknowledgements

There are many people I wish to acknowledge for their contribution during these years.

First of all, Prof. Anna Maria Siani, my mentor, who wisely guided me since my earliest steps in research. Thank you for the stimulating working environment you established through relentless commitment, trust and mutual understanding. I was immensely lucky to engage with Prof. Cristina Cornaro, a precious advisor for modelling and simulation, and Prof. Chiara Bertolin, a unique source of expertise, curiosity and motivation. I'm also indebted to Dr. Francesca Frasca, for her inexhaustible support, patient guidance and daily fun. Thank you all for having greatly enriched my academic path as a PhD student. A special mention goes to Emeritus Prof. Alfredo Colosimo, Dr. Pino Casale and Dr. Massimiliano Pedone, for the compelling talks and the affectionate companionship at our laboratory.

I had the honour and pleasure to learn from Emeritus Prof. Dario Camuffo (CNR-ISAC), who has always been keen to share his outstanding knowledge. I treasured the hospitality and worthy discussions with Emeritus Prof. Roman Kozłowski (IKiFP PAN) and Prof. Łukasz Bratasz (IKiFP PAN) during my stay in Poland. My sincere gratitude goes to Prof. Fernando-Juan Garcia-Diego, for having shared his great competence and passion for the microclimate studies.

For the microclimate monitoring campaigns in the historic libraries, I thank Dr. Paola Fiore, responsible of the CREA Meteorological Library at Collegio Romano, Dr. Daniela Fugaro, director of the Alessandrina Library, Dr. Paolo Galimberti, director of the Ca' Granda Library in Milan and the staff of the Museo Diocesano in Udine. I also express my affectionate gratitude to Dr. Luigi Iafrate, Arch. Patrizia Cavalieri and Dr. Lorenzo Teodonio, for their collaboration and support in the on-site campaigns at CREA and Alessandrina Libraries. Finally, I thank the CollectionCare project (European Union's Horizon 2020 research and innovation programme under grant agreement No 814624) for having financed the APC of open-access articles.

I would also like to thank all the members of my Doctoral school for their constructive suggestions and for the scientific activities offered in the PhD program. Lastly, I appreciate the reviewers of this thesis for the time they dedicated to examine my work and for their valuable comments to improve it.

I accomplished this journey with the support of the people I love: my caring family and lifetime friends, who trustfully encouraged me.

This work is dedicated to the loving memory of my grandmothers, who generously laid the foundations for our greater possibilities.

Short Curriculum vitae

Elena Verticchio

Personal information

Name and surname:	Elena Verticchio
Nationality:	Italian
Place, date of birth:	Rome (Italy), June 21st, 1991
E-mail:	elena.verticchio@uniroma1.it

Research experience and Educational background

Ph.D. Mobility grant
August-November 2021

- Jerzy Haber Institute, Polish Academy of Science (Krakow, Poland)

Scientific collaboration
2019 - today

- CollectionCare "Innovative and affordable service for the Preventive Conservation monitoring of individual Cultural Artefacts during display, storage, handling and transport" (H2020 GA 814624).

Professional Internship
February-September 2018

- British Library and London Metropolitan Archives (London, UK)
- Istituto Centrale per il Restauro e la Conservazione del Patrimonio Archivistico e Librario (Rome, Italy)

Master of Science (M.Sc.) in *Science and Technology for the Conservation of Cultural Heritage*. Academic year: 2015/2016.
Sapienza University of Rome, Italy

- Thesis title: Study of microclimate frames and optimisation of the sampling frequency of the thermo-hygrometric observations. Case study : two paintings by J. Sorolla in the Pio V Museum of València (Spain).

International Summer School
May-June 2017

- International Institute for Restoration and Preservation Studies (San Gemini, Italy) - *The Craft of Making and Restoring Book Bindings*

Research Project
July-November 2017

- Istituto Superiore per la Conservazione e il Restauro (Rome, Italy)

M.Sc. Mobility grant
February-May 2016

- UPV Universitat Politècnica de València (Valencia, Spain)

Bachelor of Science (B.Sc.) in *Technologies for the Conservation of Cultural Heritage*. Academic year: 2013/2014.
Sapienza University of Rome, Italy

- Thesis title: Assessment of the historic climate within the Museum of Mineralogy of Sapienza

Teaching experience

Assistant for two courses within the M.Sc.in *Science and Technology for the Conservation of Cultural Heritage* at Sapienza University of Rome: "Laboratory of Physics" (Prof. Anna Maria Siani) from 2019 to 2022 and "Archaeometry and laboratory of archaeometry" (Prof. Stefano Ridolfi) in 2020.

Fundings and Awards

- **Avvio alla Ricerca** Sapienza Università di Roma 2020
- **Joint PhD Mobility** Sapienza Università di Roma 2019
- **Student Modelling Competition** 16th IBPSA Congress 2019
- **Percorso di Perfezionamento** Sapienza Università di Roma 2018
- **Torno Subito** Regione Lazio 2018
- **IIRPS Summer school** San Gemini Preservation studies 2017
- **Laureato Eccellente** Fondazione Sapienza 2016
- **Master thesis abroad** Sapienza Università di Roma 2016

Colophon

This thesis was typeset using LaTeX. Details on the packages utilized to make this thesis, along with the LaTeX source (template) of this thesis can be found on https://andreasliudimulyo.github.io/#latex.

Final Version as of Monday 14th February, 2022.